

Saliience Network in Psychosis

Lena Palaniyappan, MBBS, MRCPsych

Thesis submitted to the University of Nottingham for the degree of
Doctor of Philosophy, dated July 2013

ABSTRACT

This thesis explores the role of a large-scale brain network comprising of the insula and anterior cingulate cortex in the pathophysiology of psychosis using structural and functional neuroimaging. Primarily, anatomical changes affecting the grey matter structure and patterns of dysconnectivity involving the insula are investigated.

Various meta-analytic studies have reported consistent reduction in insular grey matter across various psychotic disorders. Despite these robust observations, the role played by this brain region in the generation of psychotic symptoms remains unexplored. In this thesis, using a meta-analytic approach, the relevance of insula for the clinical expression of psychosis is highlighted. Further, significant reduction in the cortical folding of the insula was noted in patients with schizophrenia. Reduced gyrification is accompanied by reduced functional connectivity between the insula and the rest of the brain.

Using an effective connectivity approach (Granger Causal Analysis), the primacy of insula in driving the dorsolateral prefrontal cortex is demonstrated in healthy controls; this relationship is significantly affected in schizophrenia amounting to aberrant connectivity within a putative salience-execution loop. Reduced primacy of the salience-execution loop relates to illness severity.

It is argued that the insula, as a key region of the salience network, plays a crucial role in the generation of symptoms of psychosis. The evidence in support of this theory is discussed, together with its implications for clinical practice aimed at reducing the burden of psychosis.

எத்தொழிலை செய்தாலும் ஏதவத்தே பட்டாலும்
முத்தர் மனமிருக்கும் மோனத்தே- வித்தகமாய்
காதி விளையாடி இரு கைவீசி வந்தாலும்
தாதி மனம் நீர்க் குடத்தே தான்
- பட்டினத்தார்

யாதும் ஊரே; யாவரும் கேளிர்;
தீதும் நன்றும் பிறர்தர வாரா;
நோதலும் தணிதலும் அவற்றோ ரன்ன;
சாதலும் புதுவது அன்றே; வாழ்தல்
இனிதுஎன மகிழ்ந்தன்றும் இலமே; முனிவின்
இன்னாது என்றலும் இலமே; மின்னோரு
வானம் தண்துளி தலைஇ ஆனாது
கல்பொருது இரங்கும் மல்லல் பேர்யாற்று
நீர்வழிப் படுஉம் புணைபோல் ஆருயிர்
முறைவழிப் படுஉம் என்பது திறவோர்
காட்சியின் தெளிந்தனம் ஆதலின் மாட்சியின்
பெரியோரை வியத்தலும் இலமே;
சிறியோரை இகழ்தல் அதனினும் இலமே

- கணியன் பூங்குன்றனார்

அம்மா.... படித்துக் கற்றது அல்ல இந்த வேட்கை; உங்களைப் பார்த்துக் கற்றது.

அப்பா ... இது வேலை நாள் ஒவ்வொன்றையும் விழா நாளாக மாற்றும் உங்கள் தனித்துவத்துக்காக.

பிரியா ... ஆராய்ச்சிக்கெல்லாம் வேர் பாய்ச்சிப் படித்ததற்கும், மற்ற எல்லாவற்றிற்கும்.

ACKNOWLEDGMENTS

Peter, thanks for inducing this preoccupation, infecting with your enthusiasm and also, furnishing all those missing ‘articles’!

Bert, thanks a lot for teaching me the concept of ‘playing with softwares’.

Vijender, thanks for being a good friend, conscientious colleague and uncertified squash guru.

Tom, thanks for your early work on the insula which seeded this thesis.

Rajeev, thanks for taking some of my ideas seriously and reducing the need for me to self-cite when pursuing the wicked h-index.

To the **Wellcome Trust** for funding my Research Training Fellowship

To **Cris Glazebrook** for supporting my PhD tuition fees

To **Ed Bullmore & Karl Friston, Chris Hollis and Dorothee Auer** for supporting my Wellcome fellowship application

To **Elizabeth Liddle** for setting up my first ANOVA

To all users of the vibrant **Freesurfer mailing list** (**Douglas Greve** for VBM-SBM registration & **Don Hagler** for clarifying issues with surface area maps in particular)

To anonymous **peer reviewers** for shaping this thesis, and correctly spelling my surname in every rejection letter.

To **Joaquim Radua** for his help with the SDM software

To **Kay Head** and **Kathleen Shaw** for their help with data collection

To **Marie Schaer** for her excellent LGI script

To **Marije Jansen, Molly Simmonite** and **Kathrin Doege** for their assistance in acquiring and analyzing the data reported in this thesis.

To **MRC** for sponsoring my attendance at the Cardiff Brain Research Summer School in 2011

To **Nicol Ferrier** for making me believe I could apply for Wellcome/MRC fellowships

To **Penny Gowland** and **Olivier Mougin** for their assistance in acquiring the 7T data

To **Prof. Rajarathinam** for ensuring that I remain a curious student of Psychiatry throughout my career.

To the **Academic Faculty** of the RCPsych for Margaret Slack Award & the Research Prize 2011

To the **General Adult Faculty** of the RCPsych the Trainee Research Prize 2010

To **Tim Crow** for his constant inspiration (and of course the Mac computer!)

To **Verghese Joseph & Pavan Mallikarjun** for acquiring crucial clinical data.

To Schizophrenia and Bipolar Research Societies - **SIRS** (2012) and **IBDS** (2011) - for awarding me Travel Fellowships

To the **editors** of Neuroimage, Biological Psychiatry, Psychiatry Research: Neuroimaging, Journal of Psychiatry & Neuroscience, Human Brain Mapping, Schizophrenia Bulletin, Schizophrenia Research, Molecular Psychiatry, Brain Structure & Function, PLOSONe, Frontiers in Psychiatry, Cortex, Neuroscience & Biobehavioural Reviews and Cerebral Cortex for providing me with opportunities not only to review others' work but also to reconsider my own work in the process.

To Robert Sommers Award Society (Giessen), European Science Foundation, Guarantors of Brain, Royal College of Psychiatrists and Graduate Travel funds from the University of Nottingham for supporting my attendance at various meetings

.....

I am very grateful for numerous patients who volunteered for the imaging projects reported in this work

PREFACE

The work presented in this thesis has resulted from a collaborative effort of a team of researchers led by Prof. Peter Liddle and funded by various bodies including the Medical Research Council (Liddle), The Wellcome Trust (Palaniyappan) and internal grants from the Nottingham Institute of Neuroscience and School of Community Health Sciences (Pump Priming and Postgraduate Research Funds - Palaniyappan). Some of the imaging data used in this thesis (Chapter 5 and 6) were supported by New Investigator grant from the University of Nottingham and a Interdisciplinary Research Award from the Nottingham Institute of Neuroscience, University of Nottingham (Mallikarjun).

All the data analyses presented in this thesis were designed, performed and written up by myself. The literature searches for the meta-analyses presented in Chapters 3 and 4 were independently cross-validated by Dr. Balain. Drs. Mallikarjun, Verghese and I acquired the clinical data reported in chapters 5 and 6. Dr Balain and I acquired the clinical data reported in chapters 7 and 8. All of the chapters presented here (except some sections of chapters 1 and 9) have been published in peer-reviewed journals; a list of the published manuscripts attached as an appendix to this thesis. The contributions of the co-authors are acknowledged in each manuscript, and elaborated in the Acknowledgements section.

I was registered as a part-time PhD student throughout the period of my doctoral study. Between October 2009 and February 2012, I was supported by a HEFCE funded Clinical Lectureship (5 clinical sessions). From February 2012 onwards the Wellcome Trust supports me as a Research Fellow. I do not have any conflicts of interest related to this work. I received a Young Investigator Travel Fellowship to attend 9th Bipolar Disorder Meeting at Pittsburgh, PA, USA through a competition organized by International Bipolar Disorder Society. This award was sponsored by Eli Lilly.

Acronyms

ACC	Anterior cingulate cortex
APA	American Psychiatric Organisation
DMN	Default mode network
EEG	Electroencephalography
FDR	False-discovery-rate
FWE	Familywise Error correction
fMRI	Functional magnetic resonance imaging
GABA	Gamma amino butyric acid
LGI	Local Gyrfication Index
MEG	Magnetoencephalography
NS-SEC	National Statistics Socio-Economic Classification
PCC	Posterior cingulate cortex
ROI	Region of interest
SBM	Surface Based Morphometry
SSPI	Signs and Symptoms of Psychotic Illness
TMS	Transcranial Magnetic Stimulation
VBM	Voxel based Morphometry

Table of Contents

Abstract	1
Acknowledgments	4
Preface	vi
Acronyms	vii
Chapter 1: The Pathogenesis Of Schizophrenia: A Guided Inquiry	1
1.1 Studies of brain structure in schizophrenia	5
1.2 Localisation of grey matter deficits in schizophrenia	8
1.3 Developing a neuroanatomic model.....	12
1.4 Outline of the thesis.....	13
Chapter 2: A Hypothesis Of Insular Dysfunction	17
2.1 The nature of the structural deficits of the SN	18
2.2 Time course of structural changes in the SN	22
2.3 Effect of antipsychotics on the structure of the SN.....	24
2.4 Functional attributes of the SN: the proximal salience	26
2.5 fMRI studies of the SN in schizophrenia.....	31
2.6 Correlation of insular deficits with clinical symptoms	32
2.7 Insular dysfunction model of psychosis.....	34
2.8 Dopamine and the Salience Network	40
2.9 Unanswered questions	42
Chapter 3: The Neuroanatomy Of Psychotic Diathesis	45
3.1 Genetic Diathesis and Clinical Expression.....	45
3.2 Literature search	48
3.3 Signed Differential Mapping.....	50
3.4 Search Outcome.....	51
3.5 Results from the Diathesis Set	56
3.6 Results from the Expression Set.....	57
3.7 Salience Network Nodes and Clinical Expression	58
3.8 Neuroanatomy of the genetic diathesis	62
3.9 Neuroanatomy of clinical expression.....	64
3.10 Limitations of this work	66

Chapter 4: Structural Correlates of Hallucinations	69
4.1 Neuroanatomy of hallucinations.....	69
4.2 Literature search	72
4.3 Signed Differential Mapping.....	72
4.4 Search Outcome.....	74
4.5 Results from SDM analysis	76
4.6 The role of insular cortex in hallucinations	81
4.7 Superior temporal gyrus in hallucinations	82
4.8 Limitations of this work	83
Chapter 5: Anatomical Basis Of Morphometric Deficits	87
5.1 Interpretation of VBM deficits	87
5.2 Participants.....	90
5.3 Image acquisition	92
5.4 Voxel Based Morphometry	92
5.5 Surface Based Morphometry	93
5.6 Statistical Analysis.....	98
5.7 VBM Analysis.....	100
5.8 SBM Analysis.....	101
5.9 Relationship between SBM measures and GMV	103
5.10 The contribution of surface anatomical changes to VBM deficits	107
Chapter 6: Aberrant Cortical Gyrification In Schizophrenia.....	112
6.1 Cortical folding patterns in schizophrenia	113
6.2 Methods.....	115
6.3 Statistical Analysis: Whole Brain Cortical Maps.....	116
6.4 Statistical Analysis: Regional cortical thickness.....	117
6.5 Whole brain gyrification defects.....	118
6.6 Post-hoc tests of asymmetry and sulcogyral thinning.....	121
6.7 Search for increased gyrification	124
6.8 Insular hypogyria	125
6.9 Multimodal cortical gyrification in schizophrenia.....	128
Chapter 7: Diagnostic Specificity Of Dysconnectivity.....	131
7.1 Kraepelinian dichotomy.....	132

7.2 Participants.....	134
7.3 Image acquisition.....	137
7.4 Image processing.....	139
7.4 Statistical Analysis.....	140
7.5 Results: Core hubs	142
7.6 Results: Group differences in centrality	149
7.7 Results: Group differences in gyrification.....	153
7.8 Posthoc tests: effect of sample size and medications	158
7.9 Redistributed centrality in psychosis	160
7.10 Aberrant gyrification in psychosis	162
7.11 Strengths and limitations	163
Chapter 8: Neural Primacy Of The Salience Processing System	166
8.1 Task-positive brain systems	167
8.2 Participants.....	170
8.3 Image acquisition and processing	172
8.4 Statistical Analysis.....	174
8.5 Granger Causality	176
8.5 Relationship with illness severity.....	186
8.6 Functional Connectivity (FC)	190
8.8 Granger Causal influences from the left anterior insula	198
8.9 Impaired salience-execution loop in schizophrenia	205
8.10 Temporo-limbic dysconnectivity in schizophrenia.....	211
8.11 Strengths and limitations	212
8.12 Possible confounding effects of hemodynamic delay	213
Chapter 9: From Observations To Opportunities	216
9.1 Studies supporting the insular dysfunction hypothesis	217
9.2 Studies refuting the insular dysfunction hypothesis	223
9.3 Extensions of the insular dysfunction hypothesis	224
9.4 Is SN dysfunction specific to schizophrenia?.....	227
9.5 Neurochemical basis of SN dysfunction.....	228
9.6 SN dysfunction as a therapeutic target.....	232
REFERENCES.....	239
APPENDICES	296

Chapter 1

The pathogenesis of schizophrenia: a guided inquiry

Schizophrenia can be described as a uniquely human condition representing one end of the continuum of variations in the mental faculties that constitute the subjective experience of self and the world (Crow, 1990; Sass and Parnas, 2003). This subjectivity has made schizophrenia a difficult subject matter to study in a reliable manner, contributing in part to the significant heterogeneity of clinical observations (Strauss, 2011). Traditionally, the descriptions of the mental phenomena that form the core experience of schizophrenia have mostly been provided by clinicians and other external observers (for example, (Grange, 1962; Schneider, 1959)). These observations have variously shaped the current classificatory systems that widely used in the diagnosis, treatment and the research of schizophrenia. In recent times, absorbing first person accounts of individuals with a clinical diagnosis of schizophrenia have appeared in the literature (Rudnick et al., 2011). Excerpts from these accounts (Table 1.1) highlight the diverse nature of schizophrenia at a phenomenological level.

These first person accounts and other recorded autobiographical narratives establish schizophrenia as an illness of perceptual, affective and cognitive disturbances (Freedman, 1974). Notwithstanding the varied nature of the illness experience, these accounts are dominated by recurring attempts of patients to understand the proximal cause of their sufferings. The explanatory attempts put forward by individuals experiencing psychosis

Table 1.1: First Person Accounts of Schizophrenia

Peter Chadwick (Chadwick, 2007)	As my delusional system expanded and elaborated, it was as if I was not “thinking the delusion,” the delusion was “thinking me!” I was totally enslaved by the belief system. everything confirmed and fitted the delusion, nothing discredited it. Indeed, the very capacity to notice and think of refutatory data and ideas was completely gone. Confirmation bias was as if “galloping .,” and I could not stop it.
Roberta Payne (Payne, 2012)	When I am psychotic, I feel like I have been pressed deep within myself. My brain was giving the noise a drama, or story, of its own. Similarly, my brain created disc jockeys in the air vents of the hospital room playing Beatles’ songs.
Erin Hawkes (Hawkes, 2012)	My delusions of the Deep Meaning included dietary demands. I ate carrots (a carrots the environment), juice, but only “from concentrate” (to concentrate is good) and cereal (to see [ce] what is real).
Clara Kean (Kean, 2009)	I am disconnected, disintegrated, diminished. Everything I experience is through a dense fog, created by my own mind, yet it also resides outside my mind. I feel that my real self has left me, seeping through the fog toward a separate reality, which engulfs and dissolves this self. This has nothing to do with the suspicious thoughts or voices; it is purely a distorted state of being. The clinical symptoms come and go, but this nothingness of the self is permanently there.
Milton T. Greek (Greek, 2010)	In the first hallucination, which lasted less than a minute, I was walking toward the glass double doors of the bus station with a small lunch when I looked through the doors and saw a street person looking at me. The street person’s eyes were highly unusual—they seemed like landscapes that went back into the man’s head infinitely far, stretching on for eternity.
A written note from “Angela” (Smith, 2003)	No visitors allowed. I was fired. I do not feel very well. May I please speak to Dr. Mark Adams. In North Carolina, I am considered a chronic paranoid schizophrenic. I have no interest in answering questions, especially about my religion. I have nothing to say except to request a transfer to a professional health care facility in New York. This is known as racketeering comrade. There is probably going to be another hospitalization. It is yet to be determined if there is going to be a pseudonym and no insurance. Happy anniversary.

range from an explicit denial of schizophrenia as a disease entity to offering novel psychological formulations of how the brain operates in health and disease (for example, (Chadwick, 2007; Hawkes, 2012; Kean, 2009)). Similar efforts to understand the mechanisms behind schizophrenia have been continually made by clinicians and researchers throughout the history of psychiatry. Kraepelin listed a number of speculated pathogenetic influences in the 8th edition of his textbook, which included morbid anatomy, hereditary

predisposition, general conditions of life (with references to the effects of civilization) and injury to the germ (Kraepelin, 1919). From these various hints offered by Kraepelin, putative biological mechanisms came to be regarded as the most proximal links to the expression of the symptoms and signs of the illness. Subsequently, the interest narrowed down to the study of pathophysiology as the key to make any real progress in the treatment of schizophrenia (Unknown, 1930).

Though the scientific progress in unraveling the aetiopathogenesis of schizophrenia has been painfully slow, it is acknowledged that most of what we know currently of schizophrenia has resulted from the continued research on the neurobiological aspects (Insel, 2010). Of late, a specific emphasis has been placed on the study of brain morphology, circuitry and gene-environment interaction to further this progress (Editorial in Nature, 2010).

The idea that schizophrenia is a disease of the brain is probably as old as the idea that schizophrenia is an illness. Crichton-Browne wrote in 1879 that the highly evolved left sided cortical centres that are last to be organized during development “might suffer first in insanity” (Crichton-Browne, 1879). The suspected morbidity of the brain anatomy heavily influenced Kraepelin’s original conception of dementia praecox. He carefully included the photomicrographs of histological findings observed by Alois Alzheimer in the eighth edition of his textbook of psychiatry, to add credence to his emphasis on the morbid anatomy of dementia praecox (Kraepelin, 1919). Kraepelin, though impressed with Alzheimer’s reports, conceded that no macroscopic changes were notable in patients. Wernicke, who approached psychoses with a

neuroscientific speculation, asserted that an aberrant shunting of associative processes underlie dementia praecox, and these disturbances are “theoretically localizable” to anatomical changes in the brain (Cutting, 1987). Bleuler, though inclined towards a psychoanalytical exposition of the myriad of observations that constitute the clinical features of schizophrenia, explicitly admitted the role of the brain in this illness (Bleuler, 1950). Nevertheless he prudently acknowledged that the task of mapping changes in brain to the disturbed psychological processes, which he considered to be of primary importance, as a challenging one (Bleuler, 1950). Even the most vocal of the critics against the concept of mental illness, accept that demonstrating alterations in the brain and their relationship to the symptoms and signs of psychosis is vital for scientific progress. Thomas Szasz, in a monograph attacking the Kraepelinian and Bleulerian concepts of schizophrenia by comparing them with the syphilitic model of disease (general paresis), states “The fact that paresis is a brain disease could never have been established by studying the paretic’s thinking. Then why study the schizophrenic’s?”(Szasz, 1976). He concludes that to be qualified as a disease, anatomical lesions in the brain must be identified in schizophrenia (Pies, 1979). 20 years later, appraising the reasons for the lack of strong inferences in schizophrenia research, Carpenter and colleagues (1993) reaffirm that defining the neuroanatomic substrate is an important next step in the search for causality in schizophrenia. At this juncture, it may be pertinent to ask what insight has been gained from the 200 years of research into psychosis/schizophrenia with regard to the structure of the brain in this illness.

1.1 Studies of brain structure in schizophrenia

The earliest systematic studies of the brain in 'insanity' focused on the post-mortem changes (Haslam, 1798). The samples were limited and substantial inferences could not be made due to the difficulties in the capacity to replicate findings. Historically, the first recorded attempt of mapping brain anatomy to symptoms in psychosis was carried out by Elmer Southard, a professor of neuropathology at Harvard (Zornberg, 1999). Between 1910 and 1915, he published a series of reports on systematic microscopic and macroscopic examination of randomly selected post-mortem samples from patients with dementia praecox, focusing particularly on structural abnormalities visible to the naked eye. He reported that 45 out of these 50 brains showed "gross anomalies or other lesions" (Southard, 1915). A number of these samples had what he termed as "internal hydrocephalus," or ventricular dilatation. He did not have access to post-mortem samples from a control population. In his 1914 report, he writes "The writer has followed up his earlier work on the dementia praecox group (1910) with a more systematic anatomoclinical study of 25 cases, having a view to (a) definite conclusions as to the structurality ("organic nature") of the disease, and (b) correlation of certain major symptom groups (delusions, catatonic symptom groups, auditory hallucinosis) with disease of particular brain regions. As to (a), the **structurality of dementia praecox**, the writer feels that the disease must be conceded to be in some sense structural, since at least 90 per cent of all cases examined (50 cases, data of 1910 and 1914) give evidence of general or focal brain atrophy or aplasia when examined post mortem, even without the use of the microscope. As to (b), the **functional correlations** of this study, the results may be summed up by saying that strong correlations have

been found to support the writer's former claims that (1) delusions are as a rule based on frontal disease, and (2) catatonic symptoms on parietal-lobe disease. An equally strong correlation (3) has now been found between auditory hallucinosis and temporal-lobe disease.” Remarkably, Southard concluded that his findings support “a study of genesis than of etiology, and does not rise to the height of ascribing causes”. He commented that “to underrate the possible contributions of anatomy to this field” is a “deplorable thing” (Southard, 1915).

A revolutionary change in the field was beginning to emerge by the late 1920s when pneumoencephalography was used to study the brain structure in 19 patients who were admitted to the Stadtroda hospital near the University of Jena in Germany (Jacobi and Winkler, 1927). A wider interest in exploring the substance of brain in schizophrenia culminated from the works of Eve Johnstone and Timothy Crow using Computed Tomography in 1976 wherein they demonstrated the presence of ventricular enlargement in schizophrenia using a case-control design for the first time to address the neuroanatomical changes (Johnstone et al., 1976). The first Magnetic Resonance Imaging study by Nancy Andreasen and colleagues in 1986 opened further doors for more sophisticated studies (Andreasen et al., 1986). The next two decades saw an exponential growth of research in schizophrenia using MRI. By 2009, the year when the current doctoral study began, there were 6305 articles retrieved using the search terms MRI, schizophrenia and neuroimaging (Shenton et al., 2010). Morphometry, a group of techniques that focused primarily on measuring the physical parameters of the brain tissue, was

employed by a number of research groups across the globe and exciting insights began to emerge by the beginning of the 21st century.

The most commonly employed method to study brain structure in schizophrenia to date is the use of voxel-based morphometry (Ashburner and Friston, 2000). This technique allows an unbiased measurement of grey or white matter tissue across the entire brain in a group of patients, thus allowing a comparison to be made against a group of healthy controls. The earliest studies using the VBM technique promised identification of neural correlates of the clinical syndromes of schizophrenia (Chua et al., 1997; Wright et al., 1995), while subsequent studies have largely focused on defining the loci of neuroanatomical deviation in schizophrenia when compared to healthy controls (Ananth et al., 2002; Wright et al., 1999) (Wright 1999, Ananth 2002). In schizophrenia, grey matter has been the focal point of most of these VBM studies. This focus on the grey matter stems from a number of events throughout the history of schizophrenia research. Grey matter changes have been the focus of neuropathological studies in schizophrenia since Kraepelinian times. Alzheimer's original investigations on post-mortem samples found a modest reduction in number of cortical neurons and some evidence for gliosis (Kraepelin, 1919). Since the advent of neuroleptic medications and the emergence of neurotransmitter hypotheses in schizophrenia (Carlsson and Lindqvist, 1963), a strong focus on neuronal synapses has emerged. With the majority of neuronal synapses being located in the cortical grey matter, this tissue has become a focal point of investigation when studying anatomical changes in schizophrenia (Feinberg, 1982). It is estimated that the majority of energy consumed by the metabolic processes of

the human brain centers around the synaptic activity (Howarth et al., 2012), making the grey matter tissue particularly prone to toxic and metabolic insults that can affect a number of cognitive faculties. Further, in recent times a rejuvenation of interest in brain mapping has resulted in the understanding that normal variations in the structure of brain, especially the grey matter, could explain a number of inter-individual differences in cognitive processes (Kanai and Rees, 2011).

Schizophrenia is likely to be one of the several pathological conditions for which VBM has been most frequently employed. During the time span of the current study (October 2009 and June 2012), 127 studies have been indexed in the MEDLINE when searched using the keywords 'voxel based morphometry' and 'schizophrenia' OR 'psychosis', out of a total of 912 articles associated with 'voxel based morphometry'. Do we have any well-replicated, consistent findings with regard to the morbid anatomy of schizophrenia from the VBM studies of the grey matter?

1.2 Localisation of grey matter deficits in schizophrenia

Meta-analytical techniques are very useful in synthesizing the evidence from several systematic investigations. In neuroimaging, meta-analytical techniques have been particularly popular and have been largely employed to determine the likelihood of the spatial distribution of group differences, thus identifying the specific brain regions where in the grey matter abnormalities are localized. In schizophrenia a number of such likelihood-estimation meta-analyses to localize grey matter changes have been conducted to date. A

summary of these studies has been presented in 1.2. The coordinates identified from these meta-analyses have been plotted in figure 1.1.

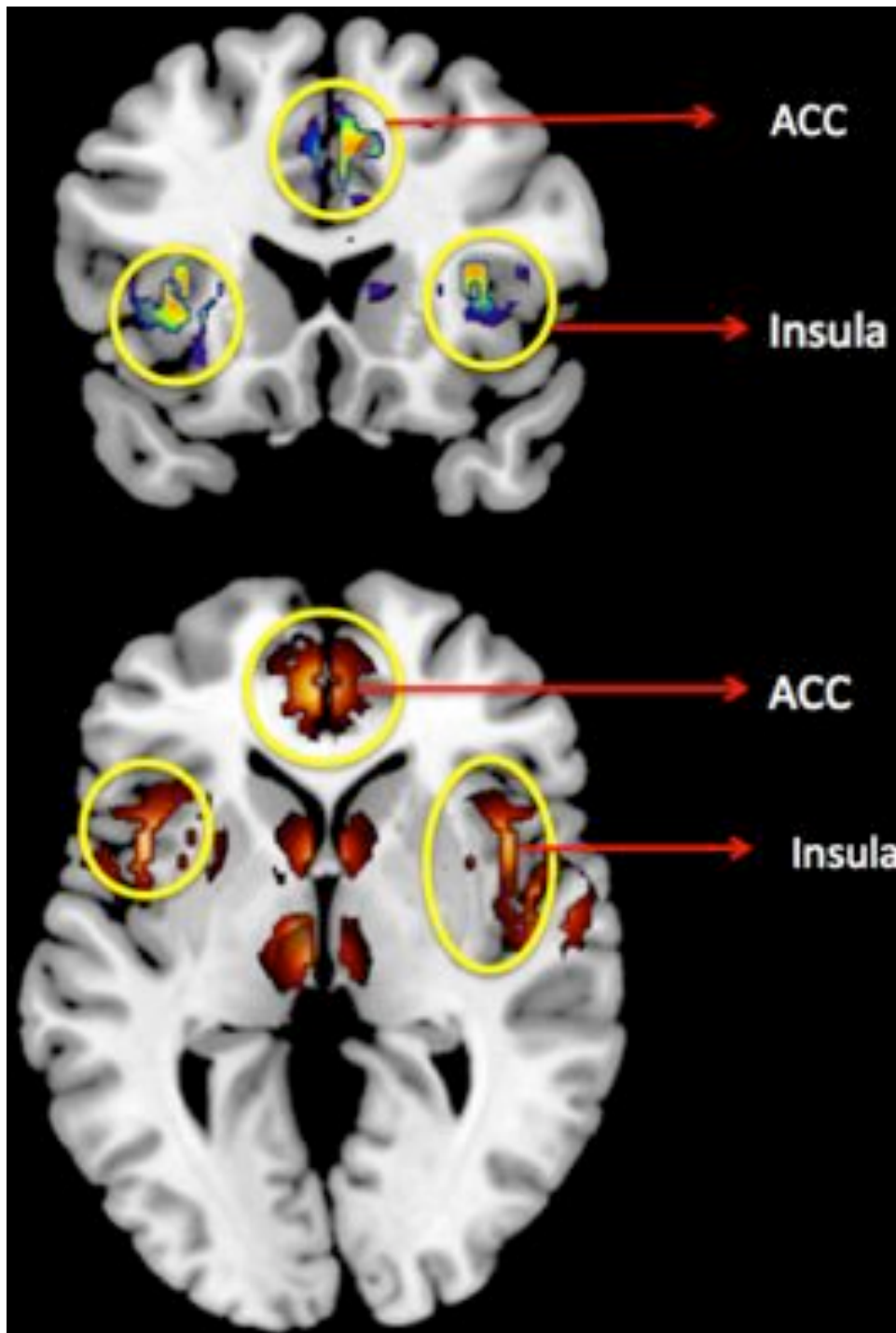


Figure 1.1: Co-ordinates derived from the VBM meta-analytic studies comparing (1) first episode schizophrenia [coronal view] and (2) mixed samples of schizophrenia with healthy controls [axial view]. Insula and anterior cingulate cortex (ACC) are encircled. Slices are selected for the best visual display of the insula and ACC nodes. The inflated co-ordinate maps are overlaid on a single subject T1 image provided with the MRICron software.

Study	Number of studies	Number of Patients / Controls	Contrast	Regions with GM reduction in patients	Meta-analytical approach
Bora 2011a	12	359/421	SCZ vs. HC	Left frontoinsular cortex, bilateral ACC, bilateral STG	SDM: Only samples with <60% males were included
Bora 2011a	39	1719/1851	SCZ vs. HC	Bilateral insula / IFG, left STG, bilateral ACC and dorsomedial frontal regions	SDM: Only samples with >60% males were included
Bora 2011b	49	1999/2180	SCZ vs. HC	Bilateral insula/inferior frontal, Bilateral thalamus, Bilateral ACC/medial frontal	SDM
Chan 2011	19	808/856	Chronic SCZ vs. HC	Bilateral insula, left IFG, left ACC, bilateral amygdala, right STG, left thalamus	GingerALE Foci >500mm3 shown in the table
Chan 2011	14	566/608	FEP vs HC	Bilateral insula, left STG, left amygdala, right IFG, right cingulate gyrus,	GingerALE Foci >500mm3 shown in the table
Ellison-Wright 2008	20	809/798	Chronic SCZ vs. HC	Bilateral insula, bilateral ACC the left IFG & middle frontal gyrus, left fusiform gyrus, right superior/middle temporal gyrus, left uncus/amygdala, right hippocampus	ALE approach: GM increases were reported in left putamen, right SFG, right fusiform.
Ellison-Wright 2008	7	170/188	FEP vs. HC	Bilateral uncus/amygdala, bilateral insula, bilateral caudate, bilateral inferior frontal gyrus, left postcentral gyrus.	ALE approach: GM increases were also reported in bilateral putamen
Ellison-Wright 2010	42	2058/2131	SCZ vs. HC	Bilateral insula, left ACC, left thalamus, bilateral medial frontal gyrus	ALE approach
Fornito 2009	37	1646/1690	SCZ vs. HC	Bilateral insula, bilateral ACC, left PCC/precuneus, left amygdala/PHG, left fusiform	GingerALE Foci >500mm3 shown in the table
Fusar-Poli 2011, 2012	8	206/202	Neuroleptic naive FEP vs. HC	Left insula, left ACC, right STG, cerebellum	SDM
Glahn 2008	31	1195/1262	SCZ vs. HC	Bilateral insula, ACC (ventral, dorsa and subgenual), left PHG, thalamus, left postcentral gyrus, left MFG	GingerALE Only the foci >400mm3 were reported
Leung 2011	6	162/165	Neuroleptic naive FEP vs HC	Bilateral caudate, bilateral insula, right MFG, right STG,	GingerALE Foci >500mm3 shown in the table
Leung 2011	9	336/484	Neuroleptic treated FEP vs.HC	Bilateral insula, left MFG and ACC, bilateral STG, right IFG, left PHG/amygdala.	GingerALE Foci >500mm3 shown in the table

Table 1.2: Meta-analyses of VBM studies comparing patients with schizophrenia and healthy controls. SCZ: Mixed samples of patients with variable duration of established schizophrenia FEP: First episode psychosis HC: Healthy controls ACC: Anterior cingulate cortex IFG: Inferior frontal gyrus STG: Superior temporal gyrus PCC: posterior cingulate cortex PHG: Parahippocampal gyrus ALE: Activation Likelihood Estimation SDM: Signed Differential Mapping

Of the several regions reported in these meta-analyses, insula shows the most consistent grey matter reduction in schizophrenia, and is identified in all of the meta-analyses irrespective of the duration of illness. Anterior cingulate cortex is the next most consistent site with GM reductions, followed by superior temporal gyrus. Interestingly, the insular cluster extends to the inferior frontal gyrus anteriorly in a number of these meta-analyses (Bora et al., 2011a, Bora et al., 2011b; Glahn et al., 2008) and to the superior temporal gyrus posteriorly in some (Ellison-Wright et al., 2008). Less consistent changes were notable in subcortical structures such as the caudate, amygdala and the thalamus. It is important to note that the remarkable consistency, at least in part, is due to the significant overlap in the studies included in these meta-analyses. Nevertheless, each of these meta-analyses focused on identifying studies that undertook a whole brain search without a priori assumptions regarding the loci of GM change in schizophrenia.

The structural changes in the insular cortex have also been noted consistently in bipolar disorder (Ellison-Wright and Bullmore, 2010), suggesting that insula has a crucial role in the pathophysiology of psychosis. But despite recent attempts to delineate the role of insula in various neuropsychiatric disorders including schizophrenia²⁻⁴, an integrative model of insular dysfunction in relation to psychosis is lacking. Insula is a highly reciprocally connected brain region^{5,6}. A fuller understanding of insular dysfunction in the pathogenesis of psychosis can be obtained by bringing together evidence from structural and functional imaging to highlight the potential role of the disrupted interaction of this structure with other brain regions in psychosis. In particular, it will be fruitful to explore the relationship

between the insula and other regions showing GM reduction in schizophrenia. To this end, we must consider whether the brain regions showing consistent GM deficits in schizophrenia, organize themselves in any constrained manner and contribute to aspects of normal brain function in healthy controls.

1.3 Developing a neuroanatomic model

There is an often-observed co-activation between the insula and the anterior cingulate cortex (ACC) across a variety of cognitive tasks suggesting the presence of a functional network involving these two regions (Taylor et al., 2009). Both functional and structural connectivity have been demonstrated between the insula and the ACC (Heuvel et al., 2009; Taylor et al., 2009) with likely extension into the inferior frontal region (Dosenbach et al., 2007; Seeley et al., 2007). This intrinsic network has been variously described as a cognitive Task Control Network and Salience Network (SN) (Dosenbach et al., 2007; Seeley et al., 2007). Menon and Uddin (2010) have recently proposed that the primary role of this network is to enable switching between a default mode (resting mode or task-negative state of brain) and executive (processing mode or task-positive) states of brain connectivity. Disrupted coordination among brain circuits, in particular between the anticorrelated networks that underlie task-related and default mode, has been postulated as a core pathophysiological feature in schizophrenia (Williamson, 2007).

The concept of parallel distributed processing models in cognition and behavioural neurology (Rumelhart and Group, 1987) has had a strong influence on the interpretation of neuroimaging literature in schizophrenia (Friston, 1998; Liddle et al., 1992). In this context, Nancy Andreasen proposed

one of the earliest heuristic neuroanatomic models of dysfunctional large-scale circuits in schizophrenia based on observations from neuroimaging studies (Andreasen et al., 1998). This model was based on the notion of cognitive dysmetria and was heavily influenced by the PET and fMRI observations on patients, with only limited references to the normal physiological organisation of a putative front-thalamic-cerebellar circuit. Nevertheless, along with other similar neurocognitive models (Braff, 1993; Frith et al., 1992; Goldman-Rakic and Selemon, 1997), this provided an experimentally testable assumption for several functional imaging studies. In a similar vein, the concept of SN provides a convenient framework to explore the pathophysiology of structural deficits in psychosis. Further, as discussed in chapter 2, it also holds the promise to integrate structural and functional abnormalities often noted, but hitherto considered in isolation in schizophrenia. However, as the primary evidence for insular dysfunction comes from structural imaging studies, it is important to establish the nature of these structural deficits in further detail. To investigate the relevance of the insula and ACC in the pathophysiology of schizophrenia, it is also important to propose a plausible model of the insular dysfunction in the context of the diverse clinical features of schizophrenia.

1.4 Outline of the thesis

The aim of this doctoral research is to investigate the nature of neuroanatomical changes in schizophrenia as outlined above in the context of the pathophysiology of psychosis. To accomplish this, 2 large datasets of magnetic resonance images in patients with schizophrenia and matched controls have been utilized. In addition, 2 meta-analyses were performed

using previously published studies investigating morphometric changes in schizophrenia.

The thesis opens with a review of the existing literature on the grey matter changes in schizophrenia highlighting the primacy of the insula and the anterior cingulate (together constituting the Salience Network, SN) in the pathophysiology of psychosis (Chapter 2). This review also highlights the missing links in the hypothesized role of the SN, some of which are investigated in detail in subsequent chapters. The rest of the thesis establishes the methods used to investigate the SN and defends the hypothesis that insula has a cardinal role in the generation of psychotic symptoms in schizophrenia.

Chapter 3 presents the results of a coordinates-based meta-analysis of several VBM studies using Signed Differential Mapping approach to address the question whether the structural changes in the SN are associated with the diathesis or the expression of schizophrenia. The findings suggest that insular abnormalities are one of the prime anatomical features in those with a clinical manifestation of schizophrenia.

Chapter 4 is an attempt to study the clinical relevance of the structural changes in the insula. It focuses on the role of the SN in one of the most frequently reported symptoms of schizophrenia: Auditory Hallucinations. Left fronto-insular cortex emerges as the structure showing the most significant grey matter reduction in relation to the auditory hallucinations in schizophrenia.

Two image analysis techniques are employed in this work: Cortical Surface Based Morphometry (SBM) and Voxel Based Morphometry (VBM).

The former technique makes use of the Freesurfer platform, while the latter is based on SPM8. The methods are described in detail in chapter 5. Results from head-to-head comparison of these two methods are reported in this chapter.

Several changes have been noted in the surface anatomical properties of the cortical sheet (mantle) in schizophrenia. Do these changes involve the SN at a whole brain level? Chapter 6 reports findings from (1) a vertex-wise analysis of cortical folding pattern and (2) corresponding changes in cortical thickness in the affected brain regions. A significant abnormality is notable in the insular cortex, suggesting a deviation in the normal cortical development affecting the insula in patients.

In chapter 7, the issue of specificity of the gyrification defects to schizophrenia in comparison with bipolar disorder is investigated. Insular gyrification defects appear to be more prominent in schizophrenia and is accompanied by overlapping reduction in the degree of functional connectivity between the insula and the rest of the brain during performance of a working memory task.

Chapter 8 is an attempt to investigate the functional relationship of insula with other brain regions in healthy controls and patients with schizophrenia. It includes results from a Granger causal analysis of functional MRI data obtained during resting state. This whole brain analysis revealed that there was a significant failure of both feed-forward and reciprocal influence between the insula and the DLPFC in schizophrenia amounting to a failure of a

physiological salience-execution loop. This abnormality was related to the burden of psychotic symptoms and processing-speed deficit seen in patients.

Chapter 9 summarises the directions provided by the present work in the scientific pursuit of the pathophysiology of psychosis and translating the insights into developing effective interventions for this debilitating illness. A critical summary of works from other research groups that followed the publication of the initial chapters of this thesis is also presented in chapter 9.

Chapter 2

A hypothesis of insular dysfunction

Voxel based morphometry (VBM), one of the most common techniques employed in studying the neuroanatomy of schizophrenia, consistently identifies grey matter reduction in the insula and the ACC constituting the Salience Network (SN). The aim of this chapter is to consider the structural deficits of the SN identified using regional morphometric methods in addition to the VBM approach in schizophrenia. The functional attributes of the insula in the context of the SN and the relevance of prediction error model will then be reviewed, along with a discussion on the relationship between insular deficits and clinical symptoms of psychosis. In the final section, an integrated model of insular dysfunction in psychosis will be proposed, followed by an outline of fundamental investigations undertaken during the present doctoral study to validate this model.

2.1 The nature of the structural deficits of the SN

Grey matter 'density' as measured by VBM is not an absolute but a proxy measure of grey matter structure as the technique of VBM is based on the probabilistic classification of voxels subjected to affine registration. Hence definitive conclusions with regard to prominent grey matter reduction across the SN cannot be made using VBM alone. Despite the differences in manual tracing methods and the issue of reliability while defining insular and ACC regions, region of interest (ROI) studies could measure the absolute morphometric properties and circumvent the problems related to image registration.

Most ROI studies exploring insular volume confirm a reduction in grey matter volume of insula in schizophrenia (Minzenberg et al., 2009; Wilmsmeier et al., 2010; Wylie and Tregellas, 2010). In addition, ROI studies address the issues of laterality and the issue of anterior vs. posterior localisation of volumetric deficits in the insula. Most ROI studies have found a bilateral volume reduction (Takahashi et al., 2009b, 2004), though some studies show a predominant left insular (Crespo-Facorro et al., 2000; Kim et al., 2003) or right insular involvement (Roiz-Santiáñez et al., 2010; Saze et al., 2007). Differentiating between the anterior and posterior subdivisions of the insula, Makris et al. (2006) showed that anterior insula had greater volume reduction than posterior insula in schizophrenia. A moderate effect size of 0.6 was noted for left anterior insular volume reduction. Such regional differences were replicated in some (Takahashi et al., 2009a), but not all studies

(Takahashi et al., 2009b, 2004). These differences are likely to be due to the inconsistencies in manual tracing for ROI studies in this anatomically complex region. To clarify this issue, a meta-analysis of ROI studies focussing on the insula was recently carried out (Shepherd et al., 2012). The pooled results from fifteen studies that met the inclusion criteria ($n = 945$) showed a medium-sized reduction of bilateral insula in people with schizophrenia (either chronic or FES), with anterior insula showing considerably larger effect sizes ($n = 605$, Hedge's $g = 0.643$, $p = .001$) compared with posterior insula ($n = 453$, Hedge's $g = 0.321$, $p = .028$) suggesting a regional anterior-posterior anatomical distinction. In summary, existing evidence suggests that bilateral insular volume is reduced in schizophrenia, with more reduction in the anterior than the posterior subdivisions.

Goldstein et al. (1999) who studied grey matter volume reductions using a parcellation method found that the largest reductions in the schizophrenia group occurred in bilateral insula and ACC. Baiano et al. (2007) systematically reviewed structural imaging studies reporting on ACC volume in schizophrenia and reported significant reduction in absolute ACC volume. Both Baiano et al. (2007) and Fornito et al. (Fornito et al., 2008), who undertook a focussed review of both VBM and ROI studies addressing ACC volume in schizophrenia, note that while functional subdivisions are noted within ACC, most morphometric studies have considered ACC as a whole. Nevertheless, when stereotactic localisation of the deficits is attempted, GM reductions in the ACC tends to localise on both dorsal and rostral subdivisions, with relatively few changes at the subcallosal region (Fornito et al., 2008).

Taken together, ROI studies on insula along with the numerous ROI studies reporting reductions in ACC volume, suggest a significant structural deficit across the SN in schizophrenia. The origins of structural deficits in grey matter are likely to be manifold. Measurement of GM volume using an ROI or VBM approach, though helpful to localise and quantify these deficits, does not indicate the underlying pathophysiology that resulted in the deficits. Volume of grey matter tissue at a locus depends on various properties such as the surface area of the brain region, degree of cortical complexity (folding or gyrification) and cortical thickness (Winkler et al., 2010). Increasingly, it is recognised that these properties have distinct developmental trajectories and genetic determinants (Eyler et al., 2011; Kochunov et al., 2010; Panizzon et al., 2009). Thus, distinguishing the contribution of thickness, surface area and gyrification changes to the GM deficits in the SN in schizophrenia is likely to provide useful leads as to the mechanism behind the deviations in the neuroanatomy observed in this illness. Though presently unknown, it is likely that these properties have distinct neuropathological correlates. An association between cortical thinning in the MRI and a reduction in the pyramidal layer thickness has been shown in schizophrenia in the frontal lobe (Williams et al., 2012). Theories of neuronal migration and cortical development suggest that a reduction in surface area could be linked to a loss of minicolumns (Casanova and Tillquist, 2008), considered by many to be the basic organisational units of cortical circuitry (Mountcastle, 1997). Formation of cortical folding, on the other hand, has been linked to the integrity of neural connectivity during early cortical development (White and Hilgetag, 2011). Evidence from studies of human fetal brains suggests that the process of development of cortical folding (gyrification) is first notable at the insular

region and proceeds in an orderly fashion (Afif et al., 2007). The periinsular sulci and the central (insular and cerebral) sulci are the first macroscopic structures visible on the lateral surface of the human fetal cerebral hemisphere as early as the 13th to 17th gestational week. This is a crucial period for neuronal migration that is considered to be important in the aetiology of schizophrenia (Akbarian et al., 1993; Fatemi and Folsom, 2009). An abnormality in cortical development during this period is likely to affect the gyrification and subsequent formation of insula. Some evidence for aberrant development comes from a study of deformation of shape of insula, which demonstrates significant reduction in the rostral end of the inferior limit of limen insulae (corresponding to antero-inferior limit of insula) in schizophrenia (Jang et al., 2006). There is also some evidence to suggest that the developmental trajectories of insula and anterior cingulate cortical thickness may be similar (Shaw et al., 2008).

Some attempts to delineate the surface based morphometric properties of thickness and surface area in the SN have been previously reported. Crespo-Facorro et al. (2000) showed significant reductions in both the volume and surface area of insular grey matter in patients with first episode of psychosis. In a larger sample of patients, these findings were not replicated (Crespo-Facorro et al., 2010) though the examination of insular thickness in an extended sample revealed significant cortical thinning (Roiz-Santiáñez et al., 2010). Similarly, Fornito et al (2008) demonstrated bilateral thinning of the ACC with an increase in surface area in patients with first episode schizophrenia. But contrary to the bulk of the evidence, there were no accompanying changes in the ACC volume in this study. In summary, it is

unclear whether the changes in SN are due to a reduction in the surface area, gyrification or cortical thickness.

Question 1: Does the VBM based GM deficits in the SN relate to the changes in the surface anatomy in schizophrenia? Which of the various determinants of GM volume (i.e. area, gyrification and thickness) is abnormal in schizophrenia, resulting in the structural deficits seen in VBM studies of the SN?

2.2 Time course of structural changes in the SN

Despite accumulating evidence regarding widespread cortical grey matter deficits in schizophrenia, the exact time course of the onset and progress of these deficits are still open to speculation. No systematic study has been carried out to date to estimate the onset of insular volume reduction in individuals with psychosis. Various cross sectional comparisons add strength to the assumption that both insular and ACC deficits predate the onset of first episode of psychosis (Chan et al., 2009; Fornito et al., 2008; Fusar-Poli et al., 2011b). Chan et al. (2009) reviewed the VBM studies in high-risk groups in addition to first episode and chronic schizophrenia. High-risk individuals showed bilateral anterior cingulate and right insular deficits. Borgwardt et al. (2007) showed that the significant deficit in the insular volume in the high-risk group (At-Risk Mental State; ARMS) may be indicative of those who developed psychosis 2 years later. A meta-analysis that predominantly included structural MRI studies investigating ARMS showed small to medium effect sizes of decreased cingulate and insular grey matter volume (in addition to prefrontal and cerebellar regions) at baseline in high-risk subjects who

show a transition to psychosis compared to high-risk subjects without transition (Smieskova et al., 2010).

Takahashi et al. (2009c) also showed that in high-risk individuals who show transition to psychosis, significant bilateral insular volume reduction is observable at baseline. Using a longitudinal design they showed that the baseline insular deficits seen in those who develop psychosis, continue to progress at a significantly higher rate ($-5.0\%/year$) when compared to the progressive reduction seen in controls ($-0.4\%/year$) or high-risk subjects without transition in 4 years ($-0.6\%/year$). Other studies that follow-up Ultra High Risk (UHR) groups demonstrate that both progressive ACC (Pantelis et al., 2003) and insular (Borgwardt et al., 2007) grey matter reduction predicts transition to psychosis. In addition to the progressive reduction during the high-risk state, there is some evidence that insular grey matter further reduces following the first episode. In a sample different from the one reported above, Takahashi et al. (2009a) compared 23 first episode patients followed up after 2 years with 26 controls and 11 chronic schizophrenia patients followed up after 2 years of initial scan. The first episode group showed the most severe loss of total insular volume ($>4\%$ in 2 years), followed by chronic schizophrenia ($>1.5\%$ in 2 years) and controls (around 0.3% in 2 years).

In summary, these studies indicate that the GM reduction in the SN is observable in high-risk individuals, predict later development of psychosis and at least in the insula, continue to progress after the first episode of illness. These studies do not indicate the time point at which the observed GM deficits make their appearance in the high-risk individuals. Most of the studies reviewed above have been carried out on clinically defined high-risk

individuals who already exhibit prodromal psychotic features. If these deficits were present even before the onset of the prodrome, this may indicate an association with the tendency to develop psychosis rather than being mere indicators of the clinical expression of a psychotic state. One way of addressing this question is investigating individuals who are at high risk due to genetic reasons rather than due to prodromal mental state.

Question 2: It is unclear as to the onset of structural deficits in the SN in the pathogenesis of schizophrenia. Are SN deficits present even before the onset of a prodrome and thus associated with a diathesis to develop psychosis?

2.3 Effect of antipsychotics on the structure of the SN

An important issue when evaluating structural deficits in schizophrenia is teasing out the confounding effect of medications. The bulk of available evidence suggests that antipsychotics have regionally specific effects on brain structure, with basal ganglia being the most susceptible to their effects (Moncrieff and Leo, 2010; Navari and Dazzan, 2009). A more recently published landmark study unfortunately did not focus on the insula or the ACC region, but revealed an association between frontal, parietal and temporal GM reduction and higher antipsychotic exposure over the course of an average of 7.2 years (Ho et al., 2011). Conflicting evidence has been presented with respect to insula in this regard. Several authors report a lack of correlation between prescribed antipsychotic dose and insular volume (Saxe et al., 2007; Takahashi et al., 2009a, 2005, 2004). Pressler et al. (2005) failed to replicate the finding of reduced insular volume in a sample of 30 chronic schizophrenia

patients, but showed that with increasing typical neuroleptic exposure the insular volume increased in their sample. In contrast, using a cross sectional VBM of a sample exposed to short-term antipsychotics, Dazzan et al. (2005) suggested that typical antipsychotics may be associated reduced insular grey matter when compared to drug free patients. However it is possible that this association is confounded by symptom burden, as there was a trend for higher positive symptom score in the treated group (Cohen's $d = 0.43$; 5.1 points difference in positive symptom score). Using a meta-regression approach when undertaking a meta-analysis of ROI studies of the insula in schizophrenia, Shepherd et al. (2012) observed no relationship between antipsychotic medication dose and insular volume differences. This finding contradicts the earlier observation reported by Leung et al (2009) who reviewed VBM studies on neuroleptic-naïve first episode patients, and compared pooled estimates from these with the pooled estimates of studies on neuroleptic treated first episode patients. In both groups, bilateral insular and ACC deficits were prominent. While caudate and temporal deficits were less extensive in the antipsychotic treated samples, insular deficits (along with parahippocampal and frontal deficits) were more pronounced in the treated samples, but this observation was not controlled for illness duration or severity. A similar pronounced defect in the treated samples was not seen for the ACC. Intriguingly, magnetic resonance spectroscopic studies suggest a long-term treatment with atypical antipsychotics may have a favorable effect on neuronal viability in the ACC (Braus et al., 2002, 2001). In line with these findings, Tomelleri et al. (Tomelleri et al., 2009) found a positive correlation between cumulative typical antipsychotic exposure and left anterior cingulate volume using VBM.

In summary, evidence indicates an uncertain association between antipsychotic exposure and reduced insula volume whereas there is some evidence that treatment protects the ACC. However the evidence that the volume deficits in both insula and ACC precede treatment in antipsychotic naïve first episode patients, and in untreated high-risk populations, suggest that the illness process itself contributes to the structural deficits in the SN.

2.4 Functional attributes of the SN: the proximal salience

Anatomical Likelihood estimation (ALE) meta-analysis of fMRI studies with insula activation (Kurth et al., 2010) in healthy individuals suggests that anterior insula is concerned with higher-level integrative process. This integration of different qualities of our coherent experience of the world sets the context for thoughts and actions. Craig (2009) assembles a large body of evidence from functional imaging studies demonstrating that the insula is active during the processing of many internal bodily stimuli (e.g. thirst, sexual arousal, heartbeat, visceral distension etc.) and external stimuli (e.g. temperature, taste, pain etc.). Similarly Augustine (1996) has concluded from a review of structural connections in primates and humans that the insula is a site of multisensory integration. Furthermore, Augustine (1996) reports that the anterior insula has a strong reciprocal connectivity with prefrontal regions. As prefrontal cortex contains representations of social and event models (Koechlin et al., 1999), this reciprocal connectivity suggests that the insula has an access to goal and plan representations. In addition, imaging studies of Stimulus Independent Thoughts reveal engagement of core midline structures of the default mode network (DMN) together with anterior insula and ACC (Christoff et al., 2009; Mason et al., 2007). Thus the SN receives information

about internal and external sensations; representations of goals and plans; and also stimulus independent thoughts.

A significant body of evidence demonstrates insular activation during a wide range of tasks that involve evaluating probability, uncertainty of an outcome (Bossaerts, 2010; Singer et al., 2009), reward and risk prediction (see Bossaerts et al. (2010) for a review). In particular, insular activity is often seen with prediction error coding. Prediction error refers to a discrepancy between an expectation and the occurrence. This discrepancy can lead to the updating of expectations about the external and internal milieu, and if necessary initiates or modifies action. Murray et al. (2008) showed that reward prediction error in healthy subjects was associated with activation of the ventral striatum along with insula and cingulate cortex, all of which were not seen in patients with psychosis. In a different fMRI study of prediction errors, the strongest correlation between risk prediction error and BOLD response was found in the insula and inferior frontal gyrus (D'Acromont et al., 2009).

Several studies suggest that the specific role of insula in prediction error paradigms is likely to be one of updating the previously existing prediction framework (Preuschoff et al., 2008; Sanfey et al., 2003; Xue et al., 2010). Activation of insula during risk evaluation predicted subsequent decision-making, indicating that insula plays a role in not only evaluating but also updating the probabilities of an outcome (Preuschoff et al., 2008; Sanfey et al., 2003; Xue et al., 2010). Insular activity during anticipated loss predicted the loss avoidance learning several months later (Samanez-Larkin et al., 2008). ACC also plays a critical role in updating the prediction models and has been shown to be involved in both social and reward related associative learning

(Kennerley et al., 2006), though it is unlikely to be the sole region for cognitive control (Baird et al., 2006; Fellows and Farah, 2005). Notably, individuals who have lesions of insula show a failure to update their prediction framework, despite having preserved ability to judge probability of events (Clark et al., 2008).

In addition to the properties of the stimulus, execution of a response also depends on the context provided by the current homeostatic state of the subject. Craig's model of 'sentient self' places insula at a central role for evaluating ongoing feeling states (Craig, 2009; Critchley et al., 2004). Craig (2009) proposes awareness of any object requires, first, a mental representation of oneself as a feeling (sentient) entity; second, a mental representation of that object; and third, a mental representation of the salient interrelationship between oneself and that object in the immediate moment ('now'): These three aspects are integrated in the anterior insula creating a state of interoceptive awareness. This is consistent with evidence that the anterior insula plays a crucial role in appraisal of self and attributing personal relevance (Enzi et al., 2009; Modinos et al., 2009a).

These observations suggest that primary role of the salience network is the integration of sensations, internally generated thoughts, and information about goals and plans, so as to update expectations about the internal and external milieu and if necessary initiate or modify action. To facilitate the description of the function of the salience network we will introduce the concept of proximal salience. An event such as an externally generated sensation, a bodily sensation or a stimulus independent thought, attains proximal salience when it generates a momentary state of neural activity

within the salience network that results in updating of expectations and if warranted by the context, initiates or modifies action.

Proximal Salience prepares one for appropriate behavioural response. To be behaviourally effective, the brain region that generates proximal salience must be tightly coupled to task related brain regions. Indeed this was clearly demonstrated by Sridharan et al (Sridharan et al., 2008), who showed that anterior insula activation precedes activation of task related brain networks. Using Granger causality analysis they proposed a role for anterior insula and anterior cingulate in switching brain states from default mode to task related activity mode, although the application of Granger Causality to fMRI data must be interpreted cautiously.

Several studies have shown that learning by means of developing new models of prediction involves changes in the resting state connectivity in both default mode and task related networks (Albert et al., 2009; Hasson et al., 2009; Lewis et al., 2009; Stevens et al., 2010) With its unique role as a switch between the DMN and task-positive networks, the SN is crucially positioned to not only enable the behavioural response but also to consolidate or update prediction models subsequent to stimulus evaluation. In complex social situations, an update of prediction models could involve attitudinal changes. Van Veen et al. (2009) observed that the insular activation during cognitive dissonance is inversely correlated with the degree of attitude change (rationalization) that follows, indicating that an optimal amount of insula activation is required for acquisition and/or alteration of beliefs.

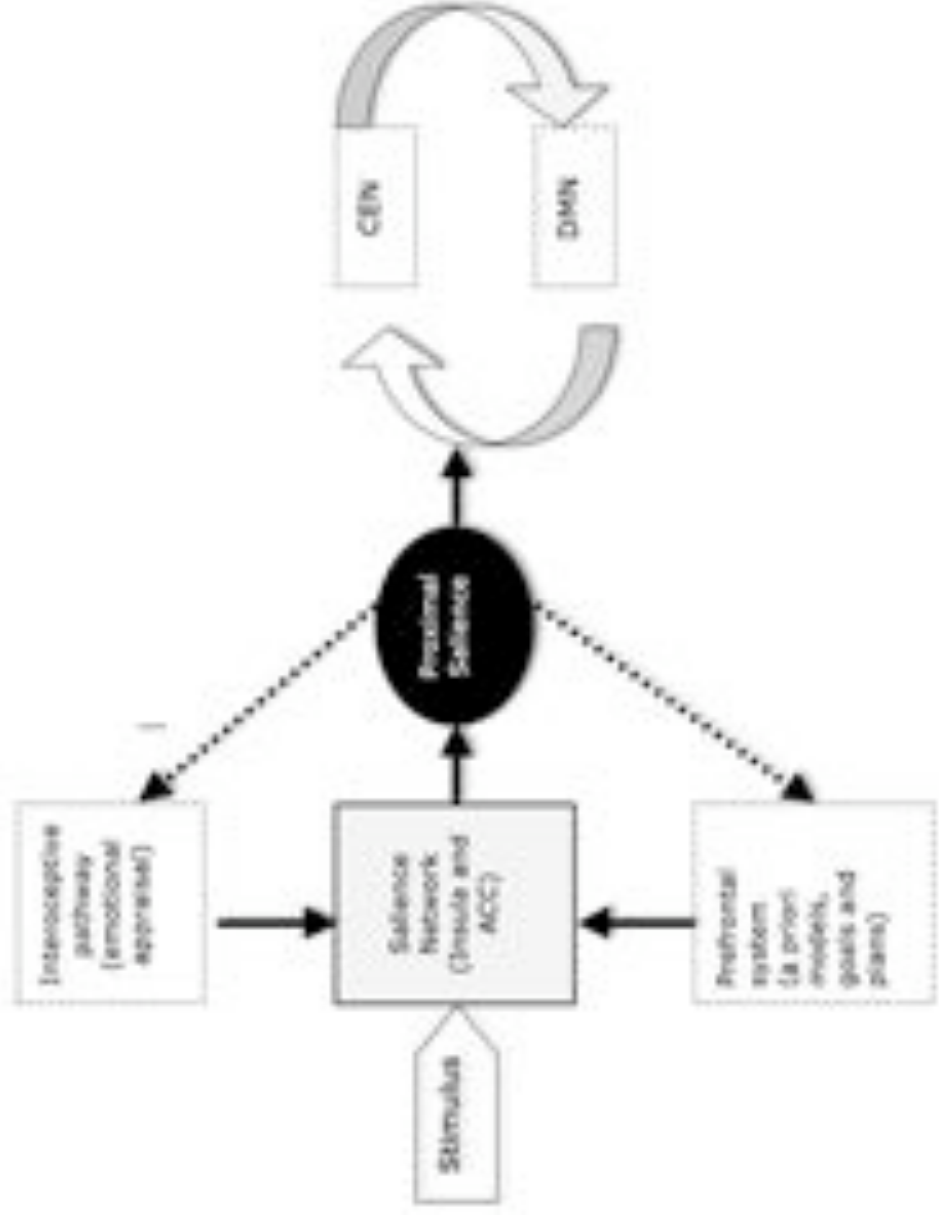


Figure 2.1: Proximal salience refers to a momentary state of neural activity within the Salience Network (SN) generated by the evaluation of external or internal stimuli. SN interacts with interoceptive pathway and prefrontal system to generate the Proximal Salience that enables a switching between resting mode to task-processing (executive) mode or vice versa.

2.5 fMRI studies of the SN in schizophrenia

Abnormalities in the functional activation of insula and ACC have been reported in schizophrenia across a variety of tasks ranging from working memory paradigms to complex social processing (Minzenberg et al., 2009; Wilmsmeier et al., 2010; Wylie and Tregellas, 2010). Studies investigating functional integration (during resting or task-related states) across multiple brain regions report a prominent reduction in connectivity involving both insula (Liang et al., 2006; Zhou et al., 2007) and ACC (Boksman et al., 2005; Honey et al., 2005) with other brain regions. Attenuated co-activation of the regions constituting the SN is noted in schizophrenia when compared to healthy controls during task execution (Henseler et al., 2009) and error processing (Polli et al., 2008). Such an effect has also been observed in patients when attending to somato-sensory stimuli (White et al., 2010b). In that study (White et al., 2010b), the reduced engagement of the SN when attending to the external stimuli was also associated with poor deactivation of the brain regions related to the default-mode (DMN). More direct evidence for an impaired interaction between the Salience Network and the DMN comes from a functional connectivity analysis of independent components in the same sample (White et al., 2010a). Notably, failure to deactivate the DMN has been shown previously in various resting state studies of schizophrenia patients and their relatives (Garrity et al., 2007; Skudlarski et al., 2010; Whitfield-Gabrieli et al., 2009). Investigating the resting state brain networks (DMN, SN, executive network comprising of dorsolateral prefrontal and inferior parietal cortex (CEN) and dorsal attention network (DAN) comprising of superior

parietal lobule, frontal eye fields and intra parietal sulcus) in schizophrenia, Woodward et al. (2011) reported a prominent disturbance in the functional connectivity measured using pairwise correlations of the DMN, CEN and DAN, but not the SN.

In summary, disrupted functional connectivity is noted across insula and the ACC in schizophrenia. There is some suggestion for an abnormal interaction between the SN and the DMN which may only be evident during task-processing. At present, it is not clear whether this abnormal interaction is related to the failure of DMN deactivation reported in schizophrenia.

Question 3: What are the functional consequences of the GM reduction in the insula? In other words, does the insular GM reduction seen in schizophrenia relate to abnormal functional connectivity during task processing?

2.6 Correlation of insular deficits with clinical symptoms

A meta-analysis of fMRI studies of active auditory hallucinations reveals prominent involvement of the insula along with bilateral Broca's area and auditory cortex (Jardri et al., 2011). From the fMRI studies, it is impossible to conclude whether the insular involvement has a causal role in the generation of hallucinations or if it is an epiphenomenon of the experience of voice-hearing. Investigating the relationship between GM deficits and hallucinations can help clarify this issue to some extent. The presence of concurrent structural and functional deficits could imply an essential role for insula in producing hallucinations.

Passivity symptoms are also shown to be related to insular dysfunction. When undertaking theory of mind tasks, patients with schizophrenia and passivity symptoms show reduced activation of right insula and anterior cingulate (Brüne et al., 2008). PET and fMRI studies have also found abnormalities in the activation of insula in addition to brain regions involved in action monitoring in patients with passivity symptoms (Schnell et al., 2008; Spence et al., 1997). Crespo-Facorro et al. (2000) has shown a significant correlation between the insular volume and severity of delusions and hallucinations though a number of other studies did not find this association (Crespo-Facorro et al., 2010; Kim et al., 2003; Saze et al., 2007).

Insular volume is related to other aspects of psychopathology as well (Takahashi et al., 2009a). A ROI study by Makris et al (2006) showed that left anterior insular volume was correlated to bizarre behaviour in schizophrenia. But some studies that do not distinguish subregions fail to find correlations with symptoms scores (Kim et al., 2003). Early PET studies suggested that reduced insular blood flow is associated with both disorganisation syndrome and reality distortion seen in schizophrenia (Liddle et al., 1992). Using arterial spin labelling, Horn et al (2009) demonstrated that along with language areas, anterior insula showed significant positive correlation of resting cerebral blood flow (rCBF) and degree of formal thought disorder. Using two independent cohorts of drug free patients, Lahti et al (Lahti et al., 2006) showed that rCBF of Broca's area along with anterior insula and anterior cingulate cortex correlated positively with disorganisation scores.

A recent VBM study of the three major psychopathological dimensions of schizophrenia has shown that insula as the most prominent brain region to

show deficits across the three clusters of positive symptoms, disorganisation and negative symptoms (Koutsouleris et al., 2008) It is worth noting that most of the studies reporting clinical correlation of insular deficits included patients taking antipsychotic medications. Antipsychotics not only reduce the severity of psychotic symptoms (especially reality distortion and disorganization) but also affect the brain structure as discussed previously. This can introduce a variability leading to inconsistencies in the relationship between clinical symptoms and brain structure.

Taken together, somewhat coherent pattern of relationship between insular deficits and symptoms of schizophrenia is noted. The clinical association with reality distortion is the most frequently investigated phenomenon, with somewhat equivocal results. Given the role of insula in proximal salience, the relationship between insular dysfunction in schizophrenia and hallucinations/delusions requires further investigations. In addition there is also some evidence for an association with disorganisation and negative symptoms.

Question 4: Is there a definite relationship between reality distortion and the GM deficit in the SN?

2.7 Insular dysfunction model of psychosis

Several investigations suggest that hallucinations are related to self-generated inner speech and passivity phenomena are related to self-generated actions (Blakemore et al., 2000; McGuire et al., 1995). Normally, these self-generated internal processes may not generate proximal salience.

However, insular activation during hallucinations suggests that the SN is generating an inappropriate proximal salience during an otherwise normal activity (Jardri et al., 2011). In particular, such an aberrant activation of insula is noted alongside a prominent absence of cingulate activation, suggesting disruption in normal SN activity (Sommer et al., 2008), and perhaps disruption to error-monitoring circuitry. The allocation of proximal salience to an event might lead to recruitment of the attentional networks required for processing the stimulus (as suggested by Seeley et al (2007)). The faulty allocation of proximal salience to an internally generated mental event would be expected to promote recruitment of the DMN and impede the normal suppression of DMN activity during tasks requiring attention to the external world. Various groups have reported the attenuation of DMN suppression during task performance (Garrity et al., 2007; Skudlarski et al., 2010; Whitfield-Gabrieli et al., 2009). Thus the internally generated mental activity might be further enhanced creating a vicious cycle of inappropriate proximal salience. In a similar vein, and consistent with a recently proposed Bayesian model of positive symptoms (Fletcher and Frith, 2009), the inappropriate allocation of proximal salience to internally generated actions could explain the passivity symptoms.

Delusions are classified as primary or secondary. Primary delusions arise when significance is attached to an incidental perception without logical justification, while secondary delusions are secondary to other abnormal mental states such as hallucinations or mood disturbances. A subjective state of uncertainty (delusional mood) or anxiety has been reported to precede the formation of primary delusions (Yung and McGorry, 1996). Conrad described

this state as a phase of apophenia that precedes full-blown delusions (Mishara, 2010). It is plausible that the insular abnormality seen in susceptible individuals during prodromal states (Borgwardt et al., 2007; Takahashi et al., 2009c; Venkatasubramanian et al., 2010) plays a role in this state of uncertainty. Insofar as the SN plays a key role in the engagement of relevant distributed circuits required for processing information (and switching-off of less relevant circuits) SN dysfunction and the associated failure of generation and response to proximal salience, would be expected to enhance the state of uncertainty.

In the context of heightened uncertainty regarding the predicted outcome of events, seemingly irrelevant incidental stimuli (both external and internal) might be allocated inappropriate proximal salience. Models of learning, such as the Rescorla-Wagner model (Rescorla and Wagner, 1972) originally developed to account for reinforcement learning, but also employed to account for incidental associative learning that is not directly related to task-performance or reward (Den Ouden et al., 2009), invoke the generation of a “teaching signal” when there is a discrepancy between the predicted outcome and the actual outcome of an event, that results in the learning of a new association between the predictor and the outcome. In a similar manner, inappropriate proximal salience might lead to the incidental stimulus acquiring unwarranted causal significance resulting in the formation of a primary delusion. Continuing deficits in the recruitment of appropriate attentional networks hamper the correct evaluation of the formed belief (updated model) while the associated reduction in uncertainty might serve to maintain the newly formed belief. Once an inappropriate model is formed, the process of

further consolidation of this model contributes to secondary delusional elaborations as suggested by Corlett et al. (2010).

Impaired regulation of switching between default mode and attention to task-relevant stimuli that is hypothesized to arise from insular dysfunction (Menon and Uddin, 2010) is likely to be related to attentional impairment and distractibility. Disturbances of attention including distractibility are features of the disorganisation syndrome in schizophrenia (Cameron et al., 2002; Liddle and Morris, 1991; Liddle, 1987; Liddle et al., 2002). Liddle et al. (1992) reported that in patients with persistent symptoms, disorganization was associated with aberrant activity of insula, anterior cingulate and adjacent medial prefrontal cortex.

It is plausible that a defect in integration of goals and plans into the state of 'interoceptive awareness' described by Craig (2009), might result in the diminution of initiation of activity characteristic of the psychomotor poverty syndrome. This might arise due to a fault within the SN itself though the possibility that a more diffuse impairment of frontal lobe function might contribute to the impairment integration of goals and plans into the state of interoceptive awareness cannot be ruled out (Sigmundsson et al., 2001). Thus, a dysfunctional SN, and associated disruption of Proximal Salience might account for many of the clinical features seen in psychosis.

It should be noted that while Menon and Uddin (2010) propose that the SN is engaged in mediating interactions between brain networks involved in externally oriented attention and internally oriented or self-related cognition, we propose that the network has a more general switching role. We propose

that the primary role of the SN is initiating the recruitment of brain regions relevant for processing currently salient stimuli while decreasing activity in networks engaged in processing previously salient stimuli. This concept does not exclude the possibility that there are brain regions that can be engaged in attending to both internal and external stimuli. Indeed under at least some circumstances, such as during tasks that require integrating information from the external world with information held in memory, we would anticipate simultaneous activity in nodes of the DMN and in other networks such as those involved in perceptual or executive processing. We consider that the terms default mode processing and task-positive processing can be misleading insofar as the DMN can be actively engaged during task performance, while networks other than the DMN are active during rest (Sridharan et al., 2008).

Question 5: The influence of insula on other brain systems, especially the executive frontal system, appears crucial for the normal physiological brain function. Is there a failure in the function of the salience-execution loop in schizophrenia?

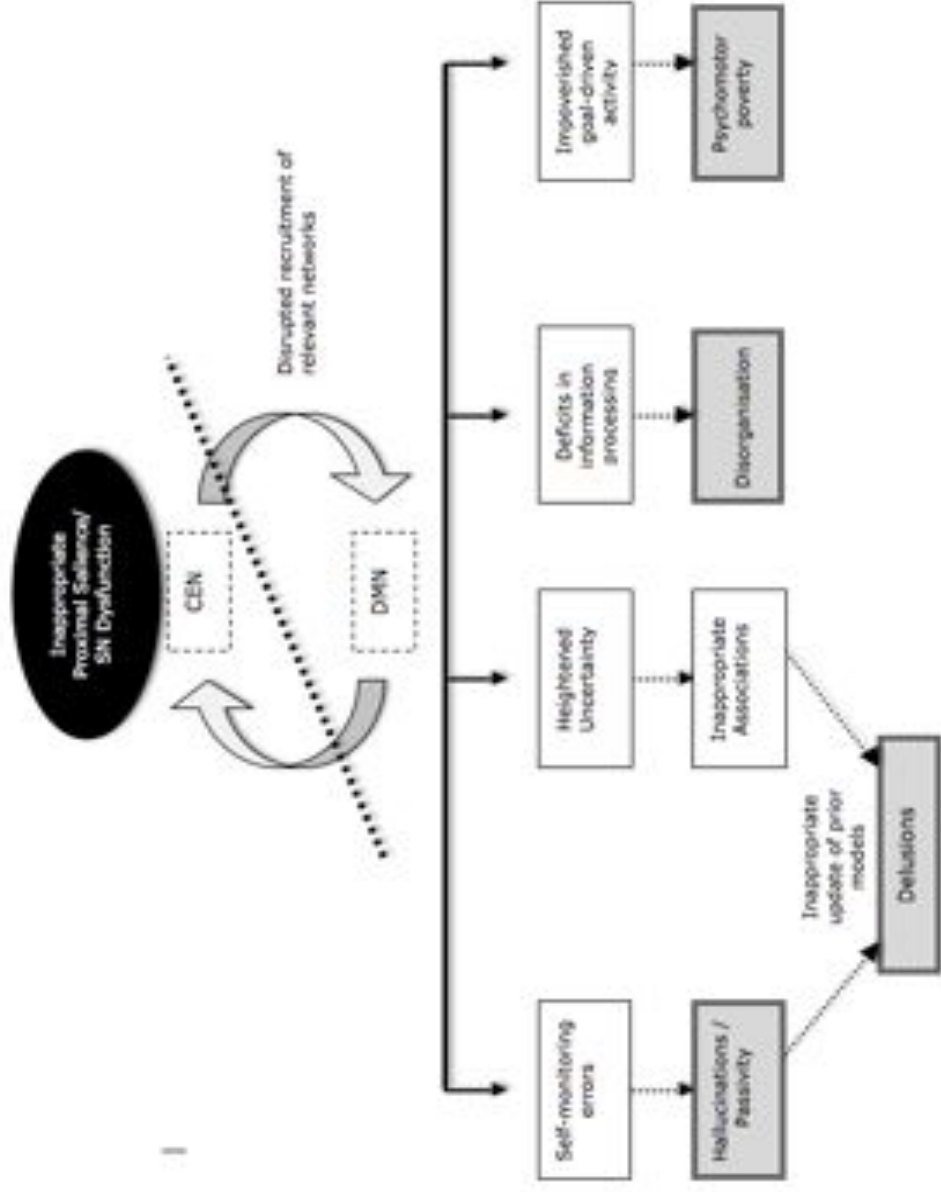


Figure 2.2: Insular Dysfunction Model of Psychosis: A dysfunction of Salience Network can lead to a cascade of events that result in clinical symptoms of psychosis. Inappropriate Proximal Salience during self generated actions result in hallucinations and passivity experiences. Proximal Salience inappropriately attached to external stimulus in the context of heightened uncertainty in unusual beliefs and delusions. A failure to engage the task-relevant network when required is associated with disorganisation. Failure to generate goal-driven activity is related to psychomotor poverty. SN: Salience Network, CEN: Central Executive Network, DMN: Default Mode Network.

2.8 Dopamine and the Salience Network

Dopamine plays a major role as the neurochemical mediator of prediction error signals (Schultz, 2010). Dopamine dysfunction has been considered to have a central role in the emergence of the state of aberrant motivational salience seen in psychosis (Kapur, 2003). The prediction error model of hallucinations and delusions (Corlett et al., 2010; Fletcher and Frith, 2009) is consistent with the dopamine hypothesis. The relationship between dopaminergic dysfunction and insula has not been systematically studied in schizophrenia so far. Nonetheless, various sources of evidence suggest that a dopaminergic abnormality is likely to be associated with the SN dysfunction in schizophrenia.

Dopamine has emerged as the primary neurochemical mediator in relation to various traits and behaviours mediated by insula (e.g. novelty seeking (Suhara, 2001), craving (Contreras et al., 2007; Naqvi and Bechara, 2010), nociception (Coffeen et al., 2008)). Moreover various studies have demonstrated the importance of dopaminergic modulation on ACC during executive tasks (Ko et al., 2009), suggesting that dopamine plays an important role in the function of the SN. Both insula and ACC are regions with relatively high extrastriatal dopamine transporters (DAT) (Wang et al., 1995; Williams and Goldman-Rakic, 1998). The synaptic availability of dopamine may be directly related to efficient insular function. A polymorphism that is shown to be associated with higher levels of DAT, which mediates dopamine reuptake from the synaptic cleft into the presynaptic terminal, is shown to be

associated with higher activation of insula and caudate along with deactivation of cingulate during verbal fluency task (Prata et al., 2009).

A high correlation between the binding of the D2/D3 ligand, [18F] Fallypride and grey matter density as measured by VBM is observed in anterior cingulate and insula, and also mid-brain regions (Woodward et al., 2009), raising the possibility that reduced grey matter across the Salience Network in schizophrenia may be directly associated with dopaminergic defects. In schizophrenia, abnormal dopaminergic transmission has been observed in the ACC (Suhara et al., 2002; Takahashi et al., 2006a). This defect may be amenable to pharmacological manipulation as shown by Dolan et al.(1995).

In summary, the insular dysfunction model of psychosis based on the SN is consistent with the dopaminergic hypothesis of psychosis. Thus the SN provides a candidate cortical framework that is consistent with and builds on the existing dopaminergic hypothesis of schizophrenia.

Nevertheless, it is important to differentiate the concept of motivational salience traditionally associated with dopaminergic dysfunction (Kapur, 2003) from the concept of proximal salience proposed here. Proximal salience refers to a momentary state generated by evaluation of external or internal stimuli in the context of interoceptive awareness. This state precedes subsequent choice of action and/or optimization of predictive models relevant for the stimuli (learning). Kapur's motivational salience refers to a process that takes place once a stimulus is evaluated: it represents the assignment of a motivational value to the external object or internal representation. In other

words, motivational salience refers to the process of attaching a tag of significance to the stimuli. While motivational salience explains stimulus-reinforcement associations, proximal salience refers to a more fundamental step in information processing: the stimulus-response association. Whereas Kapur's concept of motivational salience places emphasis on the role of the corpus striatum (Jensen et al., 2007), the concept of proximal salience places greater emphasis on the role of the insula and anterior cingulate. Nonetheless, the evidence these brain regions interact in the attribution of salience and the notion of prediction errors and dopaminergic mediation discussed in the previous sections, may serve as a common link between these two concepts.

2.9 Unanswered questions

Despite the consistency of the emerging parsimonious model in which insula dysfunctions might lead to the major symptoms of psychosis, several key questions remain unanswered before further progress in establishing the insular dysfunction in psychosis could be attempted. Several of these issues have been indicated in the previous sections of this chapter and will be investigated in further detail in the remaining chapters (Table 2.1). In addition, there are a number of important questions that emerge when considering the role of insula in the pathophysiology of schizophrenia, many of which are beyond the scope of this doctoral research. For example, with respect to structural deficits in patients, it is unclear whether there is a critical insular grey matter volume below which psychotic symptoms emerge. Furthermore, the role of the insular dysfunction in relapses and remissions that typify psychosis needs investigation. Longitudinal studies to clarify time course of

the structural and functional abnormalities in addition to studies employing novel imaging methods for studying cerebral connectivity might contribute to answering these questions. In addition studies of unmedicated cases and treatment trials are required to elucidate the effect of antipsychotics on the function of the salience network.

The proposal of a specific role for the SN in stimulus evaluation, updating of expectations and preparation for response generation, suggests several specific hypotheses that might be tested using neuroimaging procedures. Advances made through testing and falsifying these postulations could force a modification of our present understanding of the neuroanatomy of schizophrenia. On the other hand, strong inferences in support of the insular dysfunction in psychosis could lead us to the next decision point in exploiting this neurobiological concept to therapeutic advantage.

Table 2.1: Questions addressed in the present work

Research question	Thesis chapter
Are SN structural deficits associated with a genetic diathesis to develop psychosis?	Chapter 3
Is there a relationship between Auditory Hallucinations and structural defects in the SN?	Chapter 4
Does the VBM based GM deficits in the SN relate to the changes in the surface anatomy in schizophrenia?	Chapter 5
Is there a defect in cortical gyrification patterns in the SN?	Chapter 6
Is there any correspondence between structural and functional deficits affecting the insula? Are these deficits specific to schizophrenia or shared with bipolar disorder?	Chapter 7
Is the functional integrity and primacy of the salience processing system altered in schizophrenia?	Chapter 8

Chapter 3

The neuroanatomy of psychotic diathesis

Meta-analytic reviews of morphometric studies have found widespread structural changes affecting the grey matter of both insula and anterior cingulate cortex (ACC) at various stages of schizophrenia (the prodrome, first-episode, and the chronic stage) (Chan et al., 2011). It is unclear if these neuroanatomical changes are associated with a predisposition or vulnerability to develop schizophrenia rather than the appearance of the clinical features of the illness. In this chapter, two meta-analyses aimed at addressing this issue are presented. The neuroanatomical changes associated with the genetic diathesis to develop schizophrenia appear to be different from those that contribute to the clinical expression of the illness. Grey matter reduction in bilateral insula, inferior frontal gyrus, superior temporal gyrus and the anterior cingulate was seen in association with the disease expression.

3.1 Genetic Diathesis and Clinical Expression

The investigation of the pathophysiology of schizophrenia has taken a rich variety of directions in the last four decades. Despite numerous false starts, some consistencies have emerged with the aid of advanced neuroscientific methods and systematic data collection (Kane et al., 2011). Two of the most captivating of these findings support some of the earliest notions regarding the disease process proposed by Kraepelin. Kraepelin (1919) believed that there is an 'injury to the germ' in dementia praecox and discussed the role of

heredity. He was also inspired by the study of neuroanatomical aspects and considered the 'distribution of morbid changes across the surface of the cortex' to be significant in understanding the clinical presentation of the disease (Kraepelin, 1919). At present, familial risk of schizophrenia is one of the well-documented features of the illness, along with the presence of structural brain abnormalities in patients (Tandon et al., 2008).

As reviewed in the previous chapter (chapter 2), several meta-analyses have documented widespread grey matter (GM) changes in the brain in patients with schizophrenia, implicating key brain regions such as the insula, anterior cingulate cortex, medial temporal structures such as the amygdala and parahippocampal gyrus, thalamus, superior temporal and inferior frontal gyri (Chan et al., 2011; Glahn et al., 2008; Honea et al., 2005). The majority of morphometric studies have compared a group of patients with a clinical diagnosis of schizophrenia and healthy controls with no personal or family history of psychosis to identify brain regions with significant structural changes. Any significant defect observed in such a cross-sectional comparison could be attributed to several factors such as the presence and severity of schizophrenia (the expression of the illness), the effect of medications, or a tendency to develop schizophrenia (the diathesis).

The issue of whether anatomical changes are related to the expression of the illness can be addressed in part by comparing the brain structure between patients with schizophrenia and individuals with prodromal symptoms (Clinical High Risk) or with their unaffected relatives (High Risk Relatives: HRR) with whom a significant degree of genetic diathesis of the illness is likely to be shared. Fusar-Poli et al. (2011a, 2011b) previously reported two meta-

analyses employing two different methods of coordinates based likelihood estimation. One of these compared the grey matter changes in clinically high risk subjects with established psychosis (Fusar-Poli et al., 2011b) and reported GM reductions in right superior temporal, right anterior cingulate, left insula and left cerebellum in the patient group. The other meta-analysis contrasted the combined groups of clinical high risk and genetic high-risk individuals against those with established psychosis (Fusar-Poli et al., 2011a) and reported GM reductions in bilateral amygdala, left prefrontal and middle temporal gyrus and right precuneus in the patient group. The non-overlapping nature of the results of these two comparisons could be attributed to the differences in the methodology or clinical differences between the samples (e.g. duration of illness and antipsychotic medications). A crucial difference is that between the HRR group and the clinically defined Ultra-High-Risk group (Yung and McGorry, 2007). Unlike the clinically defined at-risk group, the HRR subjects do not show substantial prodromal symptoms of psychosis. Therefore the underlying structural abnormalities in this group are likely to be related to the diathesis rather than the expression of clinical symptoms.

Similarly, the anatomical changes related to the genetic diathesis can be studied by comparing healthy, asymptomatic relatives of patients with schizophrenia and healthy controls who do not have a family member with schizophrenia. Several studies have been conducted to address these questions (Boos et al., 2012; Cannon et al., 1998) but only a few have employed data-driven unbiased methods such as Voxel Based Morphometry (VBM) that allow examination of entire cortical grey matter without the need for preselecting regions of interest. In a recent meta-analytic study, Fusar-Poli

et al. (2012) contrasted genetic high-risk subjects with controls to map the neuroanatomical correlates of genetic liability. In this study they derived a contrast between HRR and controls separately, and compared this with the contrast between antipsychotic naïve first episode patients and controls; as a result the HRR group was genetically *unrelated* to the patient group. The coordinates derived from this comparison are likely to reflect both the clinical expression of the illness and the genetic liability in the HRR group that is not shared by the genetically unrelated patient group. To date, the neuroanatomical markers specifically related to the clinical expression of schizophrenia are elusive.

The focus of the present chapter is on locating and synthesizing the data from the VBM analyses that undertook direct comparisons between (a) patients with schizophrenia and their relatives (genetic high-risk group) and (b) the genetic high risk group and healthy unrelated controls, in order to identify the brain regions associated with the genetic diathesis of schizophrenia and the clinical expression of schizophrenia. To this end, Signed Differential Mapping (SDM), a meta-analytic technique that employs a probabilistic approach of locating the regions with most consistent grey matter changes from VBM studies was used. SDM takes into consideration the effect-sizes and within and between studies heterogeneity of the individual VBM studies (Radua et al., 2011).

3.2 Literature search

Medline and Scopus databases were systematically for studies using VBM published between 1995 (the year of first publication of a VBM study in

schizophrenia) to December 2011. The keywords 'schizophrenia', 'relatives', 'MRI', 'morphometry', 'voxel-based', 'family' and 'neuroimaging' were used in various combinations. The reference lists of published meta-analyses of VBM studies in schizophrenia were checked to identify studies that included relatives of schizophrenia patients. The initial hits were screened to identify only those structural MRI studies that included relatives of patients with schizophrenia (genetic high risk). Following this, Google Scholar was used to search for studies that cite the short-listed papers. Further searches were undertaken from the references listed in each of the short-listed papers. The sample characteristics and methods employed in the identified studies were scrutinized in detail by two research psychiatrists (Palaniyappan and Balain) to generate the final list of studies that satisfied the following criteria 1: Studies investigating either grey matter density or volume. 2. Spatial coordinates (MNI or Talairach space) of the significant loci must be reported 3. Whole brain voxelwise analysis (observations based on a-priori selection or small-volume correction to be excluded). We included all studies that estimated grey matter density or volume using VBM whole brain analysis and excluded those that used a Region of Interest approach to estimate the magnitude of the grey matter changes in preselected brain regions. This approach ensured that the studies that were pooled were comparable in their objective of localising grey matter deficits across the entire cortex. We then contacted the corresponding authors if any detail required for the primary meta-analysis was missing. The meta-analytic method followed the guidelines expounded by Stroup et al. (2000) (MOOSE: Meta-analysis Of Observational Studies in Epidemiology).

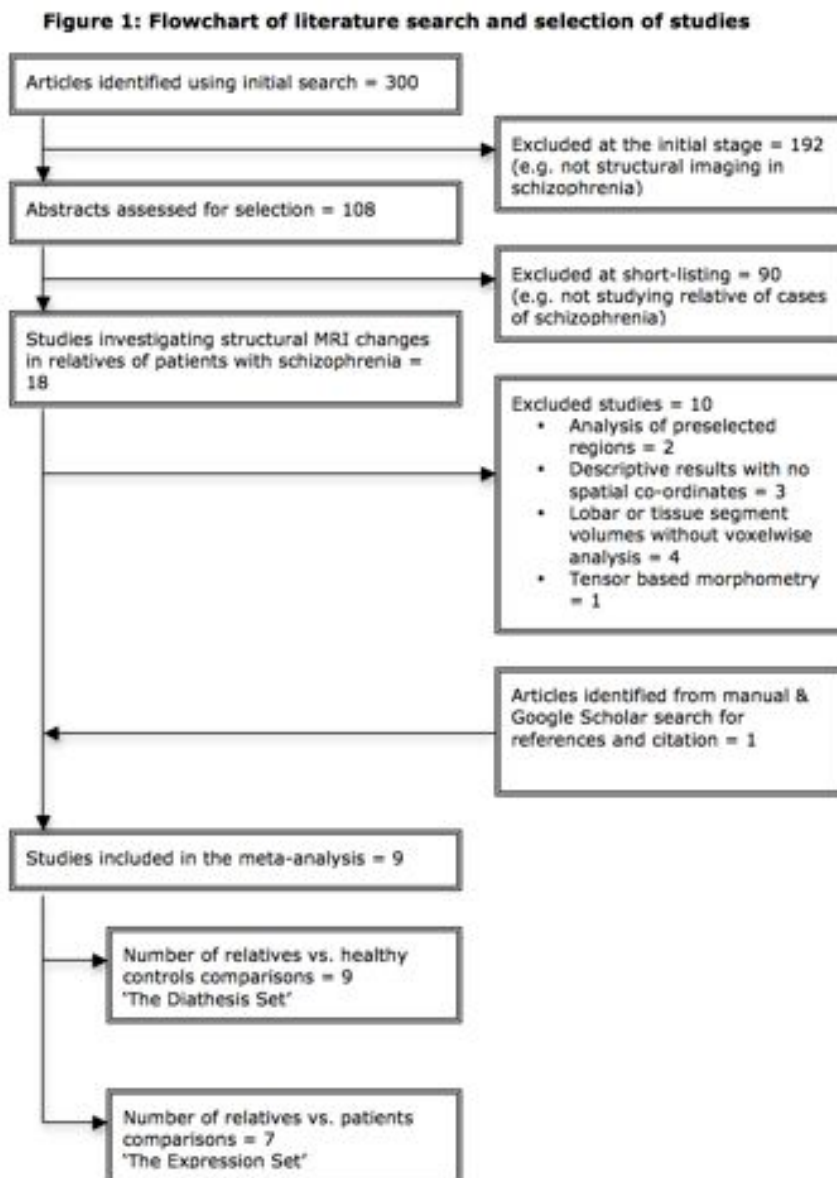
3.3 Signed Differential Mapping

The VBM comparisons between relatives of schizophrenia patients and a healthy control group (the Diathesis Set) were distinguished from the comparisons between relatives of schizophrenia patients and the patient group (the Expression Set). Two separate meta-analyses were conducted on these datasets. For each individual VBM comparison, a Gaussian kernel of 20mm half-width was employed to recreate a whole brain 'activation' map in Talairach space using the reported coordinates and the effect-size of the group differences. Thus, the voxels closer to a reported peak were estimated to have a higher effect-size, with a positive sign denoting grey matter excess (patients > relatives in the Expression Set and relatives > healthy controls in the Diathesis Set), and negative sign denoting a grey matter reduction (patients < relatives in the Expression Set and relatives < healthy controls in the Diathesis Set). In the next step, a pooled map was derived from the voxelwise mean of the individual study maps, weighted by the inverse of the variance of each study plus the between-study heterogeneity. This ensured that the studies reporting more precise results were proportionately more valued than those with less precise results. With this random-effects model, SDM also ensures that the larger studies (which are likely to have more precise effects) have proportionally more influence on the final results, and that findings are not biased towards those brain regions with more between-study heterogeneity. A permutation test (n=5000) was used for deriving the statistical significance. Standard thresholds for effect-size SDM ($p < 0.005$, cluster extent 10 voxels) (Radua et al., 2011) were used with a peak height threshold corresponding to $z=1.96$ (corresponding to 2 standard normal deviations). To ascertain if significant findings are replicable in various (n-1)

combinations of the included studies, a leave-one-out jackknife analysis was also conducted.

3.4 Search Outcome

The outcome of the search is shown in Figure 3.1.



Of the 300 initial hits identified from the search of databases, 192 studies that did not use structural MRI to investigate the grey matter morphology were excluded in the first instance. Abstracts of 108 articles were retrieved from which 18 studies investigating structural MRI changes in relatives of patients with schizophrenia were short-listed. Of these, 10 did not satisfy the predefined inclusion criteria for this meta-analysis. The remaining 8 studies, along with a single study identified from searching the citation data on Google Scholar, gave a final list of 9 studies to be included (Boos et al., 2012; Borgwardt et al., 2010; Honea et al., 2008; Hulshoff Pol et al., 2006; Job et al., 2003; Lui et al., 2009; Marcelis et al., 2003; McIntosh et al., 2004; Tian et al., 2011). These 9 studies reported data for a total of 16 VBM comparisons and included a sample of 563 healthy controls, 474 patients with schizophrenia and 733 subjects in the HRR group. 9 of these comparisons formed the Diathesis Set, while 7 formed the Expression Set that entered the SDM analysis (See Tables 1 and 2 for the details). All studies except Hulshoff Pol et al. (2006), Lui et al. (2009) and Tian et al. (2011) reported VBM results contributing to both Diathesis and Expression sets. Hulshoff Pol et al. (2006) did not compare the HRR group with controls. Lui et al. (2009) and Tian et al. (2011) did not compare the HRR group with patients. 2 comparisons contributing to the diathesis set were from a single study Lui et al. (2009), wherein patients with familial schizophrenia were distinguished from those with sporadic illness and no family history, and the two groups of relatives were separately compared with healthy controls. Honea et al. recruited several high-risk relatives who had a past history of depression. For the Expression Set, the VBM results obtained from the comparison between non-depressed subset and patients with schizophrenia were considered. For the

diathesis set, such separation of the non-depressed subset was not reported. But the results of the pooled analysis were identical even if this study was down-weighted using the proportion of non-depressed sample size. Hence only the analysis with standard weights assigned to this study is included in the final report. The sample demographic characteristics of these two sets are shown in Table 3.1.

Table 3.1: Demographic and clinical characteristics of the studies comparing relatives of patients with schizophrenia and controls

Study	Sample size		Age in years (SD)		Proportion of females		Smoothin g FWHM	MRI strength in Tesla	Image analysis
	Healthy controls	High Risk Relatives	Healthy controls	High Risk Relatives	Healthy controls	High Risk Relatives			
Boos et al. (2012)	122	186	27.5 (8.2)	27.5 (6.8)	50%	54%	4mm	1.5T	In-house analysis suite GMD
Borgwardt et al. (2010)	34	9	39.3 (9.5)	33.8 (13.1)	29%	33%	8mm	1.5T	SPM2 GMV
Honea et al. (2008)	212	213	33.3 (9.86)	36.5 (9.75)	51%	58%	10mm	1.5T	SPM2 GMV **
Job et al. (2003)	36	146	21.17 (2.37)	21.18 (2.92)	52.8%	49.3%	12mm	1T	SPM99 GMD
Lui et al. (2009) familial *	10	10	43.2 (6.3)	41.4 (3.7)	60%	50%	8mm	3T	SPM2 GMV
Lui et al. (2009) sporadic *	10	10	43.2 (6.3)	45.6 (6.2)	60%	50%	8mm	3T	SPM2 GMV
Marcelis et al. (2003)	27	32	35.5 (9.8)	35.5 (10.0)	55.5%	56.30%	4.2mm	1.5T	BAMM GMD
McIntosh et al. (2004)	49	50	35.27 (11.1)	36.52 (12.95)	53%	44%	12mm	1.5T	SPM99 GMV
Tian et al. (2011)	29	55	51.79 (5.58)	50.31 (5.10)	52%	51%	6mm	3T	SPM5 GMV

*Two independent VBM comparisons were conducted by Lui et al. **The VBM analysis was not corrected for multiple comparisons. SD: Standard Deviation. SD - Standard Deviation SPM - Statistical Parametric Mapping software. VBM - Voxel based morphometry. GMD - Grey Matter Density. GMV - Grey Matter Volume obtained using modulated VBM. FWHM - Full Width Half Maximum of Gaussian smoothing kernel.

Table 3.2: Demographic and clinical characteristics of the studies comparing patients with schizophrenia and their relatives (HRR)

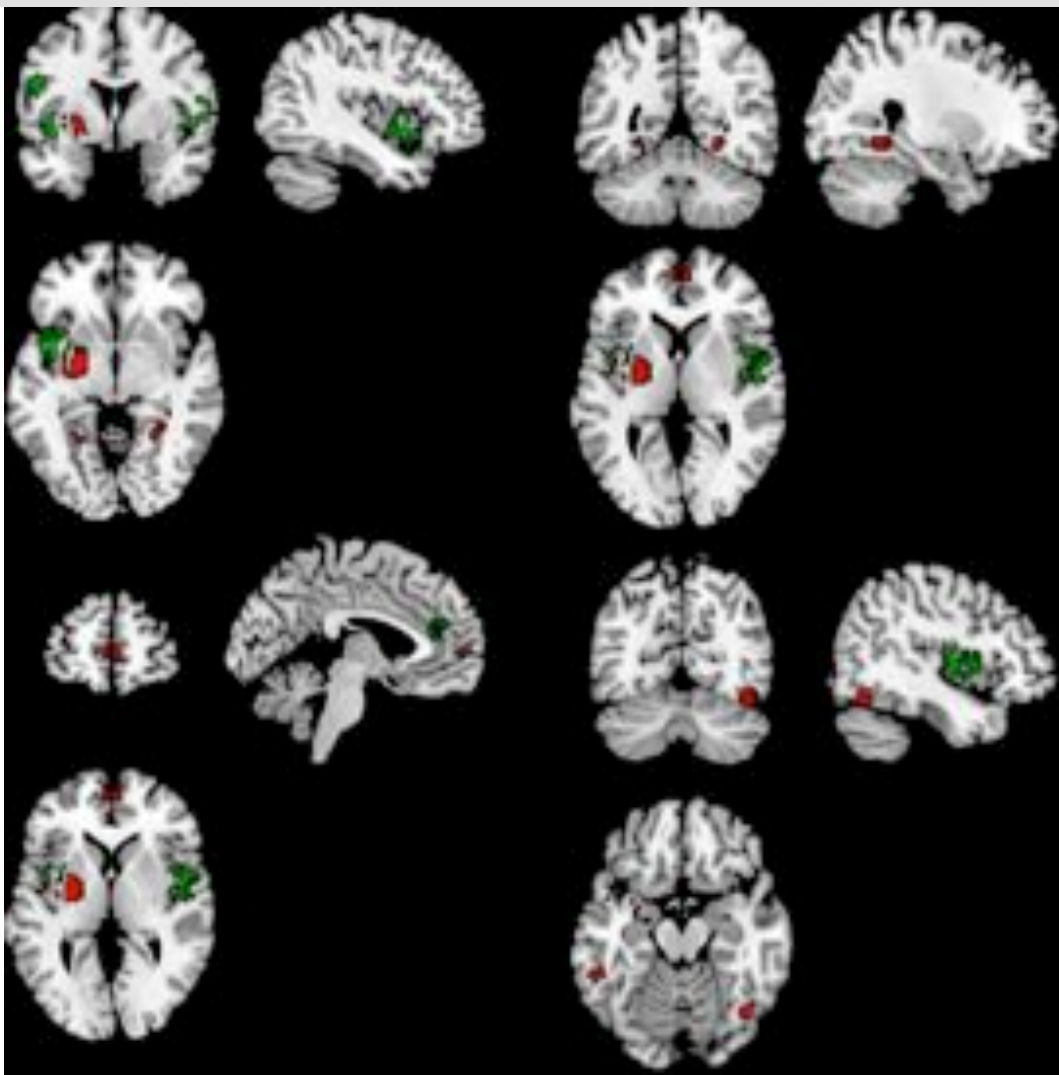
Study	Sample size	Age in years (SD)		Proportion of females		Smoothin g FWHM	Medication status of patients	Image analysis
		Patients	High Risk Relatives	Patients	High Risk Relatives			
Boos et al. (2012)	155	186	26.91 (5.6)	27.5 (6.8)	20%	54%	4mm	Y** In-house analysis suite GMD
Borgwardt et al. (2010)	37	9	39.7 (14.5)	33.8 (13.1)	24.3%	33%	8mm	Y** SPM2 GMV
Honea et al. (2008)	169	213*	36.4 (9.46)	36.5 (9.75)	22%	58%	10mm	Y** SPM2 GMV
Hulshoff Pol et al. (2006)	22	22	36.8 (10.31)	34.90 (10.86)	50%	50%	8mm	Y In-house analysis suite GMD
Job et al. (2003)	34	146	21.35 (3.66)	21.18 (2.92)	32.4%	49.3%	12mm	Un SPM99 GMD
Marcelis et al. (2003)	31	32	30.7 (7.5)	35.5 (10.0)	51.6%	56.3%	4.2mm	Y BAMM GMD
Mchintosh et al. (2004)	26	50	36.85 (13.7)	36.52 (12.95)	50%	44%	12mm	Un SPM99 GMV

*Only 63% of 213 high-risk relatives who had no past history of depression were included in the VBM. **Studies reporting statistical tests to exclude the effect of antipsychotic dose at the time of scan on the reported findings. Y - patients medicated with antipsychotics; Un - medication status unknown. SD - Standard Deviation SPM - Statistical Parametric Mapping software. VBM - Voxel based morphometry. GMD - Grey Matter Density. GMV - Grey Matter Volume obtained using modulated VBM. FWHM - Full Width Half Maximum of Gaussian smoothing kernel. All included studies employed 1.5T MRI except Job et al. who used 1T MRI.

3.5 Results from the Diathesis Set

5 out of 9 VBM comparisons showed no significant grey matter changes in HRR group compared to healthy controls (Job et al., 2003; McIntosh et al., 2004; Lui et al., 2009; Borgwardt et al., 2010; Boos et al., 2012). The studies that showed significant grey matter changes were comparable to the studies showing negative results in terms of mean sample size of HRR subjects (66 ± 83.6 vs. 80 ± 81.29), mean age of HRR subjects in years (39.72 ± 6.45 vs. 32.92 ± 9.24) and proportion of females (53% vs. 46%). The results of the SDM analysis from the 9 VBM comparisons are shown in Table 3.3. When compared to healthy controls, HRR showed a significant grey matter reduction in a cluster that included left putamen/globus pallidus (basal ganglia - BG), amygdala and parahippocampal gyrus (APHG). Grey matter reduction in HRR was also noted in left inferior temporal gyrus extending onto left fusiform gyrus (left ITG/FFG), medial prefrontal cortex (mPFC) and right parahippocampal gyrus extending onto right fusiform gyrus (Right PHG/FFG). There were no regions of grey matter excess in the HRR group. A visual display of the results using MRICron software is shown in Figure 3.2. A more lenient statistical threshold (height threshold of $z=1$, no extent thresholds) revealed grey matter reduction in the left PHG ($[-26, -54, -6]$, $Z= -1.884$ $p=0.0014$) and the right declive of the cerebellum ($[42, -64, -16]$, $z= -1.914$, $p=0.0013$).

Figure 3.2: The neuroanatomical changes related to genetic diathesis (shown in red) and the clinical expression (shown in green) displayed as a single overlay map on a template provided by MRICron. Slices are chosen for the best display of the entire overlay map. Left hemisphere is on the left of the displayed picture. Regions that emerged from the meta-analysis of Expression Set is displayed in green, Regions that emerged from the meta-analysis of Diathesis Set is displayed in red.



3.6 Results from the Expression Set

Only one (Hulshoff Pol et al., 2006) out of the 7 VBM comparisons showed no grey matter changes in patients compared to HRR group. The results of

the SDM analysis are shown in Table 3.4. When compared to HRR group, patients showed a significant grey matter reduction in a cluster that included right insula, superior temporal gyrus, pars opercularis of the inferior frontal gyrus and precentral gyrus (right Ins/STG/IFG). Grey matter reduction in patients was also noted in a cluster spanning the left insula, superior temporal gyrus extending onto left inferior frontal gyrus (left Ins/STG), a separate cluster involving the left inferior frontal gyrus (left IFG), and a fourth cluster at the left anterior cingulate and medial prefrontal cortex (left ACC/mPFC). There were no regions of grey matter excess in the patients compared to the HRR group. The bilateral insular clusters were present in all 7 of the leave-one-out sensitivity analyses, while left IFG was noted in 6 and left ACC/mPFC in 5 out of the 7 possible combinations. A visual display of the results using MRIcron software is shown in Figure 3.2. A more lenient statistical threshold (height threshold of $z=1$, no extent thresholds) revealed no additional regions with grey matter changes.

3.7 Salience Network Nodes and Clinical Expression

The primary objectives of the current study were to identify the distinct GM abnormalities associated with the genetic diathesis of schizophrenia and distinguish these from the GM abnormalities associated with the clinical expression rather than genetic liability of schizophrenia. A particular motivation was to interrogate whether a focused synthesis of the existing evidence support a role for the insula/ACC in either the genetic diathesis, or clinical expression or both. GM reduction in the left lentiform nucleus (putamen/globus pallidus), bilateral parahippocampal gyrus, left inferior temporal gyrus and fusiform gyrus and bilateral medial prefrontal cortex was

significantly associated with the genetic diathesis, while GM reduction in the bilateral insula, inferior frontal gyrus, superior temporal gyrus and left medial frontal region comprising of anterior cingulate cortex was significantly associated with the clinical expression of schizophrenia. There was no overlap in the distribution of the clusters identified from the two meta-analyses, suggesting that the neuroanatomical correlates for genetic diathesis are distinct from those that are associated with the disease expression. It should be noted that evidence from longitudinal studies provide some evidence that the development of overt psychosis is associated with a progression of grey matter deficits in the parahippocampal region in clinically defined ultra high risk individuals (UHR) (Pantelis et al., 2003) and in the left inferior temporal gyrus and right cerebellum in genetically high risk individuals (Job et al., 2005), all of which are identified as regions associated with a genetic diathesis in the present study. Even though these sites did not emerge in the meta-analysis of studies in the expression set, one cannot exclude the possibility that deficits in these regions do in fact become worse when the illness is expressed, but with an effect size too small to give a significant effect in this meta-analysis. A similar caution must also be practiced when inferring an absence of the role of insula and ACC in connection with the genetic diathesis; the presence of smaller sized insula/ACC effects in the genetic high-risk sample that becomes more apparent in the clinically symptomatic population cannot be ruled out. Nevertheless, the results presented here suggest that a relatively large portion of structural changes in insula/ACC occurs in relation to the clinically expressed psychotic disorder. This notion aligns well with the inappropriate proximal salience model in relation to the core clinical symptoms of psychosis (proposed in chapter 2).

Table 3.3: Grey matter deficits in relatives of patients with schizophrenia compared to healthy controls (Diathesis Set)

Regions	Maximum	Cluster	Cluster Breakdown	Jack-knife sensitivity	
Talairach coordinates	Z value	Uncorrected p	No. of voxels	Regions >20 voxels in size	No. of leave-one-out analyses survived by the clusters
Left lentiform nucleus (Left BG/APHG)	-34, -4, -6	0.000000514	325	Left putamen Left lateral globus pallidus Left claustrum Left thalamus Left amygdala /parahippocampal gyrus (APHG)	9 out of 9
Left Inferior temporal cluster (Left ITG/FFG)	-56,-42,-18	0.000286962	52	Left inferior temporal gyrus Left fusiform gyrus	9 out of 9
Medial prefrontal cortex (mPFC)	2, 58, 2	0.000835967	53	Left & right medial frontal gyrus	8 out of 9
Right parahippocampal cluster (Right PHG/FFG)	28,-50, -6	0.001134618	51	Right parahippocampal gyrus Right fusiform gyrus	8 out of 9

Table 3.4: Grey matter deficits in patients with schizophrenia compared to unaffected relatives (Expression Set)

Regions	Maximum	Cluster	Cluster Breakdown	Jack-knife sensitivity
	Talairach coordinates	Z value p	No. of voxels Regions >20 voxels in size	No. of leave-one-out analyses survived by the clusters
Right Insula cluster (Right Ins/STG/IFG)	48, 0, 6	-4.299 0.000014258	247 Right insula Right superior temporal gyrus Right pars opercularis Right precentral gyrus	7 out of 7
Left insula cluster	-42, 4, -6	-3.869 0.000050096	208 Left insula Left superior temporal gyrus Left inferior frontal gyrus	7 out of 7
Left inferior frontal cluster (Left IFG)	-50, 2, 22	-2.481 0.001911368	101 Left inferior frontal gyrus Left precentral gyrus	6 out of 7
Medial frontal/anterior cingulate cluster (ACC/mPFC)	-2, 46, 24	-2.264 0.002910983	54 Left medial frontal gyrus Left anterior cingulate	5 out of 7

3.8 Neuroanatomy of the genetic diathesis

A notable feature of the present analysis is that most VBM studies (5 out of 9) do not find structural differences in HRR when compared to healthy controls. This suggests that the anatomical correlates of genetic diathesis are either weak, or inconsistently identified using the VBM approach. The current results are consistent with Fusar-Poli et al. (2012, 2011a) who undertook meta-analyses of the VBM studies seeking to identify the neuroanatomical correlates of the genetic diathesis of schizophrenia. Left parahippocampal gyrus emerged as the most significant locus with grey matter reduction in HRR compared to controls (Fusar-Poli et al., 2011, 2012). But somewhat contradictory to our results, they also observed anterior cingulate cortex to be linked to the genetic diathesis. Though the primary studies that were pooled in that meta-analysis are largely overlapping with the studies that are identified in the current work, there are some important differences. Hulshoff Pol et al (2006) and Goldman et al. (2008) were not included in the current diathesis set, as the reported results were obtained from comparing a combined sample of patients and relatives (affected twin pairs) against healthy controls (unaffected twin pairs). Similarly the current study did not include the small-volume corrected results from Job et al. (2003) who undertook a motivated search of anterior cingulate and parahippocampal gyrus. It is important to note that ALE approach used by Fusar-Poli et al. (2011) discards negative findings when estimating the probability of loci in the pooled analysis (Turkeltaub et al., 2002). As a result, ALE tends to overestimate the morphometric changes in certain regions that show a high degree of between-study heterogeneity.

Studies that investigated the anatomical correlates of genetic diathesis but did not meet the inclusion criteria for both Fusar-Poli et al.'s work and the current analysis, show GM reductions at mPFC (Cannon et al., 2002; Diwadkar et al., 2006) and the ITG (Diwadkar et al., 2006) in HRR, which are in line with our results.

A meta-analysis of region-of-interest (ROI) studies addressing the neuroanatomical basis of the genetic diathesis to schizophrenia observed most significant volume reduction in the hippocampus (Boos et al., 2007). This conclusion is strongly influenced by a publication bias given that most studies measured morphometric changes in the hippocampus only, and not in other brain regions (McDonald et al., 2008). Our meta-analysis of whole brain studies identifies bilateral parahippocampal region as one of the most consistent region with structural changes in HRR. In a recent report that followed up a large cohort of individuals who met the clinical Ultra-High-Risk criteria for psychosis for a period of 2 years, left PHG showed the most prominent GM reduction in those who developed clinical psychosis compared to those who did not (Mechelli et al., 2011). This suggests that of all regions identified in the diathesis set in the present study, PHG is the one that is likely to be closely linked to the pathophysiology of schizophrenia. Parahippocampal region is considered to be a part of the limbic lobe originally described by Broca (1878). Along with amygdala, PHG assumes an important role in emotional processing and goal-directed processes (Kiehl et al., 2001; Laurens et al., 2005) in healthy controls. In chronic schizophrenia, regional blood flow to left parahippocampal gyrus is tightly linked to the various clinical symptoms (Friston et al., 1992). A reduction in the volume of the PHG is notable at the

first episode (Prasad et al., 2004) and may predict a failure to achieve remission (Bodnar et al., 2011). In the present study, the most significant cluster showing grey matter reduction in association with genetic diathesis included both putamen and parahippocampal gyrus. GM reduction in the putamen may also represent poor outcome in schizophrenia (Mitelman et al., 2009). The current observations are consistent with the suggestion that familial loading for schizophrenia could be an indicator of poor outcome (Verdoux et al., 1996).

The mean age of HRR groups in most studies included in the present analysis was higher than the average age of onset of psychosis in the general population. As a result, these HRR are likely to be individuals with a weaker diathesis for psychosis than the typical at-risk relative of a patient with schizophrenia. It is also important to note that despite the substantial contribution of genetic factors to the observed between-subjects differences in brain structure both in healthy individuals (Peper et al., 2007) and in families with schizophrenia (Brans et al., 2008), the neuroanatomical changes seen in HRR in the present study are unlikely to be entirely due to genetic mechanisms. Numerous environmental factors and shared variance between the genetic and environmental influences could affect the brain structure (Kaufman et al., 2000).

3.9 Neuroanatomy of clinical expression

Unlike the previous meta-analyses in HRR (Fusar-Poli et al., 2012), the present analysis included a direct comparison of HRR with patients who were genetically related to the HRR. Hence the current results correspond to the

neuroanatomy of disease expression, whilst controlling for the anatomical correlates of the genetic load common to both HRR and patients. Robust volumetric changes in bilateral insula were observed when patients were compared to HRR. The insula clusters were of considerable size and included a number of perisylvian/opercular structures such as the IFG, precentral gyrus and the STG. Interestingly, structural changes in bilateral insula is the most consistent finding in patients with established schizophrenia when compared to healthy controls (Bora et al., 2011a; Chan et al., 2011; Ellison-Wright and Bullmore, 2010; Glahn et al., 2008; Honea et al., 2005). The present analysis clarifies that the insula abnormalities are more likely to be related to the expression of psychosis rather than the diathesis to develop the illness. This conclusion is in line with the several studies that suggest that insular GM reduction is a feature of transition to psychosis in individuals who exhibit prodromal features and are at an enhanced clinical risk of psychosis (Fusar-Poli et al., 2011b; Smieskova et al., 2011; Takahashi et al., 2009c). An alternative explanation is that the GM reduction in the insula is related to the use of antipsychotics in those with clinical features of psychosis. Most of the studies included in this analysis reported findings from medicated samples, though only some of them statistically tested for the effect of the prescribed dose of antipsychotics on brain structure (See Table 3.2). Though several observations suggest that GM reduction could be a consequence of antipsychotic use (Ho et al., 2011; Lieberman et al., 2005), whole brain vertex-wise analysis suggests that the effect of antipsychotics is likely to be confined to regions in the frontal lobe rather than the insula (Van Haren et al., 2011).

In the current study, in addition to the insula, GM reduction in several contiguous perisylvian/opercular regions such as the STG and IFG were observed, all of which are implicated in a wider language network proposed to be abnormal in schizophrenia. Interestingly, GM reduction in STG (Takahashi et al., 2009d) IFG and ACC (Pantelis et al., 2003; Smieskova et al., 2010) has also been noted to predict transition to psychosis in clinically high-risk individuals with prodromal features.

3.10 Limitations of this work

Several limitations are notable in the present study. The number of primary studies that entered the meta-analysis is small, albeit comparable to several other published works of voxel-based meta-analyses (Radua and Mataix-Cols, 2009; Radua et al., 2010a). This limits the power of our inference though the use of effect-size based SDM safeguards against the more common type 1 error seen in other likelihood estimation approaches (Bora et al., 2010). The shortcomings of the VBM approach have been discussed in detail by Mechelli et al. (2005), and for understanding the neuro-anatomy of genetic diathesis a combination of surface based and voxel based methods may be required. Subtle surface anatomical changes that may be important for the pathophysiology of schizophrenia may be missed when using VBM. A head-to-head comparison of these two methods is presented in chapter 5. The publication bias in neuroimaging literature means that there is a tendency to overestimate the magnitude of structural changes (Ioannidis, 2011). But in the present study, a significant number of null results were included and a conservative threshold was used to identify the loci with the most robust GM

changes. Furthermore, even the use of a less stringent threshold did not reveal any overlapping changes between the diathesis and expression sets.

In a heterogeneous illness such as schizophrenia, the pathophysiology is likely to involve several neurobiological pathways. Examination of a single aspect of the human brain such as the structural changes in grey matter alone is unlikely to lead to a comprehensive insight. Nevertheless, the two meta-analyses reported in this study suggest the following speculation. Developmental abnormalities of the sensory (thalamus, FFG) and limbic (APHG/mPFC) regions associated with the schizophrenia diathesis would be expected to lead to unusual perceptual and emotional experience and/or abnormal reactions to such experiences. However, provided the executive neural systems are functioning well, the individual might cope with these experiences without expressing overt illness. However, if either a second pathological process or an extension of the primary process led to impaired function of multimodal structures such as the Salience Network (Ins/ACC) that have a supervisory role on sensory, emotional and language processing, the individual might no longer be able to cope with the abnormal perceptual and emotional experiences, and might develop overt symptoms. This observation calls for further systematic investigation of the interaction between multimodal 'cognitive control' circuits such as the Salience Network and 'lower order' sensory/emotional processing circuits to clarify or refute this supposition. Further, these observations are in line with the posited model of insular dysfunction that relates symptoms of psychosis to failed operations of the salience network (Chapter 2). This raises the question: which of the several core syndromes of schizophrenia is related to the GM reduction in the insula?

Several lines of evidence from functional MRI point towards insula having a key role in generating auditory hallucinations (Jardri et al., 2011; Kompus et al., 2011). In the next chapter, a synthesis of evidence implicating insular structural deficits in hallucinations will be presented.

Chapter 4

Structural Correlates of Hallucinations

Despite being one of the most common symptoms of schizophrenia, determining the neural correlates of auditory hallucinations still remains elusive with various studies providing inconsistent results. The inappropriate proximal salience model described in chapter 1, and the evidence linking structural changes in the insula/ACC with clinical expression of psychosis suggests that the Salience Network plays an important role in the mechanism of hallucinations. In this chapter, a voxel-based meta-analysis of studies investigating the structural correlates of auditory hallucinations in schizophrenia is reported. The insula emerged as a cardinal region along with superior temporal gyrus in this meta-analysis.

4.1 Neuroanatomy of hallucinations

Auditory hallucinations (AH) are one of the most common symptoms of schizophrenia. Several theories have been proposed to account for the mechanism of the generation of AH. These include an 'over-perceptualization' model that suggests a hyperexcitable state in the primary and secondary sensory regions (Allen et al., 2008); a source-monitoring model that suggests breakdown in the volitional assignment of self-generated speech activity leading to external misattribution (Frith and Done, 1988); and a dysfunctional episodic memory model that suggests intrusions from stored memories (Jones, 2010; Waters et al., 2006). Neuroimaging studies variously support and refute these models with no clear consensus emerging so far (Allen et al., 2007).

One of the most replicated findings in schizophrenia is the presence of structural changes in the brain (Glahn et al., 2008). Various changes have been reported across different stages of the illness both in the patients and high-risk individuals (Chan et al., 2011; Fusar-Poli et al., 2011b). It is likely that delineating structural features associated with core symptoms such as AH will help elucidate the mechanisms underlying the generation of such symptoms in schizophrenia. Recently, quantitative meta-analytic approaches have been used to determine the most likely functional anatomical substrate of AH (Jardri et al., 2011; Kühn and Gallinat, 2010). One group of functional studies investigates the regional differences in fMRI/PET activation when comparing AH state to non-AH state (Jardri et al., 2011). These differences may be secondary to the perceived AH as well as explaining the mechanism of AH, making it difficult to interpret the underlying pathophysiology. The other group of functional studies includes task-based fMRI comparing the brain activity in those with AH against those who do not experience AH (Kühn and Gallinat, 2010). The latter studies have mostly used a language task in patients, creating an inherent bias towards a greater likelihood of identifying language areas as the basis of AH. The meta-analytic results from these two groups of studies can be better understood if the structural changes that underlie AH can be delineated. Furthermore, fMRI studies observe both increased and reduced activation in the same brain regions in patients with AH (Kompus et al., 2011). Unlike the findings from fMRI studies, the structural brain changes are less likely to be an epiphenomenon of the state of AH. Consequently, delineating structural changes associated with AH might add substantially to the identification of cerebral location of abnormalities that play a casual role.

Most of the structural analyses seeking the neural correlates of AH have been conducted using a Region-of-Interest (ROI) approach. Though a number of such ROI studies found a relationship between reduced volume of superior temporal gyrus (STG), especially on the left hemisphere, and the severity of AH (Barta et al., 1990; Flaum et al., 1995; Levitan et al., 1999; Onitsuka et al., 2004; Rajarethinam et al., 2000; Sumich et al., 2005; Takahashi et al., 2006b), a significant number of studies reported a lack of association (DeLisi et al., 1994; Havermans et al., 1999; Marsh et al., 1997; Zipursky et al., 1994). Most of the ROI investigations in this context were driven by a specific hypothesis regarding the involvement of temporal cortex. This approach, while being statistically powerful, fails to identify other potentially relevant brain regions that may be crucial in the symptom generation. For example, none of the previous ROI studies have focused on regions such as insula or anterior cingulate cortex that have been highlighted as important nodes in functional imaging studies.

In the present study, a meta-analytic approach is used to combine whole brain morphometric studies investigating the structural correlates of hallucinations and investigated if the reported changes are consistent with existing models of symptom generation in schizophrenia. Signed Differential Mapping (SDM) is a meta-analytic technique that expands on the powerful probabilistic approach of Anatomical Likelihood Estimation (Radua and Mataix-Cols, 2009) and has been recently modified to take the effect-sizes and their intra- and inter-study variability into account (Radua et al., 2011). SDM has been used in synthesising VBM studies reporting grey matter changes in patients compared to controls in various psychiatric disorders

(Bora et al., 2010; Chen and Ma, 2010; Pan et al., 2011; Radua et al., 2010b). Though most of the previous meta-analyses of VBM studies were based on group differences (T maps) as in the previous chapter of this thesis, for the purpose of localizing the consistent grey matter changes in relation to hallucinations, the focus is on coordinates identified using a *correlational* analyses.

4.2 Literature search

Using the Medline, Scopus and Web of Knowledge databases, a comprehensive search for studies using VBM published between 1995 (the year of first publication of a VBM study in schizophrenia) to December 2011 was undertaken independently by 2 research psychiatrists (Palaniyappan and Balain). The keywords ‘hallucination’, ‘voice’, ‘MRI’, ‘morphometry’, ‘voxel-based’, ‘voxelwise’ and ‘neuroimaging’ were used. We also undertook further searches from the references used in the identified papers. Using Google Scholar, we additionally searched for studies that cite the identified papers. We included all studies that investigated grey matter VBM correlates of auditory hallucinations measured using a standardized rating scale in schizophrenia and excluded those that used a Region of Interest approach rather than a whole brain analysis. We then contacted the corresponding authors if any detail required for the primary meta-analysis was missing. We followed the guidelines suggested by Stroup et al. 2000 (MOOSE: Meta-analysis Of Observational Studies in Epidemiology).

4.3 Signed Differential Mapping

For each study, SDM was initially used to recreate a whole brain map in Talairach space of the effect-size of the correlations. This was achieved by estimating the effect size of the peak coordinates and applying an un-normalized Gaussian kernel of 20mm half-width to the voxels surrounding them. Thus, the voxels closer to a reported peak were estimated to have a higher effect-size, with a positive sign denoting a positive correlation, and negative sign denoting a negative correlation. In the next step, a pooled map was derived from the voxelwise mean of the individual study maps, weighted by the inverse of the variance of each study plus the between-study heterogeneity. With this random-effects model, SDM ensures that the larger studies have proportionally more influence on the final results, and that findings are not biased towards those brain regions with more between-study heterogeneity. A permutation test is used for deriving the statistical significance. Standard thresholds for effect-size SDM were used ($p < 0.005$, cluster extent 10 voxels) (Radua et al., 2011) along with a minimum peak height value of $z > 2$ (instead of $z > 1$) to focus on the most consistent findings from the individual correlational studies.

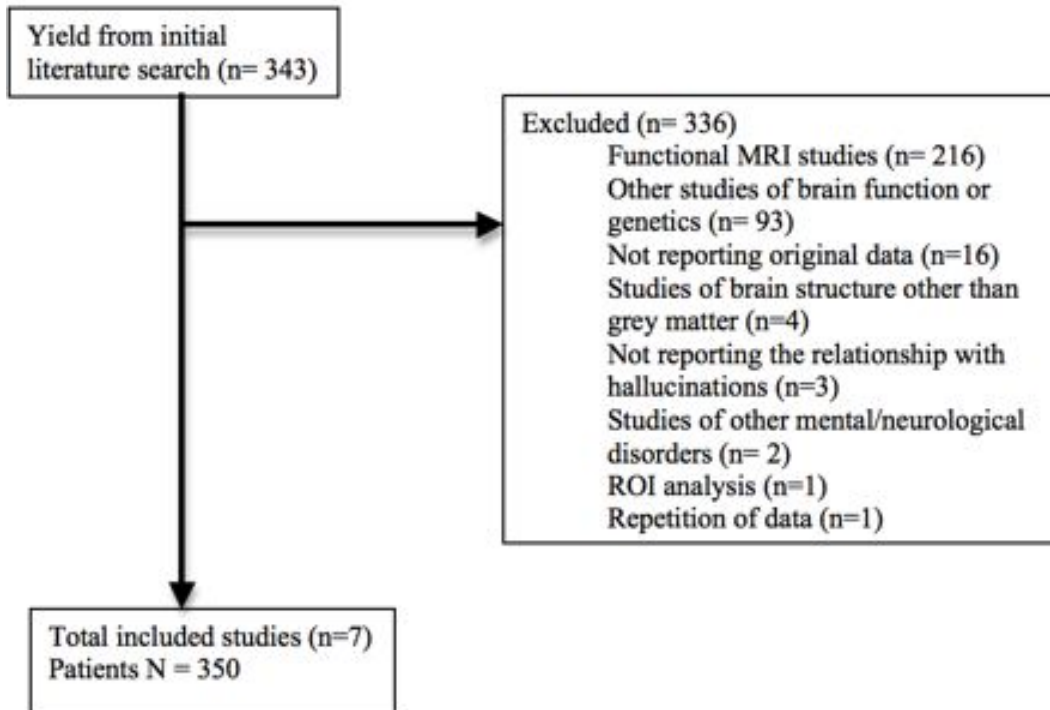
SDM differs from ALE (Anatomical Likelihood Estimation) in that both positive and negative group differences are recreated in the same map (signed map), thus avoiding the same voxel being significant in opposite directions. This feature is particularly useful when synthesizing VBM based correlational analyses, as symptom scores can be associated with both reduced and excessive grey matter volume at a locus. A direct comparison of ALE and SDM methods suggests that the influence of multiple coordinates identified in a single study on the overall results is comparatively less when

SDM method is employed (Bora et al., 2010). Thus SDM reduces the risk of false positive localization even when the number of primary studies included in an analysis is small. Furthermore, only those studies that conducted an unbiased whole brain analysis are included in the SDM. In order to prevent biases towards pre-selected brain regions, SDM establishes that *within* one study, the same threshold must be applied throughout the whole brain - although this threshold might be different *between* studies. Though VBM studies vary in the statistical thresholds used for correcting multiple comparisons, SDM does not assume statistical significance of voxels reported but instead uses these coordinates to approximately recreate the statistical parametric map for meta-analytic synthesis. In order to check whether results could be biased by small lenient studies, a jack-knife sensitivity analysis was undertaken to demonstrate the robustness of the results. The mean maps showing statistically significant positive and negative correlations with severity of hallucination were visualized using MRICron (<http://www.cabiatl.com/mricro>). SDM was employed in line with the instructions provided with the software (www.sdmproject.com).

4.4 Search Outcome

The outcome of the search is shown in Figure 4.1.

Figure 1: Inclusion of studies



Of the 343 studies identified in the search of databases, 319 were excluded because they did not report the relationship between grey matter morphology (quantified at voxel level) and hallucinations in schizophrenia, and 17 were excluded because they did not report new data. Further details regarding the excluded studies are provided in figure 4.1. Seven datasets including a total of 350 patients were eligible for the final analysis (García-Martí et al., 2008; Gaser et al., 2004; Modinos et al., 2009b; Neckelmann et al., 2006; Nenadic et al., 2010; O'Daly et al., 2007; Shapleske et al., 2002). All except one study used a correlation approach to study the structural correlates. The meta-analysis was conducted twice, first using standard weights, and later down-weighting the study by Shapleske et al. (2002) to reflect the decrease in power associated to the use of a binary variable

assuming a linear trend. As the results were nearly identical, only the findings of the latter approach are reported. Two studies in the final sample had a partial sample overlap (Gaser et al., 2004; Nenadic et al., 2010). The meta-analysis was carried out both with and without the latter study to test the stability of the results. The sample demographic characteristics are shown in Table 4.1.

4.5 Results from SDM analysis

The results of the SDM analysis are shown in Table 4.2. There were no areas of positive correlation in grey matter volume with AH. There were two significant clusters of negative correlation with maximum peaks occurring in left insula and right superior temporal gyrus. The left insular cluster showed a higher likelihood of relationship and demonstrated high replicability (7 out of 7) in the jack-knife sensitivity analysis (a procedure wherein the analysis was repeated for 7 times in subsets of 6 studies, leaving one out at a time), with a significant association evident in all 7 studies. This cluster had its maximum in the insula, and extended to Broca's area (BA 44) anteriorly and superior temporal gyrus (BA 22) posteriorly. The right superior temporal gyrus (STG) cluster had its maximum at BA 22, and extended to include the insular region and subcentral sulcus. For right STG cluster, a significant association was found in 3 out of 7 studies. Jack-knife analysis revealed that the negative correlation between the right STG cluster and auditory hallucinations was evident 6 out of 7 times. No relevant differences were observed between the studies who had detected statistically significant correlations at the right STG cluster (García-Martí et al., 2008; Nenadic et al., 2010; O'Daly et al., 2007) and those which had not (Gaser et al., 2004; Modinos et al., 2009b;

Neckelmann et al., 2006; Shapleske et al., 2002) in terms of mean age (36 ± 10 vs. 35 ± 10 years), proportion of females (31% vs. 25%), duration of illness (8 ± 9 vs. 11 ± 9 years), mean sample size ($N = 48\pm 44$ vs. 49 ± 35) or use of uncorrected threshold (33% vs. 50%). There were small areas of significant between-study heterogeneity in bilateral insula, but funnel plots of the peaks showed that findings were driven by many studies with both large and small standard errors, and no studies reporting effects in opposite direction or other gross abnormalities were detected. The results are displayed in Figure 4.2.

Table 4.1: Demographic and clinical characteristics of the included studies

Study	Sample Size	Left handed	Software	Statistical threshold	Proportion of females	Illness duration in years (mean (SD))	Medication Status	Age in years (mean (SD))	Hallucination Rating Scale
Garcia-Marti et al. (2008)	18	0%	SnPM	P<0.05 FDR corrected	0%	NA*	medicated	35.71 (6.11)	PSYRATS AHRS
Gaser et al. (2004)	85	0%	Deformation-based morphometry	P < 0.001 uncorrected	39%	8.9 (8.2)	medicated	36.2 (10.9)	SAPS
Modinos et al. (2009)	26	NA	SPM5	FWE corrected p<0.05	50%	13.6 (11)	medicated	36 (12)	PSYRATS AHRS
Neckelmann et al. (2006)	12	NA	SPM99	p < .001 (uncorrected).	NA	NA	medicated	19 to 51	BPRS
Nenadic et al. (2010)	99	NA	SPM2	Uncorrected p<0.01	42%	NA	medicated	36.2 (s.d. 11.2)	SAPS
O'daly et al. (2007)	28	0%	Permutation based VBM	<1 FP cluster	11%	8 (8)	medicated	33 (10)	BPRS
Shapleske et al. (2002)	72	25%	Permutation based VBM	<1 FP cluster	0%	11.5 (7.8)	medicated	34.1(8.5)	SAPS

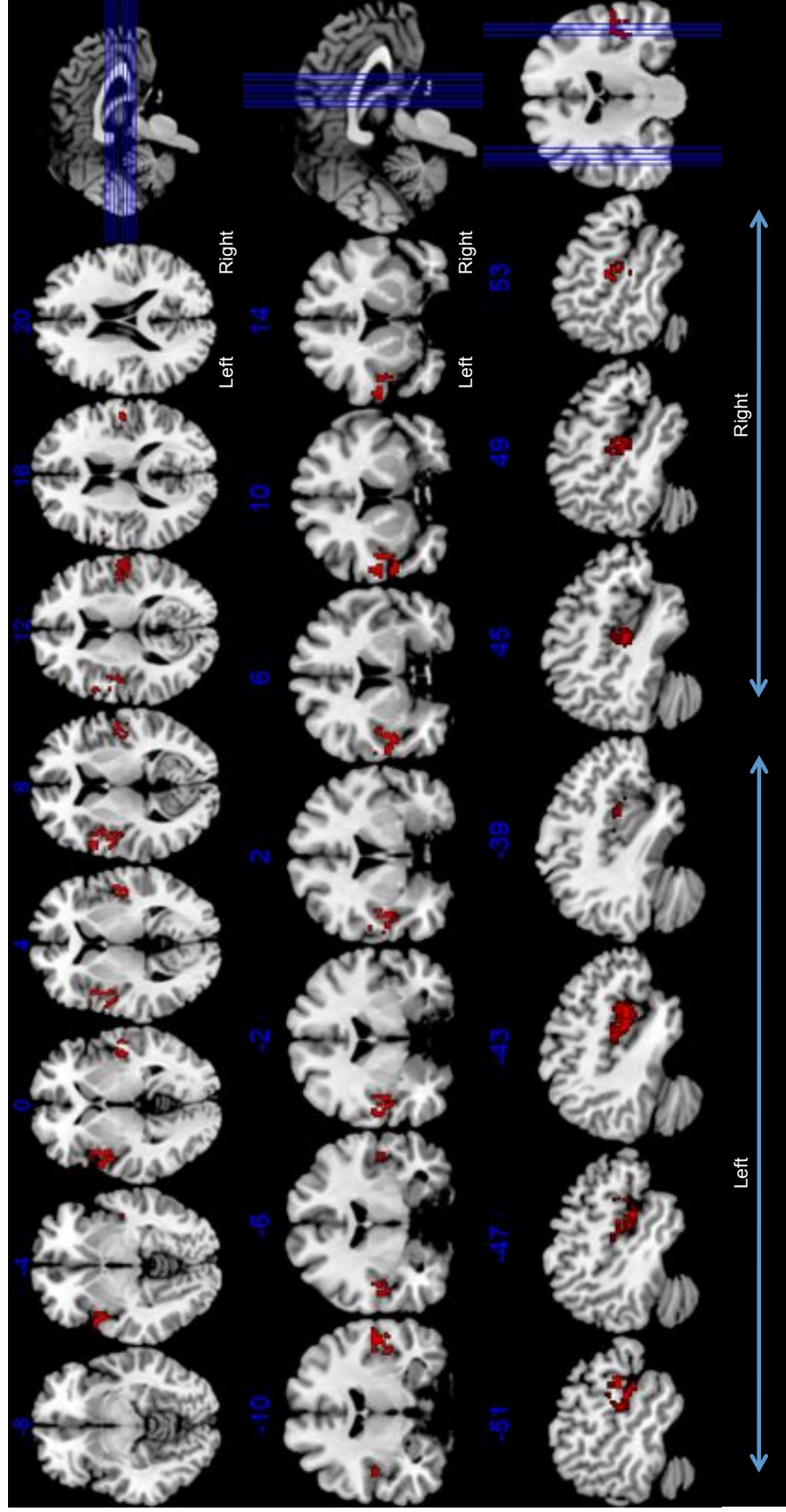
*Mean age of onset of hallucinations 18.7 years. SD: Standard Deviation. SAPS: Scale for the Assessment of Positive Symptoms. BPRS: Brief Psychiatric Rating Scale. PSYRATS-AHRS: The Psychotic Symptoms Rating Scales - Auditory Hallucination Rating Scale. FDR: False Discovery Rate. FWE: Familywise Error. s.d. Standard Deviation

Table 4.2: Structural correlates of the severity of hallucinations in schizophrenia

Regions	Direction of correlation	Maximum coordinates	Cluster	Cluster Breakdown		
		Talairach coordinates	Z value	Uncorrected p	No. of voxels	Regions >60 voxels in size
Left Insula cluster	Negative	-42,-4,2	-3.565	0.000001	717	Left insula Left superior temporal gyrus, BA22 Left inferior frontal gyrus, BA44
Right Superior Temporal Gyrus cluster	Negative	58,-6,10	-2.016	0.0008	318	Right superior temporal gyrus, BA22 Right insula

SDM: Signed Differential Mapping BA: Brodmann Area

Figure 4.2: Regions showing negative correlation between grey matter density and severity of hallucinations in schizophrenia. Left insula and right superior temporal gyrus showed significant associations. The overlay map is generated and displayed on a template provided by MRIcron. Slices are chosen to provide the best display of the overlay. For the axial and coronal views, left side of each slice represents left hemisphere. In the bottom row, first four sagittal slices represent left hemisphere.



DISCUSSION

4.6 The role of insular cortex in hallucinations

A meta-analytic approach has been used for the first time to detect the structural correlates of AH in schizophrenia. The current findings implicate a major role for the insula along with other regions traditionally regarded as language areas in the pathophysiology of AH. The robust relationship observed between AH and left insular cluster is consistent with the emergence of left insula and Broca's areas as the significant correlates during active hallucinations (Jardri et al., 2011). The present observations complement the meta-analytic literature of fMRI and PET in AH and support the notion that functional defects observed in the insula and language areas during AH are unlikely to be merely a consequence of the experience of AH.

Fronto-insular cortex forms a part of the Salience Network, a large-scale brain circuit that integrates switching between task-positive and resting mode of brain activity (Sridharan et al., 2008). The salience network plays a key role in integration of internally and externally generated sensations, with information about goals and plans, so as to update expectations about the internal and external milieu and if necessary initiate or modify action (Menon and Uddin, 2010). As predicted in chapter 2, the role of insula in evaluation of internal/external stimuli accompanied by assignment of momentary salience (or 'proximal salience') may be crucial in generation of hallucinations. Insular dysfunction could result in failure to evaluate internal speech in light of its

context and hence an inappropriate allocation of proximal salience to internally generated speech.

4.7 Superior temporal gyrus in hallucinations

In contrast to the insula, which has been sparsely studied in relation to hallucinations using a ROI approach, the STG has been the target of various ROI studies as highlighted previously (Sun et al., 2009). In the present study, in addition to the right STG involvement, the left STG (BA 22) was also related to the severity of AH. These results are in agreement with various ROI studies in schizophrenia (Sun et al., 2009), reinforcing that the bilateral STG grey matter reduction seen in hypothesis-driven ROI studies is replicable when conducting whole brain morphometric analyses. These structural changes may underlie the STG dysfunction seen when performing language-processing tasks in fMRI in patients with AH (Jardri et al., 2011; Kühn and Gallinat, 2010).

Insofar as there was no association between AH and medial temporal structure, the current findings provide no support for the dysfunctional episodic memory hypothesis. Nevertheless, Waters' cognitive model of AH proposes a combined deficit in contextual memory and intentional inhibition of intrusive memories, suggesting the possible involvement of a network wider than the traditional memory related medial temporal regions in the mechanism of AH (Waters et al., 2004, 2006). The proximal salience model of insular dysfunction accommodates the possibility of an increase in 'mind-wandering' due to the failure to 'switch-off' the 'default mode' of brain activity (chapter 2).

This resting state brain activity has been associated with both Stimulus Independent Thoughts and memory retrieval (Binder et al., 1999).

The observation of a relationship between grey matter reduction and hallucinations may not be symptom specific, as most VBM studies except two (Gaser et al., 2004; Nenadic et al., 2010) did not adjust for the influence of other psychotic symptoms on this relationship. Gaser et al. (2004) also showed a lack of relationship between severity of hallucinations and symptom scores other than delusions in the study sample. This issue was indirectly addressed by Garcia-Marti et al. (García-Martí et al., 2008) who undertook a whole brain search seeking grey matter correlates of total symptom burden and showed that the regions correlating with hallucinations were different from those relating to overall symptom severity. Nevertheless, brain activation during AH seems to involve the insula and STG irrespective of the presence or absence of psychosis (Diederer et al., 2011). This suggests that the current findings of structural deficits in the insula and STG are likely to be specific to the symptom of AH.

4.8 Limitations of this work

An important limitation of this meta-analysis is the lack of sufficient number of studies, but a sample of size of 350 patients is comparable to other studies using the SDM methodology (Radua and Mataix-Cols, 2009; Radua et al., 2010b). Furthermore, when compared to ALE approach, effect-size SDM reduces the false positive inclusions by including the regions showing both positive and negative correlations in the same pooled map, and by taking intra-study variance and between-study heterogeneity into account. A head to

head comparison between ALE and SDM by Bora et al. (2010) demonstrated the accuracy of SDM even in the presence of notable between-studies heterogeneity. The studies included in the current analysis were heterogeneous in terms of image analysis methods and rating scales used. This is a common issue in anatomical likelihood estimates used in neuroimaging. The jack-knife sensitivity analysis suggests that methodological differences have not influenced the pooled effect in the reported clusters. All subjects considered in the present report had hallucinations despite taking antipsychotic medications, with two studies including only those patients with treatment-resistant hallucinations (Modinos et al., 2009b; O'Daly et al., 2007). As a result the sample included may not be representative of majority of patients with auditory hallucinations that respond to antipsychotic treatment, and the observed neural correlates may be more relevant for persistence of hallucinations rather than a tendency to hallucinate in patients with schizophrenia. . Further, the reported correlations may have been affected by the variable effect of antipsychotics on cortical grey matter. It is pertinent to note that Spencer et al. (2007) reported a positive correlation restricted to males between auditory hallucinations and grey matter density in right superior temporal gyrus, in un-medicated individuals with intellectual disability considered to be 'at risk of psychosis'. The effects of antipsychotics on grey matter remain a subject of debate, but longitudinal studies do not identify focal grey matter changes in the insula and superior temporal gyrus to be related to antipsychotic use (Ho et al., 2011; van Haren et al., 2011). Females were under-represented and statistical adjustment for gender was reported in two studies (Gaser et al., 2004; Nenadic et al., 2010). Only one of the studies reported a gender specific analysis (Modinos et al., 2009b), demonstrating a

lack of gender differences. Relevant to the current findings is a recent meta-analysis of VBM studies seeking to estimate the effect of gender on the grey matter deficits in schizophrenia (Bora et al., 2011b). This study reported that though more extensive grey matter deficits are seen in males with schizophrenia, gender-balanced samples consistently show deficits in left insula and right STG regions. None of the included studies have systematically evaluated the relationship between duration of illness and the severity of hallucinations. But exclusion of studies with lower or higher duration of illness has not affected the results of the meta-analysis, as demonstrated by the sensitivity analysis.

A meta-analytic study published around the same time as this chapter, reviewed 8 studies (n=307 patients with hallucinations) (Modinos et al., 2013). This study observed that the severity of AVHs was significantly associated with grey matter reductions in the left and marginally with the right superior temporal gyri. Interestingly, insular focus did not appear in this study. This is likely to be related to the non-specific inclusion criteria whereby studies that did not directly investigate the grey matter correlations of hallucinations with VBM approach were also included. Somewhat unusually, this VBM meta-analysis also included a single fMRI study, which showed activation focus on the STG (Plaze et al., 2006). In addition, the largest weighted study in this analysis (van Tol, Modinos, Aleman et al., unpublished) was an unpublished report available only to the authors of this meta-analysis. This large study remains unpublished to date (June 2013), making it difficult to compare the reasons for the differences in the conclusion.

Meta-analytic synthesis of the unbiased whole brain structural studies of AH supports the hypothesis that AH arises from an inappropriate assignment of momentary salience to internal speech, mediated by a reduction in the grey matter of bilateral insula, Broca's area and right STG. A focused exploration of the insula in future using both structural and functional studies in unmedicated samples may help to confirm the insular dysfunction hypothesis in AH. Given that grey matter reduction as measured using VBM is related to the clinical expression (chapter 3) and one of the common symptoms of schizophrenia (chapter 4), understanding the anatomical nature of the information 'picked up' by VBM studies becomes paramount in making further inroads into the pathophysiology of this illness. A direct comparison of surface-based and voxel-based morphometric approaches is reported in the next chapter (chapter 5).

Chapter 5

Anatomical basis of voxel based morphometric deficits in schizophrenia

As noted in the previous two chapters, Voxel Based Morphometric (VBM) studies have provided an important line of evidence to support the role of insula in the pathophysiology of schizophrenia. Nevertheless, the biological or tissue-related property measured by the VBM approach is unknown to date. While simultaneous histological study of brain tissue will be the gold standard approach to address this question, significant inroads can be made if the morphological (surface anatomical) properties captured by the VBM approach could be clarified. In this chapter, the proportional contribution of the anatomical properties of the cortical mantle such as thickness, surface area and gyrification to the group differences in grey matter volume (GMV) observed using VBM is investigated in a sample of 57 patients with schizophrenia and 41 healthy controls. Multiple mediation analysis revealed that while SBM measures make distinct but regionally variable contribution to the VBM differences, a large proportion of the group difference observed using VBM is not explained by the individual surface anatomical properties.

5.1 Interpretation of VBM deficits

Voxel Based Morphometry (VBM) is a widely used method to quantify grey matter abnormalities in disease states (Ashburner and Friston, 2000). Since its initial application to study structural changes in schizophrenia (Wright et al., 1995), the technique of VBM has evolved significantly. One of the major

criticisms of VBM is that the technique is very sensitive to the image registration procedures. Conditions that result in systematic differences in image alignment may produce spurious results (Bookstein, 2001), though the significance of this is refuted (Ashburner and Friston, 2001). This issue is especially relevant for conditions such as schizophrenia, where abnormalities of sulcal patterning around the lateral fissure (Csernansky et al., 2008) can produce group differences in aligning grey matter images for VBM, in particular affecting the perisylvian regions such as insula and the surrounding operculum that are commonly observed to have GMV deficit in schizophrenia (Koutsouleris et al., 2008; Meisenzahl et al., 2008). Recent updates of VBM improve on registration methods (Ashburner, 2007), thus addressing the criticisms raised by Bookstein (2001) to certain extent.

Surface based morphometric (SBM) methods such as Freesurfer circumvent some of the problems associated with VBM by undertaking computations of morphometric properties in the 'native space' (Dale et al., 1999). The computationally intensive surface based techniques provide distinct cortical thickness and surface area measures that are shown to be both genetically and phenotypically independent (Panizzon et al., 2009; Winkler et al., 2010). Group differences emerging in a VBM study could be variously attributed to cortical thinning, altered gyrification (cortical folding) or abnormalities in the surface area (Mechelli et al., 2005). Despite the increasing number of studies that employ both VBM and SBM together to study brain structure in disease states (Cerasa et al., 2011; Chee et al., 2011; Lehmann et al., 2009), the relationship between VBM derived Grey Matter

Volume (GMV) and SBM derived measures of thickness, gyrfication and surface area is unclear.

The importance of structural changes in understanding the pathophysiology of schizophrenia has been well established (McCarley et al., 1999; Shenton et al., 2001). A significant number of VBM investigations of the neuroanatomy of schizophrenia have been published in the last two decades (Ellison-Wright et al., 2008; Glahn et al., 2008; Honea et al., 2005; Leung et al., 2009). Despite the significant spatial heterogeneity of the reported findings, meta-analysis of VBM studies estimate a high likelihood of grey matter deficits in specific regions such as bilateral insula, temporal cortex and anterior cingulate in schizophrenia (Ellison-Wright et al., 2008; Glahn et al., 2008; Honea et al., 2005; Leung et al., 2009). Cortical thickness (Kuperberg et al., 2003) maps identify regions of structural changes that overlap to some extent with the regions showing GMV reduction in VBM. Focused analyses of the spatial overlap between VBM and SBM in schizophrenia have previously revealed that either thickness or surface area changes were present in clusters that had significant reduction in GMV (Narr et al., 2005; Voets et al., 2008) with some suggestion that cortical folding differences could account for the some of the regional differences . These findings indicate that changes in the anatomical properties of the cortical mantle (thickness, cortical folding or surface area) may underlie the GMV reduction seen in schizophrenia.

In the present study, the relationship between the GMV and anatomical properties of the cortical mantle is investigated in regions showing significant VBM changes in schizophrenia. The hypothesis that SBM measures will mediate the group differences in GMV observed in the VBM analysis was

directly tested. Given the partial overlap in the spatial distribution of VBM and cortical thickness measured using both surface-based (Narr et al., 2005; Voets et al., 2008) and voxel-based methods (Hutton et al., 2009) in previous studies, regional differences were expected in the influence of surface based measures on VBM findings.

5.2 Participants

Data acquired from 98 subjects (57 with schizophrenia and 42 healthy controls) were used in this study. Regional Ethics Committees (Nottinghamshire & Derbyshire) approved the study and all participants provided written informed consent.

Patients were initially referred by clinicians attached to community mental health teams and rehabilitation services including the early intervention in psychosis teams and hence represent a predominantly early phase sample. The diagnosis of schizophrenia was made in accordance with the procedure of Leckman (1982) using data from all available sources to make diagnosis according to DSM IV criteria. The predominant subtypes of schizophrenia in the sample included Paranoid [DSM-IV 295.30] (n=47), Undifferentiated [DSM-IV 295.90] (n=7) and Disorganized [DSM-IV 295.10] (n=3). All patients were in a stable phase of schizophrenia (defined as a change of no more than 10 points in their Global Assessment of Function (GAF; DSM-IV (APA, 1994)) score, assessed six weeks prior and immediately prior to study participation) and the mean duration of illness was 4.3 years. Subjects with neurological disorders, current substance dependence, IQ < 70 using Quick Test (Ammons & Ammons, 1962), and diagnosis of any other axis I disorder were

excluded. All patients were receiving treatment with antipsychotic medications (average dose in chlorpromazine equivalents was 288.7mg, range: 100 to 1200mg). 3 were on clozapine (mean chlorpromazine equivalents: 683.33mg), while 54 were on non-clozapine atypical antipsychotics (mean chlorpromazine equivalents: 266.77mg). Chlorpromazine equivalent doses were computed using data presented by Woods (2003) (for non-clozapine atypicals) and Chong et al. (2000) (for clozapine). In the case of Risperidone Consta injection, 25 mg Consta injection every 14 days was taken to equate to 4 mg oral risperidone per day, in accordance with the recommendation of the British National Formulary (Joint Formulary Committee, 2008). Patients with schizophrenia were interviewed on the same day of the scans by a research psychiatrist and symptom scores assigned according to the SSPI (Liddle et al., 2002).

Healthy controls were recruited from the local community via advertisements and comprised 41 subjects free of any psychiatric or neurological disorder matched groupwise in age (\pm 3 years) and socio-economic status (measured using National Statistics - Socio Economic Classification (Rose and Pevalin, 2003) to the patient group. Controls had similar exclusion criteria to patients; in addition subjects with history of psychotic illness in first-degree relatives were excluded. One control subject was excluded in the final analysis due to a movement artifact in the MRI image that precluded volumetric computations, giving a final sample of 57 patients and 41 controls for the present analysis.

5.3 Image acquisition

Magnetic resonance scans were collected using a Philips 3-T imaging system equipped with 8-channel phased array head coil. The scanning protocol included a single high-resolution three-dimensional T1-weighted MPRAGE volume of isotropic voxel size $1 \times 1 \times 1 \text{ mm}^3$, flip angle 8° , field of view $256 \times 256 \times 160 \text{ mm}^3$. Head motion was minimized by using cushion pads, and providing reassurance at the beginning of the procedure. Quality check to exclude motion artefacts was carried out by 2 researchers (Palaniyappan & Liddle) independently using predefined criteria (see appendix 1).

5.4 Voxel Based Morphometry

VBM-DARTEL analysis was used to investigate the differences in the GMV between the two groups. Image analysis was carried out using SPM8 (<http://www.fil.ion.ucl.ac.uk/spm>) implemented in Matlab 2010b (Math Works, Natick, MA, USA) with the default parameters. Diffeomorphic Anatomical Registration using Exponentiated Lie algebra (DARTEL)(Ashburner, 2007) procedure was used to create a study-specific template for tissue segmentations and a high-dimensional normalization protocol. Smoothed, modulated, grey matter images normalized to MNI space were used for the statistical analysis. Smoothing was carried out using isotropic Gaussian kernel of 8mm full-width at half-maximum. To identify clusters showing GMV differences, an independent samples t test (controls vs. patients) was carried out with intracranial volume as a global covariate. The total intracranial volume (ICV) for each subject was calculated as the sum of the volumes of the three tissue segmentations (grey matter, white matter, and cerebro-spinal

fluid (CSF)) using SPM8. A Familywise Error Rate of 0.01 was used along with a spatial threshold of 200 voxels to obtain the statistical t maps. The conservative height and extent threshold for VBM analysis were chosen with the primary objective of isolating relatively few clusters with robust GMV changes across a considerable spatial extent (200 voxels) in order to obtain corresponding surface anatomical properties such as gyrification and surface area, which are difficult to interpret in small clusters. All cortical clusters that emerged significant in the analysis were chosen for further analysis. Subcortical structures were not included, as surface based measures such as thickness and gyrification are not applicable to them. For the chosen regions, Marsbar (Brett et al., 2002) was used to generate cluster specific binary masks. The clusters that emerged from VBM analysis were not specific to clearly demarcated anatomical regions and often extended to subcortical structures. In order to achieve anatomical specificity for further analysis using SBM, the cluster specific masks were refined using the anatomical boundaries specified by Automated Anatomical Labelling (AAL) Atlas (Tzourio-Mazoyer et al., 2002) for the predominant cortical region represented by each cluster. This 'trimming' procedure produced 'inclusive' binary masks that only included those voxels that were present in both AAL parcellation and the VBM derived clusters, limiting the masks to the cortical mantle for which SBM metrics can be obtained. These binary masks were then used to obtain constrained mean GMV from all voxels included within the cluster using Marsbar.

5.5 Surface Based Morphometry

Surface extraction was carried out using FreeSurfer version 4.5.0 (Fischl et al., 1999). The preprocessing was carried out according to the standard

description available at (<http://surfer.nmr.mgh.harvard.edu/>). Briefly, following skull-stripping and intensity correction, the grey-white matter boundary for each cortical hemisphere was determined using tissue intensity and neighbourhood constraints. The resulting surface boundary was tessellated to generate multiple vertices across the whole brain before inflating. All surfaces were visually inspected following an automated topology fixation procedure, and remaining minor defects were manually corrected as recommended by the software guidelines. The expansion of the resulting grey-white interface created the pial surface with a point-to-point correspondence. This was followed by spherical morphing and spherical registration. Cortical thickness, surface area and volume measures were computed using the methods developed by Fischl and Dale (Fischl and Dale, 2000).

Local gyrification indices (LGIs) were obtained using the method of Schaer (2008) using images reconstructed through the Freesurfer pipeline. Schaer's method is a vertex-wise extension of Zilles' gyrification index, which gives a ratio of the inner folded contour to the outer perimeter of the cortex (Zilles et al., 1988). Using the grey-white interface constructed via surface registration and cortical inflation using Freesurfer, a pial surface is first obtained by constructing a set of lines perpendicular to the grey-white interface. In the second step, an outer 'hull' surface is generated by means of a morphological closing operation which ensures that the local curvature at all points on the outer 'hull' surface is less than the curvature of a 15mm radius sphere (a radius chosen to ensure that the hull surface does not dip into the sulci). Schaer originally chose the 15mm sphere for the closing operation to ensure

that the hull surface does not dip into the sulci and remains tight but external to the sulcal dips. We followed the same procedure in the present study.

This hull surface acts as the outer perimeter while the original pial surface provides the inner perimeter. Both inner and outer surfaces are tessellated with numerous vertices formed by the meeting points of triangles. For each vertex (j) on the outer surface, a spherical region of interest is created with the vertex as the centre and a standard 25mm radius. 25mm radius is chosen so an uninterrupted Gaussian smooth map that retains the ability to distinguish anatomically discrete local maxima along the primary sulci is produced (Schaer et al., 2008). The resulting spherical regions yield two area measures for each vertex. The outer measure ($Area^j_o$) is area of that part of the hull defined by the intersection of this sphere with the hull surface. To measure the corresponding pial surface area, the pial region of interest for the given vertex on outer hull surface is determined as follows. Initially all vertices within $Area^j_o$ (on the hull surface) are identified. Following this, the nearest pial vertex to each of these hull vertices is identified. These pial vertices define the outline of pial mesh, whose area is then calculated using sum of areas of all included triangular tessellations ($Area^j_p$). The ratio of the pial surface area to the outer surface area gives the local gyrification index for each vertex on the outer surface ($Area^j_p/Area^j_o$). These outer surface values are redistributed to the pial surface using a weighted sum of all outer surface LGIs to which each pial vertex contributed during the prior computation. The weighting was inversely proportional to the distance of the hull vertex from the pial vertex. Thus the LGI for each vertex on the pial surface reflects the amount of cortex buried in

its locality. Schaer's method has been employed to study gyrification in various conditions such as first episode psychosis (Janssen et al., 2009), depression (Zhang et al., 2009), mental retardation (Zhang et al., 2010) and 22q11 deletion (Schaer et al., 2009), and a fuller description is available at (<http://surfer.nmr.mgh.harvard.edu/fswiki/LGI>).

The binary masks obtained from VBM were registered on to a Freesurfer average image using the *bbregister* registration function in Freesurfer. This is a boundary based affine registration method that aligns images by maximizing the intensity gradient across tissue boundaries (Greve and Fischl, 2009). ROI labels were created using the outline of the masks and the labels were unwarped back onto each subject's native image. The native space labels (ROIs) were then projected onto midthickness surface obtained from each subject in line with Voets et al. (Voets et al., 2008)). Thickness, surface area and LGI values were obtained by averaging respective values from all the vertices included within the defined clusters for each subject (Figure 5.1).

Table 5.1: Demographic features of the sample

	Patients with schizophrenia	Healthy controls
Number	57	41
Gender (male/female)	50/7	39/2
Handedness (right/left)	52/5	34/7
Age range in years	19 to 47 (26.1; 7.5)	18 to 44 (28.0; 6.6)
Mean parental NS-SEC (SD)	2.5(1.6)	2.0 (1.4)

NS-SEC: National Statistics – Socio Economic Status; SD: standard deviation

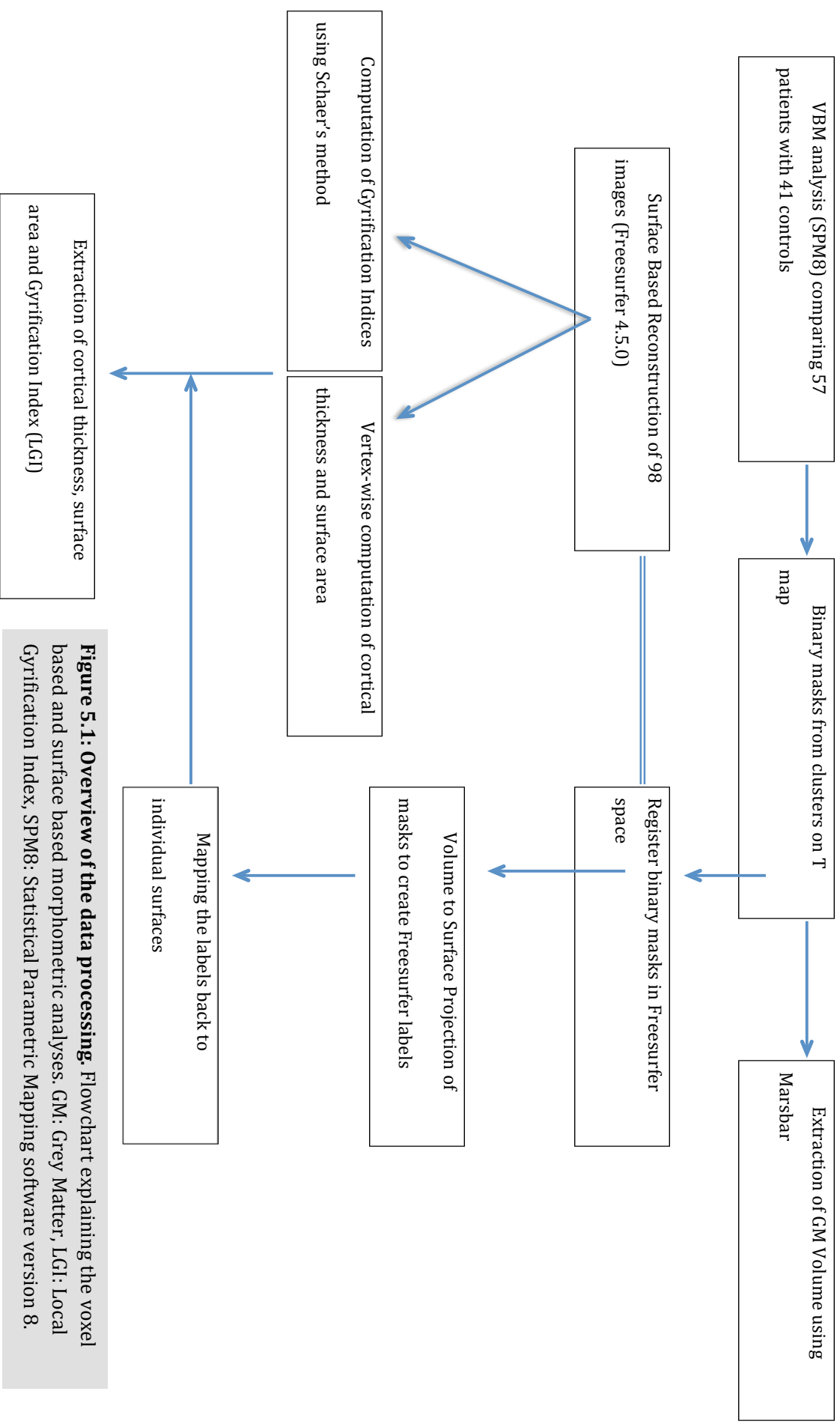


Figure 5.1: Overview of the data processing. Flowchart explaining the voxel based and surface based morphometric analyses. GM: Grey Matter, LGI: Local Gyrrification Index, SPM8: Statistical Parametric Mapping software version 8.

5.6 Statistical Analysis

Group differences in the global tissue volumes and the SBM measures from the clusters were tested using unpaired t tests. Pearson's bivariate correlation was used to test the association between global tissue volumes obtained using SBM and VBM. For regional SBM measures derived from the clusters of interest, a criterion p value set as $p=0.0125$ was employed for the four clusters.

The mediation model used in this study is shown in Figure 5.2. The multiple mediation model for each VBM cluster involved predicting GMV (dependent variable, DV) from diagnosis (independent variable, IV). The predictor was the diagnostic group membership and mediators (M) were the corresponding SBM variables (surface area, thickness and gyrification index) in each cluster. Intracranial volume was included as a covariate in the models.

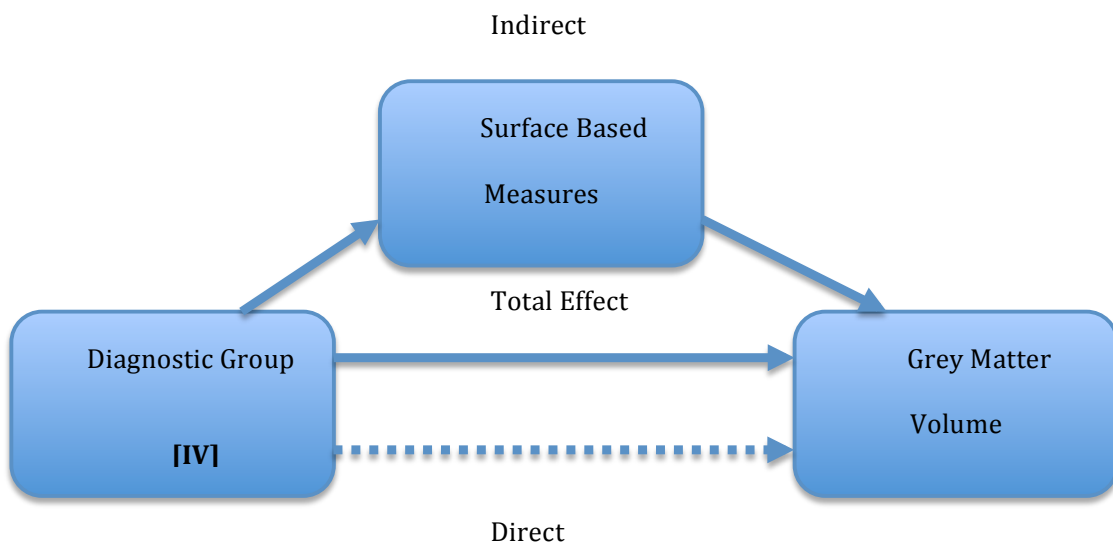
Analyses of mediation effects of the SBM variables on the relationship between IV and DV was carried out using Preacher & Hayes model of indirect mediation (Preacher and Hayes, 2004). The mediation analysis tests the hypothesis that a proportion of the variance in a dependent variable (i.e. GMV) that is predicted by variance in an independent or predictor variable (i.e. diagnosis) can be accounted for by the mediator variables (i.e. SBM measures such as gyrification), in the sense that the independent variable accounts for variance in the mediator variable and in turn, this variance in the mediator variable accounts for a proportion of the variance of the dependent variable. The adjustable parameters of the model represent the unidirectional influence between pairs of variable in the model. The best fitting values of the parameters are estimated by using the General Linear Model to solve the

linear equations that describe the relationships within the model. This analysis differs from multiple regression which estimates the proportion of variance in the dependent variable accounted for by each of several independent predictor variables while allowing for the variance accounted for by the other predictors in the model. In other words, the mediation analysis partitions the variance explained by the predictor into a part that is independent of the mediating variable, and a part that is accounted for via the mediating variable.

The Preacher and Hayes procedure used in this analysis evaluates the total, direct, and indirect effects of diagnostic status on GMV through the three SBM measures. Both a summary indirect effect (from all mediators) and individual indirect effect of each mediator was obtained. In the context of the present study, total effect in each cluster refers to the effect of diagnosis on the GMV of the cluster. The direct effect refers to the influence of diagnosis on GMV that is not mediated by the SBM measures. The summary indirect effect refers to the influence of diagnostic status on the GMV that is accounted for by the relationship between diagnosis and the three SBM measures. The individual indirect effects refer to the influence of diagnostic status on the GMV that is accounted for by the relationship between diagnosis and each of the individual SBM measures. The three SBM measures were entered simultaneously to allow investigation of the indirect effects of the different anatomical properties whilst controlling for the others. A bootstrapping approach with 5000 simulations was used to test the significance and bias-corrected 95% confidence intervals of the indirect effects (Preacher and Hayes, 2008). Effect ratios were also obtained for direct and indirect effects,

which express the proportion of the total effect that can be explained by either the direct (unmediated) or the indirect (mediated) effects (Preacher and Hayes, 2004). In other words, an indirect effect ratio of 0.25 would mean that a quarter (25%) of the total effect of the diagnostic status on the GMV is explained by the SBM measures.

Figure 5.2: The mediation model. The multiple mediation model for each cluster with VBM changes include the corresponding SBM measures (gyrification, thickness and surface area) as mediators of the relationship between diagnostic status and GMV. IV: Independent Variable, DV: Dependent Variable, M: Mediators.



RESULTS

5.7 VBM Analysis

The VBM comparison between patients and controls revealed five clusters with significant reduction in GMV (Figure 5.3). There were no regions with increased GMV in schizophrenia. As expected, bilateral insula emerged as

regions of significant GMV reduction, along with left thalamus, left precuneus and left middle temporal region. Binary masks were derived for right and left insula in addition to left middle temporal and left precuneus clusters. The MNI coordinates of the four cortical clusters and also the thalamic cluster are shown in Table 5.2.

Table 5.2: Clusters showing reduced GMD in schizophrenia compared to controls

Region	MNI Coordinates of peak difference			Size (voxels)	Tmax
	x	y	z		
Left Middle Temporal	-48	-56	18	704	6.98
Right Thalamus	10	-20	12	261	6.41
Left Insula	-38	16	0	203	5.61
Right Insula	44	6	0	418	5.60
Left Precuneus	-10	-60	46	248	5.49

MNI: Montreal Neurological Institute

5.8 SBM Analysis

SBM measures of thickness, area and LGI showed significant group differences that were variable according to the brain region (Table 5.3). In both left insula and left temporal cluster, significant group differences were seen in all three surface anatomical measures. In the left precuneus, significant reduction in surface area and gyrification but not thickness was seen. In the right insula, despite there being reductions of magnitude comparable to those observed in other clusters, the reduction in SBM measures did not reach statistical significance, though there was a trend towards significant reduction in surface area in the patients.

Table 5.3: Grey Matter Density, Cortical Thickness, Surface Area and Gyrification Index in schizophrenia compared to controls

Region		Healthy Controls	Patients	Percentage reduction	p value
Left Temporal	Grey Matter Density	0.55(0.07)	0.47(0.05)	14.54%	NA
	Surface Area	890.1 (98.9)	833.0 (113.3)	6.42%	=0.01*
	Thickness	2.63(0.15)	2.48(0.20)	5.70%	<0.001*
	Gyrification Index	3.50 (0.16)	3.37 (0.18)	3.71%	<0.001*
Left Insula	Grey Matter Density	0.63(0.06)	0.57(0.06)	9.52%	NA
	Surface Area	222.3(35.0)	204.8(31.8)	7.87%	=0.01*
	Thickness	3.44(0.35)	3.25(0.26)	5.52%	=0.004*
	Gyrification Index	4.78(0.49)	4.40(0.39)	7.95%	<0.001*
Right Insula	Grey Matter Density	0.61(0.06)	0.55(0.05)	9.84%	NA
	Surface Area	291.1 (57.5)	271.9(43.3)	6.60%	=0.06
	Thickness	3.63(0.42)	3.53(0.41)	2.76%	=0.23
	Gyrification Index	5.05(0.53)	4.87(0.87)	3.56%	=0.25
Left Precuneus	Grey Matter Density	0.54(0.08)	0.46(0.06)	14.8%	NA
	Surface Area	573.6(145.8)	460.4(93.7)	19.74%	<0.001*
	Thickness	2.39 (0.23)	2.36(0.22)	1.26%	=0.46
	Gyrification Index	3.04(0.22)	2.88(0.27)	5.26%	=0.001*

*Significant at an adjusted p value of p=0.0125

5.9 Relationship between SBM measures and GMV

Total tissue volumes (grey and white matter) obtained using SBM and VBM in each group are shown in Table 5.4. Within each group, significant correlation was seen between the global volumes obtained using the two methods.

The mediation models were significant in all four regions, implying that a considerable proportion of variance in the GMV is explained by the diagnostic status (Table 5.5). The SBM mediators, when entered into the mediation analysis, showed regionally differing pattern of mediating influence between diagnosis and the GMV. A significant overall indirect effect (mediated by the SBM measures) was observed for left insula, left precuneus and left temporal with an indirect effect ratio of 64%, 47.3%, and 36.5% respectively. The overall indirect effect was insignificant for right insula, where 79.7% of the effect of diagnosis on GMV was direct and not mediated via the SBM measures. With respect to the individual surface anatomical properties, gyrification was an influential mediator in the left insula (effect ratio of 17.8%) and left temporal clusters (effect ratio of 13.5%) while surface area was the primary mediator in the left precuneus cluster (effect ratio of 42.1%). Thickness had a significant mediating influence on the effect of diagnosis on GMV in left temporal (effect ratio of 13.5%) and left insular clusters (effect ratio of 30.1%). Table 5.5 displays the effects of the models along with the indirect effect ratios for each of the mediators in the models.

Table 5.4: Global Tissue Volumes in schizophrenia compared to controls

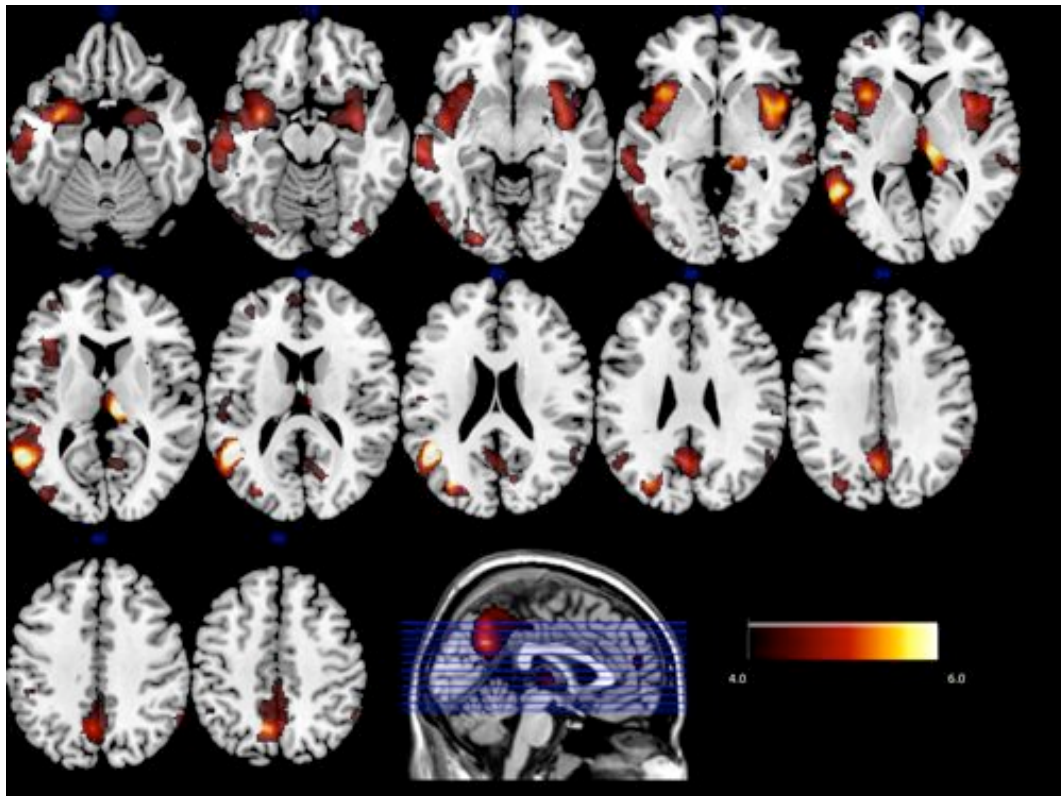
	Patients	Controls	T statistics of group differences
Total Grey Matter Volume in mls (SD)			
SPM-VBM	700.4 (60.45)	747.8 (64.22)	3.728**
Freesurfer-SBM	585.5 (59.90)	645.9 (55.09)	5.091**
SBM-VBM Correlation	r =0.812**	r =0.835**	-
Total White Matter Volume in mls (SD)			
SPM-VBM	492.5 (42.88)	522.9 (48.45)	3.277*
Freesurfer-SBM	473.0 (48.41)	505.2 (55.39)	3.051*
SBM-VBM Correlation	r= 0.844**	r= 0.869**	-

SD: Standard Deviation, SPM-VBM: Statistical Parametric Mapping – Voxel Based Morphometry, SBM – Surface Based Morphometry. *p<0.01; **p<0.001

Table 5.5: The effect of Surface Based Measures on the diagnostic differences in Grey Matter Density (* coefficient greater than zero at $p < 0.05$)

	Coefficient	SE	P values	Bootstrap 95% CI	Effect Ratio
Left Temporal					
Model	$R^2 = 0.66$; $F[5,92]=35.97$, $p < 0.00001$				
Total effect	0.052	0.010	<0.001	-	100%
Direct effect	0.033	0.010	<0.005	-	63.5%
Indirect effect (via mediators)	0.019	0.006	-	(0.008; 0.033)*	36.5%
Gyrification	0.007	0.004	-	(0.002; 0.018)*	13.5%
Surface Area	0.005	0.004	-	(-0.002; 0.015)	9.5%
Thickness	0.007	0.004	-	(0.002; 0.018)*	13.5%
Left Insula					
Model	$R^2 = 0.667$; $F[5,92]=36.82$, $p < 0.00001$				
Total effect	0.0422	0.011	<0.001	-	100%
Direct effect	0.0152	0.010	0.129	-	36.0%
Indirect effect (via mediators)	0.0270	0.008	-	(0.013; 0.042)*	64.0%
Gyrification	0.0075	0.004	-	(0.002; 0.018)*	17.8%
Surface Area	0.0069	0.006	-	(-0.005; 0.019)	16.3%
Thickness	0.0127	0.005		(0.005; 0.023)*	30.1%
Right Insula					
Model	$R^2 = 0.723$; $F[5,92]=47.90$, $p < 0.00001$				
Total effect	0.0354	0.009	<0.001	-	100%
Direct effect	0.0282	0.008	<0.001	-	79.7%
Indirect effect (via mediators)	0.0072	0.005	-	(-0.005; 0.018)	20.3%
Gyrification Index	0.0006	0.003	-	(-0.005; 0.006)	1.7%
Surface Area	0.0029	0.005	-	(-0.006; 0.011)	8.2%
Thickness	0.0037	0.004		(-0.003; 0.013)	10.4%
Left Precuneus					
Model	$R^2 = 0.524$; $F[5,92]=20.22$, $p < 0.00001$				
Total effect	0.0484	0.013	<0.001	-	100%
Direct effect	0.0255	0.130	<0.001	-	52.7%
Indirect effect (via mediators)	0.0229	0.008	-	(0.009;0.042)*	47.3%
Gyrification Index	0.0021	0.003	-	(-0.002;0. 009)	4.3%
Surface Area	0.0204	0.008	-	(0.008;0.038)*	42.1%
Thickness	0.0004	0.002	-	(-0.003;0. 006)	0.9%

Figure 5.3: VBM Clusters: Voxel Based Morphometry showing gray matter reduction in schizophrenia compared to controls. Regions that survive family-wise error correction ($p = 0.01$) are displayed. Of these regions, five cortical clusters extended to more than 200 voxels in size. See Table 2 for further details. Colour bar represents t scores



DISCUSSION

5.10 The contribution of surface anatomical changes to VBM deficits

Using VBM and SBM on a cross sectional sample with schizophrenia, the present study has shown that the differences in GMV observed using VBM are partially mediated by surface anatomical properties such as gyrification, surface area and thickness. Reduced gyrification and surface area were observed in three out of four clusters examined, while reduced thickness was observed in two clusters. But the mediating effect of the surface anatomical features on GMV is regionally variable with a large proportion of the group differences seen in VBM (between 36% and 79.7% in the present study) not being accounted for by the three surface based measures.

There are several possible reasons why only a modest proportion of variance in GMV is explained by SBM measures. Though there is a high degree of correlation between the total tissue volumes determined by the two methods (Table 5.4), the difference in the magnitude of the absolute volume of total grey matter estimated by the two methods suggest that the definition of GM/CSF boundary by SBM and VBM are dissimilar. Such measurement differences might introduce artefactual errors such that the computed values are an imprecise estimate of the relevant grey matter feature they are intended to represent. The artefactual noise would be expected to decrease the estimated proportion of variance in GMV explained by SBM measures. For example, a systematic error in the probabilistic determination of grey matter

voxels at a specific region in one group could contribute to spurious VBM defects that are not correlated with SBM measures. In this context, the presence of subtle abnormalities in sulcal pattern in schizophrenia, especially around the Sylvian fissure (Csernansky et al., 2008), could lead to less accurate alignment when using volume based registration (Anticevic et al., 2008).

Secondly, these observations show that different SBM measures account for the greatest amount of GMV variation in different clusters. This suggests that there might also be regional variations in the nature of the morphological abnormality within a single cluster, thereby weakening the overall relationship between each SBM measure and the GMV for that cluster. This inhomogeneity might be present across and/or within subjects. Regions with large variations between subjects in surface anatomy may fail to show significant group differences in SBM studies, though for the composite GMV measure, the variance within groups may be less pronounced. Some evidence for the latter was observed at the right insula in this sample, where a comparatively large variance for gyrification was noted. As a result, the clusters that show significant group differences in a VBM map are not necessarily homogenous in terms of the underlying morphological change.

Varying combination of structural changes that include gyrification, surface area contraction and cortical thinning contribute to the findings in a VBM study. While isolated cortical thinning or surface area reduction could result in reduced GMV in some regions, it is possible that in other regions modest non-significant changes in several of the SBM measures might combine to produce a significant GMV reduction. In such circumstances, SBM features

may provide a more sensitive index of grey matter abnormality. Using both VBM and SBM may better identify regions with isolated surface anatomical changes of comparatively smaller effect. This conclusion is largely consistent with previous observations that suggest only a partial overlap exist between regions showing VBM changes and those showing cortical thickness changes (Hutton et al., 2009; Voets et al., 2008). Voets et al (2008) studied the spatial distribution of SBM based thickness changes and VBM based GMV changes. In regions that showed VBM deficits but no cortical thinning, a reduction in surface area was observed. The direct contribution of the SBM measures to the observed VBM changes was not investigated in the previous studies.

While neither GMV nor SBM measures are directly related to molecular aspects of grey matter structure, SBM measures can be related more directly to specific developmental processes. Accumulating evidence suggests that thickness and surface area are independently heritable properties with differing developmental trajectories (Joyner et al., 2009; Panizzon et al., 2009; Rimol et al., 2010; Winkler et al., 2009, 2010). According to Rakic's radial unit hypothesis (Rakic, 1988), symmetrical neuronal proliferation in the ventricular zone along with a tangential expansion contributes to the development of surface area. Non-symmetrical proliferation with radial neuronal migration contributes to cortical thickness. The disproportionate scaling factors for thickness and surface area observed both within and across the species reflect a tight ontogenic and phylogenic control over the cortical anatomy (Herculano-Houzel et al., 2010; Im et al., 2008). As a result, the identification of brain regions with specific surface anatomical changes is likely to be

informative in the study of pathophysiology of disorders of cortical development such as schizophrenia.

A specific contribution of cortical gyrification to the VBM based GMV is reported for the first time. Gyrification is closely linked to the process of neuronal migration and cortico-cortical connectivity in the developing brain (White and Hilgetag, 2011). The gyrification measured used in the present study is a composite measure combining both the spatial frequency of sulcal fissures and the depth of these fissures in a given region (Schaer et al., 2008). Either or both of these differences in cortical folding could contribute to VBM based GMV changes in schizophrenia.

The relationships between VBM based GMV and SBM measures were investigated in a sample of patients with schizophrenia. The observations relate to the differences between schizophrenia and healthy age matched controls, and may not apply for VBM based GMV differences measured in other disease states. Further, the present sample is predominantly male, precluding a direct generalization of these observations to female subjects. A previous observation suggests that significant sex by diagnosis interactions are not observed for GMV though thickness profiles may be different between the genders (Narr et al., 2005). Both VBM and SBM measures are indirect measures. In the present study cortical clusters with significant GMV increase were not observed in schizophrenia; the mediating effect of SBM measures may be different in regions with pathological increase in GMV.

In summary, multiple distinguishable aspects of cortical development such as gyrification, surface area expansion and regional cortical thickness are

impaired in schizophrenia. These alterations contribute to the grey matter deficit observed in schizophrenia using VBM based GMV. Significant regional variation in the relationship between surface based measures and VBM suggests that reduced GMV is an index of diverse pathophysiological processes in different brain regions. Studies investigating the mechanisms of disease expression in schizophrenia such as those using genetic association methods may be better informed when using both SBM and VBM in a complementary fashion.

The observation that is of specific interest to the current work is the difference in the mediating effect of surface anatomical changes to the VBM deficit of the left and the right insula. Whilst a substantial portion of the volumetric changes in the right insula are not explained by surface anatomical changes, the GMV changes of the left insula are largely mediated by changes in either thickness or gyrification. These two properties require further consideration for us to understand the nature of insula structural deficits in schizophrenia, especially on the left hemisphere. In the next chapter, a detailed evaluation of gyrification changes across the entire brain surface in the same sample of patients is reported.

Chapter 6

Aberrant Cortical Gyrification in Schizophrenia

As noted in the previous chapter, surface anatomical properties such as gyrification and thickness are significantly altered in patients with schizophrenia resulting in localized patterns of morphometric changes in patients. Schizophrenia is considered to be a disorder of cerebral connectivity associated with disturbances of cortical development. Disturbances in cortical connectivity at an early period of cortical maturation can result in widespread defects in the complexity of cortical folding (i.e. gyral and sulcal formation, also called as gyrification). Investigating the anatomical distribution of gyrification defects can provide important information about neurodevelopment in schizophrenia and will clarify if insula is affected by a putative developmental aberration in patients. In this chapter, we present automated surface based morphometric assessment of gyrification on 3-dimensionally reconstructed cortical surfaces across multiple vertices that cover the entire cortex in the same sample of patients who were shown to have significant VBM deficits in chapter 5. Patients with schizophrenia reveal a prominent reduction of cortical folding around the perisylvian fissure, involving the left insula.

6.1 Cortical folding patterns in schizophrenia

Schizophrenia is regarded as a disorder of connectivity associated with neurodevelopmental abnormality (Friston, 1998). Despite accumulating evidence for disturbances in functional connectivity (Pettersson-Yeo et al., 2011), it is unclear how these findings are related to defective cortical development.

Developmental aberrations can affect several characteristic anatomical features of the grey matter surface. Cortical development is constrained by both the need for developing a cost-efficient wiring scheme wherein signal transmission is quick and effective (Casanova and Tillquist, 2008), and the limitations on the total brain size partly to facilitate parturition (Deacon, 1990; Montagu, 1961). This is facilitated by a substantial expansion of surface area along with a high degree of cortical folding, despite relatively minor gain in cortical thickness during evolutionary development (Laughlin and Sejnowski, 2003). This remarkable dissociation between thickness and surface area persists in human adult brains (Toro et al., 2008).

Axonal connections in the developing brain are considered to be one of the several factors that influence the morphology of the cortical surface (Hilgetag and Barbas, 2005). In particular, a widely accepted model of cortical morphogenesis suggests that the appearance of cortical convolutions is dependent on the underlying neuronal connectivity (Essen, 1997). Disturbances in regional cortical gyrification can be a surrogate marker for disruptions in neuronal connectivity during development (Essen, 1997; White and Hilgetag, 2011).

As discussed previously in chapter 2, the majority of studies examining neuroanatomical changes in schizophrenia have employed voxel-based morphometry (VBM) and report consistent volume reduction bilaterally in the insula and anterior cingulate cortex (ACC). Compared to the number of VBM studies, relatively few have attempted to locate gyrification defects within the entire cortex in schizophrenia (see White & Hilgetag (2011) for a detailed review). Most previous investigations have quantified differences in gyrification at preselected regions of interest (ROI), especially the cingulate (Wheeler and Harper, 2007; Yücel et al., 2002) and the prefrontal cortex (Bonnici et al., 2007; Falkai et al., 2007; Vogetley et al., 2000). As a result, unlike the robust evidence localizing volumetric changes in schizophrenia to the insula, the spatial distribution of focal gyrification abnormalities in schizophrenia is currently unclear. Nonetheless, there is a consistent trend for region-of-interest studies to report hypergyria in the most anterior regions of the frontal cortex (Harris et al., 2004a; McIntosh et al., 2009) suggesting that there are consistent abnormalities in gyrification in schizophrenia. If widespread abnormalities are present, this might reflect a deviation of the neurodevelopmental processes that produce gyrification; abnormalities confined to specific pathways might indicate a more focal defect that affects regions that are mutually connected. In particular, the insula is a region of specific interest while investigating cortical folding in schizophrenia, not only due to its relevance to the illness (as discussed in the previous chapters), but also as it has been shown to be one of the earliest brain regions to develop gyrification (Chi et al., 1977; Kalani et al., 2009; Wai et al., 2008) with an accelerated growth rate when compared to the surrounding cortical plate during fetal development (Rajagopalan et al., 2011) .

The search for the brain region with most significant gyrification defect in schizophrenia is hampered by several methodological issues (Mangin et al., 2010). Zilles' gyrification index (the ratio between the inner folded contour and the outer curvature) (Zilles et al., 1988), though commonly used (White and Hilgetag, 2011), does not capture the regional changes that are associated with subtle deviations in cortical connectivity. Its use is further limited by the use of 2-dimensional slices whose orientation and thickness could bias the measurements leading to inconclusive results.

To address these issues, we undertook a blinded automated assessment of gyrification in multiple vertices across the whole of 3-dimensionally reconstructed cerebral surfaces in a sample of 57 patients, in whom VBM deficits have already been demonstrated (Chapter 5) in comparison with 41 controls. On account of the need for stringent correction for multiple comparisons when undertaking a whole brain search, this study would only be anticipated to detect regions with a large effect size of between-group differences but nonetheless offers the possibility of determining whether or not substantial abnormalities of gyrification occur in multiple brain regions in schizophrenia, including the insula and the anterior cingulate cortex. Further, to investigate if cortical thinning is associated with the pathogenetic processes resulting in abnormal gyrification, cortical thickness was also studied in regions showing gyrification abnormalities in schizophrenia.

6.2 Methods

A detailed description of participants recruited for this study has been provided in chapter 5 and 6. In brief, the sample comprised of 98 subjects (57

with schizophrenia and 41 healthy controls), mostly referred from community mental health teams representing a predominantly early phase sample. The demographic properties of this sample are described in Table 5.1.

Image acquisition parameters are also described in Chapter 5. Surface extraction was completed using FreeSurfer version 4.5.0 (Dale et al., 1999). The preprocessing was performed as described by Dale (1999) and reported in detail for this sample in the previous chapter (chapter 5). Cortical thickness values were computed using the methods developed by Fischl and Dale (2000).

Local gyrification indices (LGIs) were obtained using the method of Schaer (2008) using images reconstructed through the FreeSurfer pipeline. Schaer's method is a vertex-wise extension of Zilles' gyrification index, which gives a ratio of the inner folded contour to the outer perimeter of the cortex (Zilles et al., 1988). This method has been described in detail in chapter 5. This procedure yield a local gyrification index (LGI) for each vertex on the pial surface that reflects the amount of cortex buried in its locality.

6.3 Statistical Analysis: Whole Brain Cortical Maps

Each vertex-wise LGI measurement of the subjects' surface was mapped on a common spherical coordinate system (fsaverage) using a spherical transformation. Maps were smoothed using a Gaussian kernel of 5 mm. A general linear model controlling for the effect of age and total cortical surface area was used to estimate differences in gyrification between the groups at each vertex of the right and left hemispheric surfaces. Total surface area was chosen as a covariate as it has a linear relationship with gyrification (Luders et

al., 2006). This model allowed for the possibility that the slope for the relationship between LGI and total surface area may be different in different brain regions(Luders et al., 2006). Query Design Estimate Contrast (QDEC) tool in the Freesurfer program was used to generate the contrasts. Monte Carlo permutation cluster analyses was carried out with 10,000 simulations to identify significant clusters with vertex-wise group differences (cluster inclusion threshold $p=0.0001$). To examine the effect of gender, we carried out the same analysis after excluding the 9 female subjects. To produce a visual display of the group comparison (t maps) we used the reconstructed grey-white boundary of the fsaverage image, which allows anatomical landmarks to be illustrated clearly.

6.4 Statistical Analysis: Regional cortical thickness

Using ANCOVA, the mean values of cortical thickness from each of the significant clusters obtained from the gyrification analysis were compared between the two groups. Age, gender and global mean thickness were used as covariates. The significance levels of group comparison of mean thickness within clusters were Bonferroni corrected to allow for the number of clusters examined. To relate LGI to cortical thickness within regions that showed abnormalities in both thickness and LGI, Pearson correlation was computed between mean LGI and cortical thickness values after removing the variance due to age, gender and appropriate global covariates for thickness (global mean thickness) and LGI (global mean LGI) in the entire sample (patients and controls). This was followed by Fisher's r -to- z transformation to compare the correlation in the two groups. Correlations were also sought between the

thickness and gyrification measures and antipsychotic dose in chlorpromazine equivalents in the patients group (Wood).

RESULTS

6.5 Whole brain gyrification defects

There were no significant differences in demographic features including age ($t(1,96) = -1.32, p=0.17$) and parental socioeconomic status (Mann-Whitney U Test, $Z = -1.46, p=0.16$) between the two groups (Table 6.1). The mean total symptom score on the SSPI was 10.3 out of a maximum of 80 (range: 0 to 29), indicating a low symptom burden. The mean score on Reality Distortion (delusions and hallucinations) among the patient group was 3 (range: 0 to 7). The mean score on Psychomotor Poverty dimension was 2.9 (range: 0 to 9) and on Disorganisation dimension was 0.74 (range: 0 to 4).

Whole brain analysis revealed four clusters in the left hemisphere and a single cluster in the right hemisphere with significant reduction in gyrification in patients compared to controls. The largest cluster included left insula extending to pars opercularis and superior temporal gyrus. Other clusters are shown in Figure 6.1 and Table 6.1. The right hemispheric cluster included the junction between caudal superior temporal and inferior parietal regions. No regions with increased gyrification in the patients were noted at this threshold. Exclusion of 9 female subjects did not alter the results substantially.

Table 6.1: Clusters showing group differences in gyrification [threshold for inclusion in a cluster p=0.0001]

Cortical Region	Talairach coordinates of the centroid	Cluster Size (mm ²)	Clusterwise probability
Left Insula	-37,-1,1	6094	0.0001
Left caudal superior and middle frontal cortex	-23,4,47	2345	0.0001
Left parieto-occipital sulcus	-11,-65,31	2339	0.0001
Left superior temporal/ inferior parietal junction	-43,-61,14	698	0.0001
Right superior temporal/ inferior parietal junction	49,-53,11	543	0.0001

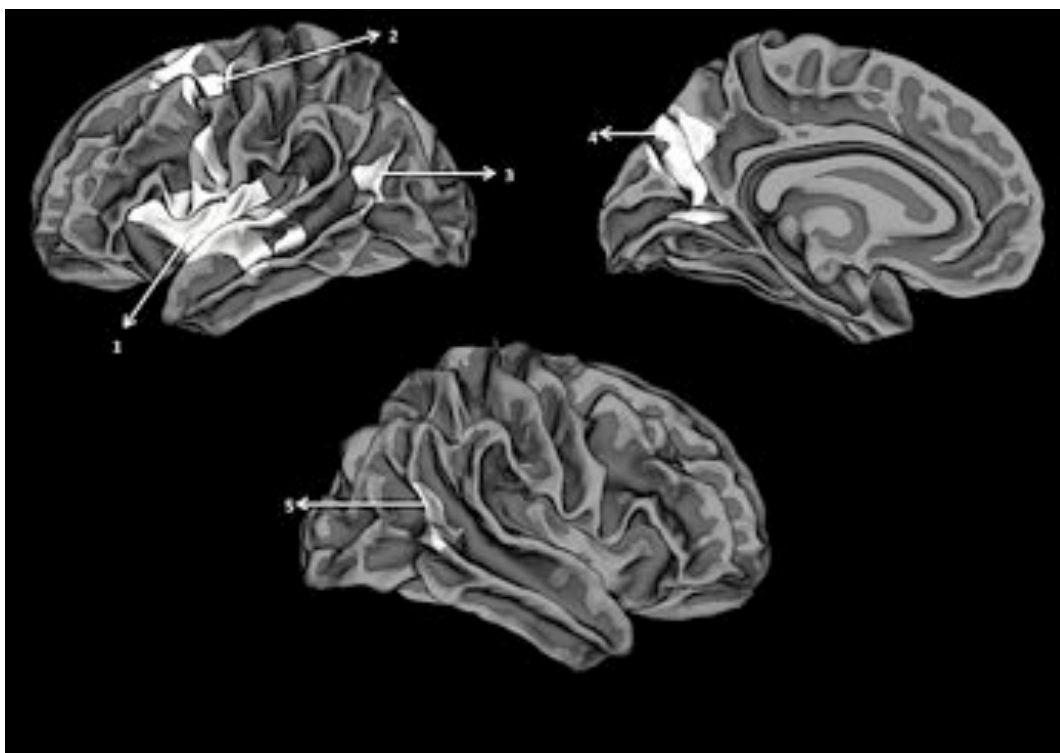


Figure 6.1: Clusters showing hypogyria in schizophrenia compared to healthy controls displayed on a reconstructed average white matter surface (fsaverage). All displayed clusters survived multiple testing using Monte-Carlo simulation with a cluster inclusion criterion of $p=0.0001$. Left hemisphere (top panel): 1. Left Insula extending to inferior frontal gyrus and superior temporal gyrus 2. Left caudal middle and superior frontal cluster 3. Superior temporal /inferior parietal cluster 4. Left parieto-occipital cluster extending to precuneus. Right hemisphere (bottom): 5. Right superior temporal / inferior parietal cluster.

Table 6.2: Percentage reduction in gyrification and thickness in patients compared to controls. LGI: Local Gyrification Index (no units). SD: Standard deviation.

Cortical Region	Mean LGI (SD)			Mean thickness in mm (SD)		
	Patients	Controls	Percentage reduction in patients	Patients	Controls	Percentage reduction in patients
Left Insula	4.47(0.30)	4.85(0.47)	7.84%*	2.61(0.12)	2.75(0.11)	5.09% ^a
Left caudal superior and middle frontal	2.88 (0.19)	3.07(0.15)	5.88%*	2.42 (0.15)	2.41 (0.16)	-0.41% ^c
Left parieto-occipital sulcus	3.02 (0.23)	3.21(0.23)	5.94%*	2.24(0.16)	2.28(0.13)	1.75% ^c
Left superior temporal/inferior parietal junction	3.28 (0.18)	3.43(0.15)	4.67%*	2.45(0.19)	2.53(0.16)	3.16% ^c
Right superior temporal/inferior parietal junction	3.42(0.15)	3.55(0.19)	3.67%*	2.47(0.21)	2.60(0.20)	5% ^b

*: Clusterwise significance at $p=0.0001$ (permutation test $n=10,000$)

a: Bonferroni corrected $p<0.0001$

b: Bonferroni corrected $p<0.1$

c: Bonferroni corrected $p>0.1$

The average reduction in gyrification within clusters ranged from 7.84% to 3.67% (Table 6.3). The greatest degree of hypogyria was seen in the left insula. Significant cortical thinning was observed only in the left insula ($F[1,93]=30.1$, corrected $p = 0.007 \times 10^{-6}$) with a trend towards thinning in the right temporal cluster ($F[1,93]=6.06$, corrected $p = 0.08$) in patients (Table 6.2). In the left insula, there was a significant correlation between gyrification and thickness for the whole sample ($r=0.22$, $p=0.028$, $n=98$) with a significant difference between patients and controls in this relationship ($r[\text{patients}]=0.30$, $r[\text{controls}]=-0.17$, Fisher's r -to- z test $p=0.023$). The correlation was significant in patients but not in controls. There were no significant correlations between the gyrification or thickness values and current antipsychotic dose or total disease duration in any of the examined clusters.

6.6 Post-hoc tests of asymmetry and sulcogyral thinning

Given the prominent hypogyria noted in the left insular cluster, a post-hoc analysis of hemispheric differences in gyrification and thickness was carried out. By drawing ROI labels guided by landmarks on the fsaverage surface a homologous mask was generated on the right insula. To ensure comparability, the Destrieux parcellation scheme (Destrieux et al., 2010) was used for visual inspection of the contiguous regions included in the respective ROI labels from each hemisphere. This right insula mask was mapped back on to the surface of each subject using the same spherical coordinate system used for the initial analysis. The right homologous insular cluster showed a 4.13% reduction in LGI in patients with a trend towards statistical significance (mean (SD) LGI in controls=4.84(0.45), patients= 4.64(0.63), uncorrected $p=0.08$). Comparison of asymmetry index ($AI = (\text{Left}-\text{Right}) \times 100 / (\text{Left}+\text{Right})$) revealed

a significant group difference in the asymmetry of insular gyrification ($t(1,96)=2.028$, $p=0.045$; AI in controls = 0.16 L>R, AI in patients = -1.5 R>L). A significant cortical thinning (4.61%) was also noted in the right homologous cluster in patients compared to controls (mean (SD) thickness in mm in controls=2.82(0.13), patients= 2.69(0.13), uncorrected $p<0.001$). No significant hemispheric differences in thickness was notable between the two groups ($t(1,96)=0.825$, $p=0.412$; AI in controls = -1.17 R>L, AI in patients = -1.45 R>L).

Various observations suggest that in healthy controls, cerebral gyri are generally thicker than the sulci (Hilgetag and Barbas, 2005; Welker, 1990). Among many possible mechanisms that can produce such a difference, the variation in axonal tension during development is thought to be an important mechanism (Essen, 1997). The major sulci were separated from the gyri within the hypogyric insular cluster by overlaying the cluster mask on Destrieux atlas (Destrieux et al., 2010) and mean thickness was computed for the three gyral (short insular gyrus, inferior frontal opercular gyrus and superior temporal gyrus) and sulcal regions (anterior, superior and inferior circular sulci) included in the mask. Long insular gyrus was not included as due to its inconsistent appearance; the central sulcus of the insula and the long insular gyri were grouped in the same label in the parcellation scheme. An ANCOVA with diagnosis as between subjects factor, and regions (sulcal vs. gyral) as within-subjects factor, with age, gender and global thickness as covariates revealed no significant interaction between diagnosis and the sulcogyral division ($F(1,93)=1.62$, $p=0.206$). Both sulcal (partial eta = 0.16,

$p < 0.0001$) and gyral regions (partial $\eta = 0.11$, $p = 0.001$) showed significant thinning in schizophrenia when compared to controls.

Figure 6.2: Clusters showing hypergyria in schizophrenia compared to healthy controls. The clusters are displayed on the anterior aspect of a reconstructed average white matter surface (fsaverage). All displayed clusters survived multiple testing using Monte-Carlo simulation with a cluster inclusion criterion of $p = 0.05$. 1. Right frontomarginal cluster 2. Left frontomarginal cluster. No other hypergyric clusters were observed in the vertex-wise analysis.

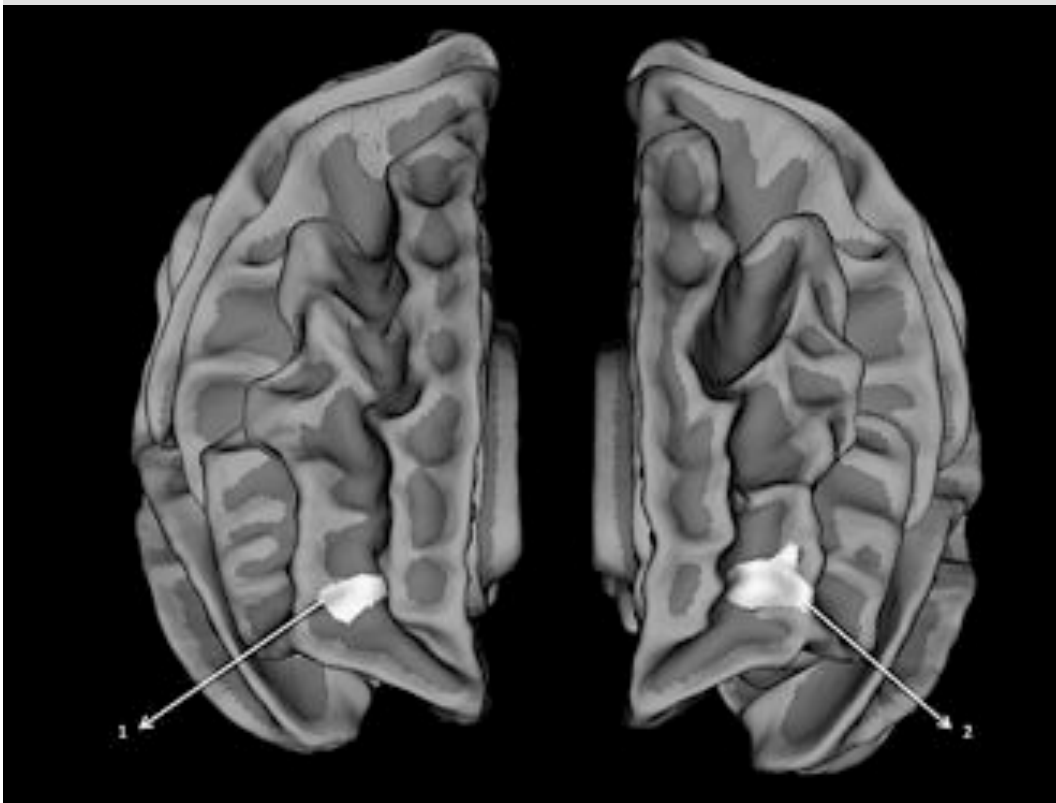


Table 6.3: Clusters showing increased gyrification in patients at a lower threshold for inclusion in a cluster [p=0.05]

6.7 Search for increased gyrification

Despite the substantial sample size, the need for stringent correction for multiple comparisons in a whole-brain vertex-wise search creates a risk of failing to identify cerebral regions in which there are relatively small abnormalities. Using a region of interest approach to test the specific hypothesis of abnormal frontal gyrification in the same sample (Palaniyappan et al., 2011), our group has previously shown that hypergyria is localized to a circumscribed part of the prefrontal cortex, and the normal laterality of the frontal gyrification was reversed in patients. This effect might not survive the stringent correction for multiple comparisons in the current study; as a result we used a more lenient statistical threshold to search for regions showing

Cortical Region	Talairach coordinates of the centroid	Cluster Size (mm²)	Clusterwise probability
Right frontomarginal	32, 50,1	144	0.039
Left frontomarginal	-29, 48,1	260	0.030

hypergyria. Bilateral frontomarginal hypergyria in patients was observed in this analysis. These results are shown in Table 6.3.

DISCUSSION

6.8 Insular hypogyria

Using a surface based vertex-wise morphometric approach we observed a significant reduction in gyrification in patients with schizophrenia. The hypogyria was more pronounced in the left hemisphere, with the greatest reduction occurring in the left insula, extending onto superior temporal gyrus and sulcus posteriorly and the Broca's area anteriorly. These extensions of the insular cluster are larger than that could be accounted for by the smoothing employed in the present study, consistent with the concept that the fronto-insular cortex acts as a coordinated unit (Craig, 2009; Seeley et al., 2007).

Gyrification maps used in the present study contain information about distribution of cortical convolutions and resulting complexity based on the amount of grey matter that is buried in the neighbourhood of multiple vertices on the pial surface. Insofar as the degree of folding across the different regions in the cortex varies with the rate of maturation of those regions (Finlay et al., 2001; Hill et al., 2010; Rajagopalan et al., 2011; Toro et al., 2008), the gyrification metrics provide crucial information about neurodevelopmental aberrations. To quantify gyrification, we used Schaer's LGI, which captures changes in both the frequency and the depth of sulcogyral transitions in the cortical surface (Schaer et al., 2008). Thus LGI reflects the biological process of cortical folding more closely than measuring either the sulcal depth (Cachia et al., 2008) or frequency of curvature changes (Narr et al., 2001) independently. Nonetheless the current results are comparable to those

obtained using a sulcal-wise gyrification measure in a selected group of patients with persistent hallucinations by Cachia et al. (2008). Though the defect was more pronounced on the left, consistent with many previous observations (Cachia et al., 2008; White and Hilgetag, 2011), we also found a trend towards hypogyria on the right insula along with a significant group difference in the hemispheric asymmetry. Patients exhibited a reversal of the normal tendency for greater insula gyrification on the left.

The significant insular hypogyria might be partially explained using the tension-based morphogenetic theory (Essen, 1997) which suggests that cortical folding is a result of radial tension during brain development, wherein established axonal networks resist radial while allowing tangential expansion. It is likely that insular connections with more medial grey matter preclude outward expansion of its grey matter, leading to sequestration of the insula within lateral fissure during normal development. Some support to the existence of such a medial tract comes from studies on interoceptive system in primates (Craig, 2003) and olfactory system in other animals (Buchanan and Johnson, 2011). Given that insular folding is deficient in schizophrenia, it is likely that connectivity of insula to more medial regions of grey matter, possibly cingulate cortex, is impaired in schizophrenia. As discussed in chapters 1 and 2, The connections between the two paralimbic structures, insula and anterior cingulate, constitutes the Salience Network (Seeley et al., 2007). This observation that the hypothesized state of insular dysfunction and the resultant failure in the generation of proximal salience during stimulus evaluation is likely to have a significant contribution from the developmental abnormalities in schizophrenia.

Differential changes in the thickness of gyri and sulci would be expected if the insular hypogyria were solely due to fewer axonal connections creating less axonal tension. But no differences were observed between the sulci and the gyri. It is likely that developmental factors other than axonal tension account for folding. The principal mechanical effect of cortical folding has been noted to produce differential thickness changes in the superficial and deep layers of cortical laminae of the sulci and gyri (Hilgetag and Barbas, 2006, 2005), the examination of which requires a cytoarchitectural study. The current observation of combined gyral and sulcal thinning in the hypogyric insular cluster suggest that in addition to reduced connectivity, other mechanisms contributing to the development of the cortex may be affected in schizophrenia. Goldman-Rakic and Rakic (1984) examined the effect of the timing of prenatal cortical lesions on subsequent gyrification and suggested that neuronal migration, which eventually contributes to the thickness of cortical sheet predates gyrification. Investigating the gyrification of regions showing cortical thinning in adolescents with schizophrenia, Janssen et al. (2009) found no correlation between gyrification and thickness in most regions and suggested that cortical thinning may be a late developmental phenomenon in schizophrenia. The current results are largely consistent with Janssen et al. (2009), though we did observe a correlation between these two metrics in left insula which was specific to patients. It is likely that in healthy controls, the degree of gyrification is not the principal determinant of cortical thickness. On the contrary, the association of hypogyria with sulcogyral thinning in patients may suggest that a developmental disturbance, possibly predating the dissociation between radial and tangential cortical expansions during early phases of cortical development (Martínez-Cerdeño et al., 2006).

This is supported by the observation that insula is one of the earliest brain structures to show gyrification and neuronal differentiation and thus forms a core zone of sulcal and gyral maturation during the normal intrauterine growth (Afif et al., 2007).

6.9 Multimodal cortical gyrification in schizophrenia

Most of the other regions showing hypogyria in schizophrenia (inferior frontal, superior temporal and inferior parietal regions), belong to the multimodal (heteromodal) association cortex described by Mesulam (2000). A pathological perturbation in the development of multimodal association areas has been previously suggested as the core deficit in schizophrenia (Ross and Pearlson, 1996). In healthy individuals, the regions constituting the multimodal association cortex show a prolonged maturational trajectory, attaining peak grey matter density at a later stage of development when compared to unimodal sensory regions (Gogtay et al., 2004). This slow maturation may be linked to the relatively higher degree of cortical folding normally observed in these regions (Finlay and Darlington, 1995). An abnormally premature, delayed or arrested growth peak in these regions could putatively account for the reduced gyrification observed in schizophrenia. But the present observation that reduced gyrification is not limited to multimodal regions but extends to paralimbic cortices supports the hypothesis that a developmental abnormality in the connectivity within and between paralimbic and multimodal association areas is a characteristic feature of schizophrenia. Alternatively, the combined paralimbic and multimodal hypogyria could be related to a shared defect in foetal thalamocortical connectivity in schizophrenia (Lewis, 2000). According to the tension based morphogenesis model, if the axonal

tension is the primary determinant of gyrification then a weakening of connectivity affecting specific pathways may result in relatively greater tension in other pathways leading to local hypergyria (White and Hilgetag, 2011), suggesting that the increased gyrification observed in the frontomarginal region could be developmentally related to the extensive hypogyria noted in other multimodal/paralimbic regions. In fact, the presence of hypergyria in anteriormost regions of frontal cortex has been shown to predict the development of schizophrenia in high-risk individuals (Harris et al., 2004b).

Gender differences have been noted in some (Narr et al., 2004; Vogeley et al., 2000) but not all (Bonnici et al., 2007; Cachia et al., 2008) studies investigating gyrification in schizophrenia. The present sample is predominantly male precluding a meaningful analysis of gender effect on gyrification in schizophrenia. Hence the results presented here must be interpreted with caution for mixed samples. All patients in the present study were taking antipsychotic medications. The effect of antipsychotics on brain structure is a matter of debate, but similarly to Cachia et al. (2008), no correlation was found between gyrification and antipsychotic dose in the preceding 6 weeks. It is possible that earlier treatments could have affected the brain structure. The results presented here should be interpreted cautiously until replicated in unmedicated samples.

In summary, the present study demonstrates a significant abnormality in cortical gyrification in schizophrenia. The localisation of these changes to insula and regions of multimodal association cortex and the observed relationship of insular hypogyria with reduced cortical thickness in patients suggests a prominent role for a developmental abnormality of connectivity of

the insula and the multimodal cortex in the pathophysiology of schizophrenia. Future studies focussing on the interaction between insula and the multimodal association regions are required to test the functional consequences of these gyrification defects.

An important approach required to appreciate the pathophysiology of schizophrenia is delineating the unique and shared neurobiological features between schizophrenia and bipolar disorder with psychosis. In the next chapter, the issue of specificity of gyrification defects in schizophrenia and the spatial overlap between functional connectivity deficits and gyrification deficits are investigated.

Chapter 7

Diagnostic specificity of gyrification defects and functional connectivity

Insula is a major cortical hub with wide ranging functional connectivity across the entire brain (chapter 2). When the entire cerebral surface anatomy is examined, patients with schizophrenia reveal a prominent reduction of cortical folding involving the left insula (chapter 6). Two questions arise from this observation 1. Is this prominence of insular hypogyria specific to the diagnosis of schizophrenia? 2. Do patients with prominent insular hypogyria show corresponding loss of the prominence of insula as a functional hub? In this chapter, gyrification and functional connectivity hub architecture (degree centrality) were studied in a sample of 39 subjects with established schizophrenia, 20 subjects with psychotic bipolar disorder, and 34 healthy controls. A combined reduction in gyrification and functional connectivity of the left insula was more prominent in schizophrenia than in bipolar disorder with psychosis. This study also revealed disturbances in the integrity of gyrification and functional connectivity in relation to the Kraepelinian 'line of divide' between schizophrenia and bipolar disorder.

7.1 Kraepelinian dichotomy

Significant nosological uncertainty over Kraepelin's description of two major psychotic disorders persists to date. While several observations suggest the existence of overlapping pathophysiological processes in schizophrenia and bipolar disorder (Whalley et al., 2012), the point of rarity in brain structure and function at which the two disorders differ is elusive.

Structural imaging studies have mostly used voxel based morphometric approach to differentiate the two disorders. Meta-analytic conjunction approaches seeking the anatomical likelihood of the overlap between the two disorders reveal shared VBM deficits in bilateral insula and anterior cingulate cortex (Ellison-Wright and Bullmore, 2010). So far, direct comparisons have not established any regional brain changes that separate these two illnesses. It is possible that subtle changes exist in the surface anatomy that is not captured by studying volumetric changes in the grey matter (as shown in chapter 5). Some support for this notion comes from Rimol et al. (2012), who observe that while volume changes occur in both groups, deformation of the cortical surface appears more specific to schizophrenia. Cortical gyrification (or folding) is a promising surface anatomical marker to study schizophrenia and bipolar disorder (White and Hilgetag, 2011). Cortical folding patterns are established during early phases of development, and are likely to be affected by a higher burden of aberrant neurodevelopment reported in schizophrenia (Demjaha et al., 2011). In addition, as folding patterns are tightly linked to underlying neural connectivity (White and Hilgetag, 2011), gyrification appears to be a compelling candidate to investigate the Kraepelinian dichotomy.

There is an increasing realization that the functional integration, rather than regional specialization in the brain, is likely to be abnormal in psychosis, with several studies in schizophrenia suggesting an inefficient recruitment of distributed brain regions during task performance (Pettersson-Yeo et al., 2011). To date, fMRI studies contrasting bipolar disorder and schizophrenia have mostly used task activation approaches, and observe similar regional brain dysfunction in both disorders (Whalley et al., 2012). This approach does not directly address the possible differences that may exist in the efficiency of cerebral recruitment in the two groups and fails to capture the system-level disintegration in the neural networks. In recent times, several approaches have been proposed to measure the integrative functions of brain regions using fMRI. A promising method is studying the number of instantaneous functional connections (or correlations) between a region and the rest of the brain, also called Degree Centrality (DC) (Buckner et al., 2009). This approach has established the notion of cortical hubs, specialized brain regions that show high DC and thus influence a number of other brain regions. The core architecture formed by cortical hubs is consistent and stable in healthy human brain, but highly vulnerable to pathological processes (Buckner et al., 2009; Drzezga et al., 2011). Both structural and functional studies indicate the loss of prominence of multimodal cortical hubs and the emergence of peripheral hubs in unimodal cortex in schizophrenia (Bassett et al., 2008; Li et al., 2012). Whether such a shift in the cortical topology is specific to schizophrenia is yet to be investigated.

Behavioural (Chen et al., 2005) and electrophysiological studies (Hamm et al., 2012) comparing patients with bipolar disorder schizophrenia suggest that

early sensory processing deficits may be specific to schizophrenia, with fMRI studies finding converging group differences localized to unimodal regions such as the extrastriate visual association cortex (Curtis et al., 2001; Ongür et al., 2010). On the other hand, paralimbic brain regions constituting large scale brain networks such as the insula and anterior cingulate cortex show prominent but shared structural alterations in the two disorders when VBM approach is employed (Ellison-Wright and Bullmore, 2010). In the light of these observations, overlapping abnormalities in the structure and function across the two psychotic disorders were expected in the multimodal brain regions and the limbic/paralimbic cortex, while schizophrenia specific defects were expected to be restricted to unimodal sensory processing areas.

A sample of patients with either bipolar disorder with psychotic symptoms (BPP) or schizophrenia (SCZP) and healthy controls were recruited to study the cortical gyrification from structural MRI and the DC from functional MRI using an executive/working memory task (n-back). In addition to examining the integrity of the core cortical hub architecture, the emergence of peripheral hubs were also examined in patients. The three groups were compared with each other; in addition a conjunction analyses was also carried out to identify the degree of overlap (or similarity) in the abnormalities common to both disorders.

7.2 Participants

The data used in the current chapter were obtained from an independent sample, different from the one reported in chapters 5 and 6.

The original sample consisted of 43 patients with schizophrenia, 22 patients with bipolar disorder and 40 controls, but 11 subjects (3 patients with schizophrenia, 2 with bipolar disorder and 6 controls) were excluded due to due to movement artefacts, while 1 subject with schizophrenia did not complete the n-back acquisition protocol as planned. From the sample of 93 subjects with n-back data, 2 patients with schizophrenia and 1 with bipolar disorder had poor quality structural scans due to excessive movement, providing a final sample size of n=90 for gyrification analysis. Good quality resting fMRI data was available for 38 patients with schizophrenia, 19 with bipolar disorder and 35 healthy controls. There were no differences in the symptom severity (mean (SD) in the included group= 10.5(7.7), excluded group= 11.3(9.5), $p=0.86$) between patients who were included or excluded in the analysis.

The final sample consisted of 39 patients satisfying DSM-IV criteria for schizophrenia, 20 patients with bipolar disorder with psychotic features and 34 healthy controls. Patients were recruited from the community based mental health teams (including Early Intervention in Psychosis teams) in Nottinghamshire and Leicestershire, UK. The diagnosis was made in a clinical consensus meeting in accordance with the procedure of Leckman et al.(1982), using all available information including a review of case files and a standardized clinical interview (Symptoms and Signs in Psychotic Illness (SSPI)(Liddle et al., 2002)). All patients were in a stable phase of illness (defined as a change of no more than 10 points in their Global Assessment of Function (GAF, DSM-IV) score, assessed six weeks prior and immediately prior to study participation). No patient had a change in antipsychotic,

antidepressant or mood stabilizing medications in the six weeks prior to the study. Subjects with age <18 or >50, subjects with neurological disorders, current substance dependence, or IQ < 70 using Quick Test (Ammons and Ammons, 1962) were excluded. 54 out of 59 patients were receiving psychotropic medications. The median Defined Daily Dose (WHO Collaborating Centre for Drug Statistics and Methodology, 2003) was calculated separately for antipsychotics, mood stabilisers (including lithium) and antidepressants. Patients were interviewed on the same day as the scan and symptom scores assigned according to the SSPI.

Healthy controls were recruited from the local community via advertisements and included 34 subjects free of any psychiatric or neurological disorder group-matched for age and parental socio-economic status (measured using National Statistics - Socio Economic Classification(Rose and Pevalin, 2003)) to the patient group. Controls had similar exclusion criteria to patients; in addition subjects with personal or family history of psychotic illness were excluded. A clinical interview by a research psychiatrist was employed to ensure that the controls were free from current axis 1 disorder and history of either psychotic illness or neurological disorder. The study was given ethical approval by the National Research Ethics Committee, Derbyshire, UK. All volunteers gave written informed consent. The sample characteristics are shown in Table 6.1.

Table 7.1: Demographic and clinical features

	Healthy controls (n=34)	Patients with bipolar disorder (n=20)	Patients with schizophrenia (n=39)	F/ χ^2
Gender (male/female)	23/11	13/7	30/9	$\chi^2=1.2$, p=0.55
Handedness (right/left)	31/3	18/2	34/5	$\chi^2=4.0$, p=0.41
Age in years (SD)	33.76(9.0)	35.25(10.8)	34.18(9.3)	F=0.16, p=0.86
Mean parental NS-SEC (SD)	2.00(1.3)	1.8(1.2)	2.4(1.5)	F=1.33, p=0.27
Accuracy in % (SD)	92.38(8.2)	91.77(6.1)	86.14(14.0)	F=3.46, p=0.036
Mean total SSPI score	-	7.50(8.1)	11.74(7.4)	F=3.78, p=0.06
Reality Distortion	-	0.44(1.3)	2.21(2.6)	F=7.48, p=0.008
Disorganisation	-	1.28(2.1)	1.36(1.3)	F=10.04, p=0.003
Psychomotor Poverty	-	2.77(3.5)	1.92(3.2)	F=0.03, p=0.86

NS-SEC: National Statistics – Socio Economic Status; SD: standard deviation; SSPI – Symptoms and Signs of Psychotic Illness. The total SSPI score can vary between 0 and 80. Reality distortion (delusions and hallucinations) can vary between 0 and 8. Psychomotor poverty (anhedonia, underactivity, poverty of speech and flat affect) can vary between 0 and 16. Disorganisation (inappropriate affect, disordered thought form and poor attention) can vary between 0 and 12.

7.3 Image acquisition

Blood oxygenation level-dependent (BOLD) fMRI datasets were acquired on a 3 Tesla Philips Achieva MRI scanner (Philips, Netherlands). To enhance sensitivity, dual-echo gradient-echo echo-planar images (GE-EPI) were acquired (Gowland and Bowtell, 2007), using an eight-channel SENSE head coil with SENSE factor 2 in anterior-posterior direction, TE1/TE2 25/53 ms, flip angle 85°, 255 x 255 mm field of view, with an in-plane resolution of 3 mm x 3 mm and a slice thickness of 4 mm, and TR of 2500 ms. For the n-back task,

at each dynamic time point a volume dataset was acquired consisting of 40 contiguous axial slices acquired in descending order. 410 dynamic time points were acquired during an entire n-back session, with 2 sessions in total per subject. For the resting-phase fMRI, 240 time points were acquired during the 10 minutes resting phase wherein the subjects were instructed to keep their eyes open and to relax, without the need to focus on any particular task with the same acquisition parameters as above (40 axial slices in descending order, 240 time points per resting acquisition).

A magnetisation prepared rapid acquisition gradient echo image with 1 mm isotropic resolution, 256 x 256 x160 matrix, TR/TE 8.1/3.7 ms, shot interval 3 s, flip angle 8°, SENSE factor 2 was also acquired for each participant for reconstructing the anatomical surface.

A visual n-back task was used with a button press response in 2 sessions of fMRI recording. 7 task-blocks each of 110 seconds duration were presented in each session. Each task-block consisted of 0-back, 1-back and 2-back conditions (randomly selected alphabets) of 30 seconds duration each presented in a random sequence, with 10 seconds interval between the conditions. On screen instructions preceded every condition indicating the type of response required (0, 1 or 2 back). Each condition included 4 target and 11 non-target stimuli with a 2 seconds inter-stimulus interval. To ensure adequate task comprehension and performance, all participants performed a practice version of the task outside the scanner prior to scanning. All scanned participants successfully identified in excess of 80 % of targets in the practice task. The performance accuracy of this task is presented in Table 7.1.

7.4 Image processing

The fMRI data was preprocessed using SPM8 (<http://www.fil.ion.ucl.ac.uk/spm>) and Data Processing Assistant for resting-state fMRI (Chao-Gan and Yu-Feng, 2010)). After an initial correction for slice-timing differences, spatial realignment to the first image was carried out. Participants were excluded if movement parameters exceeded 3 mm. An interpolation method (ArtRepair: <http://cibsr.stanford.edu/tools/human-brain-project/artrepair-software.html>) was used to correct movement artefacts. A single weighted summation of the dual-echo dynamic time course was obtained for each subject (Posse et al., 1999), followed by retrospective physiological correction using RETROICOR (Glover et al., 2000). Unified segmentation based spatial normalization and smoothing using a Gaussian kernel of 8 mm Full-Width at Half Maximum was carried out. Following this, linear detrending and filtering using a band pass filter (0.01-0.08 Hz) was done to eliminate low frequency fluctuations and high frequency noise. Finally, variance accounted for by six head motion parameters, global mean signal, white-matter signal and CSF signal was removed by regression before conducting the degree centrality (DC) analysis. The same preprocessing procedure was followed for both n-back data and resting data.

Preprocessed data was analysed by deriving degree centrality measure for every grey matter voxel using the cortical hub analysis procedure described by Buckner et al., (2009) and implemented in the REST software (Chao-Gan and Yu-Feng, 2010). For each voxel, the BOLD time course was

extracted and correlated with every other voxel in the brain. For each voxel j the number of strong voxel-to-voxel correlations (defined as correlation coefficient $r > 0.25$) was computed to determine the DC of j . The threshold of 0.25 was chosen to minimize the risk of inclusion of voxels whose correlation with the index voxel could be accounted for by noise in the centrality estimate for the index voxel. For each subject, a map with DC values for every grey matter voxel was obtained. These maps were then z-transformed to enable group comparisons. The computation of normalized DC maps was done separately for both resting state acquisition and the n-back acquisition.

For gyrification analysis, cortical surfaces were reconstructed using FreeSurfer version 5.1.0. The preprocessing was performed using standard procedures as described by Dale et al. (1999). To measure cortical folding patterns for each of the several thousands of vertices across the entire cortical surface, the method advocated by Schaer et al (2008) and described in chapter 6 was used.

7.4 Statistical Analysis

Core-hub centrality: To determine the core cortical hub architecture, the significant clusters with high DC across the entire sample were identified using one sample t test (FWE corrected error rate of 5%, cluster extent threshold = 30 voxels). A single mean value of the normalized DC measure in each voxel included in the core hubs was computed for each subject; this represented the mean DC of the core (DCC). An ANCOVA was used to compare the DCC among the three groups, after taking into account the effect of age and gender. The effect of including the overall n-back accuracy scores

as covariates was also tested, as this was significantly different among the groups. This analysis was repeated for the centrality maps derived during resting state.

Spatial distribution of group differences: To examine the differences between the two disorders in DC on a voxelwise basis across the entire brain, direct between-group comparisons (SCZP vs. BPP contrast) were carried out with a familywise error corrected type 1 error rate of 5% at a voxelwise threshold of $p=0.001$. In addition, each patient group was compared with the control group, at the same statistical threshold. All group comparisons included age, gender and n-back accuracy scores as covariates. This analysis was repeated for the centrality maps derived during resting state.

Gyrification analysis: The vertex-wise LGI measurement for each subject was mapped on a common spherical coordinate system (*fsaverage*) to enable group comparisons. A general linear model controlling for the effect of age and gender was used to compute differences in gyrification between the groups at each vertex of the right and left hemispheric surfaces. Query Design Estimate Contrast (QDEC) tool in the Freesurfer program was used to generate the contrasts. To correct for multiple testing Monte-Carlo simulations ($n=10,000$) were used to identify clusters that survived a type 1 error rate of 5% at a cluster inclusion threshold of $p=0.05$. In a different sample of subjects (chapter 6) it has been shown that both increased and decreased gyrification in schizophrenia is observable at this threshold.

Degree of overlap between the two disorders: To compute the topographical overlap in the abnormalities seen in BPP and SCZP, an intersection (overlap) mask and a combination (union) mask were derived for the contrasts controls vs. SCZP and controls vs. BPP. Then the Dice-coefficient of similarity (DCS)(Drzezga et al., 2011; Zou et al., 2004) was calculated between the 2 groups for the two imaging modalities (DC and gyrification maps). Conjunction measures such as DCS provide more reliable results when every signal of interest is included in the individual contrasts (Duncan et al., 2009). To enable this, an uncorrected threshold of $p=0.05$ was used when extracting the intersection and the combination masks. A DCS value of 100% means that the disorders have perfect spatial agreement in the distribution of abnormalities across the brain.

7.5 Results: Core hubs

The core hub regions showing significant DC in the entire sample is shown in Table 7.2 and Figure 7.1. The results of the one sample t test of centrality maps derived from resting state fMRI in the entire group are shown in table 7.3 and figure 7.2. The core hubs observed during the resting state were essentially the same as the core hubs noted in the n-back data (Figure 7.3). Cerebellum and dorsolateral prefrontal cortex were more prominent during n-back task, while the right insula was more prominent during rest.

Comparison of the mean DCC during n-back across the three groups revealed no significant differences ($F[2,87]=1.25$, $p=0.29$; mean (SD) of DCC in controls = 0.54(0.23), SCZP = 0.46(0.32), BPP = 0.47(0.17)). Age ($F[1,88]=16.4$, $p<0.001$), but not gender ($F[1,88]=1.35$, $p=0.25$) had a

significant effect on DCC during n-back. The inclusion of n-back accuracy ($p=0.3$) or the exclusion of age and gender as covariates did not affect the results ($p=0.22$). Similarly, the comparison of the mean DCC during resting state across the three groups revealed no significant differences ($F[2,87]=0.22$, $p=0.81$; mean (SD) of DCC in controls = $0.67(0.33)$, SCZP = $0.60(0.39)$, BPP = $0.63(0.33)$). Age ($F[1,87]=25.5$, $p<0.001$), but not gender ($F[1,87]=0.58$, $p=0.45$) had a significant effect on the resting-state DCC. The exclusion of age and gender as covariates did not affect the results ($p=0.71$).

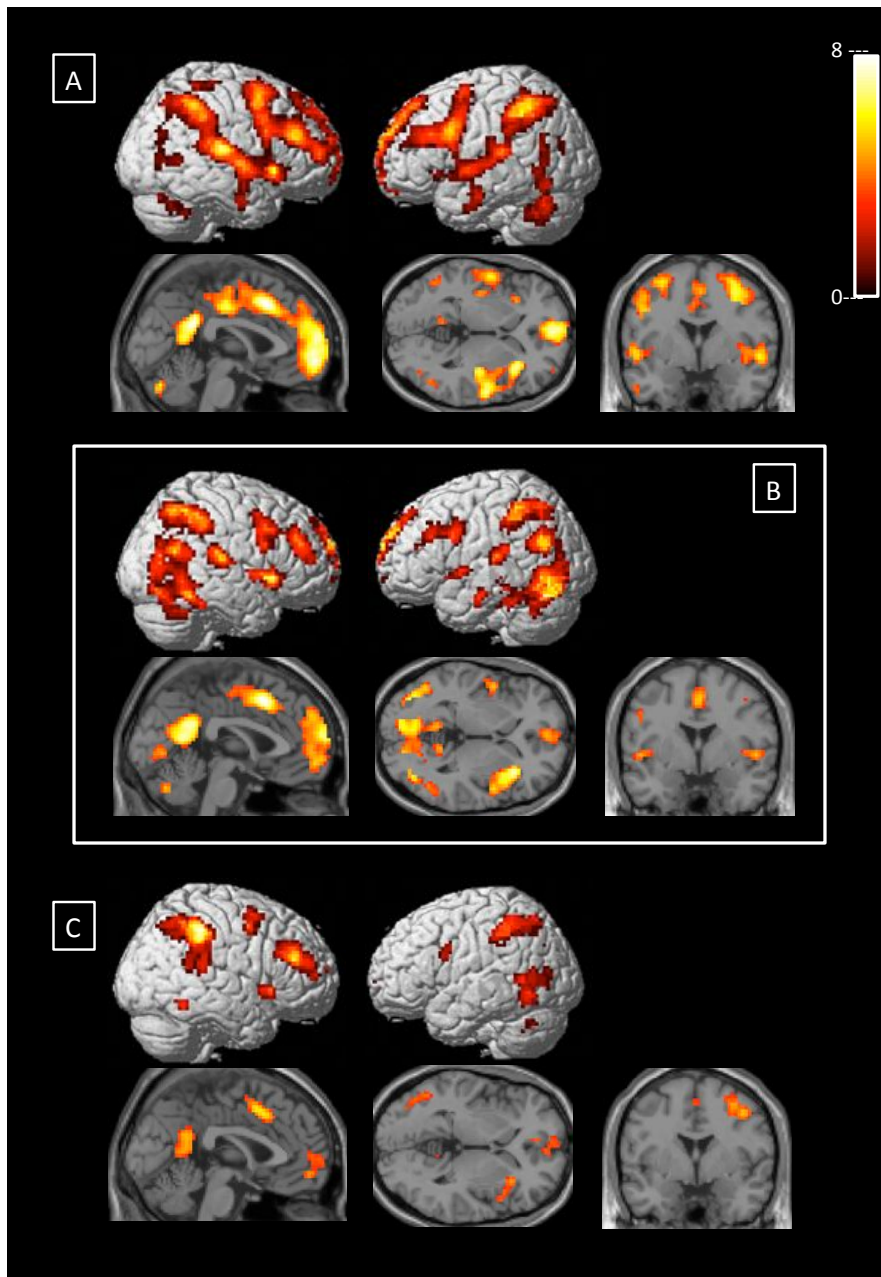


Figure 7.1: One sample T test of degree centrality in the three groups from the n-back data. Images are rendered on surfaces using xjview, with coronal, axial and sagittal slices (at $x=0,y=0,z=0$) selected to display core hubs not visible on the rendered surface. For display purposes, the images are thresholded at uncorrected $p=0.001$, with cluster extent of $k=30$. A. Controls B. Schizophrenia C. Bipolar disorder

Table 7.2: Coordinates of maximum clusters derived from whole brain analysis of degree centrality during n-back test representing significant cortical hubs in the entire sample (including patients and controls) (FWE corrected $p < 0.05$, $k=30$)

Brain region	Peak MNI coordinates (x,y,z) in mm	Peak T intensity	Cluster extent (number of voxels)
Left inferior/superior parietal lobule and superior temporal gyrus.	-42 -42 42	13.66	1433
Right inferior/superior parietal lobule and superior temporal gyrus.	48 -42 45	13.21	1381
Posterior cingulate/precuneus	-6 -48 24	12.76	488
Medial superior frontal gyrus	3 15 45	12.65	1332
Right middle/inferior frontal gyrus (DLPFC)	42 39 24	11.72	691
Left cerebellar crus	-9 -75 -27	10.97	150
Left middle/inferior frontal gyrus (DLPFC)	-48 9 27	10.40	270
Right cerebellar crus	30 -63 -33	9.14	67
Left middle temporal gyrus	-57 -12 -24	8.14	51
Right inferior temporal gyrus	57 -9 -30	7.84	45
Right inferior temporal gyrus	51 -51 -15	7.76	67
Left precentral gyrus	-30 0 57	7.21	49
Left superior temporal gyrus	-51 0 0	6.70	52
Right lingual / fusiform gyrus	21 -72 -9	6.47	77

FWE = cluster level family-wise correction for multiple comparisons.

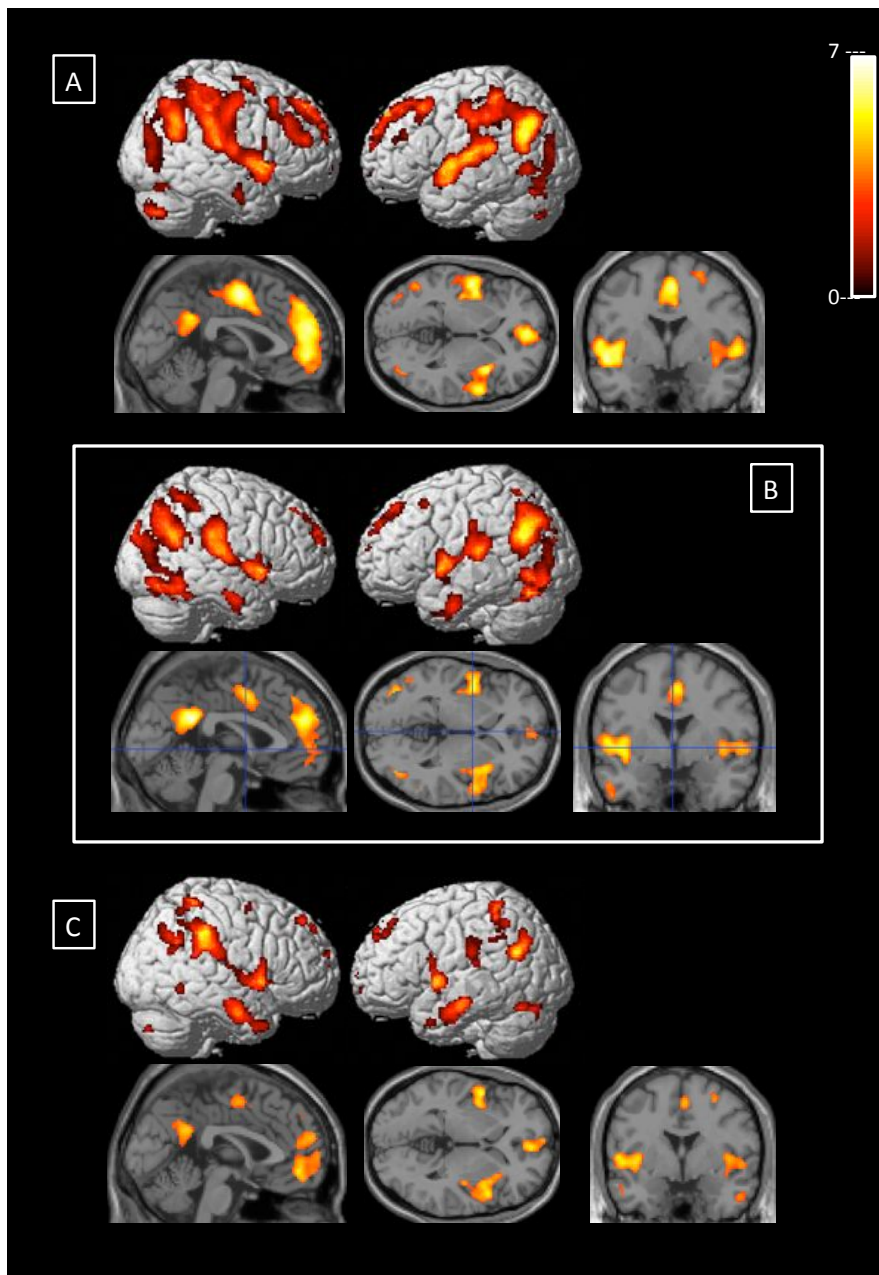


Figure 7.2: One sample T test of degree centrality at rest in the three groups. Images are rendered on surfaces using xjview, with medial and coronal views selected to display core hubs not visible on the rendered surface. For display purposes, the images are thresholded at uncorrected $p=0.001$, with cluster extent of $k=30$. A. Controls B. Schizophrenia C. Bipolar disorder.

Table 7.3: Coordinates of maximum clusters derived from whole brain analysis of degree centrality representing significant cortical hubs in the entire sample (including patients and controls) during rest (FWE corrected $p < 0.05$, $k = 30$)

Brain region	Peak MNI coordinates (x,y,z) in mm	Peak T intensity	Cluster extent (number of voxels)
Left inferior parietal and superior/middle temporal gyrus	-52, -64, 26	11.52	1653
Medial superior frontal and anterior cingulate gyrus	6, 50, 14	10.10	2931
Right inferior parietal and superior temporal gyrus	56, -62, 24	9.75	980
Posterior cingulate/precuneus	-2, -48, 28	9.73	714
Left insula, supramarginal/superior temporal gyrus	-42, 0, 0	9.71	1852
Supplementary motor area and dorsal anterior cingulate	2, -2, 50	9.62	677
Right insula, supramarginal and superior temporal gyrus	38, 10, -2	9.49	3728
Right middle and inferior temporal gyrus	56, -10, -24	8.06	191
Left middle/superior occipital gyrus	28, -80, 18	7.19	293
Left fusiform / middle occipital and middle temporal gyrus	-50, -64, -2	7.08	924
Left middle and inferior temporal gyrus	-56, -6, -24	7.00	179
Right fusiform/lingual gyrus extending to cerebellum declive	26, 58, -12	6.87	323
Left middle frontal gyrus	-34, 16, 52	6.62	68
Right inferior temporal gyrus	50, -52, -14	6.39	70
Left superior parietal/precuneus	-16, -58, 58	6.27	85
Right superior and middle frontal gyrus	26, -2, 62	5.53	37

FWE = cluster level family-wise correction for multiple comparisons.

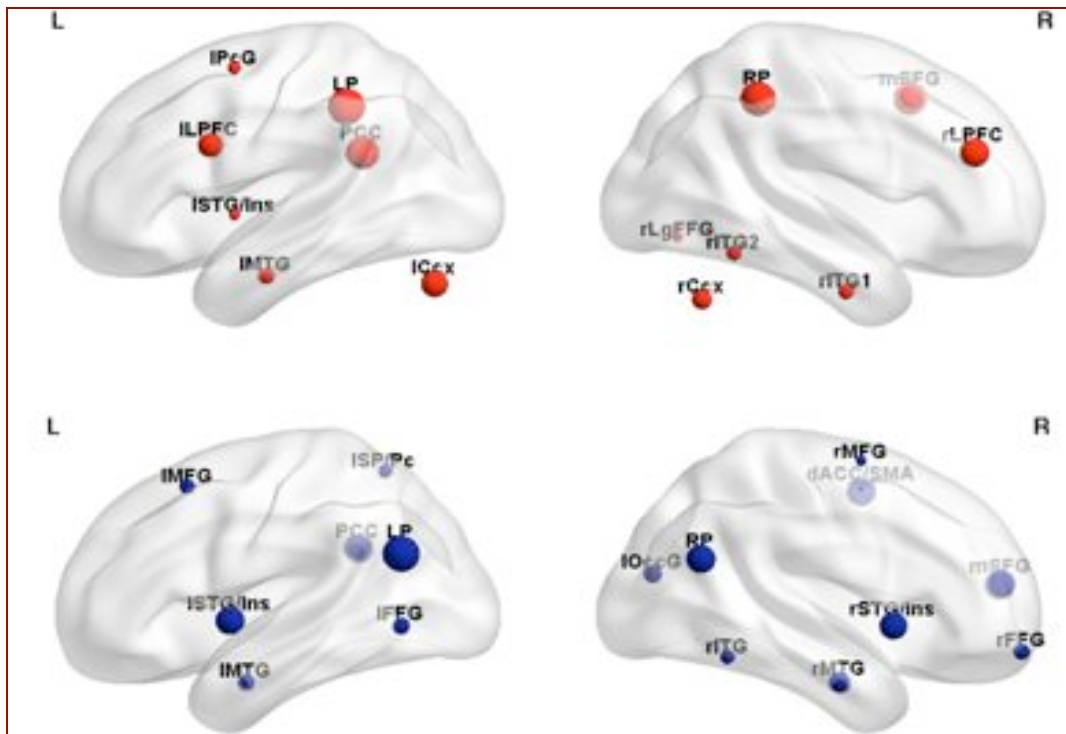


Figure 7.3: Cortical hubs from resting and task-performance data. The hubs were derived from one sample T test of the entire sample (controls, schizophrenia and bipolar groups). Top panel represents n-back data. Bottom panel represents resting data. The size of the nodes represents the T values from the one sample T test. Labels are derived from the peak coordinates for each cluster. The nodes are displayed using the BrainNet Viewer (<http://www.nitrc.org/projects/bnv/>) on a partially inflated template brain surface.

TOP: Left parietal cortex (LP), Right parietal cortex (RP), Posterior cingulate/precuneus (PCC), Medial superior frontal gyrus (mSFG), Right lateral (middle/inferior) prefrontal cortex (rLPFC), Left cerebellar crus (LCcx), Left lateral (middle/inferior) prefrontal cortex (lLPFC), Right cerebellar crus (RCcx) Left middle temporal gyrus (lMTG), Right inferior temporal gyrus (rITG1 and rITG2), Left precentral gyrus (lPcG), Left insula and superior temporal gyrus (lSTG/Ins), Right lingual / fusiform gyrus (rLgFFG). BOTTOM: Left parietal cortex (LP); Medial superior frontal and anterior cingulate gyrus (mSFG); Right parietal cortex (RP); Posterior cingulate/precuneus (PCC); Left insula, and superior temporal gyrus (lSTG/Ins); Supplementary motor area and dorsal anterior cingulate (dACC/SMA); Right insula and superior temporal gyrus (rSTG/Ins); Right middle and inferior temporal gyrus (rMTG); Left middle/superior occipital gyrus (lOccG); Left fusiform gyrus (lFFG); Left middle temporal gyrus (lMTG); Right fusiform gyrus (rFFG); Left middle frontal gyrus (lMFG); Right inferior temporal gyrus (rITG); Left superior parietal/precuneus (lSP/Pc); Right superior and middle frontal gyrus (rMFG)

7.6 Results: Group differences in centrality

Voxelwise comparisons revealed significant differences among the groups (Table 7.4) in the DC of several brain regions during n-back performance. In both groups, there was a decrease in DC relative to controls in the right insula, though the location of the cluster was more posterior than expected. Both groups of patients showed higher DC in bilateral hippocampus/parahippocampal regions extending to the thalamus (Figure 7.4). In addition, SCZP showed significant increase in DC in left fusiform/lingual and inferior occipital gyrus. Compared to BPP, patients with SCZP showed higher centrality in left calcarine/lingual gyrus and anterior cerebellum but reduced DC in right supramarginal gyrus.

The group comparison for the resting state centrality analysis is shown in Table 7.5. In general, the group differences were less prominent for resting fMRI. Most notably, the group contrasts revealed that patients with SCZ had higher DC in the cerebellar crus and fusiform gyrus compared to patients with BPP during both rest and n-back task performance. Patients with BPP had higher DC in right supramarginal gyrus compared to SCZ during both rest and n-back task performance. When compared to controls, patients with schizophrenia had prominent increase in DC of the fusiform and parahippocampal clusters in both the resting and n-back data.

Table 7.4 : Degree centrality differences between patients and controls during n-back task (uncorrected $p < 0.001$, $k = 30$).

Comparison	Brain region	Peak MNI coordinates (x,y,z) in mm	Peak T intensity	Cluster extent (no. of voxels)
Controls>Schizophrenia	Right superior temporal gyrus*	33 6 -24	5.39	48
	Right insula*	45 -15 3	4.95	137
	Left superior frontal gyrus	-3 36 60	4.54	35
	Left inferior frontal gyrus*	-39 24 12	4.37	64
	Left inferior parietal lobule	-42 -54 42	4.24	37
Controls>Bipolar	Right insula*	45 -12 3	4.51	102
Schizophrenia>Controls	Left fusiform, lingual and inferior occipital gyrus*	-21 -81 -9	6.29	434
	Bilateral hippocampus, parahippocampal gyrus and thalamus*	-36 -33 -12	5.72	438
Bipolar>Controls	Right fusiform, lingual and inferior temporal gyrus	36 -63 -12	4.58	154
	Right hippocampus and parahippocampal gyrus *	24 -24 -9	5.59	164
	Left hippocampus, parahippocampal gyrus and thalamus	-30 -42 -3	5.31	363
	Left caudate	-9 6 -12	4.47	49
	Right inferior temporal	51 -48 -27	4.37	51
Bipolar>Schizophrenia	Right supramarginal gyrus*	57 -39 39	4.24	96
Schizophrenia>Bipolar	Cerebellum Anterior Lobe*	36 -48 -30	4.80	83
	Left calcarine sulcus and lingual gyrus*	-6 -84 0	3.85	37

* Regions that survive cluster level family-wise correction at $p < 0.05$ for multiple comparisons.

Figure 7.4: Group differences in degree centrality from n-back fMRI in patients with schizophrenia compared to bipolar disorder. Illustrations drawn on a single subject structural image with slices selected for the best display of regions showing differences in the two sample t test. Top panel (A) displays schizophrenia vs. controls contrast; Middle panel (B) displays bipolar disorder vs. controls contrast. In A and B, warm colours refer to higher degree centrality in controls. Bottom panel (C) shows schizophrenia>bipolar disorder contrast in the upper row and bipolar disorder>schizophrenia contrast in the lower row. Colour bars show scales of T values.

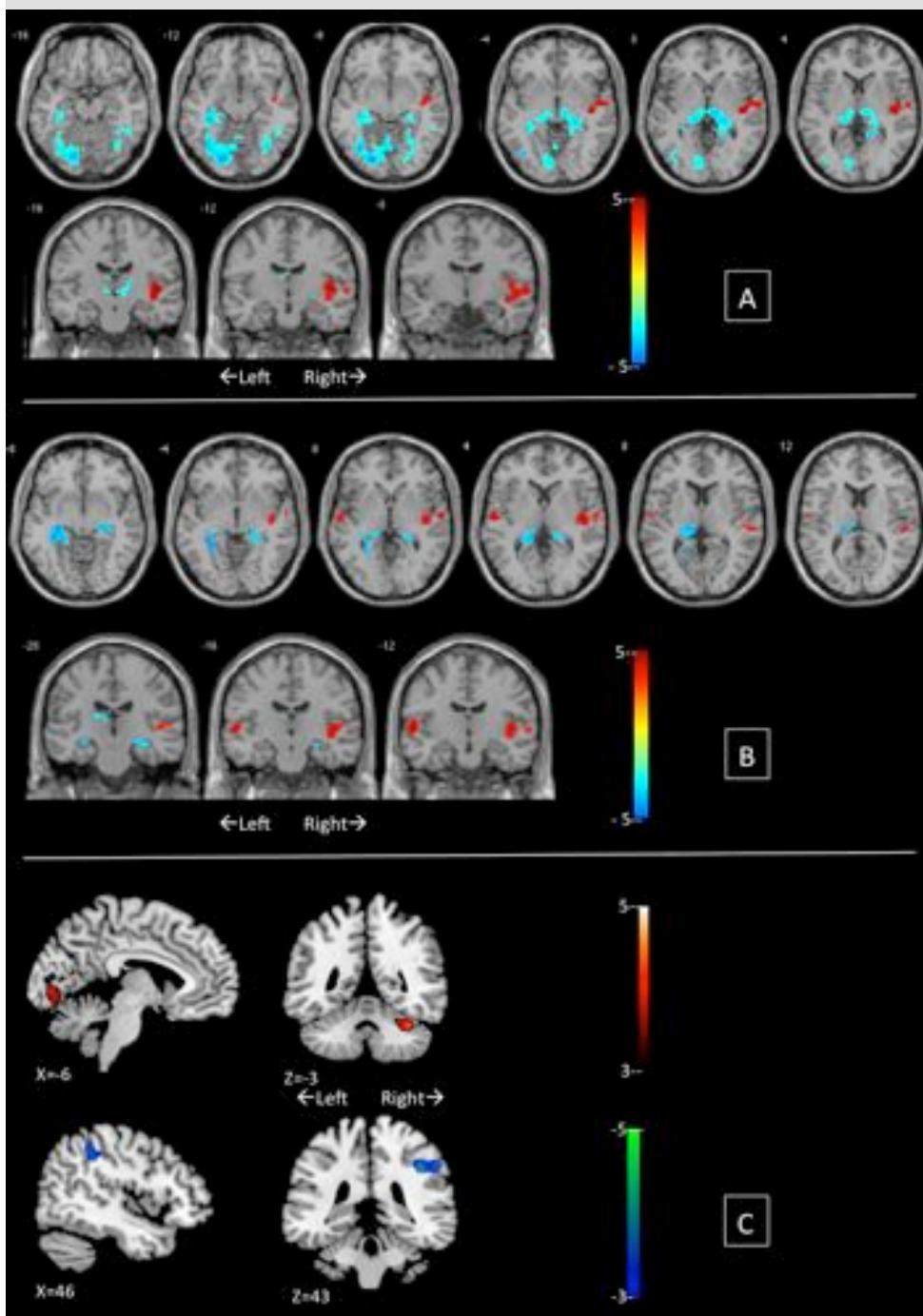


Table 7.5 : Degree centrality differences between patients and controls during rest (uncorrected p<0.001, k=30). *FWE p<0.05

Comparison	Brain region	Peak MNI coordinates (x,y,z) mm	Peak T intensity	Cluster extent (no. voxels)
Controls>Schizophrenia	Paracentral lobule	2 -32 56	4.48	117
	Right precentral gyrus	36 -24 46	4.44	401
	Cerebellum posterior lobe and crus	44 -70 -42	4.42	264
	Right middle frontal gyrus	44 38 18	4.40	100
	Left inferior frontal gyrus	-42 30 12	4.25	104
	Left superior temporal gyrus	-50 4 -10	4.24	98
	Anterior cingulate	0 42 -4	3.82	41
	Left precentral gyrus	-36 -18 58	3.67	66
	Left postcentral gyrus	-50 -8 42	3.65	37
	Right precentral gyrus	46 -12 46	4.49	112
Controls>Bipolar	Left precentral gyrus	-48 -10 44	3.93	74
	Left inferior temporal and fusiform gyrus*	-42 -16 -38	5.58	1305
Schizophrenia>Controls	Right inferior temporal and fusiform gyrus*	36 -18 -36	5.33	736
	Right fusiform gyrus	28 4 -44	4.61	89
	Right parahippocampal gyrus	28 -30 -14	4.33	76
	Right inferior temporal gyrus	50 -24 -22	4.95	78
Bipolar>Controls	Right temporal pole	42 10 -34	4.58	139
	Left temporal pole	-52 14 -24	4.06	38
	Left inferior temporal gyrus	-54 -20 -22	3.89	112
Bipolar>Schizophrenia	Right supramarginal gyrus	56 -36 36	4.44	90
Schizophrenia>Bipolar	Right cerebellar crus	46 -44 -38	4.40	31
	Right fusiform gyrus	28 0 -46	3.88	36

7.7 Results: Group differences in gyrification

Significant group differences were also noted in gyrification, with more prominent reduction in the SCZP group. Right lingual, left posterior cingulate, and bilateral orbital fronto-insular regions showing reduced gyrification in SCZP compared to BPP (Table 7.6/ Figure 7.5).

Regions showing combined gyrification and n-back DC differences in SCZP vs. BPP contrasts are displayed in figure 7.6. The DCS test revealed 25% overlap in the topography of gyrification abnormalities (when compared to controls) and 51% overlap in the topography of DC abnormalities between BPP and SCZP (See Table 7.7 and Figure 7.7).

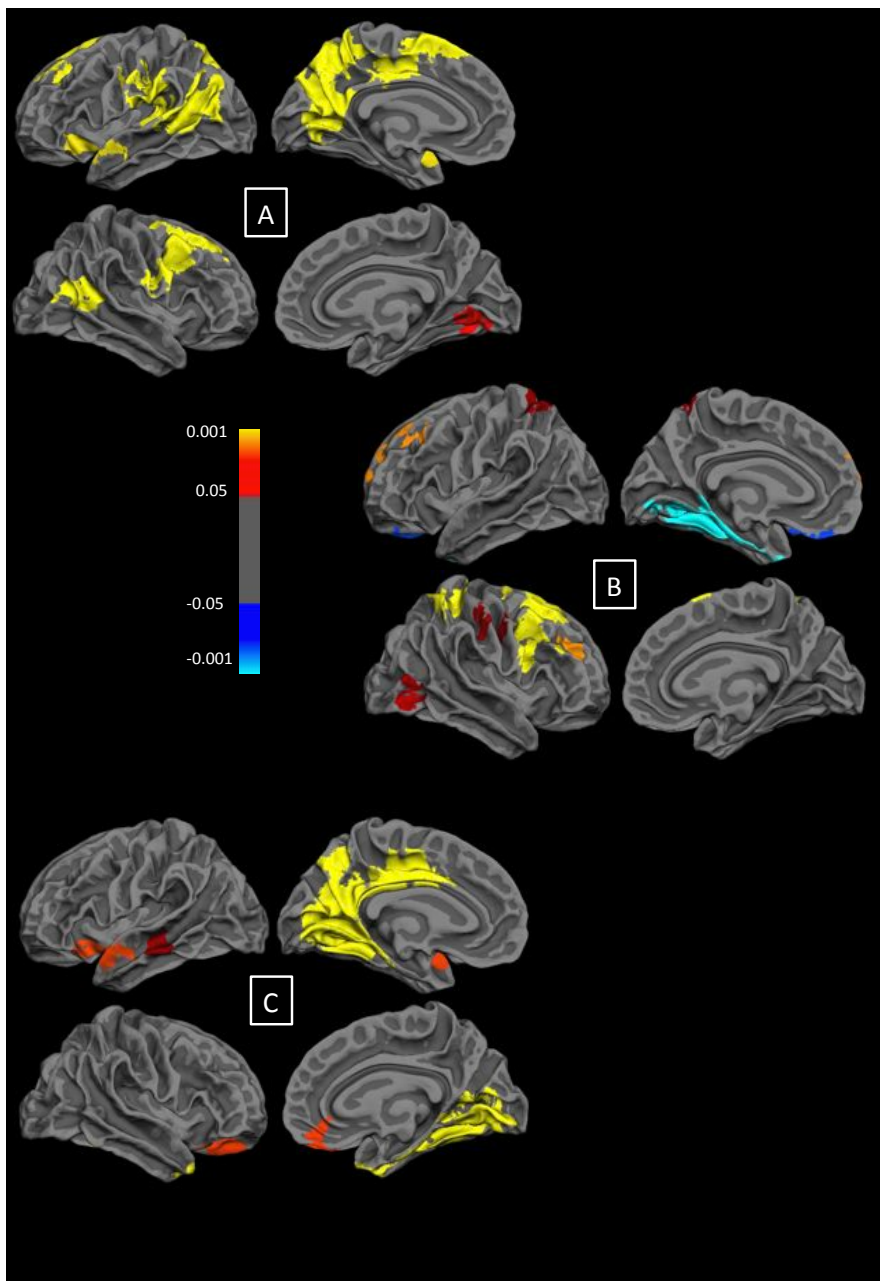


Figure 7.5: Clusters showing differences in gyrification among controls, patients with schizophrenia and bipolar disorder. A. Schizophrenia vs. Controls contrast. B. Bipolar disorder vs. controls contrast. For A and B, warm colours (red-yellow) indicate controls>patients; cool colours (blue-cyan) indicate patients>controls. C. Schizophrenia vs. bipolar contrast. For C, warm colours indicate Bipolar Disorder>Schizophrenia. Color bar is a scale of p value of clusters surviving multiple testing using Monte-Carlo simulation with a cluster inclusion criterion of $p=0.05$. All results are displayed on a reconstructed average white matter surface (fsaverage). Left hemisphere is on the upper row and right hemisphere on the bottom row of each panel of images.

Table 7.6: Gyrfication differences between patients and controls (cluster inclusion threshold p=0.05).					
Comparison	Brain region	Peak MNI coordinates (x,y,z) in mm	Clusterwise probability	Cluster extent in mm²	
Controls> Schizophrenia	Right caudalmiddlefrontal*	36,22,44	0.0001	3238	
	Right inferiorparietal/ superior temporal *	60,-55,13	0.0002	1430	
	Right lingual	22,-69,-1	0.012	916	
	Left Insula*	-35,5,-18	0.001	1207	
	Left precuneus/posterior cingulate *	-6,-45,56	0.0001	5847	
	Left superiorfrontal*	-17,46,37	0.0001	2680	
	Left middle temporal*	-63,-50,6	0.0001	3360	
	Left supramarginal*	-62,-23,30	0.0001	2446	
	Right caudalmiddlefrontal*	36,23,42	0.0001	3312	
Controls> Bipolar	Right rostralmiddlefrontal	35,39,25	0.0029	966	
	Right superiorparietal*	31,-38,66	0.0002	1231	
	Right postcentral	56,-13,38	0.0457	633	
	Right lateraloccipital	53,-72,14	0.0335	671	
	Left caudalmiddlefrontal	-31,28,36	0.0031	1093	
	Left superiorparietal/precuneus	-26,-45,68	0.046	722	
	Schizophrenia> Controls				
	None				
	Bipolar> Controls	Left fusiform gyrus*	-31,-69,-1	0.0001	3022
Left medialorbitofrontal		-5,28,-32	0.0333	559	
Right lingual gyrus*		21,-69,-2	0.0001	5533	
Bipolar> Schizophrenia	Right lateral orbitofrontal	22,27,-27	0.007	1005	
	Left posterior cingulate*	-5,-8,37	0.0001	8573	
	Left middle temporal	-64,-28,-11	0.046	723	
	Left insula / lateral orbitofrontal	-29,20,-23	0.007	981	
Schizophrenia>Bipolar	None				

*Clusters that survived correction for multiple comparisons using Monte-Carlo simulations (n=10,000 iterations; clusterwise probability p=0.001)

Figure 7.6: Overlap between gyrification and degree centrality changes in the schizophrenia vs. bipolar disorder contrasts. Both contrasts were thresholded at uncorrected $p < 0.05$ to increase the sensitivity of the conjunction analysis and displayed on white matter surface of reconstructed template cortical surface (fsaverage) using FreeSurfer. 1. Left anterior insula 2. Left middle temporal gyrus 3. left lingual gyrus/calcarine fissure 4. Left precuneus 5. Left posterior cingulate 6. Right lingual gyrus/calcarine fissure

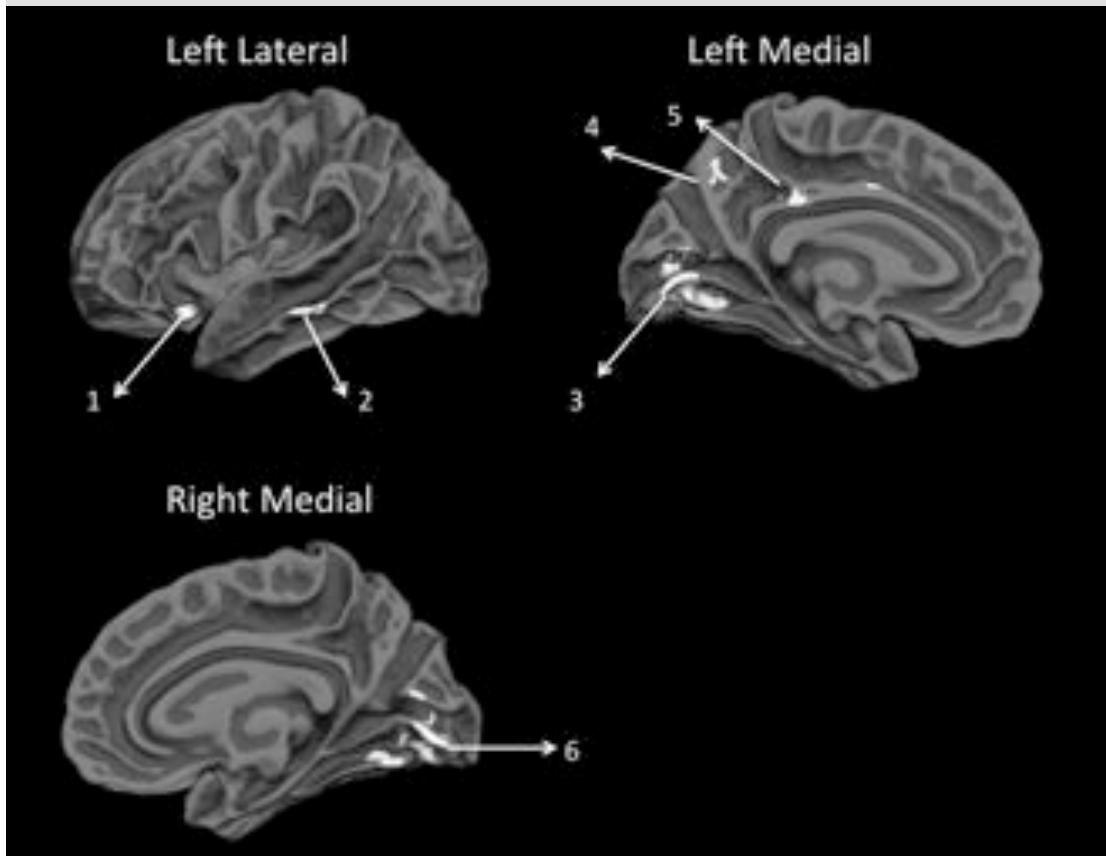
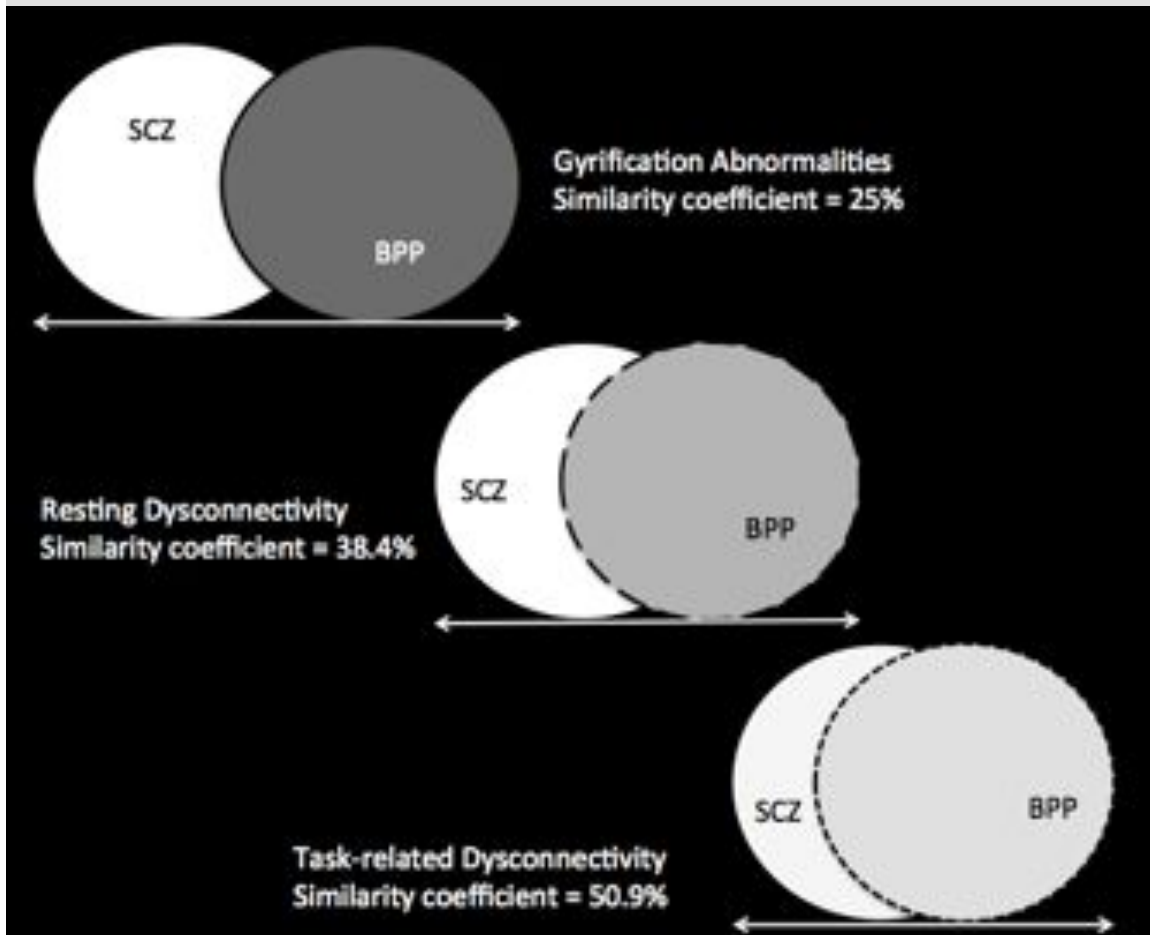


Table 7.7: Dice coefficients of spatial overlap between the two psychotic disorders in contrasts with healthy controls

Contrast	Spatial extent of gyrification contrast (no. of vertices) at p=0.05	Spatial extent of centrality contrast during n-back(volume in mm3) at p=0.05	Spatial extent of centrality contrast during rest(volume in mm3) at p=0.05
Schizophrenia vs. Controls (A)	43375	375516	282872
Bipolar disorder vs. Controls (B)	16864	274050	165536
Union (A'U'B)	42277	481224	371896
Intersection (A'N'B)	5299	122528	76512
Dice coefficient	25.1%	50.92%	38.45%

Figure 7.7: Graphical display of the similarity coefficients presented in the Table 7



7.8 Posthoc tests: effect of sample size and medications

To address whether the difference in sample size affects the observed centrality and gyrification differences between the two groups, an additional analysis was carried out comparing the BPP group (n=20, 7 females, mean age (SD) = 35.2(10.8)) with a sub-sample of gender and age matched patients with SCZP selected from the original sample. 20 SCZP (see the table 7.8 below) were identified to repeat the head-to-head comparison with BPP group for differences in centrality and gyrification. In both comparisons, with reduced degrees of freedom, there was a reduction in the effect size of the observed differences necessitating the use of a reduced statistical threshold (uncorrected $p < 0.001$ for centrality and clusterwise threshold of $p < 0.05$ for gyrification). But the regional localization of the group differences remained essentially the same, with the SCZP group showing higher left calcarine/lingual and cerebellar DC, but reduced right lingual and left posterior cingulate gyrification when compared to the BPP group. One sample t test of DC within the subsample of SCZP continued to show the localization of core hubs in bilateral superior temporal, inferior parietal, posterior cingulate, cerebellar crus and DLPFC regions. These observations suggest that the differences in the relative size of the samples do not explain the observed differences between the SCZP and BPP groups in the present study.

Table 7.8: Clinical and demographic variables in a sub-sample of patients with schizophrenia matched to patients with bipolar disorder

	Patients with bipolar disorder (n=20)	Sub-sample of patients with schizophrenia (n=20)
Gender (male/female)	13/7	14/6
Age in years (SD)	35.25(10.8)	34.4(10.9)
Mean parental NS-SEC (SD)	1.8(1.2)	2.2(1.7)
Mean total SSPI score	7.50(8.1)	12.7(7.7)
Reality Distortion	0.44(1.3)	2.6(2.6)
Disorganisation	1.28(2.1)	1.45(1.4)
Psychomotor Poverty	2.77(3.5)	3.0(4.1)
Mean n-back accuracy in % (SD)	91.77(6.1)	86.13(10.7)

NS-SEC: National Statistics – Socio Economic Status; SD: standard deviation; SSPI – Symptoms and Signs of Psychotic Illness. The total SSPI score can vary between 0 and 80. Reality distortion (delusions and hallucinations) can vary between 0 and 8. Psychomotor poverty (anhedonia, underactivity, poverty of speech and flat affect) can vary between 0 and 16. Disorganisation (inappropriate affect, disordered thought form and poor attention) can vary between 0 and 12.

Antipsychotics and mood-stabilisers could affect the functional and structural imaging measures investigated in the present study. To test this effect, the defined daily dose (DDD) of prescribed antipsychotics (details given in Supplementary Material 1) in the entire sample of patients (both SCZP and BPP) was related to core hub centrality and to the mean degree centrality and cortical gyrification indices of clusters emerging as significant from the SCZP vs. BPP group contrasts using Spearman’s correlations (as the DDD was not normally distributed). No significant relationships were observed (all $p > 0.3$, ρ -0.09 to 0.09) in this analysis.

In contrast to antipsychotics, which were prescribed to both patients with BPP and SCZP, the use of mood stabilizers was restricted to patients with BPP in this sample. Therefore, correlations were sought between the DDD of mood stabilisers (lithium, valproate, lamotrigine and carbamazepine) and the DC and gyrification indices as above, within the BPP group. No significant

relationships were observed (all $p > 0.2$, ρ -0.27 to 0.15) in this analysis as well.

Given the limited sample size, not powered to detect such correlations if present, one cannot confidently rule out the influence of medications on either centrality or gyrification. But the lack of correlation between the prescribed dose and the MRI measures suggest that at least in this sample, the observed group differences in these measures cannot be attributed to the linear effect of medications.

DISCUSSION

7.9 Redistributed centrality in psychosis

To our knowledge, this is the first study to use combined surface anatomical and functional connectivity approach to study the neural basis of the diagnostic discontinuity in psychosis. The current results show that while a degree of overlap exists between the two disorders in the functional connectivity and cortical gyrification, significant differences between the disorders are notable especially in the visual processing regions. While the core hub of functional connectivity seems to be preserved in both patient groups, the emergence of a higher degree of connectivity in the hippocampus/parahippocampus and thalamic regions and a reduction in the connectivity of the right posterior insula was observed in both patient groups.

A reduction in the centrality of right insula in both groups is consistent with a large body of evidence implicating this region in the emergence of psychotic

symptoms, though the locus of maximum change was more posterior than expected. In both SCZP and BPP, peripheral hubs emerged in the parahippocampal complex extending to the thalamus. This is consistent with Meyer-Lindenberg et al.'s (Meyer-Lindenberg et al., 2005) observation of inappropriate recruitment and connectivity of the parahippocampal regions during working memory performance in schizophrenia. It is important to note that the regional distribution of the connectivity differences is likely to differ according to the cognitive paradigm used. For example, an overactivation of medial temporal structures in BPP compared to SCZP has been noted when performing emotion/reward or memory based tasks, but not in tasks involving language or executive functions (Whalley et al., 2012).

Interestingly, in contrast to the BPP group who had an increase in the DC of lateral parietal cortex (supramarginal gyrus), part of the core connectivity hub, the SCZP group displayed an increase in DC of the anterior cerebellum and extrastriate visual cortex during both n-back and resting state, suggesting a conjoint dysfunction of these two regions. Focused examination of cerebellar connectivity during rest suggests that amidst an overall reduction in the cortico-cerebellar connectivity, the connectivity between extrastriate visual cortex and cerebellum appears to be increased in SCZP (Collin et al., 2011).

In general, the spatial extent of both DC and gyrification abnormalities was numerically larger in SCZP than BPP (Table 7.7). Interestingly, the similarity coefficient was higher in the n-back than in the resting fMRI or gyrification analysis. This finding highlights the importance of using multiple neuroimaging tools to investigate the current issue of diagnostic discontinuity. Further it

suggests that when external constraints such as task demands are present, 'schizophrenia-like' functional abnormalities are likely to be seen in BPP.

Abnormal visual information processing appears to be specific to SCZP and their relatives when compared to BPP and their relatives (Kumar et al., 2010). This corroborates the current findings that imply diagnostic specificity involving visual processing regions. It is worth noting that the extrastriate visual cortex, where we find combined gyrification and functional connectivity defects in schizophrenia, shows a predilection for developmental disturbances that affect cortical maturation (Braddick et al., 2003). Ongur et al. (2010) found significantly reduced coherence between extrastriate visual cortex and other brain regions during rest in schizophrenia when compared to bipolar disorder. Sui et al (2011), using independent component connectivity analysis during auditory oddball task performance, observed a predominantly visual cortex component to discriminate SCZP from BPP. SCZP fail to recruit the extrastriate cortex during semantic decision and verbal fluency (Curtis et al., 2001), but show greater engagement during facial affect processing when compared to BPP (Delvecchio et al., 2012). Inefficient functional connections in these regions could result in inflated centrality but reduced task related efficiency (Curtis et al., 2001).

7.10 Aberrant gyrification in psychosis

In line with the results reported in the previous chapter in a different set of subjects with schizophrenia, a predominant reduction in gyrification involving lateral prefrontal region, insula and superior temporal regions was noted in SCZP. BPP had reduced gyrification predominantly involving lateral prefrontal

and superior parietal regions when compared to controls, but showed increased gyrification in posterior cingulate, lingual gyrus and the left fronto-insular cortex when compared to SCZP. The two groups showed relatively less spatial overlap in the extent of gyrification abnormalities (25%) compared to the functional connectivity measures. A prominent overlap in the reduction in gyrification was noted in the lateral prefrontal cortex in both patient groups (Figure 7.5).

Combined (and specific) reduction in cortical gyrification and functional connectivity in SCZP (compared to BPP) involved calcarine, lingual and fusiform regions, left insula and middle temporal gyrus (Figure 7.6). This implies that prominent developmental deviations accompanied by functional consequences that separate the two disorders may involve the Salience Network (left insula) and extrastriate visual regions. In contrast, the other nodes of the Salience Network (right insula and ACC) do not show such schizophrenia-specific gyrification/centrality changes.

7.11 Strengths and limitations

A specific strength of the present study is the recruitment of bipolar disorder cases who also experience psychotic symptoms during the course of their illness (BPP), in contrast to previous studies that recruited bipolar disorder irrespective of the presence of psychotic symptoms (Calhoun et al., 2012; Sui et al., 2011). Further, a multimodal approach was employed studying structural and functional anatomy during rest and a cognitive task. Nevertheless several limitations must be considered when interpreting these results. Firstly, the sample size of BPP group was small compared to the

SCZP and control groups, but this is unlikely to have influenced the current results as shown using additional analysis. The overall proportion of female subjects was low, though the groups were well matched for gender distribution. Most patients were taking antipsychotic medications, with several patients in the BPP group also being exposed to mood stabilisers. To our knowledge there is no evidence that these medications have differential effect on cortical gyrification or centrality measures, though volumetric measures appear to be affected by both antipsychotics and lithium (Hafeman et al., 2012). In the present sample, no significant associations were found between antipsychotic DDD (SCZP/BPP) or mood stabiliser DDD (BPP only) and core hub centrality or cortical gyrification. Existing evidence predicts that at least in the short-term, antipsychotics could reduce overall functional connectivity (Lui et al., 2010); the present observation that SCZP show higher connectivity in visual processing regions compared to BPP is in the opposite direction, suggesting that medications alone cannot explain all of the present findings. Nevertheless one cannot completely exclude the effect of prescribed medications on the current observations. A recent post-mortem study suggests that abnormal gyrification in cerebellar vermis is a feature of schizophrenia (Schmitt et al., 2011). As the surface based morphometric approaches do not reconstruct the cerebellum, the present gyrification analysis was restricted to the cerebral surface only.

This study provides critical evidence delineating neurobiological underpinnings of the diagnostic boundaries of psychosis and highlights the ability of connectivity based neuroimaging measures to inform nosological classification. These observations open the question as to whether treatment

selection during early psychosis could be better informed by utilizing neuroimaging markers that differentiate the two disorders, alongside the existing symptom-based decision-making.

In both patient groups, the centrality of anterior insula does not appear to be significantly disturbed, while bilateral posterior insula shows a loss of widespread connectivity especially during task performance. It is possible that the abnormalities in the functional connectivity of the right insula in patients with psychosis is not diffuse, but affects specific key nodes of the brain, with both abnormal increases and decreases in the connectivity. This can lead to preserved centrality in the presence of aberrant interactions with other networks. This needs to be further investigated through a focused seed based analysis. One such analysis is presented in chapter 8.

Chapter 8

Neural primacy of the salience processing system in schizophrenia

For effective information processing two large-scale distributed neural networks appear to be critical: a multimodal executive system anchored on the dorsolateral prefrontal cortex (DLPFC) and a salience system anchored on the anterior insula. A critical component of the insular dysfunction hypothesis (proposed in chapter 2) is the suggestion that the interaction between these two systems will be affected in schizophrenia. Whole-brain Granger causal modelling using resting fMRI reveals a significant failure of both the feed-forward and reciprocal influence between the insula and the DLPFC in schizophrenia. Further, a significant failure of directed influence from bilateral visual cortices to the insula was also seen in patients. These findings provide compelling evidence for a breakdown of the salience-execution loop in the clinical expression of psychosis.

8.1 Task-positive brain systems

Several functional brain imaging studies support the existence of two 'task-positive' brain systems that facilitate efficient performance of tasks that require focused attention (Seeley et al., 2007). One of these large-scale networks, termed the Salience Network (SN), is anchored in the right anterior insula (rAI) and dorsal ACC (dACC), and has predominant limbic and subcortical components. The SN is involved in integrating external stimuli with internal homeostatic context, thus marking objects that require further processing (Menon and Uddin, 2010; Seth et al., 2011; Singer et al., 2009). A second network comprised of the dorsolateral prefrontal cortex (DLPFC) and lateral parietal regions, termed the central executive network (CEN), operates on the identified salient stimuli to enable task performance (Seeley et al., 2007). These two networks are thought to interact at various levels to enable coordinated neural activity (Medford and Critchley, 2010). Firstly, the rAI is thought to causally influence the anticorrelation between the CEN and a set of brain regions involved in self-referential activities that constitute the default mode network (DMN) (Sridharan et al., 2008). Thus the rAI has a strong causal influence enabling the recruitment of contextually relevant brain regions. Secondly, along with dACC and thalamus, rAI forms a tonic-alertness loop that forms a vital subcortical-limbic system in a hierarchical attention processing stream (Sadaghiani et al., 2010). In addition, during task performance the dACC acts in conjunction with the DLPFC to form a cognitive control loop that modulates the behavioural response (Miller and Cohen, 2001).

Converging evidence from structural and functional neuroimaging studies indicate a crucial role for both the rAI (chapters 2, 3 and 4) and the DLPFC (Callicott et al., 2000; Weinberger et al., 1992) in the pathophysiology of schizophrenia. A number of neuropathological and imaging studies have found abnormalities in the DLPFC, with robust evidence implicating a failure of excitatory-inhibitory neuronal balance in this region (Lewis et al., 2005). Several pooled analyses of structural imaging studies have confirmed that the most consistent grey matter abnormalities across the different stages of schizophrenia occur in the nodes of the SN, especially the anterior insula (Ellison-Wright et al., 2008; Glahn et al., 2008). fMRI studies suggest that an inefficient recruitment of the frontoparietal executive system is often noted alongside SN dysfunction during task performance (Hasenkamp et al., 2011; Kasperek et al., 2013; Minzenberg et al., 2009; Nygård et al., 2012). The presence of SN dysfunction in schizophrenia has also been shown in studies seeking instantaneous functional correlations (also known as functional connectivity) in the Blood Oxygen Level Dependent (BOLD) time-series between the rAI and several nodes of the SN (Guller et al., 2012; Pu et al., 2012; Tu et al., 2012), and this within-network SN dysconnectivity is related to cognitive dysfunction (Tu et al., 2012). Similar findings of reduced connectivity within the SN in schizophrenia also emerge when seeking time-lagged (-5 to +5 seconds) rather than instantaneous correlations between the BOLD signal from brain regions constituting large-scale networks (White et al., 2010a). It is possible that the disintegration of the salience processing system anchored on the rAI has a causal role in the inefficient cerebral recruitment noted in schizophrenia. To our knowledge, no neuroimaging studies have so far investigated whether a failure in the feed-forward causal influence from the

salience processing system to the executive system is present in schizophrenia.

Following the terminology of Friston (1994) in this chapter the term functional connectivity (FC) is employed to denote the instantaneous, zero-time lagged correlation between brain activity occurring at spatially distinct sites. Correlation does not demonstrate a causal relationship between variables and therefore the existence of functional connectivity does not imply that activity in one region causes that in another, or even that the regions have a direct neural connection. Brain regions showing significant FC are functionally coupled and may reflect components of a single but spatially distributed system (i.e. a large scale brain network). Granger causal connectivity is a measure of effective connectivity; the presence of Granger causal connectivity from a region A to another region B implies that the neuronal activity in region A precedes and predicts the neuronal activity that occurs in region B. These two regions, A and B, may not show instantaneous functional coupling that is characteristic of a single large-scale system. Thus Granger Causal Analysis (GCA) is a more useful approach to study the causal relationships that may exist across networks. But it must be borne in mind that such 'causal' relationships identified between two regions may indeed be indirect and mediated by a third region not considered in bivariate approaches.

To investigate the 'causal' influences between the salience processing and the executive systems, Granger causality analysis was applied to task-free resting state fMRI. Task-free conditions minimize potentially confounding effects of between-group performance differences and permit the investigation of fundamental components of neurophysiological function. The 'causal'

influence of the rAI over the multimodal brain regions constituting the executive system was hypothesized to be reduced in schizophrenia. It was also predicted that any abnormality in the feed-forward influence would be accompanied by a reciprocal diminution of the feedback from the executive system to the rAI, resulting in a dysfunctional salience-execution loop in patients. In addition, using a mediation model the relationship between the abnormalities in the functional connectivity (FC) of the SN and the 'causal' outflow from the salience processing to the executive system was studied. Finally, the relationship between illness severity in patients and the dysfunction of the salience-execution loop was investigated.

8.2 Participants

The data used in the current chapter were obtained from the same sample reported in chapter 7 for resting fMRI analysis. This sample consisted of 38 patients satisfying DSM-IV criteria for schizophrenia and 35 healthy controls. In addition to the description reported in chapter 7, the present study also used the information regarding duration of illness collected from case-files; the current occupational and social dysfunction quantified using the Social and Occupational Functioning Assessment Scale (SOFAS) (Goldman et al., 1992) and speed of cognitive processing, a consistent and prominent cognitive deficit in schizophrenia, assessed using the Digit Symbol Substitution Test (Dickinson et al., 2007). DSST was administered using a written and an oral format with a mean DSST score computed from the two formats. [This adaptation was carried out as a part of the current doctoral work with data from a different group of participants reported in Palaniyappan et al. (2013)].

36 out of 38 patients were receiving treatment with antipsychotics (clozapine n=5, other atypical antipsychotics n=25, typical neuroleptics n=5, combined typical and atypical agents n=1) and had no change in their prescriptions for the 6 weeks preceding the scan. The median Defined Daily Dose (WHO Collaborating Centre for Drug Statistics and Methodology, 2003) of antipsychotics was 1 (range from 0 to 5.6).

Table 8.1: Demographic and clinical features

	Patients with schizophrenia	Healthy controls	t/χ^2
Number	38	35	-
Gender (male/female)	29/9	25/10	$\chi^2=0.23$, $p=0.63$
Handedness (right/left)	33/5	31/4	$\chi^2=0.05$, $p=0.82$
Age in years (SD)	34.5(9.1)	33.5(9.1)	$t=0.46$, $p=0.65$
Mean parental NS-SEC (SD)	2.4(1.5)	2.1(1.3)	$t=0.79$, $p=0.43$
Mean DSST score	42.4(10.0)	57.4(9.4)	$t=6.5$, $p<0.0001$
Mean SOFAS score	53.9(12.8)	-	-
Median duration of illness in years (range)	6.5(28)	-	-
Median Defined Daily Dose of antipsychotics (range)	1.0(5.57)	-	-
Mean total SSPI score	12.1(7.3)	-	-
Reality Distortion	2.26(2.6)	-	-
Psychomotor Poverty	2.84(3.5)	-	-
Disorganisation	1.39(1.3)	-	-

DSST – Digit Symbol Substitution Test; NS-SEC: National Statistics – Socio Economic Status; SD: standard deviation; SOFAS – Social and Occupational Functioning Assessment Scale; SSPI – Symptoms and Signs of Psychotic Illness. The total SSPI score can vary between 0 and 80. Reality distortion (delusions and hallucinations) can vary between 0 and 8. Psychomotor poverty (anhedonia, underactivity, poverty of speech and flat affect) can vary between 0 and 16. Disorganisation (inappropriate affect, disordered thought form and poor attention) can vary between 0 and 12.

8.3 Image acquisition and processing

Details of the resting fMRI image acquisition are provided in chapter 7. fMRI data was preprocessed using SPM8 (<http://www.fil.ion.ucl.ac.uk/spm>) and Data Processing Assistant for resting-state fMRI (Chao-Gan and Yu-Feng, 2010)). Data were corrected for slice-timing differences and spatially realigned to the first image of the dataset. Movement parameters were assessed for each participant, and participants were excluded if movement exceeded 3 mm. Further, ArtRepair was employed to correct movement artefacts using an interpolation method (<http://cibsr.stanford.edu/tools/human-brain-project/artrepair-software.html>). The first 5 volumes of functional images were discarded to allow stability of the longitudinal magnetization. A single dataset was produced from a weighted summation of the dual-echo dynamic time course (Posse et al., 1999). During scanning, cardiorespiratory cycles were monitored by means of a cardiogram and pneumatic belt. This information was transformed to frequency domain to remove the variance on BOLD signal modulations due to cardiorespiratory activity. This procedure, called RETROICOR (retrospective image correction), was performed in accordance with the original description (Glover et al., 2000). The functional scans were then spatially normalized using the unified segmentation approach and smoothed using a Gaussian kernel of 8 mm Full-Width at Half Maximum. Following this, linear detrending and filtering using a band pass filter (0.01-0.08 Hz) was done to eliminate low frequency fluctuations and high frequency noise. Finally, variance accounted for by nuisance covariates including six head motion parameters, global mean signal, white-matter signal and CSF signal was removed by regression before conducting a seed based regional functional connectivity analysis.

Selection of the seed region : As the primary hypothesis tested here is related to the influence of right anterior rAI on the executive system, the anatomic location of the rAI seed was determined using functional activation data during a 2-back task performed by all subjects included in the study (one sample t-test, FWE corrected $p < 0.05$). A 6-mm radius sphere centered on the local maxima ($x=33, y=21, z=-3$) corresponding to the rAI was used as the seed region for further analysis. The location of this seed (Figure 8.10) corresponds to the anterior compartment of the insula that is frequently mapped to the behavioral domains of attentional processing and socio-emotional function (Klein et al., 2013).

Granger causality: Granger's principle suggests that a time series (X) exerts a causal influence (termed as Granger causality) on another time series (Y) if the preceding states of X predict the state of Y uniquely, over and above the variance explained by the preceding states of Y itself. In the present study the following were estimated; (a) X to Y effects: the Granger causal effects of the time series of the anterior insula seed region (X) on every other grey matter voxel in the brain (Y) and (b) Y to X effects: the Granger causal effect of every other grey matter voxel on the rAI. The path coefficient maps for the Granger causality were generated using a time lag order of 1 (one TR, 2.5 seconds). In contrast to Sridharan et al. (Sridharan et al., 2008), signed path-coefficients were used (Hamilton et al., 2011a; Zang et al., 2012) instead of F-residuals so as to infer the probable excitatory or inhibitory effects of the directed physiological influences. The path coefficient of +1 from region X to Y in this model suggests that one unit of change in the activity of region X in a specific direction brings a unit change in the activity of region Y in the

same direction in the context of Granger-causality. This is referred to as excitatory influence. Similarly, a path coefficient of -1 from region X to Y suggests that one unit of change in the activity of region X in a specific direction brings a unit change in the activity of region Y in the opposite direction (this is referred to as inhibitory influence). In contrast to residual-based GCA models where the net causal flow is calculated by subtracting x-to-y from y-to-x effects, bivariate GCA allows for the physiological possibility that bi-directional influences of opposite effects could simultaneously exist in the brain. Further, the signed-path coefficient maps allow parametric statistical analysis for group level inference (Hamilton et al., 2011a). This helped us to determine the multimodal brain region that showed most significant difference between the patients and controls in the causal influence to and from the rAI.

Bivariate first-order coefficient based voxelwise Granger causality analysis (GCA) was performed using the REST software (www.restfmri.net), using Chen's method of signed path-coefficients.

Functional connectivity: To compute functional connectivity (FC), Pearson's correlation coefficients were calculated between the mean time series of the rAI seed region and every voxel in the brain for each subject. Resulting voxel-wise correlation coefficients were then converted to produce whole-brain z-maps using a Fisher transform for further second level statistical analyses.

8.4 Statistical Analysis

The FC and GCA maps from each individual subject were analysed using separate one-sample t-test for the entire sample (both patients and controls)

with a familywise error (FWE) corrected $p < 0.05$ for positive and negative coefficients. This threshold was used to ensure that the clusters emerging in the one sample t-test are unlikely to be due to a type 1 error. From the results, search volume masks were derived for the FC and GCA to constrain the subsequent between-group analyses. These masks represented regions with significant instantaneous positive correlation or anticorrelation with the seed region, and significant excitatory or inhibitory influence to and from the seed region in the whole sample. Between group analyses were conducted using an unpaired t-test (FWE corrected $p < 0.05$), with the search volume corrected for the masks used in the analyses. For regions showing significant group differences at the FWE corrected threshold, follow-up one-sample t tests were conducted to investigate the direction of the Granger-causal influence in each group separately. These tests were Bonferroni corrected for a total of 8 follow-up comparisons. In addition to such constrained analyses, a whole brain between-group analysis (at uncorrected $p < 0.001$) was also carried out in order to identify informative group differences that may exist in regions outside the masks derived from one-sample t-tests. As this exploratory search has a higher likelihood of identifying false positive clusters, an additional extent criterion of $k=30$ was applied. Age and gender were used as covariates in all group level analyses. Within the patient group, bivariate correlations were used to examine the influence of antipsychotic medications on the mean coefficients within the clusters that emerged as significant from the two-sample t-tests in both FC and GCA comparisons. All group level analyses were carried out using the SPM8 software and the toolboxes MarsBar (marsbar.sourceforge.net) and xjview (www.alivelearn.net/xjview8), in addition

to MRICron (<http://www.mccauslandcenter.sc.edu/mricro/mricron/>) to visualize the results.

Mediation Analysis: Mediation analysis was carried out using Preacher and Hayes model (Preacher and Hayes, 2004), predicting the Granger influence of rAI on the time course of signal in the DLPFC (dependent variable, DV) from diagnosis (independent variable, IV). The mediator (M) of this relationship was the first eigenvariate of the functional connectivity between rAI and the clusters showing significant diagnostic effect in the functional connectivity (FC) analysis. This eigenvariate represented the typical connectivity in each subject between the rAI and each of the voxels showing abnormal FC in schizophrenia. The total effect of diagnostic status on the rAI to DLPFC influence was evaluated, and this effect was partitioned to direct effect and the indirect effect mediated by the presence of functional dysconnectivity related to the rAI. A bootstrapping method with 5000 iterations was used to test the 95% confidence intervals of the indirect effects (Preacher and Hayes, 2008).

RESULTS

8.5 Granger Causality

In the entire sample (patients and controls, one-sample t test), rAI exerted a significant excitatory influence on the bilateral DLPFC, inferior parietal regions and left cerebellar crus. Significant inhibitory influence of the rAI was noted at bilateral supplementary motor region and bilateral precentral regions, in addition to right posterior insula. Bilateral DLPFC in turn had a significant inhibitory influence on the rAI. In addition, dACC and PCC had significant

inhibitory influence, while pre-supplementary motor area (pre-SMA) and temporal pole had significant excitatory influence on the rAI. These results are shown in Figure 8.1 and Table 8.2.

Table 8.2: One sample T test (patients and controls) of the directed causal influence to and from right anterior insula

Regions	MNI coordinates (x, y, z) in mm	Mean (SD) path coefficient in controls	Mean (SD) path coefficient in patients	Peak intensity (T) and cluster size (k=voxel count) [§]
Regions positively influenced by rAI				
Right inferior parietal (supramarginal, BA40)	50,-44,52	0.071(0.07)	0.086(0.08)	T=8.15,k=784
Right middle and inferior frontal (BA10,BA46)	38,40,24	0.095(0.07)	0.058(0.06)	T=7.75,k=900
Left cerebellum crus	-30,-64,-32	0.070(0.08)	0.039(0.06)	T=6.33,k=79
Left inferior parietal (supramarginal, BA40)	-52,-42,38	0.058(0.07)	0.066(0.08)	T= 6.18 ,k=321
Left inferior frontal	-52,34,0	0.071(0.10)	0.058(0.08)	T=6.00 ,k=47
Right orbitofrontal and superior temporal	48,16,-12	0.114(0.18)	0.114(0.15)	T=5.72 ,k=38
Left inferior and middle frontal	-36,44,12	0.104(0.12)	0.045(0.08)	T=5.55 ,k=34
Regions negatively influenced by rAI				
Supplementary Motor Area (left and right)	10,-8,56	-0.054(0.05)	-0.039(0.05)	T= 7.57 ,k=383
Left Precentral and Postcentral	-58,-10,22	-0.077(0.07)	-0.047(0.06)	T=7.52 ,k=526
Right Precentral and Postcentral	62,0,22	-0.068(0.07)	-0.037(0.05)	T= 6.93 ,k=276
Right posterior insula	42,-8,6	-0.067(0.08)	-0.040(0.05)	T=6.45 ,k=89
Left Precentral and Postcentral	-22,-30,60	-0.033(0.05)	-0.034(0.04)	T= 5.67 ,k=37
Regions exerting positive influence on rAI				
Left Supplementary motor area, ACC	-10,2,50	0.059(0.07)	0.034(0.04)	T=6.54, k=55
Right Supplementary motor area, ACC	10,-6,56	0.060(0.08)	0.049(0.06)	T=6.65,k=31
Regions exerting negative influence on rAI				
Left middle and inferior frontal	-34,40,16	-0.052(0.06)	-0.025 (0.04)	T=6.28,k=120
Right middle frontal (BA10, BA46)	36,50,16	-0.054(0.06)	-0.031(0.04)	T=6.25 ,k= 307
Left superior medial frontal, ACC	2,44,26	-0.031(0.04)	-0.024 (0.03)	T=5.92 ,k=34
Left inferior frontal	-54,28,8	-0.034(0.06)	-0.036 (0.04)	T=5.82 ,k= 50
Right inferior frontal	44,24,26	-0.042(0.05)	-0.033(0.05)	T=5.77 ,k= 30
§ Familywise Error corrected p<0.05				

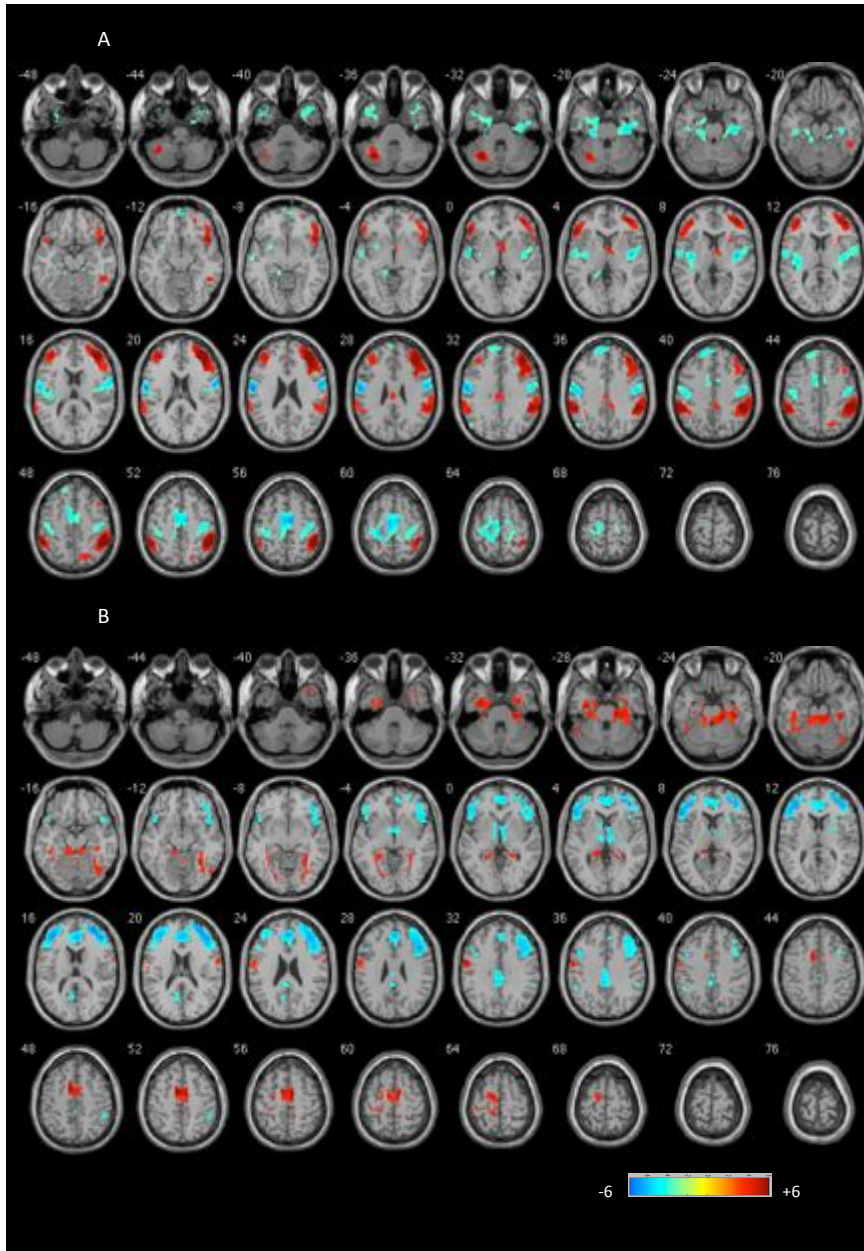


Figure 8.1: Granger causal influence to and from the right anterior insula. Top panel A depicts the influence of right anterior insula on the rest of the brain (x to y). Bottom panel B depicts the influence of regions from the rest of the brain on right anterior insula (y to x). The figures show the results of the one sample T test of GCA maps on all subjects (patients and controls). Illustrations drawn on a single subject structural image showing axial slices using xjview at $p < 0.001$ uncorrected, $k = 30$. Colour bar shows a scale of T values. Warm colours suggest excitatory influence, while cold colours suggest inhibitory influence.

Two sample t-tests revealed significant differences between patients and controls in the ‘causal’ outflow from the rAI to the rDLPFC. In controls, the rAI exerted a significant excitatory influence on right DLPFC ($t(34) 7.42$, corrected $p < 0.001$), while in the patients, this influence was weak ($t(37) 2.06$, uncorrected $p = 0.047$). In addition there was a group difference in the effect of rAI on precuneus at an uncorrected threshold ($p < 0.001$, $k = 30$), where the controls exhibited an excitatory influence ($t(34) = 3.14$, uncorrected $p = 0.004$) while the patients exhibited an inhibitory influence ($t(37) = -2.18$, uncorrected $p = 0.036$). Patients also showed a significant reduction in the ‘causal’ influence from bilateral visual cortex and right hippocampal formation to the insula when compared to controls. These group differences are shown in Figure 8.2 and Table 8.3.

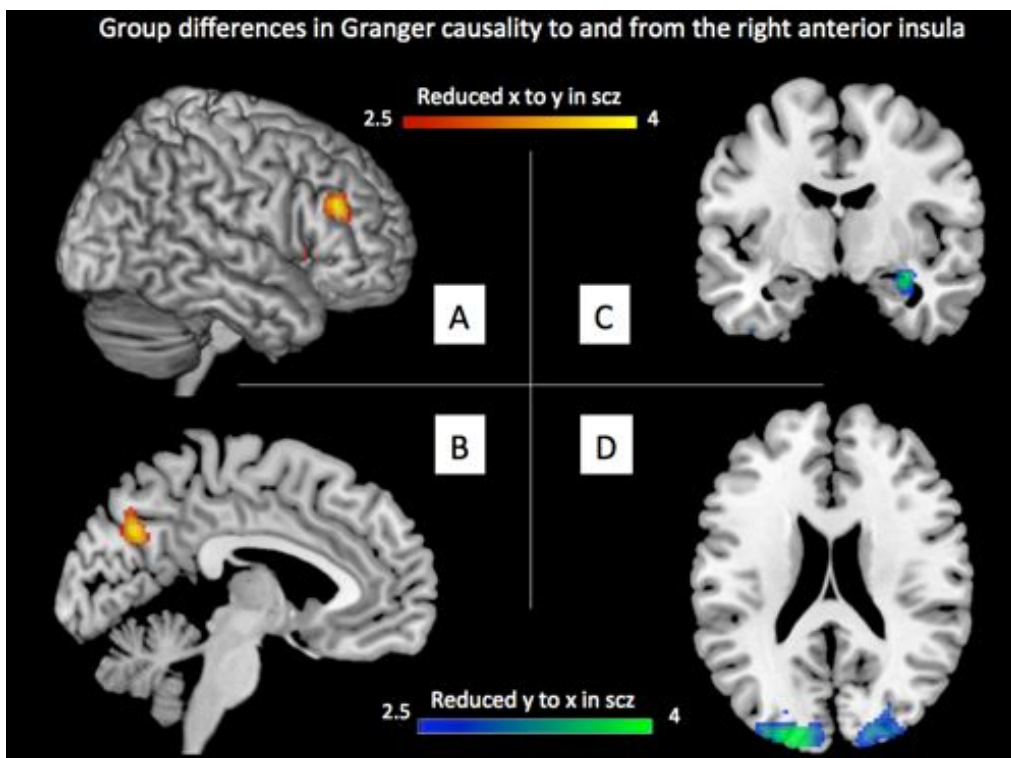


Figure 8.2: Group differences in Granger causality to (y to x) and from (x to y) the right anterior insula in patients with schizophrenia compared to healthy controls. Illustrations drawn on a single subject structural image with slices selected for the best display of regions showing differences in the two-sample t test. Color bar shows a scale of T values. Blue-green areas shows regions where patients had reduced y to x path coefficients (i.e. less excitatory influence on the insula) than controls, while red-yellow colored areas show regions where patients had reduced x to y (i.e. less excitatory influence from the insula) path coefficients than controls. A. Surface rendered image showing right DLPFC region with most significant reduction in the Granger-causal influence from the right anterior insula. B. Precuneus (x=-4) C. Hippocampal formation (y=-6) D. Bilateral visual cortex (z=18).

In order to investigate the effects of influences of the rDLPFC on the rest of the brain, voxelwise GCA was performed using a 6mm spherical ROI placed in the rDLPFC node showing the significant group difference. The results of the one sample t-tests of GCA based on the rDLPFC seed are presented in the Figure 8.3, and Table 8.4). The SN was the primary site of dysfunctional 'causal' influence on the rDLPFC in patients. Patients had a significantly reduced excitatory effect from the bilateral (more ventral) insula and the dACC to the rDLPFC in addition to a significant loss of inhibitory effect of the rDLPFC on the bilateral anterior insula and dorsal ACC (Figure 8.4, Table 8.5).

None of the x to y or y to x path coefficients from the rAI or the DLPFC seed regions showed significant correlations with antipsychotic dose equivalents (all $p > 0.2$).

Table 8.3: Two-sample T test of the difference in the directed influence to and from the right anterior insula in patients and controls.

Regions	MNI coordinates (x, y, z) in mm	Mean (SD) path coefficient in controls	Mean (SD) path coefficient in patients	P value, peak intensity and cluster size (k = voxel count)
Causal outflow from the rAI (x to y coefficients)				
Right middle frontal**	48,34,24	0.103(0.08)	0.027(0.08)	P(SVC)=0.035, T=3.85, k=32 Controls>Schizophrenia
Left precuneus	-4, -70,32	0.072 (0.14)	-0.039(0.10)	P(unc.)<0.001, T=3.93,k=72 Controls>Schizophrenia
Causal inflow to the rAI from rest of the brain (y to x coefficients)				
Left superior occipital, cuneus (BA18 and BA19)*	-18,-92,22	0.045(0.05)	-0.035 (0.09)	P(cFWE.)=0.006, T=4.74 ,k= 351 Controls>Schizophrenia
Right hippocampus and parahippocampal gyrus	32,-8,-16	0.031(0.07)	-0.025(0.05)	P(unc.)<0.001, T=3.97 ,k=33 Controls>Schizophrenia
Right superior occipital, cuneus (BA18 and BA19)	24,-90,16	0.034(0.05)	-0.030 (0.08)	P(unc.)<0.001, T=3.91 ,k=112 Controls>Schizophrenia
**P(SVC), Familywise Error corrected within the search volume at p<0.05.				
*P(cFWE), Cluster level familywise error corrected at p<0.05.				
P(unc.), the clusters observed using a more lenient criteria of p<0.001 are thresholded using an extent cluster k=30 in the unconstrained search.				

Table 8.4: One sample T test of the directed causal influence to and from right DLPFC in patients and controls

Regions	MNI coordinates (x, y, z) in mm	Mean (SD) path coefficient in controls	Mean (SD) path coefficient in patients	Peak intensity (T) and cluster size (k=voxel count) §
Regions positively influenced by rDLPFC				
Left cerebellum posterior lobe/crus	-44 -70 -38	0.078(0.06)	0.020(0.04)	T=6.67 k=111
Right middle frontal gyrus	44 36 34	0.091(0.07)	0.056(0.08)	T=6.45, k=140
Right superior parietal lobule and angular gyrus	42,-66,50	0.090(0.10)	0.060(0.08)	T=6.13, k=280
Left superior parietal lobule	-26,-68,56	0.081(0.10)	0.050(0.10)	T=5.7 k=44
Regions negatively influenced by rDLPFC				
Right insula, superior temporal gyrus and parietal operculum	36 -24 16	-0.044(0.05)	-0.035(0.04)	T=6.94, K=170
Left insula	-34 -14 14	-0.041(0.04)	-0.028(0.04)	T=5.94 k=39
Right posterior insula	44,12,-12	-0.070(0.07)	-0.046(0.09)	T=5.56, k=69
Regions exerting positive influence on rDLPFC				
Anterior midcingulate	2,14,42	0.071(0.06)	0.023(0.06)	T=6.05, k=76
Right anterior insula	34,22,0	0.072(0.06)	0.021(0.06)	T=6.02, k=35
Regions exerting negative influence on rDLPFC				
Left angular gyrus (inferior parietal lobe)	-46,66,38	-0.043(0.06)	-0.029(0.05)	T=5.25, k=31
§ Familywise Error corrected p<0.05, k=30				

Figure 8.3: Granger causal influence to and from the right dorsolateral prefrontal cortex (rDLPFC). Top panel A depicts the influence of rDLPFC on the rest of the brain (x to y). Bottom panel B depicts the influence of rest of the brain on rDLPFC (y to x). The figures show the results of the one sample T test of GCA maps on all subjects (patients and controls). Illustrations drawn on a single subject structural image showing axial slices using xjview at $p < 0.001$ uncorrected, $k=30$. Colour bar shows a scale of T values. Warm colours suggest excitatory influence, while cold colours suggest inhibitory influence.

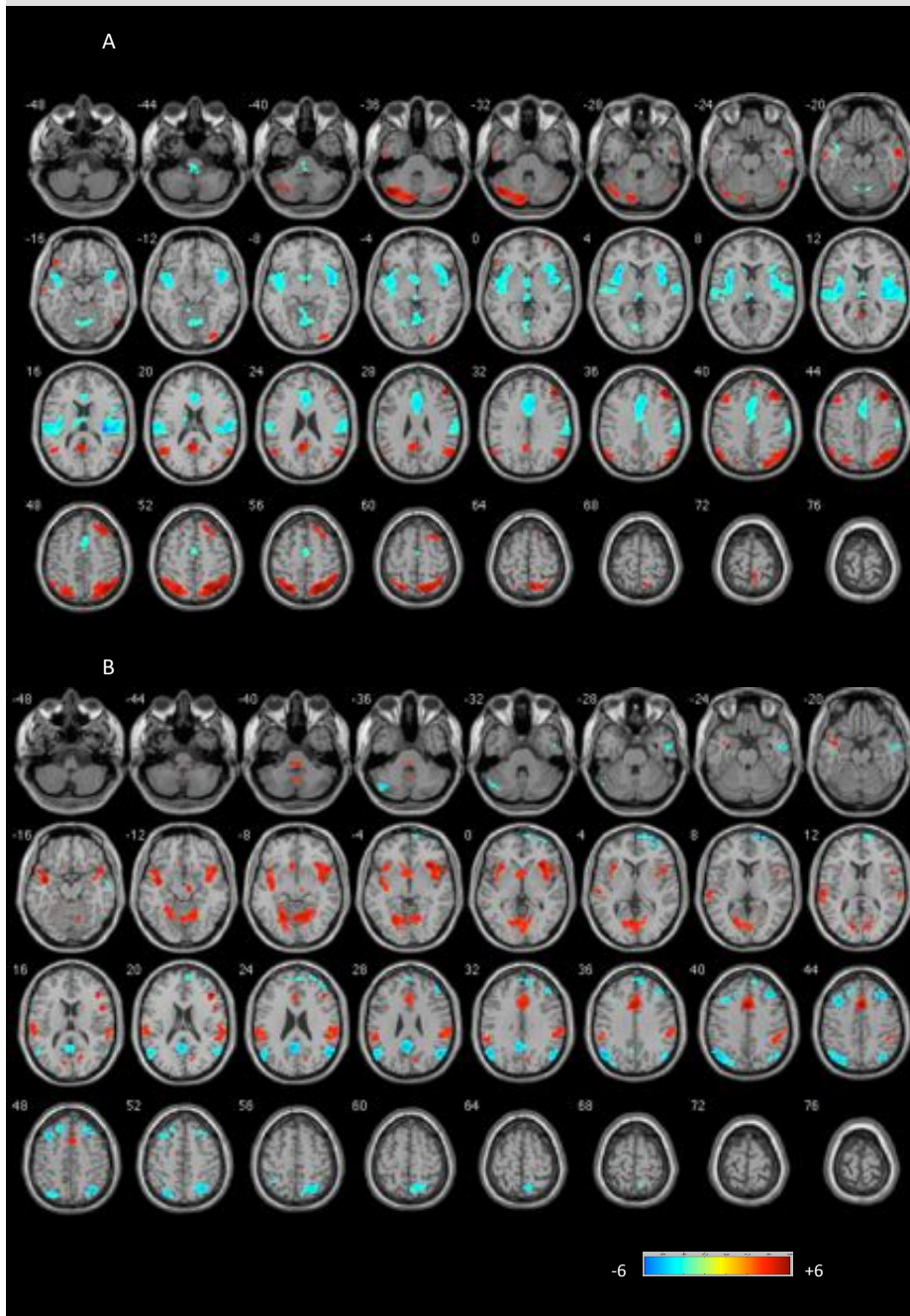


Figure 8.4: Group differences in Granger causality to (y to x) and from (x to y) the right DLPFC in patients with schizophrenia compared to healthy controls. Illustrations drawn on a single subject structural with slices selected for the best display of regions showing differences in the two sample t test. Left sided panel displays group differences in x to y maps; Right sided panel displays group differences in y to x maps. Color bar shows a scale of T values. Blue areas show regions where patients had greater (i.e. less inhibitory) path coefficients than controls, while red colored areas show regions where controls had greater (i.e. more excitatory) path coefficients than patients.

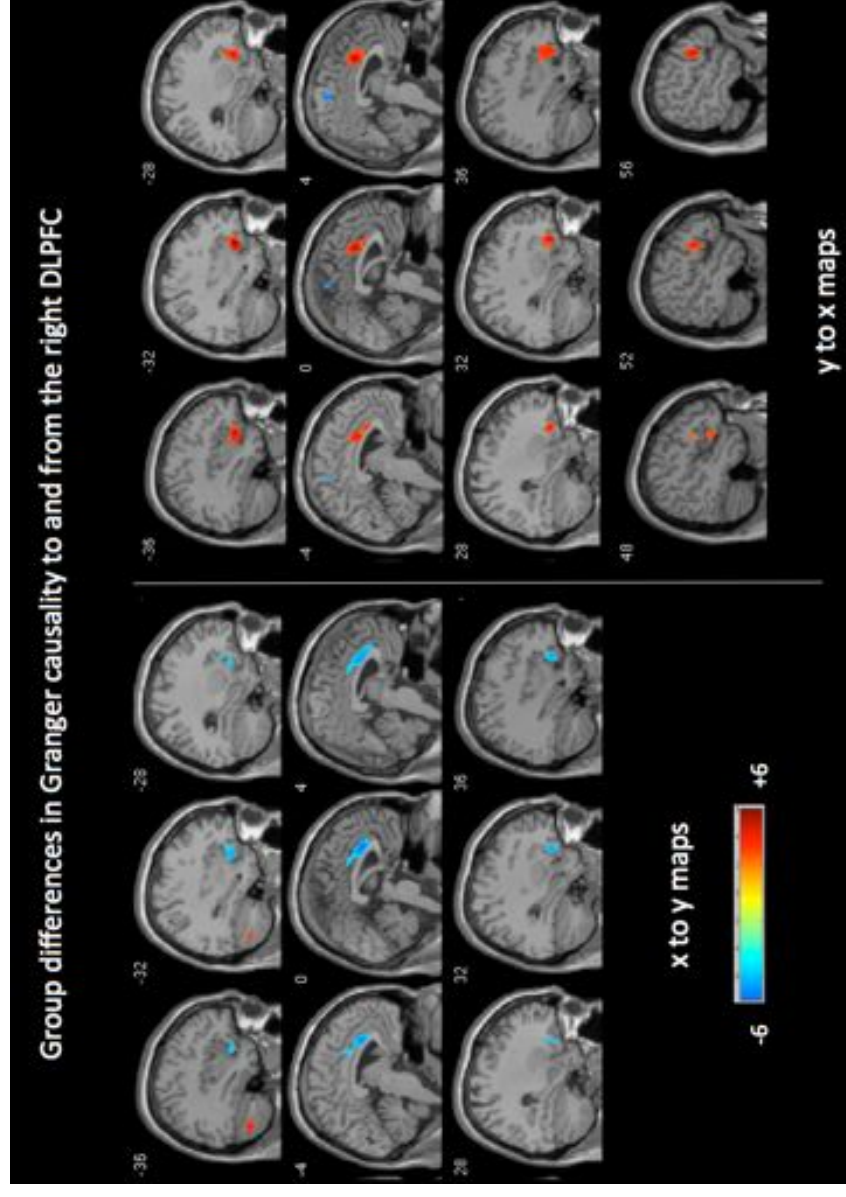


Table 8.5: Two-sample T test of the difference in the directed influence of right DLPFC on rest of the brain between patients and controls.

Regions	MNI coordinates (x, y, z) in mm	Mean (SD) path coefficient in controls	Mean (SD) path coefficient in patients	P value, peak intensity and cluster size (k = voxel count)
Causal outflow from the DLPFC (x to y coefficients)				
Bilateral dorsal anterior cingulate**	0,28,20	-0.079(0.06)	-0.009(0.06)	P(cFWE)=0.01, T=-4.91, k=452 schizophrenia>controls
Left cerebellum posterior lobe / crus	-42,-70,-34	0.075(0.06)	0.018(0.03)	P(unc.)<0.001, T=4.74, k=164 controls>schizophrenia
Right anterior insula and orbitofrontal cortex	34,26,-14	-0.052(0.06)	0.013(0.07)	P(unc.)<0.001, T= -4.48 k=180 schizophrenia>controls
Right inferior frontal operculum	54,18,14	-0.059(0.10)	0.022(0.06)	P(unc.)<0.001, T=-4.23 k=163 schizophrenia>controls
Left anterior insula and orbitofrontal cortex	-32,18,-14	-0.041(0.05)	0.018 (0.07)	P(unc.)<0.001, T=-4.22, k=146 schizophrenia>controls
Right cerebellum posterior lobe/ crus	16,-78,-32	0.053(0.09)	-0.010(0.05)	P(unc.)<0.001, T=3.62, k=38 controls>schizophrenia
Causal inflow to the DLPFC from rest of the brain (y to x coefficients)				
Left anterior insula and orbitofrontal cortex**	-32,22,-12	0.046(0.04)	-0.009(0.04)	P(cFWE)<0.001, T=5.98, k=523 controls>schizophrenia
Bilateral dorsal anterior cingulate**	2,18,30	0.068(0.05)	0.001(0.05)	P(cFWE)=0.001, T=5.83, k=481 controls>schizophrenia
Inferior frontal gyrus**	56,16,14	0.054(0.05)	-0.008(0.04)	P(cFWE)=0.022, T=5.05, k=243 controls>schizophrenia
Right anterior insula and orbitofrontal cortex**	32,28,-14	0.062(0.05)	-0.007(0.05)	P(cFWE)<0.001, T=5.05, k=539 controls>schizophrenia
Parietooccipital sulcus and precuneus	-14,-56,20	-0.040(0.07)	0.026(0.07)	P(unc.)<0.001, T=3.97, k=32 schizophrenia>controls
Supplementary Motor Area BA6	4,-26,64	-0.047(0.06)	0.021(0.08)	P(unc.)<0.001, T=3.96, k=70 schizophrenia>controls
Right cerebellum posterior lobe and crus	14,-82,-32	-0.035(0.05)	0.020(0.06)	P(unc.)<0.001, T=3.83, k=37 schizophrenia>controls

**P(cFWE), Cluster level familywise error corrected at p<0.05 (cluster inclusion threshold p<0.001). P(unc.) clusters observed using peak threshold p<0.001 and an extent threshold k=30 in the unconstrained search.

8.5 Relationship with illness severity

In the present study, a significant failure of the directed influences within a salience-execution loop comprised of rAI, rDLPFC and dACC was observed. Further there was a significant failure of directed influence to and from several other brain regions (other than dACC and DLPFC) and the rAI. This includes a reduction in the Granger-causal inflow from bilateral visual cortices and right hippocampus to the rAI, and from the rAI to precuneus in patients. In light of this, the relationship between illness severity and these abnormal Granger-causal interactions was investigated in patients.

SSPI scores on Reality Distortion, Disorganisation and Psychomotor Poverty, measured on the same day of scanning, provide information regarding the symptom burden that persist despite antipsychotic treatment. In addition, cognitive deficits (reduced DSST score), longer duration of illness and higher functional disability (reduced SOFAS score) also indicate illness severity. The variables reflecting disease severity (three SSPI scores, duration of illness, DSST score, SOFAS score) showed significant bivariate relationships (mean of absolute correlation coefficients $|r|=0.34$).

The net Granger-causal influences (computed as $[(x\text{-to-}y) - (y\text{-to-}x)]$ coefficients) among the three nodes in the salience execution loop were highly correlated ($|r|=0.46$). Similarly, the Granger-causal influences to and from rAI to regions showing most significant between-group differences (rAI to precuneus, from left and right visual cortex and right hippocampal region to rAI - reported in Table 8.2) were also correlated with each other ($|r|=0.3$). Therefore, three separate principal component analyses were performed to extract first unrotated principal

factors explaining the largest proportion of variance in (i) the measures of illness severity (ii) the causal interactions among rAI, rDLPFC and dACC, (iii) the causal influences to and from rAI to regions showing most significant between-group differences. This data reduction approach reduced the likelihood of type 1 errors occurring due to multiple testing of the relationships among the various neuroimaging and symptom variables.

An 'illness severity' factor explaining 40% of variance, a 'salience-execution loop' factor explaining 52% of variance, and a 'visual inflow' factor explaining 48.5% of variance emerged from this analysis (Table 8.6). To study the relative contribution of the salience-execution loop factor and the visual inflow factor in predicting the illness severity, a multiple regression analysis was conducted with antipsychotic dose as a covariate. There was no significant collinearity among the independent variables. All variables (covariate and predictors) were entered in a single step in the regression model.

The model had a significant fit ($F[3,34]=4.03$, $R^2=0.26$, $p=0.015$). Illness severity was significantly predicted by both reduced integrity of the salience-execution loop ($\beta= -0.71$; $t=-2.8$, $p=0.008$) and reduced integrity of the visual inflow to the rAI ($\beta= -0.32$; $t=-2.1$, $p=0.04$). Antipsychotic dose had a trend level association with higher dose being prescribed for patients with more severe illness ($\beta= 0.27$; $t=1.9$, $p=0.064$). Further details are presented in Table 8.6 and Figure 8.5.

Figure 8.5: Relationship between illness severity, salience-executive loop integrity and visual inflow to right anterior insula. Variables with loading >0.4 in each of the first unrotated principal factor are shown as components in the figure. Factor scores are indicated using appropriate positive or negative sign. The β , t and p values are parameter statistics derived from a multiple regression analysis to predict the illness severity factor from the salience-executive loop and the visual to rAI inflow factors. rAI: right anterior insula, DLPFC: dorsolateral prefrontal cortex; dACC: dorsal anterior cingulate cortex.

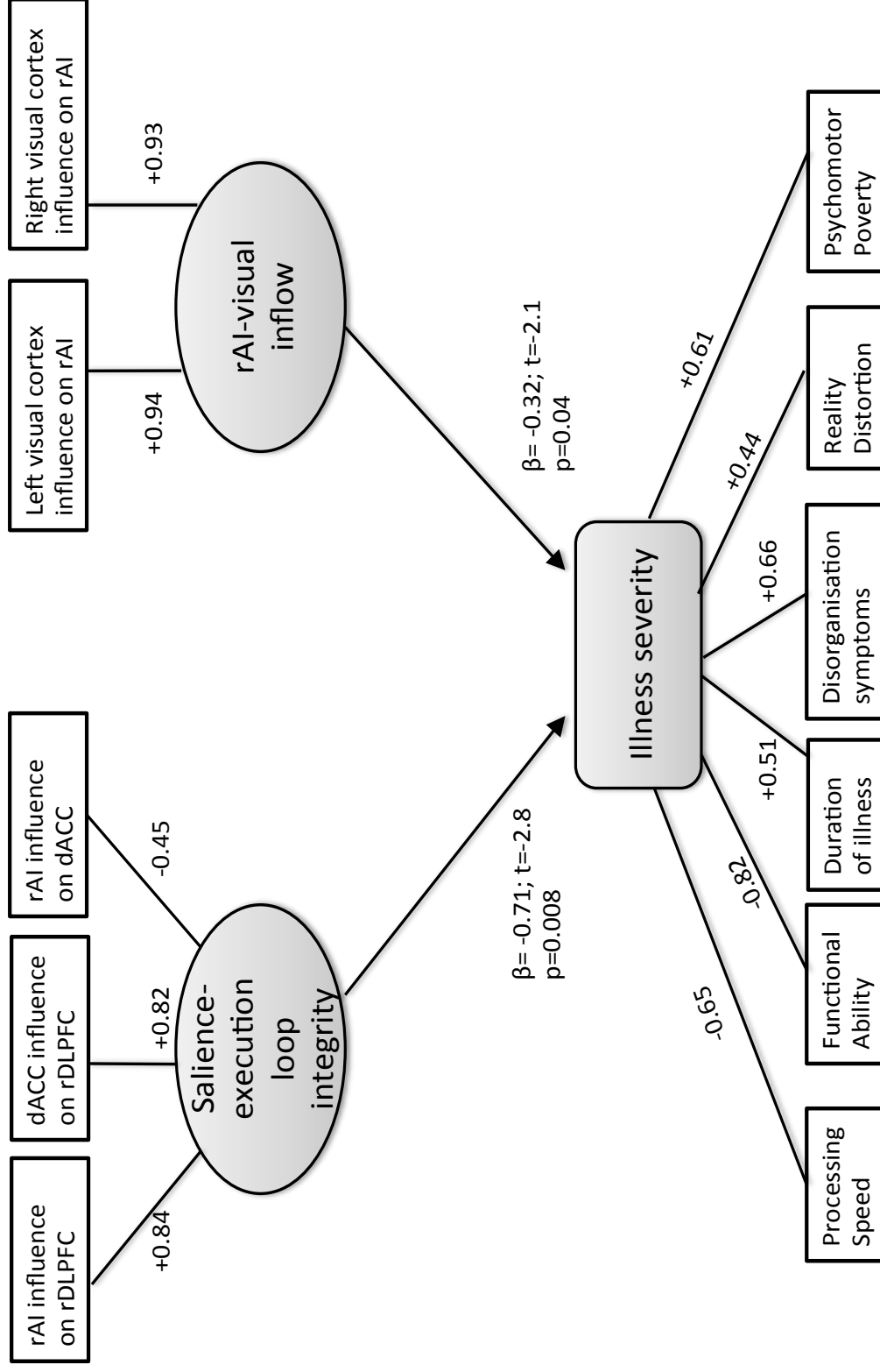


Table 8.6: Principal components (first unrotated factors) relating to illness severity, salience-execution loop integrity and visual inflow to rAI in patients with schizophrenia

Variables	Factor loading	Interpretation of the principal factor based on major components (variables with loading >0.4)
Illness severity (40% of variance)		
Social and occupational functioning (SOFAS) score	-0.82	Higher factor scores seen in patients with poor functional ability, poor processing speed and higher burden of disorganisation, psychomotor poverty and reality distortion.
Disorganisation score (SSPI)	+0.66	
Processing speed score (DSST)	-0.65	
Psychomotor Poverty score (SSPI)	+0.61	
Duration of illness	+0.51	
Reality Distortion score (SSPI)	+0.44	
Causal influence within the salience-execution loop (53% of variance)		
rAI to rDLPFC influence	+0.84	Higher factor scores seen in patients with higher excitatory influence from rAI and dACC to DLPFC, and reduced excitatory influence from rAI to dACC. (In the present sample, this pattern is observable in healthy controls and is suggestive of normal physiological integrity of the salience-execution loop)
dACC to rDLPFC influence	+0.82	
rAI to dACC influence	-0.45	
Visual inflow to rAI (48.5% of variance)		
Left visual cortex to rAI influence	+0.94	Higher factor scores seen in patients with higher excitatory influence from visual cortex to rAI. (In the present sample, this pattern is observable in healthy controls and is suggestive of normal physiological integrity of the visual input to rAI)
Right visual cortex to rAI influence	+0.93	
Right hippocampus to rAI influence	+0.35	
rAI to precuneus influence	+0.28	

8.6 Functional Connectivity (FC)

One-sample t-tests of FC maps reflecting functional coupling between rAI and rest of the brain revealed significant positive correlation with several regions constituting the SN (bilateral anterior insula, extending to anterior and midcingulate, bilateral inferior frontal, middle frontal and superior temporal gyrus, supramarginal gyrus, putamen and thalamus). In addition, positive correlation was also noted at right middle temporal gyrus and small clusters located bilaterally in the dorsal precuneus. Extensive anticorrelation was noted between the rAI seed and nodes constituting the DMN including the PCC/ventral precuneus, angular gyrus and parahippocampal region. The results are shown in Figure 8.6 and Table 8.7.

Two sample t-tests comparing the FC maps of patients and controls revealed significant differences in the rAI connectivity with key paralimbic regions including bilateral temporal pole, parahippocampal region and the amygdala. In the right temporal pole, patients showed no significant functional connectivity (one-sample $t(37)=0.24, p=0.81$) while controls showed a significant positive correlation (one-sample $t(34)=7.42$, corrected $p<0.001$). At the left temporal pole, patients showed an anti-correlation (one-sample $t(37)=-4.9$, corrected $p<0.001$), while controls had a positive correlation (one-sample $t(34)=3.78$, corrected $p<0.001$).

A similar dissociation in the FC between the two groups was also noted in other limbic clusters when using an uncorrected threshold of $p<0.001$, $k=30$ [periaqueductal grey matter (two-sample $t=3.74, k=60$; patients, one-sample $t(37)=-3.06, p=0.004$; controls, one-sample $t(34)=2.42, p=0.021$) and right

parahippocampal/amygdala (two-sample $t=4.36, k=159$; patients, one-sample $t(37)=-2.72, p=0.010$; controls, one-sample $t(34)=3.51, p=0.001$]. Left DLPFC and left posterior insula showed significant group difference (schizophrenia>controls) at the uncorrected threshold. At the left DLPFC, a significant anticorrelation in controls (one-sample $t(34)=-5.88, p<0.001$) and absence of significant correlation in patients (one-sample $t(37)=0.41, p=0.69$) was noted. At the left posterior insula, a significant positive correlation was seen in the patients (one-sample $t(37)=5.75, p<0.001$) while controls had no significant correlation (one-sample $t(34)=0.70, p=0.49$). The group differences are shown in Table 8.8 and Figure 8.7.

The eigenvariate derived from the clusters showing either reduced or increased FC in patients showed no significant correlations with antipsychotic dose equivalents (both $p>0.2$).

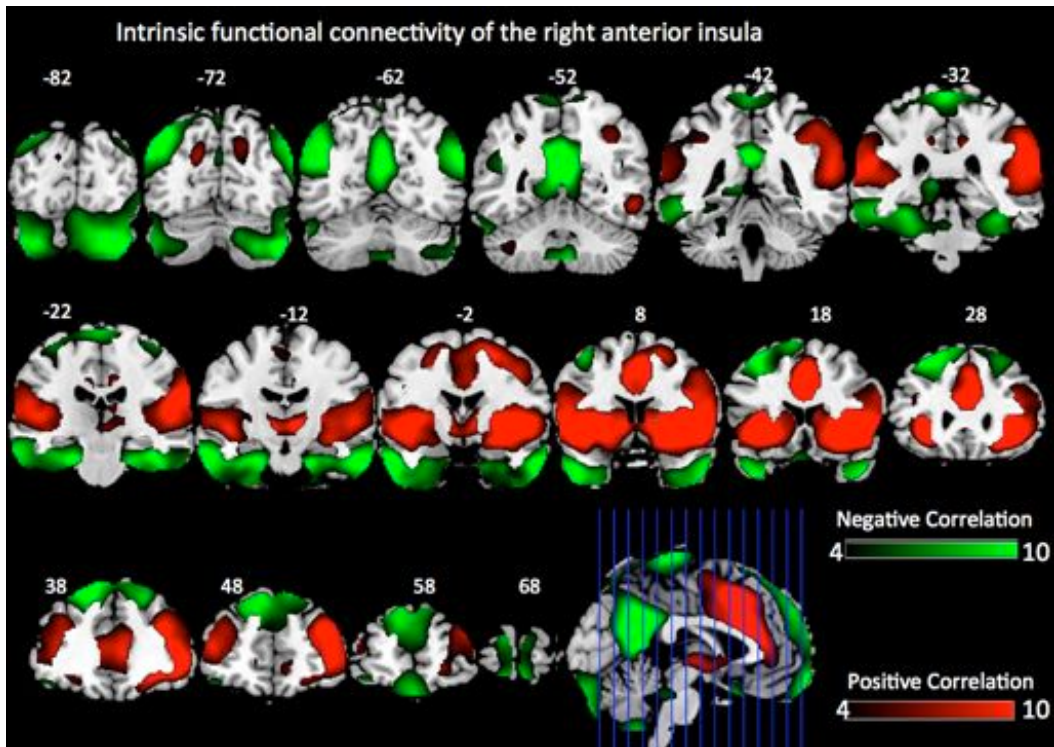


Figure 8.6: Functional connectivity of the right anterior insula. The figure depicts the results of the one sample T test of z transformed voxelwise correlation maps on all subjects (patients and controls). Illustrations drawn on a single subject structural image showing coronal slices using MRICron at family-wise error corrected $p < 0.05$, $k = 30$. Color bar shows a scale of T values. Red colored areas show positive correlation, while green colored areas show anticorrelation with the seed region.

Table 8.7: One sample T test (patients and controls) of intrinsic functional connectivity between right anterior insula and rest of the brain

Regions	Peak MNI coordinates (x, y, z) in mm	Mean (SD) correlation coefficient in controls*	Mean (SD) correlation coefficient in patients*	Peak intensity (T) and cluster size (k=voxel count) [§]
Regions showing positive correlation				
Bilateral anterior insula, extending to anterior and midcingulate, bilateral inferior frontal, middle frontal and superior temporal gyrus, supramarginal gyrus, putamen and thalamus	32,20,0 -32,20, -2 4,12,46	0.257(0.07)	0.249(0.08)	T=82.2, k=31948
Right middle temporal gyrus	54, -52, -8	0.151(0.17)	0.130(0.16)	T=8.0, k=124
Right anterior midcingulate	12, -28,36	0.167(0.16)	0.135(0.20)	T=8.0, k=80
Left precuneus	-16, -74,30	0.111(0.13)	0.123(0.14)	T=7.6, k=161
Left anterior midcingulate	-12,-28,36	0.121(0.14)	0.140(0.19)	T=7.1, k=137
Right precuneus	18, -70,34	0.137(0.16)	0.120(0.19)	T=6.2, k=138
Left inferior parietal	-34,-44,38	0.122(0.16)	0.125(0.19)	T=6.1, k=50
Regions showing negative correlation				
Right inferior temporal, fusiform and parahippocampal region	60, -6 -28	-0.164(0.09)	-0.199(0.11)	T=14.2, k=4044
Right posterior cingulate / precuneus	2, -58,22	-0.236(0.12)	-0.189(0.12)	T=13.9, k=2018
Left inferior temporal gyrus, fusiform and parahippocampal region	-58, -2 -34	-0.175(0.06)	-0.172(0.10)	T=13.4, k=11792
Left angular gyrus	-44, -70, 40	-0.253(0.11)	-0.201(0.17)	T=13.1, k=2181
Bilateral ventral and superior medial prefrontal	-38,16,56	-0.229(0.13)	-0.186(0.17)	T=12.4, k=5373
Right angular gyrus	58, -66,26	-0.215(0.14)	-0.182(0.18)	T=11.8, k=1239
Bilateral paracentral lobule	-2, -34,72	-0.127(0.12)	-0.146(0.16)	T=10.9, k=1185
Posterior lobe and tonsil of cerebellum	4, -54,-50	-0.167(0.16)	-0.119(0.15)	T=9.3, k=297
Left medial frontal gyrus	-4,14,-26	-0.097(0.17)	-0.183(0.18)	T=7.53, k=77
Left orbitofrontal cortex	-44, 32 -18	-0.134(0.14)	-0.150(0.18)	T=6.5, k=126
Left precentral gyrus	-36,-24,62	-0.105(0.15)	-0.115(0.16)	T=6.38,k=126
Right precentral gyrus	40, -22,66	-0.099(0.15)	-0.131(0.17)	T=6.3, k=96
* Values are z transformed. § Voxel level familywise error corrected p<0.05, k=30				

Table 8.8: Two-sample T test of the difference in the instantaneous functional connectivity of right anterior insula with the rest of the brain between patients and controls

Regions	MNI coordinates (x, y, z) in mm	Mean (SD) correlation coefficient in controls	Mean (SD) correlation coefficient in patients	P value, peak intensity and cluster size (k = voxel count)
Controls>Schizophrenia				
Right superior temporal pole**	44,14,-24	0.211(0.17)	0.005(0.13)	P(cFWE)=0.028, T=5.09, k=582
Left superior temporal pole extending to parahippocampal/amygdala**	-44,14,-26	0.094(0.15)	-0.092(0.12)	P(cFWE)=0.011, T=4.95, k=801
Right parahippocampal/amygdala region	36,-10,-22	0.106(0.18)	-0.064(0.15)	P(unc.)<0.001, T= 4.36, k=159
Periaqueductal grey matter	6,-24,-18	0.069(0.17)	-0.089(0.18)	P(unc.)<0.001, T= 3.74, k=60
Schizophrenia>Controls				
Left middle frontal	-34,30,36	-0.186(0.19)	0.0117(0.18)	P(unc.)<0.001, T= -4.67, k=285
Right posterior insula	42,-12,18	0.017(0.14)ns	0.165(0.18)	P(unc.)<0.001, T= -3.91, k=52
**P(cFWE), Cluster level familywise error corrected at p<0.05 (cluster inclusion threshold p<0.001). P(unc.), clusters observed using peak threshold p<0.001 and an extent threshold k=30 in the unconstrained search.				

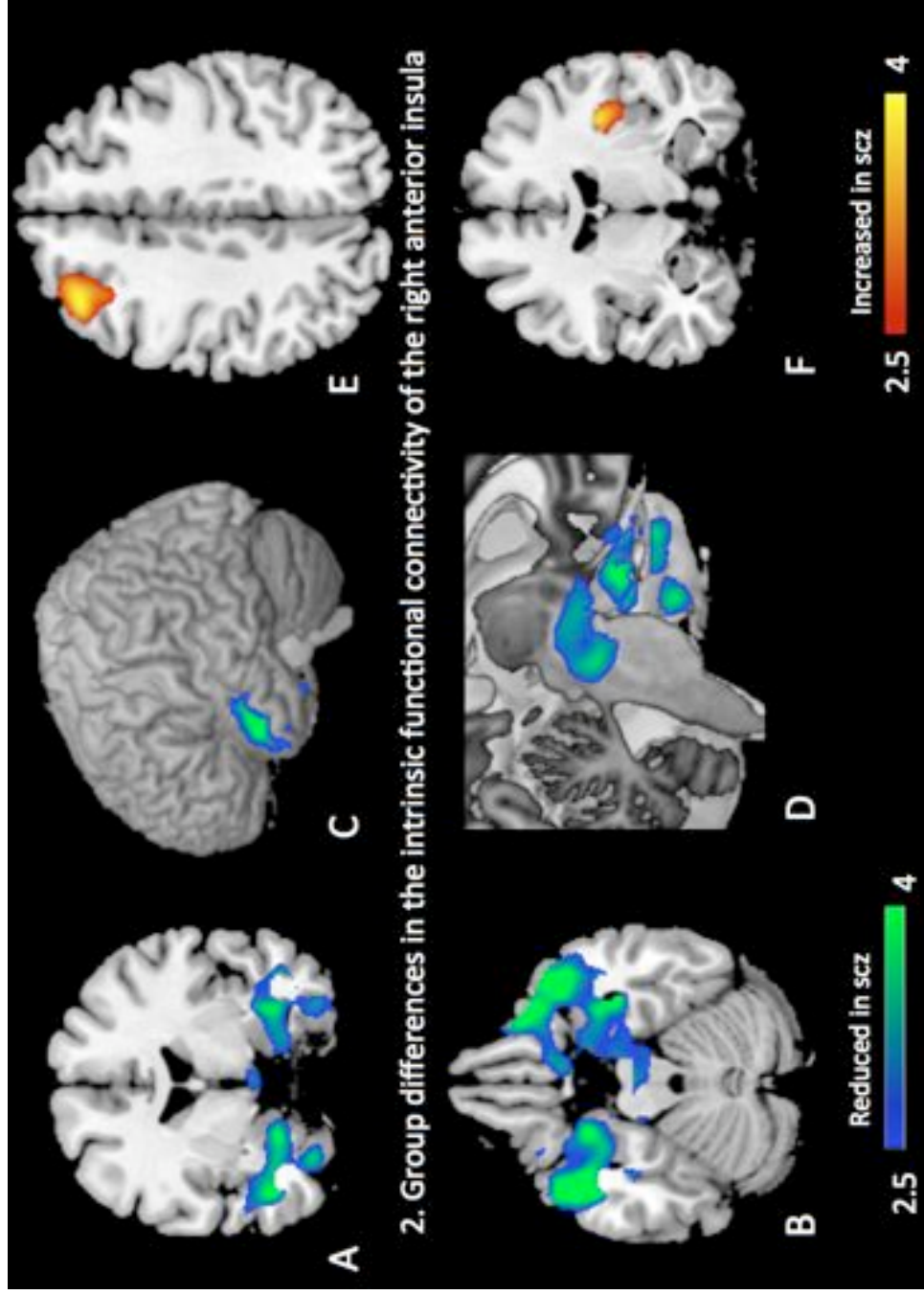


Figure 8.7: Group differences in functional connectivity of the right anterior insula in patients with schizophrenia compared to healthy controls. Illustrations drawn on a single subject structural with slices selected for the best display of regions showing differences in the two-sample t test. Color bar shows a scale of T values. Red-yellow colored areas show regions where patients had greater Fisher's r-to-z correlation scores than controls, while green-blue colored areas show regions where patients had lower z Fisher's r-to-z scores than controls. A and B. Amygdala / parahippocampal region ($y=-6$, $z=-21$) C. Surface rendered image showing left superior temporal pole D. Magnified cut section ($x=6$) of surface rendered image showing periaqueductal grey matter E. Left middle frontal region ($z=42$) F. Right posterior insula ($y=-12$).

Table 8.8: Two-sample T test of the difference in the instantaneous functional connectivity of right anterior insula with the rest of the brain between patients and controls

Regions	MNI coordinates (x, y, z) in mm	Mean (SD) correlation coefficient in controls	Mean (SD) correlation coefficient in patients	P value, peak intensity and cluster size (k = voxel count)
Controls>Schizophrenia				
Right superior temporal pole**	44,14,-24	0.211(0.17)	0.005(0.13)	P(cFWE)=0.028,T=5.09, k=582
Left superior temporal pole extending to parahippocampal/amygdala**	-44,14,-26	0.094(0.15)	-0.092(0.12)	P(cFWE)=0.011,T=4.95,k=801
Right parahippocampal/amygdala region	36,-10,-22	0.106(0.18)	-0.064(0.15)	P(unc.)<0.001,T= 4.36,k=159
Periaqueductal grey matter	6,-24,-18	0.069(0.17)	-0.089(0.18)	P(unc.)<0.001,T= 3.74,k=60
Schizophrenia>Controls				
Left middle frontal	-34,30,36	-0.186(0.19)	0.0117(0.18)	P(unc.)<0.001,T= -4.67,k=285
Right posterior insula	42,-12,18	0.017(0.14)ns	0.165(0.18)	P(unc.)<0.001,T= -3.91,k=52
**P(cFWE), Cluster level familywise error corrected at p<0.05 (cluster inclusion threshold p<0.001). P(unc.), clusters observed using peak threshold p<0.001 and an extent threshold k=30 in the unconstrained search.				

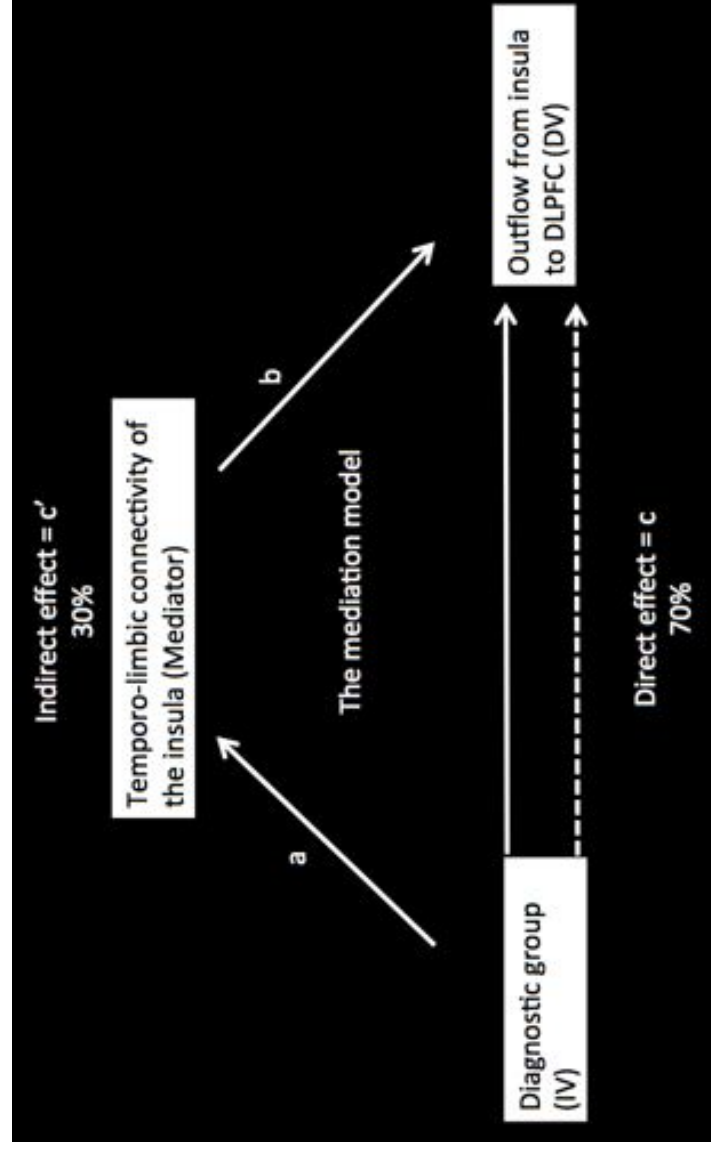


Figure 8.8: The mediation model. A single mediation model with the first eigenvariate of functional connectivity between the right anterior insula and the temporolimbic clusters (bilateral temporal pole, hippocampal formation and periaqueductal grey) as a mediator of the relationship between diagnostic status and the directed influence (x to y) from right anterior insula to right DLPFC. IV: independent variable, DV: dependent variable

8.8 Granger Causal influences from the left anterior insula

A number of previous observations suggest that the right anterior insula is a major node in the Salience Network and plays a crucial role in the interactions between large-scale networks (Seeley et al., 2007; Sridharan et al., 2008; Supekar and Menon, 2012). Studies examining the resting state connectivity of right and left anterior insula (AI) often observe a significant overlap, though the pattern of connectivity related to the Salience Network is strongly right lateralized (Cauda et al., 2012, 2011). To explore the causal interactions from the left AI, the GCA analysis was repeated (described in the Methods section of the manuscript) using a left AI seed. A 6-mm radius sphere centered on the local maxima ($x=-33$, $y=21$, $z=-3$) of functional activation corresponding to the left AI during a 2-back task performed by all subjects was used as the left AI seed region.

One sample t test of GCA maps from left AI : In the entire sample (patients and controls, one-sample t test), left AI exerted a significant excitatory influence on the bilateral DLPFC and bilateral inferior orbitofrontal cortex. Significant inhibitory influence of the left AI was noted at bilateral supplementary motor region, precuneus and bilateral precentral regions. Bilateral DLPFC in turn had a significant inhibitory influence on the left AI. In addition, dACC also had significant inhibitory influence on the left AI. Overall, this pattern of causal influence was very similar to those observed using rAI seed. These results are shown in Figure 8.9 and Table 8.9.

Between-groups comparison of GCA maps from left AI: Between group (Controls vs. Schizophrenia) analysis conducted using two-sample t-

test (FWE corrected $p < 0.05$), with the search volume corrected for the mask derived from one sample t test did not reveal any significant differences in the causal influences to and from left AI. At an uncorrected peak height threshold $p < 0.001$ and cluster extent threshold $k=30$, patients showed a reduction in the inhibitory influence from the left AI to bilateral medial frontal gyrus and precentral gyrus. Similar to the findings from the rAI seed, patients also showed a reduction in the excitatory influence from visual cortex to the left AI, at this uncorrected threshold ($p < 0.001$, cluster extent $k=30$). Overall, this suggests that the abnormalities in the causal influence from the anterior insula in general, and the salience-execution loop (AI to DLPFC feedback) in particular, more prominently involve the right hemisphere. More details are presented in Table 8.10.

Spatial similarity analysis: To determine the degree of topographical overlap between the Granger causal outflow maps from the right and the left AI across the entire sample, a spatial similarity analysis was carried out using the masks derived from the one-sample t tests of right and left AI (x-to-y) GCA maps. Firstly, an intersection (overlap) mask and a combination (union) mask were created from the two original masks derived from the one-sample t tests. The Dice-coefficient of similarity (DCS) was then calculated using the intersection and the combination masks (Zou et al., 2004). Conjunction measures such as DCS provide more reliable results when every signal of interest is included in the individual contrasts (Duncan et al., 2009). To enable this, an uncorrected threshold of $p=0.001$ was used when extracting the intersection and the combination masks. A DCS value of 100% means that the

both maps have perfect spatial agreement in the distribution of causal influences across the brain.

The DCS test revealed 73% overlap in the topography of causal influences from right and left AI in the entire sample. Of the 27% observed dissimilarity, voxels present in the right AI GCA maps but not in the left AI maps contributed to 21.2% (i.e. 78.5% of the total dissimilarity), with the remaining 5.8% arising from voxels present in the left, but not in the right AI GCA maps. Examination of the conjunction maps revealed that despite the similar distribution of the clusters in both maps, rAI had a larger spatial extent of causal influence (no. of voxels) than the left AI in these clusters (Figure 8.10).

Group specific differences between the right and left AI GCA maps : A paired t test between the x to y rAI seed maps and left AI seed maps across the entire sample did not reveal any regions of significant differences (at uncorrected $p < 0.001$, cluster extent = 30). Interestingly, when the paired t test was restricted within the patient group, three significant clusters with higher Granger causal influence from the right AI compared to the left AI were noted (Figure 8.10). There were no differences between the left and right AI maps in the healthy controls.

Table 8.9: One sample T test (patients and controls) of the directed causal influence to and from left anterior insula

Regions	MNI coordinates (x, y, z) in mm	Mean (SD) path coefficient in controls	Mean (SD) path coefficient in patients	Peak intensity (T) and cluster size (k=voxel count) [§]
Regions positively influenced by left AI				
Left superior temporal and orbitofrontal gyrus	-46,17,-13	0.107(0.11)	0.069(0.08)	T=7.6, k=195
Right inferior orbitofrontal / insula	48,20,-10	0.080(0.09)	0.069(0.08)	T=7.3, k=232
Left middle frontal gyrus	-37,46,14	0.077(0.11)	0.040(0.06)	T=5.6, k=196
Right middle frontal gyrus	39,43,26	0.060(0.08)	0.030(0.07)	T=5.1, k=50
Regions negatively influenced by left AI				
Left precentral gyrus	-56,-5,24	-0.063(0.08)	-0.024(0.04)	T=6.5, k=263
Right precentral gyrus	58,-3,24	-0.058(0.07)	-0.020(0.04)	T=6.3, k=194
Supplemental Motor Area	9,-8,60	-0.031(0.04)	-0.030(0.05)	T=5.7, k=48
Right precuneus	14,-37,2	-0.058(0.06)	-0.030(0.07)	T=5.6, k=73
Right postcentral gyrus	38,-24,55	-0.052(0.08)	-0.023(0.04)	T=5.1, k=110
Regions exerting positive influence on left AI				
Anterior lobe of cerebellum	1,-30,-19	0.036(0.05)	0.035(0.06)	T=5.4, k=163
Left Supplementary motor area	-8,-3,60	0.053(0.09)	0.061(0.09)	T=4.9, k=48
Regions exerting negative influence on left AI				
Left superior temporal pole	-47,17,-11	-0.035(0.05)	-0.33(0.05)	T=5.9, k=67
Right middle and inferior frontal	46,24,25	-0.040(0.03)	-0.034(0.05)	T=5.9, k=459
Right inferior frontal gyrus	48,20,-9	-0.029(0.05)	-0.036(0.04)	T=5.6, k=70
Left middle frontal gyrus	-37,42,16	-0.047(0.05)	-0.30(0.05)	T=5.3, k=254
Right anterior cingulate	6,43,17	-0.026(0.05)	-0.044(0.05)	T=5.2, k=133
§ Familywise Error corrected p<0.05				

Table 8.10: Two-sample T test of the difference in the directed influence to and from the left anterior insula in patients and controls.

Regions	MNI coordinates (x, y, z) in mm	Mean (SD) path coefficient in controls	Mean (SD) path coefficient in patients	Peak intensity and cluster size (k = voxel count), P(unc.)<0.001
<i>Causal outflow from the left AI (x to y coefficients)</i>				
Left precentral gyrus	-55,-7,25	-0.082(0.09)	-0.019(0.05)	T= 3.89 , k= 49 Schizophrenia> Controls
Right medial frontal gyrus (right rectus)	6,55,-15	-0.074(0.14)	0.020(0.07)	T= 3.81 , k= 69 Schizophrenia> Controls
Left medial frontal gyrus (left rectus)	-9,49,17	-0.055(0.10)	0.015(0.06)	T= 3.79 , k= 31 Schizophrenia> Controls
Right precentral and postcentral	64,-2,18	-0.06(0.07)	-0.004(-.05)	T=3.76 , k= 49 Schizophrenia> Controls
Right superior medial frontal	9,61,7	-0.06(0.09)	0.014(0.06)	T=3.64 , k= 109 Schizophrenia> Controls
<i>Causal inflow to the left AI from rest of the brain (y to x coefficients)</i>				
Left middle occipital gyrus (BA19)	-30,-96,12	0.063(0.09)	-0.045 (0.14)	T= 3.96 , k=37 Controls> Schizophrenia
P(unc.) clusters observed using a peak threshold p<0.001 and cluster extent threshold k=30 in the unconstrained search. None of the clusters survived FWE corrected p<0.05 for multiple testing.				

Figure 8.9: Granger causal influence to and from the left anterior insula. Top panel A depicts the influence of left anterior insula on the rest of the brain (x to y). Bottom panel B depicts the influence of rest of the brain on left anterior insula (y to x). The figures show the results of the one sample T test of GCA maps on all subjects (patients and controls). Illustrations drawn on a single subject structural image showing axial slices using xjview at $p < 0.001$ uncorrected, $k = 30$. Color bar shows a scale of T values. Warm colours suggest excitatory influence, while cold colours suggest inhibitory influence.

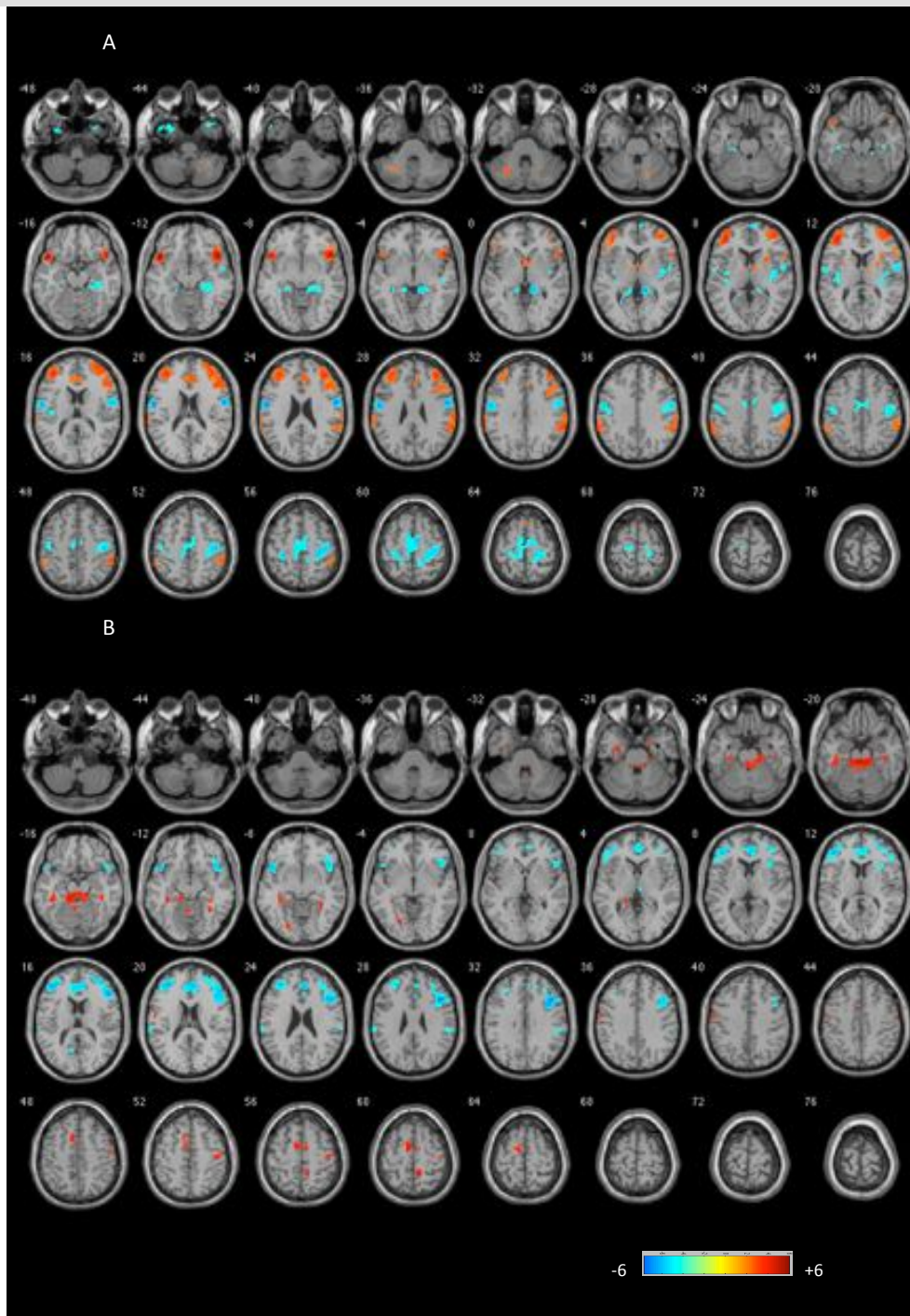
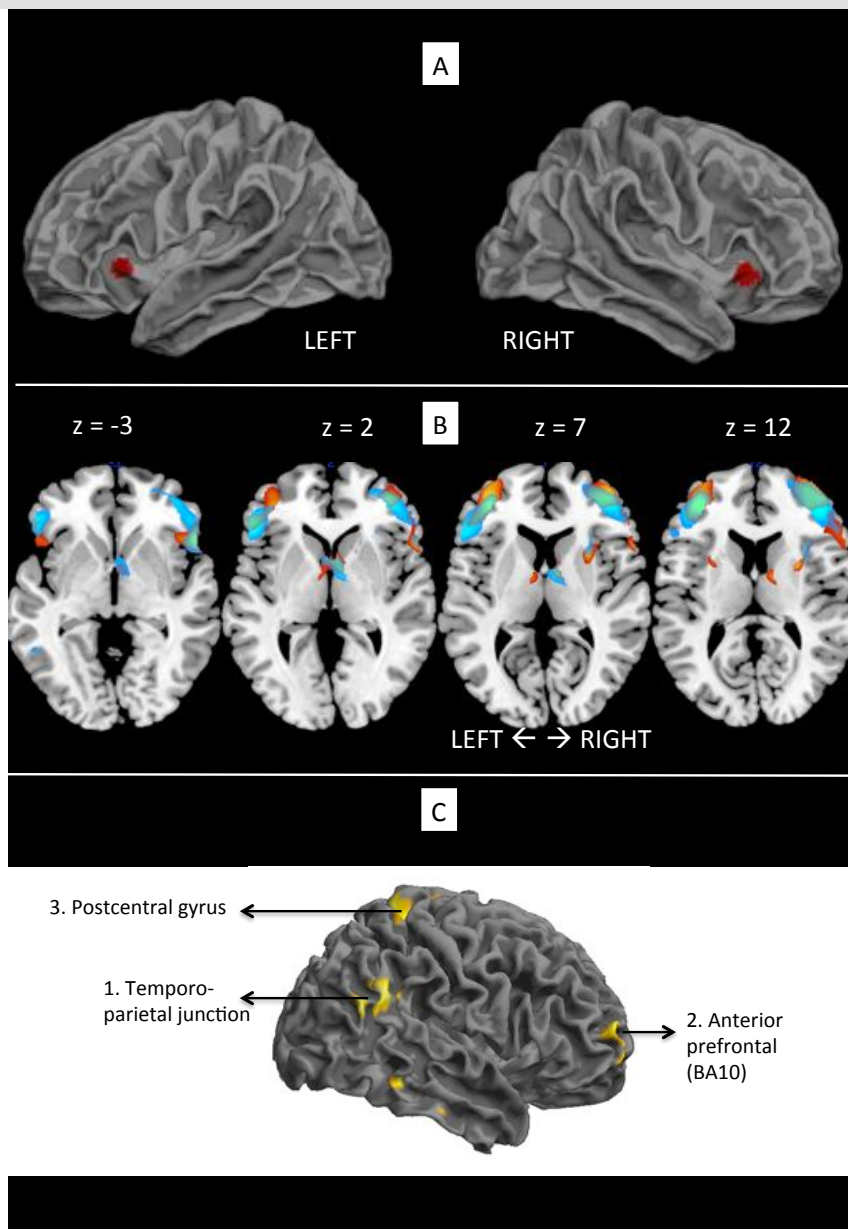


Figure 8.10: Hemispheric lateralisation of Granger causal influences from anterior insula. A: Right ($x=33,y=21,z=-3$) and Left ($x=-33,y=21,z=-3$) anterior insula seed regions projected on a reconstructed average white matter surface (fsaverage) using Freesurfer software. B. Spatial overlap of causal influence from right (blue-cyan) and left (red-yellow) anterior insula seeds. Each overlay is derived from the one sample T test of the corresponding seed based GCA maps on all subjects (patients and controls). Illustrations drawn on a single subject structural image showing axial slices using MRICron at $p<0.001$ uncorrected, $k=30$. Slices selected for the best display of lateral prefrontal cortex. C. Differences in the Granger causal (x to y) influence between right and left anterior insula using a paired t test in patients with schizophrenia ($n=38$). Three clusters showing greater causal influence from right ($>$ left) anterior insula emerged in patients. 1. Temporo-parietal junction (cluster $p_{FWE}=0.006$; $k=431$; $T=5.74$, peak $(x,y,z) = 56,-56,30$) 2. Anterior prefrontal (BA10) (cluster $p_{FWE}=0.042$; $k=268$; $T=5.17$, peak $(x,y,z) = 34,64,-6$) 3. Postcentral gyrus (cluster $p_{FWE}=0.021$; $k=324$; $T=4.63$, peak $(x,y,z) = 12,-40,64$). There were no regions showing excessive casual influence from left ($>$ right) anterior insula seed. No differences in the GCA maps between the right and left anterior insula were notable in healthy controls.



DISCUSSION

8.9 Impaired salience-execution loop in schizophrenia

Though deficits in brain regions involved in processing stimulus salience and cognitive control have been repeatedly shown in schizophrenia, this is the first study that directly investigates the ‘causal’ relationship between the dysfunctions observed in these two systems. Using Granger causal analysis, patients with schizophrenia are shown to have significantly reduced neural influence from the rAI, a key node in the salience processing system, to the DLPFC, a crucial node in the executive loop (Table 8.11). Further the most significant abnormality in the influences to and from the DLPFC in patients with schizophrenia involved the nodes of the SN - the dACC and the anterior insula. These observations confirm the primary hypothesis that the interaction between the paralimbic salience processing system and the multimodal executive system is significantly diminished in schizophrenia (Figure 8.11).

Table 8.11: Test performance of the insula-DLPFC Granger Influence. Using a cut-off of zero (no Granger influence between insula and DLPFC), the groups are stratified as ‘test positive’ and ‘test negative’. Test Accuracy statistics are computed for the entire sample.

Sensitivity	37%	
Specificity	97%	
Accuracy	66%	
Predictive value of positive test	93%	
Predictive value of negative test	59%	
Likelihood ratio of positive test	12.9	
‘Cut-off’ of 0	Schizophrenia	Controls
Negative GC	14	1
Positive GC	24	34

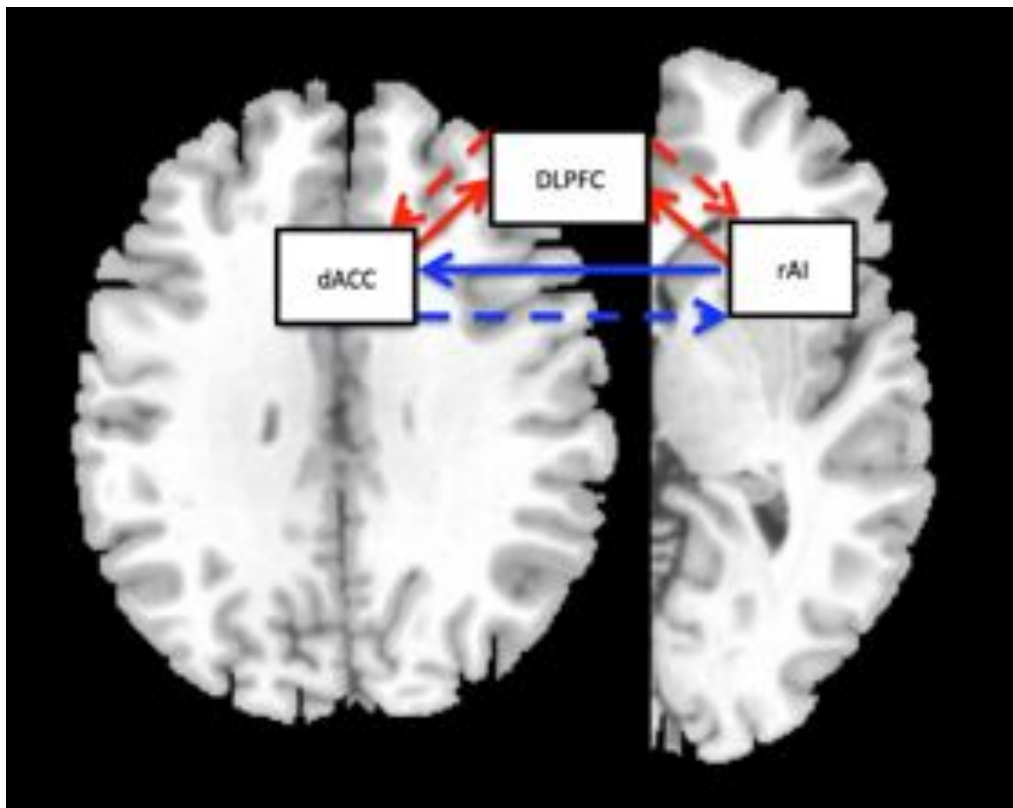


Figure 8.11: Summary of the Granger causal inferences. Right anterior insula (rAI) has excitatory influence on both dorsal anterior cingulate cortex (dACC) and dorsolateral prefrontal cortex (DLPFC), in turn both of these regions inhibit the rAI in controls. Solid lines represent a positive Granger influence, dashed lines represent a negative Granger influence. Lines drawn in red indicate the pathways that show significant abnormalities in schizophrenia when compared to controls. The interaction between the DLPFC and both nodes of the Salience Network (rAI and dACC) are affected in schizophrenia. The rAI to dACC loop is relatively intact in schizophrenia.

Van Snellenberg et al., (2006) concluded that the magnitude of working memory performance reduction in schizophrenia is associated with degree of attenuation of DLPFC activation. Inefficient DLPFC recruitment is apparent when the task becomes more challenging (Potkin et al., 2009). It is not simply the failure to recruit frontoparietal systems that is associated with the reduced

task performance, but there is a conjoint failure to deactivate or 'switch-off' the task-irrelevant DMN system that includes multimodal midline structures such as the ventromedial prefrontal cortex (Nygård et al., 2012) and PCC/Precuneus (Hasenkamp et al., 2011) in addition to parahippocampal regions (Whitfield-Gabrieli and Ford, 2012). Successful anticorrelation between these two networks appears crucial for effective task performance, and this anticorrelation is affected in schizophrenia (Whitfield-Gabrieli and Ford, 2012). The SN has been proposed to regulate the two competing brain systems (Seeley et al., 2007; Sridharan et al., 2008). The present observation that during rest, the influence of the rAI on the DLPFC and to some extent on the precuneus is diminished in schizophrenia suggests that the inefficient cerebral recruitment associated with cognitive dysfunction in schizophrenia is likely to result from a failure of paralimbic-multimodal integration rather than a focal DLPFC dysfunction alone. Further, the abnormal reciprocal influence from DLPFC was more ventrally located in the insula, highlighting the somewhat selective loss of prefrontal influence predominantly directed to the socio-emotional frontoinsula cortex (Kurth et al., 2010).

In patients with schizophrenia, both the excitatory influence of dACC onto DLPFC, and the inhibitory influence from the DLPC onto dACC were significantly reduced. ACC is frequently coactivated with DLPFC during task performances, irrespective of the nature of the stimulus and response (Koski and Paus, 2000). Several computational models suggesting bidirectional flow of information between ACC and DLPFC have been put forward, with both feed-forward and feedback influences proposed in addition to indirect influences via other brain structures (Mars et al., 2012). But to date, the

detailed topography of these circuits remains unclear. Tracer injection studies from rhesus monkeys indicate that ACC exerts both prominent excitatory and inhibitory effects on the DLPFC (Medalla and Barbas, 2009). Barbas (2000) suggests that DLPFC has no direct limbic connections, though it is likely to access limbic signals via paralimbic structures including the ACC. Interestingly, in schizophrenia at least in the superficial layers of the ACC, inhibitory neurons appear to be reduced in their density (Reynolds et al., 2001). The prominent failure of the bidirectional communication between the dACC and the DLPFC observed in this sample suggest that the transfer of limbic signals onto the DLPFC is abnormal in schizophrenia. It is, however, important to note that both ACC and DLPFC are large brain regions with significant heterogeneity in the functional specialization of neuronal subsets (Johnston et al., 2007), hence generalizing the present results derived from selected coordinates to entire dACC/DLPFC circuitry may not be appropriate.

It is worth noting that in the original description of the SN using FC, Seeley et al. (Seeley et al., 2007) hypothesized that in task-free settings the SN and CEN are negatively correlated with the DMN but are minimally correlated with one another. The current observations suggest that in fact, at rest, while the SN exerts an excitatory influence on the DLPFC, in turn the DLPFC exerts an inhibitory influence on the SN. It is possible that a well-balanced salience-execution loop exists during rest, and on the arrival of appropriate stimulus that violates expectancies of the resting state, this balance is perturbed with an increase in the positive influence of SN over the DLPFC, and a reduction in the negative influence of the DLPFC over the SN leading to a reverberating

excitatory process in this loop. This speculation requires verification from direct electrophysiological studies during task performance.

Patients with reduced 'causal' influence within the salience-execution loop had poor occupational and sociofunctional ability, cognitive dysfunction characterized by reduced processing speed and higher symptom burden in the domains of disorganisation, psychomotor poverty and reality distortion despite antipsychotic treatment. A similar, albeit less prominent relationship was observed between reduced visual inflow to rAI and higher illness severity in patients. This predictive relationship observed between the impairments in the directed influences within the salience-execution loop and the symptom burden validates the notion that an impaired 'switching' function of the SN contributes to several core symptoms of schizophrenia and contributes to functional disability (chapter 2). Given that the patients in this sample were in a clinically stable phase, this relationship is likely to reflect the role of the salience processing system on the 'trait-like' aspects of the clinical presentation of schizophrenia. In the present study, both reduced visual inflow to the rAI, and the impaired 'causal' connectivity within the salience-execution loop predicted reduced processing speed. This reconciles previous findings that reported impaired processing speed both in relation to functional hypofrontality (Molina et al., 2009), and structural dysconnectivity involving occipitofrontal fasciculi (Palaniyappan et al., 2013), and affirms the cardinal role of rAI in the pathophysiology of schizophrenia.

A reduction in the 'causal' inflow from the visual cortex to the rAI in schizophrenia was not predicted *a priori*. Nevertheless, in line with the mounting evidence implicating a failure of bottom-up processes in psychosis (Javitt, 2009) and their relationship with anhedonia, apathy, negative symptoms and cognitive dysfunction (Javitt, 2009), the present results suggest that insular dysfunction is characterized by both a reduced visual inflow and frontal outflow. Thus the SN is likely to form a crucial link in the hierarchical processing (sensory regions → salience network → executive network) abnormalities that contribute to the clinical expression of schizophrenia.

Right anterior portion of the temporoparietal junction (TPJ), along with right anterior insula and anterior prefrontal cortex (aPFC), participates in a ventral attention system associated with the function of orienting to salient external stimuli (Corbetta and Shulman, 2002; Wen et al., 2012). In patients with schizophrenia, there is a stronger right lateralization of the causal influence from the anterior insula to right TPJ and aPFC, while the causal influence of right AI on the right DLPFC is significantly reduced when compared to healthy controls. The results presented here suggest that in schizophrenia, a possible imbalance between the bottom-up stimulus processing circuitry and top-down cognitive control circuitry exists at the level of right anterior insula. This phenomenon of putative stimulus processing imbalance is likely to explain a number of cognitive deficits noted in schizophrenia (Gilbert and Sigman, 2007), and requires further experimental exploration using cognitive tasks that modulate stimulus saliency.

8.10 Temporo-limbic dysconnectivity in schizophrenia

A prominent loss of instantaneous positive correlation between the rAI and bilateral temporal pole was observed in patients. Unlike healthy controls who showed a positive correlation, patients showed an anticorrelation between rAI and bilateral medial temporal lobe structures. Temporal pole is a prominent paralimbic region with a crucial role in socioemotional processing (Olson et al., 2007). In patients with schizophrenia medial temporal structures form a significant component of the task-negative DMN (Garrity et al., 2007), but often fail to 'switch-off' during cognitive tasks. The presence of significant disconnectivity between rAI and temporolimbic system suggests that the abnormalities in the SN-mediated switch-off of DMN during task performance could affect the medial temporal region in particular. Further, temporal poles have a role in feeding semantically processed environmental stimuli to the insula (Craig, 2009). The temporo-insular disconnectivity in schizophrenia merits further investigation in this context.

Meyer-Lindenberg et al (2005) observed that the attenuated deactivation of the temporolimbic system is related to frontal inefficiency in schizophrenia. The degree of rAI- temporolimbic functional dysconnectivity in schizophrenia was found to explain a significant portion of the reduced influence of insula on DLPFC, suggesting that an adaptive paralimbic gating of executive system is disorganised in patients (Dichter et al., 2010).

8.11 Strengths and limitations

A whole brain Granger causality analysis was employed, instead of choosing a priori ROIs, which enabled us to study the Granger-causal influence of the insula across every grey matter voxel in an unconstrained fashion. Further the current observations from the rAI seed region were confirmed using a reverse inference method, by seeding the DLPFC region that showed a prominent diagnostic effect. fMRI acquisition during a task-free resting state was used, so that the inferences are not influenced by differences in effort or task performance in patients. Nevertheless, it is possible that there are systematic differences in the resting state achieved by patients compared to controls that could explain the differences noted in the present study. Such differences are difficult to quantify in the fMRI set-up, though existing studies suggest that resting state is likely to be less confounded by diagnostic differences than task fMRI studies in schizophrenia (Whitfield-Gabrieli and Ford, 2012). The labeling of a path coefficient from X to Y as excitatory (or inhibitory) reflects a positive (or negative) sign of the Granger causal coefficient when the BOLD signal in region Y is regressed on the BOLD signal in region X at a preceding point in time. However, increased firing of inhibitory neurons might result in an increase on local blood flow and hence an increase in BOLD signal. Therefore, excitatory and inhibitory Granger casual influences between BOLD time courses do not necessarily correspond directly to excitatory and inhibitory neurotransmission, respectively. As a result, models of neural activity drawn from fMRI BOLD signals must be cautiously interpreted.

It is worth noting that processing speed scores were used to assess cognitive dysfunction and an exhaustive cognitive testing was not carried out on the current patient sample. Studies exploring the cognitive landscape of schizophrenia have demonstrated that a broad cognitive deficit that spans multiple domains of cognition is present in a substantial number of patients (Dickinson et al., 2011). In particular, information-processing speed has emerged as the single most consistent cognitive deficit (Dickinson et al., 2007; Rodríguez-Sánchez et al., 2007). In future, more detailed exploration of other cognitive domains that are influenced by the salience-execution loop integrity is warranted.

8.12 Possible confounding effects of hemodynamic delay

Differences in hemodynamic delay between brain regions might in principle confound inferences based on neural delays. In particular, Smith et al (2011) reported that when GCA was applied to modelled data in which hemodynamic delay varied randomly between subjects, the identification of causal influences was only slightly above chance. However, using hemodynamic responses derived from real data, Schippers et al. (2011) demonstrated that GCA identified causal influences in group studies with good sensitivity and specificity.

When using random effects analysis in which the effect of interest is compared with variance between subjects, the detection of a significant group effect implies the occurrence of a systematic delay in neural and/or hemodynamic response. The results obtained by Schippers et al (2011) indicate that the effects are most likely to be neural. This conclusion is

supported by the fact that the regions involved are served by different arteries and therefore group effects due to hemodynamic delay would only be expected if there were differences in arterial transmission times that were consistent across subjects. However any such systematic differences would be expected to be similar in the two hemispheres, yet neither the effects reported by Sridharan et al. (2008), nor those that are observed here are symmetrical across the hemispheres. Furthermore, examination of the timing of regional neural activity using magnetoencephalography (Brookes et al., 2012) demonstrates appreciable neural delays between occipital cortex and insula during various visual tasks consistent with the present findings that occipital cortex exerts a Granger causal influence on insula.

An additional issue raised by Smith et al (2011) is the possibility that in a Granger causality analysis, findings might be distorted by zero-lag correlations 'bleeding into' the time-lagged relationships. Significant zero-lag correlations between insula and other brain regions have been shown to occur at different locations from the Granger causal effects of insula on other brain regions.

To our knowledge this is the first study to examine time-directed neural primacy effects during task-free resting state in schizophrenia. These findings extend the neuronal network level models informing the pathophysiology of this illness. Effective cognitive control requires successful suppression of distractors (e.g. spontaneous internal thoughts), but at the same time must be responsive to unexpected stimuli, which though irrelevant to the task are salient for our homeostatic defense (Su et al., 2011). The concept of 'proximal salience' refers to the switching between brain states (e.g. task-focused, resting or internally-focused and sensory-processing states) brought on by a

momentary state of neural activity within the salience processing system, anchored in the rAI and the dACC (chapter 2). The breakdown of the causal influence to and from the salience processing system in schizophrenia can be inferred as amounting to a failure of proximal salience mechanism. The present study highlights the importance of studying the pathways of failed interaction between large-scale networks in the pathophysiology of schizophrenia. Further, it raises the question of whether the indices of failed integration between the large-scale networks, especially the paralimbic SN and the multimodal CEN, could be employed in prognostic classification and treatment monitoring of patients with psychotic symptoms.

Chapter 9

From neuroimaging observations to therapeutic opportunities

The data presented in the previous chapters of this thesis has supported the notion that SN dysfunction is a viable mechanistic model for understanding the pathophysiology schizophrenia. In this concluding chapter, evidence supporting and refuting the role of salience network in schizophrenia that emerged after the publication of the insular dysfunction hypothesis proposed in this thesis is initially considered. The putative neurochemical basis for the SN dysfunction in schizophrenia is then discussed, followed by a suggestion that the SN dysfunction could be a therapeutic target for a combined pharmacological and cognitive training treatment approach in psychosis. This combination approach, termed as Brain Network Modulation, could exploit neuronal plasticity to reverse a key pathophysiological deficit in schizophrenia.

9.1 Studies supporting the insular dysfunction hypothesis

In this section a summary of studies conducted elsewhere, but supporting the major findings and hypotheses put forward in the previous chapters of this thesis, is provided.

Morphometric studies: The prominence of the structural deficits in the insula noted using VBM studies has been further clarified using a number of region-of-interest studies that specifically focus on the insula. A meta-analysis of ROI studies focussing on the insula was recently published (**Shepherd et al.**, 2012). The pooled results from fifteen studies that met the inclusion criteria (n = 945) showed a medium-sized reduction of bilateral insula in people with schizophrenia (either chronic or first episode), with reductions in anterior insula showing considerably larger effect sizes than the reductions in posterior insula, suggesting a regional anterior-posterior anatomical distinction, as discussed in chapter 2.

Pu et al. (2012) studied a large sample of patients with early stages of paranoid subtype of schizophrenia (mean duration of 18 months) and reported reduced grey matter volume in bilateral anterior insula and ACC. Patients with longer duration of illness showed greater volumetric deficit in the left anterior insula. Patients with more severe hallucinations showed greater volumetric deficit in the right anterior insula. Functional connectivity analysis with the clusters identified in the VBM analysis as seeds revealed a significant reduction in within-network connectivity (especially between bilateral insula) for the SN in patients. Further, patients with more severe burden of hallucinations had weaker connectivity between ACC and anterior insula.

Moran et al. (2013a) studied bilateral insular volume of a selected group of childhood onset schizophrenia patients (n = 98) and found significantly lower right, left and total insular volumes than healthy volunteers (n = 100). Right insular volume negatively correlated with positive symptoms, while both left and right insula volumes were positively correlated with overall functioning. Siblings of childhood onset schizophrenia patients (n = 71), did not differ from controls, confirming the meta-analytic findings reported in chapter 3 that the insular deficits are more related to the illness state than a familial endophenotype.

Task-fMRI studies: Gradin et al. (2013) used fMRI to assess the neural correlates of reward processing in schizophrenia. Interestingly, while controls activated both reward-task related regions (striatum, amygdala/hippocampus and midbrain) and the insula-ACC salience network in response to rewards, patients showed activations that were restricted to the insula-ACC salience network system. When the dopamine-rich substantial nigra was used as a seed in the functional connectivity analysis, controls showed significant connectivity with amygdala, parahippocampal region, insula and putamen. Patients, compared to controls, showed a pattern of anticorrelation between the midbrain and the right insula, resulting in significant difference between the two groups on head-to-head comparison. The extent of this dysconnectivity correlated with increased psychotic symptoms.

In a dichotic auditory cognitive task individuals with schizophrenia exhibited decreased upregulation of an executive network including dACC and anterior insula, and attenuated downregulation of DMN regions as compared to controls (**Nygård et al., 2012**). These results emphasise that

contextually-relevant brain function is contingent not just on the recruitment of task-relevant regions but also the controlled dampening of the action of potentially disruptive systems, both of which are ascribed to the dynamic switching function of the SN.

Resting state studies: In healthy controls SN connectivity at rest predicts working memory performance (Tu et al., 2012). In contrast, in patients it does not but rather is negatively correlated with the severity of negative symptoms in these individuals (Tu et al., 2012). Such findings support the hypothesis that SN connectivity disturbance is a pathophysiological mechanism of schizophrenia.

Orliac et al. (2013) studied 26 schizophrenia patients using resting-state functional magnetic resonance imaging and found reduced functional connectivity within both DMN and SN in patients with schizophrenia. Within the SN, greatest reduction in connectivity was noted in the striatum, and this correlated with the severity of delusion and depression in patients.

Mamah et al. (2013) conducted a resting-state functional connectivity study of 35 patients with bipolar disorder and 25 patients with schizophrenia, and 33 controls. Mean connectivity within and between five neural networks were studied (default mode, fronto-parietal (FP), cingulo-opercular (CON), cerebellar and salience (SN)). It is important to note that while most previous studies have used the two terms Salience Network and Cingulo-Opercular network interchangeably, in this study, ventral anterior cingulate (aCC), lateral anterior prefrontal cortex (aPFC), and orbitofrontal (al) were grouped as SN, while dorsal ACC and anterior insula were defined as cingulo-opercular

network. In bipolar disorder, significant reduction in within-network connectivity was restricted to cingulo-opercular network; patients with schizophrenia showed intermediate levels of connectivity between controls and patients with bipolar disorder. The connectivity of both CON and SN with cerebellar network was abnormal in both groups of patients, while the connectivity between FP and CON was abnormal only in schizophrenia whereas the connectivity between CON and SN was abnormal only in bipolar disorder. Higher amount of disorganisation in patients was associated with the dysconnectivity between both CON/SN and cerebellum.

A very interesting study (Moran et al., 2013b) was published at the same time coinciding with the paper reporting the data in chapter 8. This study directly tests the insular dysfunction hypothesis using resting state functional connectivity, Granger causality and structural equation modelling. In a sample of 44 patients with schizophrenia and 44 controls, Moran et al. observed reduced functional connectivity between right ventral insula and DMN nodes (positive correlation in controls, absent or negative correlation in patients); between right anterior insula and both DLPFC and PCC. In a striking similarity with the observations reported in chapter 8, the authors of this study found that the Granger influence from right dorsal anterior insula to both DLPFC and PCC was reduced in patients, and this reduction correlated with the poor performance on a sustained attention task. These findings stand as independent replication of the work reported in this thesis and strengthen the notion that insular dysfunction operates as a failure to generate proximal salience and “switching” between networks in schizophrenia.

Manoliu et al. (2013b) recently presented another direct independent confirmation of the insular dysfunction theory by demonstrating that the dependence of DMN/CEN interactions on right anterior insular (rAI) activity is altered in 18 patients with schizophrenia (compared to 20 controls). The functional connectivity of the right anterior insula within the SN was reduced in patients; but the interaction between DMN and CEN was abnormally increased and related to the severity of hallucinations in the acute stage. The decreased rAI activity of the SN was associated with both hallucinations and increased functional connectivity between DMN and CEN. In addition, the time-lagged connectivity between SN and DMN/CEN was reduced. Furthermore, in a separate report, this group described aberrant functional connectivity between ICA derived SN and CEN in 12 patients with schizophrenia during psychotic remission (**Manoliu et al., 2013a**); this increased SN-CEN connectivity was related to the severity of negative symptoms. Reduced SN activation and reduced DMN deactivation along with impaired anti-correlation between DMN and CEN during task performance was noted to be a prominent abnormality by **Kasperek et al. (2013)** in a sample of patients with first episode of schizophrenia, after 1 year of remission. The observations made by Kasperek et al. in a remitted sample of patients with first episode of schizophrenia draw parallels to Manoliu et al.'s report. Manoliu et al.'s demonstration of insula-dependent dysregulation of DMN/CEN interaction is very convincing evidence in favor of the hypothesis tested in this thesis. It is important to note that these two studies report an unusually high strength of correlation between imaging variables and clinical ratings, raising the suspicion of noise, possibly related to the very small

sample size that is not suited to estimate the true effect size of the underlying relationships.

Electrophysiological studies: Electroencephalogram (EEG) data show recurrent periods of quasi-stable brain states lasting for 60-120ms. These microstates (Lehmann et al., 1987) are thought to reflect binding/integration of neural information and are linked to momentary content of thought and information processing. Using combined fMRI-EEG independent component analysis, a microstate reflecting the activity of the SN and another reflecting the frontoparietal CEN have been identified. **Nishida et al.** (2013) investigated the duration and the sequence of transformation from the SN-microstate to the CEN-microstate in patients with schizophrenia, frontotemporal dementia, Alzheimer's dementia and controls. They did not observe any change in the duration of the SN-microstate in schizophrenia (though this was reduced in frontotemporal dementia). Interestingly, unlike in healthy controls, in both FTD and schizophrenia, transition from CEN to SN was more favored than the transition from SN to CEN-microstate. This result supports that notion of the loss of insular primacy in schizophrenia, in line with the results presented in chapter 8.

Investigating schizophrenia-related disturbance to cerebral function is often confounded by systematic differences between patients and controls in task performance. Although studying resting-state activity arguably lessens these between-group effects, it can be contended that resting-state experiments merely employ a poorly controlled cognitive task. In contrast, single-pulse transcranial magnetic stimulation (spTMS), by which localised neuronal populations are directly activated, enables the investigation of

haemodynamic responses in a non-confounded manner. It has been shown that sp-TMS of precentral gyrus induced significant reductions in haemodynamic peak amplitude in schizophrenia compared to controls in regions including thalamus and anterior insula, and further that thalamo-insular functional connectivity was reduced in patients (Guller et al., 2012); importantly this suggests that these and other SN functional deficits are not wholly due to impaired task performance in individuals with schizophrenia.

9.2 Studies refuting the insular dysfunction hypothesis

Resting-state SN connectivity with a fronto-insular seed was recently reported to be unaffected by schizophrenia, despite significant connectivity reductions in both DMN and CEN (Woodward et al., 2011). A recent fMRI study investigating the modulation of intra- and inter-network connectivity by working memory load in individuals with schizophrenia and matched controls reported that increased working memory load led to increased anticorrelation between SN and DMN, and increased correlation between SN and CEN in both groups. Nevertheless, schizophrenia-related dysconnectivity in these measures was observed to be similar in magnitude across rest and all working memory loads (Repovš and Barch, 2012).

Overall, there is strong evidence for SN structural and functional abnormality in schizophrenia, though not all studies agree. While clinical and methodological heterogeneity are likely to be important factors in explaining these discrepancies, the emerging pattern suggests that the observation of within network dysconnectivity may require task-processing experiments, while inter-network dysconnectivity (e.g. subcortical-SN dysconnectivity) may

be more apparent at resting state. Systematic examination of both task-related and sample-related effects on a broad range of SN connectivity measures in schizophrenia is required to clarify this issue. Of note is the fact that SN dysconnectivity at resting state becomes apparent when larger samples are studied (Pu et al., 2012).

Williamson and Allman (2012) find that the evidence supporting aberrant interactions between SN and DMN/CEN to be non-specific and insufficient to explain the symptom burden of schizophrenia. These authors suggest that the coordinated role of dACC and PCC, along with auditory cortex and hippocampus is likely to be specific for schizophrenia whereas the interactions among ventral anterior cingulate cortex (ACC), orbital frontal cortex, and amygdala are likely to be crucial for the expression of bipolar disorder. These networks (and their respective dysfunctions) are supposed to converge on the so-called representational network comprising of DLPFC, temporal poles and the fronto-insular cortex. While this postulate is not a refutation of the SN dysfunction hypothesis, it shifts the focus from insula to subregions of ACC. Further, this review rightly points out that insular dysfunction is likely to be non-specific across the two psychotic disorders (schizophrenia and bipolar disorder), which is likely to be true, as shown in chapter 7 of this thesis. On the other hand, the lack of specificity of insular dysfunction to the diagnostic description of schizophrenia does not necessarily rule out the importance of normalizing its function in pursuit of effective treatment strategies for psychosis.

9.3 Extensions of the insular dysfunction hypothesis

Menon (2011) published an extensive review of the role of large-scale networks in cognitive dysfunction seen across several psychiatric disorders including autism, schizophrenia, bipolar disorder, frontotemporal dementia, ADHD and Alzheimer's disease. He advances a triple network model that places SN dysfunction as central to the cognitive psychopathology across various disorders. Citing the work presented in chapter 2 (proximal salience model figure) of this thesis, Menon adapted and further extended the link between SN function and different domains of psychopathology. (Unfortunately, a report on the contraction of the surface area of SN carried out as a part of this doctoral study has been wrongly cited as functional connectivity analysis by this author).

Insular dysfunction has been recently invoked to explain symptoms of a number of other neuropsychiatric disorders such as a migraine, ADHD, behavioural problems of Alzheimer's dementia and depression. Salience network is often included in the description of a putative 'pain matrix' - brain regions involved in generating the perception and response related to painful stimuli (Legrain et al., 2010). **Xue et al. (2012)** observed that patients with migraine show aberrant increase in connectivity within the SN, and greater connectivity between both the DMN and right CEN and the insula. In this sample, greater connectivity between both the DMN and rCEN and the insula correlated with duration of migraine. This suggests an interesting relationship between disorders of pain perception and hallucinations that requires further exploration. In a brain-wide analysis of functional connectivity in a very large cohort of patients with ADHD (n=249), increased coupling between the anterior cingulate gyrus and anterior insula was observed recently (**Ji et al.**,

2011). This observation suggests that different modes of insular dysfunction could be present in closely related psychiatric disorders. A resting-state functional connectivity analysis in 20 patients with Alzheimer's dementia, and 17 healthy elderly control subjects revealed increased connectivity within the SN and decreased connectivity within the DMN in patients (Balthazar et al., 2013). The increase in SN connectivity was related to higher degree of behavioural disturbances (agitation, irritability, aberrant motor behavior, euphoria, and disinhibition) in patients.

Stip et al. (2012) have proposed an interesting concept that suggests that the insular dysfunction in psychosis may contribute to the weight gain that is often seen in patients on antipsychotic treatment. In a cohort of 24 patients with schizophrenia, 4 months of treatment with olanzapine resulted in significant weight gain. This was associated with a higher increase in sensitivity to appetitive stimuli in insular cortices, amygdala and cerebellum in patients compared to controls. According to these authors, an abnormal response to visual food cues could be associated with inappropriate proximal salience generation in the insula, induced by antipsychotics acting to repair a dysfunctional SN. Similarly, **Moran et al. (2012)** have invoked SN dysfunction to explain the abnormally high rates of smoking seen in patients with schizophrenia. They observed exaggerated reduction in the SN connectivity when challenged by nicotine for smokers who have schizophrenia compared to smokers who do not have this condition. They argue that this implies that there is an inherent disease-related weakening of SN circuits that are also involved in nicotine addiction. This is supported by the observation of aberrant salience network connectivity in response to smoking related cues,

over and above the changes noted when food-related cues are presented to smokers (Claus et al., 2013).

An extensive review of structural and functional imaging studies in psychotic depression suggests that the insula deficits noted in schizophrenia are likely to be present in psychotic depression as well (Busatto, 2013). In particular, studies comparing psychotic and non-psychotic depressed individuals have supported the view that the insula and prefrontal cortex have a specific role in the emergence of psychotic symptoms in depression. More recently, McGrath et al. (2013) have made an interesting observation that identifies two subgroups of patients with depression who show substantially different treatment response: the group with insular hypometabolism (measured using PET) responded better to CBT while those with increased insular metabolism responded more favorably to antidepressant therapy.

9.4 Is SN dysfunction specific to schizophrenia?

Grey matter reduction in the anterior insula and ACC is not a feature specific to schizophrenia. Such reduction is seen in bipolar disorder (Ellison-Wright and Bullmore, 2010), depression (Bora et al., 2012) and also in fronto-temporal dementia (Olabi et al., 2012). On a similar note, reduced insular gyrification has also been reported in other psychiatric conditions where development in early childhood is disrupted (Hyatt et al., 2012; Kelly et al., 2013). The dysconnectivity involving insula and other distributed large-scale networks are reported in various other cognitive-psychiatric syndromes including ADHD (Yu, 2013), depression (Hamilton et al., 2012) and PTSD (Daniels et al., 2010; Sripada et al., 2012). But such non-specificity is not

surprising, given that the insula performs what appears to be a cardinal function in stimulus selection and response initiation (proximal salience). A notable feature emerging from the studies reported in this work is the observation that not all patients with schizophrenia show a significant degree of SN dysfunction. As shown in table 8.11 (chapter 8), while majority of patients show a significant insular dysfunction, the remaining (with less severe illness) do not show the same degree of abnormality affecting the SN. This suggests that specific SN-dysfunction ‘neurotypes’ can be identified within a sample of patients with severe psychiatric disorders. At this stage, one could speculate that this sub-group will respond differently to treatment compared to the sub-group with no SN-dysfunction. Some evidence to support this SN-based prediction of treatment response has already been shown by McGrath et al. (2013).

Taking together the replications, near-replications, refutations and revisions of the insula dysfunction model in psychosis, it is increasingly clear that (1) the SN related deficits are unlikely to be specific to schizophrenia, but apply to wide range of disorders wherein cognitive dysfunction and perceptual abnormalities are commonplace (2) Even within a specific clinical condition (e.g. schizophrenia), subgroups of individuals with varying degrees/types of SN dysfunction are likely to exist, implying that SN-focused treatment selection may improve outcomes across these disorders. In the next section, we consider the neurochemical basis in pursuit of SN dysfunction as a therapeutic target.

9.5 Neurochemical basis of SN dysfunction

At present, the neurochemical basis of the several crucial functions of the SN in relation to proximal salience is unknown. Given the complexity of the functions ascribed to the SN, it is reasonable to expect significant modulatory role for a number of key neurotransmitters such as dopamine, glutamate, GABA, noradrenaline and acetylcholine. In the context of the pathophysiology of schizophrenia, an important issue is to understand the neurochemical basis of the SN dysfunction in relation to psychotic symptoms.

Numerous observations provide circumstantial evidence for the role of dopaminergic system in the physiology of the SN (reviewed in chapter 2). More direct evidence comes from pharmacofMRI studies wherein dopaminergic drugs are administered to study changes in functional connectivity. D2/D3 agonist pramipexole increases the connectivity between ventral striatum (VS) and the anterior insula when anticipating monetary rewards (Ye et al., 2011). Similar effects are observed when a single dose of 100mg levodopa is administered to healthy volunteers. In this case, levodopa increases the resting state functional connectivity between the VS and the SN (Cole et al., 2012). On the other hand, 3mg of haloperidol reduces the resting state connectivity between the VS and the SN (Cole et al., 2012). Consistent with the later observation, D2 antagonist sulpride also reduces the activity of both VS and ACC in response to rewarding stimuli (McCabe et al., 2011). These observations suggest that dopamine has a crucial role in the interaction between the striatum and the SN.

Given the importance of SN in enabling stimulus-response associations, a crucial role for GABA in the physiology of SN is highly likely. Several lines of evidence for this notion come from animal studies. In midbrain, GABA

interneurons code for the expectancy in associative learning paradigms. GABAergic neurons counteract excitatory drive from primary reward when the reward is expected (Cohen et al., 2012). In the absence of such GABAergic modulation, more frequent dopaminergic bursts are observed (Lobb et al., 2010) with a faster associative learning and a tendency to have higher risk preference (Parker et al., 2011). Cytoarchitectural studies of insula suggest an abundance of GABA interneurons that receive direct input from the midbrain dopaminergic pathways (Ohara et al., 2003). Disruption of early trophic influence on GABA interneuron development leads to selective loss of parvalbumin containing GABA interneurons in the insula and visual cortex (Canty et al., 2009), suggesting that GABA deficits might play a major role in functional deficits arising from abnormal development of these regions. In human subjects, variations in GABA-RA2 genotype influence insular activation during anticipatory processing (Villafuerte et al., 2011) highlighting the role of GABA in insular function. Pregabalin, a GABA potentiator, reduces insular activation during anticipatory processing (Aupperle et al., 2011), while the benzodiazepine lorazepam reduces insular response to emotional face processing (Paulus et al., 2005). Further, GABA agonist baclofen reduces resting cerebral blood flow to bilateral insula (Franklin et al., 2011). Interestingly, an opposite effect on insular rCBF is noted when NMDA antagonist ketamine is administered in subanaesthetic doses (Långsjö et al., 2005), indicating that the GABA/Glu coupling potentially mediates the function of the aFI. Ketamine, which produces a preferential blockade of the glutamate receptors on the inhibitory GABA interneurons, increases the glutamate turnover in ACC, as evidenced by an increase in glutamine level (Rowland et al., 2005). Further, associative learning mediated by the insula is associated

with changes in both the glutamate levels (Ferreira et al., 2005; Gussew et al., 2010) and increased GABAergic (GAD67+) interneuron activity (Doron and Rosenblum, 2010).

In a meta-analysis of MRS studies in schizophrenia, medial prefrontal cortex (including the ACC) showed significant reduction in glutamate levels but an increase in glutamine concentration (Marsman et al., 2011). It is important to note that most MRS spectra in the studies considered by Marsman et al. (Marsman et al., 2011) did not have sufficient resolution to reliably separate glutamine and glutamate signals. Further, the MRS Glx (glutamate+glutamine) measurements could reflect any of the three (synaptic extracellular, glial or neuronal) compartments of the glutamate/glutamine pool in the brain tissue. This precludes meaningful interpretation of this data in terms of the SN dysfunction in schizophrenia. So far, in vivo measurement of Glu/GABA from the aFI has not been reported in patients with schizophrenia though several studies have highlighted the usefulness of the GABA/Glu quantification from the insula in other disease states, especially fibromyalgia (Foerster et al., 2012; Harris et al., 2009, 2008). The most relevant study in this context was carried out on patients with a depressive disorder. Horn et al (2010) investigated the relationship between Glx at the ACC and the functional connectivity of the SN and observed a linear relationship in depressed patients, but not in healthy controls. Patients with severe depression also had a significant reduction of Glx concentration. This observation supports the notion that the integrity of SN in schizophrenia could have a similar relationship to Glutamate concentration, though this issue is yet to be investigated. Relative balance between GABA and Glu in the ACC is

likely to be important in modulating the BOLD response across both the DMN and task-positive networks (Falkenberg et al., 2012; Northoff et al., 2007).

Several other neurotransmitter systems also influence the activity of the SN. Nicotine normalises the ketamine induced increase in the rCBF of the SN (Rowland et al., 2010), suggesting a role for cholinergic transmission. A recent assessment of the in vivo distribution heteromeric $\alpha 4\beta 2$ neuronal nicotinic acetylcholine receptor (nAChR), using 2-[^{18}F]F-A-85380 PET showed that cortical nAChR density was highest in the insular and anterior cingulate cortices, suggesting an important role of the nicotinic receptors in its functions (Picard et al., 2013). Beta-adrenergic blockade diminishes the responsiveness of the SN to fear stimuli (Hermans et al., 2011). The degree of regional brain activation in response to a given task and functional connectivity of a region with other nodes is likely to be influenced by interactions among several neurotransmitter systems (Pauli et al., 2012). With a note of caution on the oversimplification of the available evidence, we may assume that dopamine has a crucial role in the interaction of the SN with subcortical sites, whilst the within-network connectivity of the SN and the interaction of the SN with other large-scale networks may predominantly depend on the Glu/GABA neurotransmission.

9.6 SN dysfunction as a therapeutic target

From the numerous studies that are reviewed above and from the data presented in the previous chapters, it is evident that the SN dysfunction forms a crucial cog in the wheel of the complex pathophysiological process that results in the expression of several of the psychotic symptoms in

schizophrenia. Importantly, pharmacological manipulation of the SN function appears to be a feasible strategy in treating psychotic symptoms. Increasingly it is being realized that drugs targeting a single neurotransmitter system (the so-called magic bullet approach) provide insufficient translational benefit(Sams-Dodd, 2005). Network pharmacology, which aims to address large-scale brain network dysfunctions in brain disorders, is proposed as an alternative strategy for drug development(Hopkins, 2007).

Reorganization of brain networks involves habitual reallocation of neural resources on demand(Hebb, 1949). This plasticity of functional networks open the possibility that such reorganization could be achieved, at least in part, through focused cognitive training(Castellanos et al., 2010; Lewis et al., 2009; Voss et al., 2012). This approach has been advocated for anxiety disorders, with specific training approaches proposed to address targeted dysfunctional networks underlying anxiety symptoms(Sylvester et al., 2012). Combination of network pharmacology to improve plasticity of connections, along with targeted cognitive training is likely to be a powerful approach to address dysfunctional brain networks. This combined approach can be termed as Brain Network Modulation (BNM), and has a potential to address several of the symptoms of schizophrenia. This is especially important as a number of observations suggest that isolated pharmacological approaches could often elicit compensatory or feedback mechanisms, which either reduce the effectiveness of treatment or cause additional unwanted effects(Gardner et al., 2005).

The emergence of repetitive transcranial magnetic (rTMS) and direct current stimulation (tDCS) approaches offer very promising noninvasive

physical interventions to modulate network plasticity. Meta-analysis indicates that rTMS applied to temporoparietal junction ameliorates persistent hallucinations in schizophrenia (Slotema et al., 2012), with preliminary evidence suggesting that modulation of the anterior insular connectivity predicts treatment response (Vercammen et al., 2010). Anterior insula, due to its sequestered location, is often considered to be beyond the reach of rTMS or tDCS approaches. Our current observation of the existence of a rAI-rDLPFC 'causal' feedback loop raises the possibility of modulating anterior insula, by focused targeting of the more accessible rDLPFC.

In schizophrenia targeted cognitive training addressing working memory deficits has been shown to be associated with improved BOLD activation in prefrontal regions (Haut et al., 2010). One cognitive approach that bears several properties of being a SN oriented training method is mindfulness training (Tang et al., 2012; Zeidan et al., 2011). Neuroplastic changes in the anterior cingulate cortex and insula has been consistently observed along with changes in other fronto-limbic nodes and default mode network structures (see Holzel et al. (Hölzel et al., 2011) for a review). While different degree of mindfulness training are present in various psychological therapies and meditations approaches, two crucial components of mindfulness are (1) attention to the present moment instead of delving into memory / mind-wandering and 2) the suspension of cognitive elaboration/appraisal of present perceptions (Farb et al., 2012a). Experienced meditators show stronger functional connectivity between the posterior cingulate (DMN node), dACC (SN node), and dorsolateral prefrontal cortices (CEN node) (Brewer et al., 2011). Several studies indicate that mindfulness practices improve the degree

of deactivations seen in cortical midline structures constituting the DMN(Ives-Deliperi et al., 2011; Pagnoni et al., 2008). Mindfulness also increases the BOLD correlation between nodes of the SN and relevant sensory cortex when attending to a stimulus, while increasing the anticorrelation with irrelevant sensory cortices(Kilpatrick et al., 2011). Practicing mindfulness meditation has been shown to increase the recruitment of anterior insula during interoceptive attention, and influence the connectivity between posterior and the anterior insula(Farb et al., 2012b). A reduction in the perception of pain and anxiety through the practice of mindfulness is associated with (1) increased ACC engagement in anticipation of the pain stimulus and (2) reduced lateral prefrontal cortex but increased posterior insula engagement on presentation of the pain stimulus(Gard et al., 2011). Interestingly, in a large sample of long-term meditators, pronounced increase in gyrification was noted in the right anterior insula when compared to non-meditators(Luders et al., 2012), suggesting that recurrent practice of mindfulness based approaches may have a significant effect on both the connectivity and morphology of aFI.

Another approach that bears some promise in manipulating the SN and its interaction with other distributed networks is neurofeedback using realtime fMRI (RtfMRI) or EEG. In real-time fMRI based neurofeedback subjects can be trained to influence the amplitude of fMRI signal from a specific brain region while receiving operational information about the signal(Johnston et al., 2010). Neurofeedback has been shown to be effective in modulating cortico-subcortical connectivity in patients with Parkinson's disease(Subramanian et al., 2011). Both upregulation and downregulation of BOLD activity in several nodes of the SN appears to be possible using this technique in both healthy

volunteers(deCharms et al., 2005; Hamilton et al., 2011b; Johnston et al., 2010) and patients with mental disorders(Linden et al., 2012). Patients with schizophrenia successfully trained in neurofeedback paradigms and the potential of this technique in addressing symptoms of psychosis is being increasingly appreciated(McCarthy-Jones, 2012). In a small sample of patients with schizophrenia (n=9), volitional control of the hemodynamic response in bilateral anterior insula was achieved using neurofeedback after 2-weeks of training(Ruiz et al., 2011). On learning insular self-regulation, patients showed an improved accuracy in recognizing faces showing the emotion of disgust. This improvement positively correlated with the capacity to self-regulate right anterior insula. RtfMRI training was also associated with an increase in the effective connectivity among insula, amygdala and mPFC and an overall increase in the causal inflow density to the ACC(Ruiz et al., 2011).

It is important to note that there is no randomized trial evidence for neurofeedback in schizophrenia. While mindfulness based approaches have been shown to have certain positive effects on psychotic symptoms, the clinical use of this technique is far from established. Though current understanding of synaptic mechanisms suggests that modulation of neurotransmitters could influence neuronal network plasticity(Du et al., 2004; LeBeau et al., 2005), there have been no trials of Brain Network Modulation (combined cognitive training approaches and pharmacological/TMS treatments targeted at brain networks) in psychosis. As we understand more about brain states and their alterations in schizophrenia, clinical utility of these approaches could become readily achievable. A crucial next step is to characterize the neurochemical basis of the proximal salience and SN

dysfunction, and evaluate the proof for the concept of BNM approach of neural plasticity. The concept of SN dysfunction promises a viable target for brain-network focused approaches that can guide treatment developments in the near future.

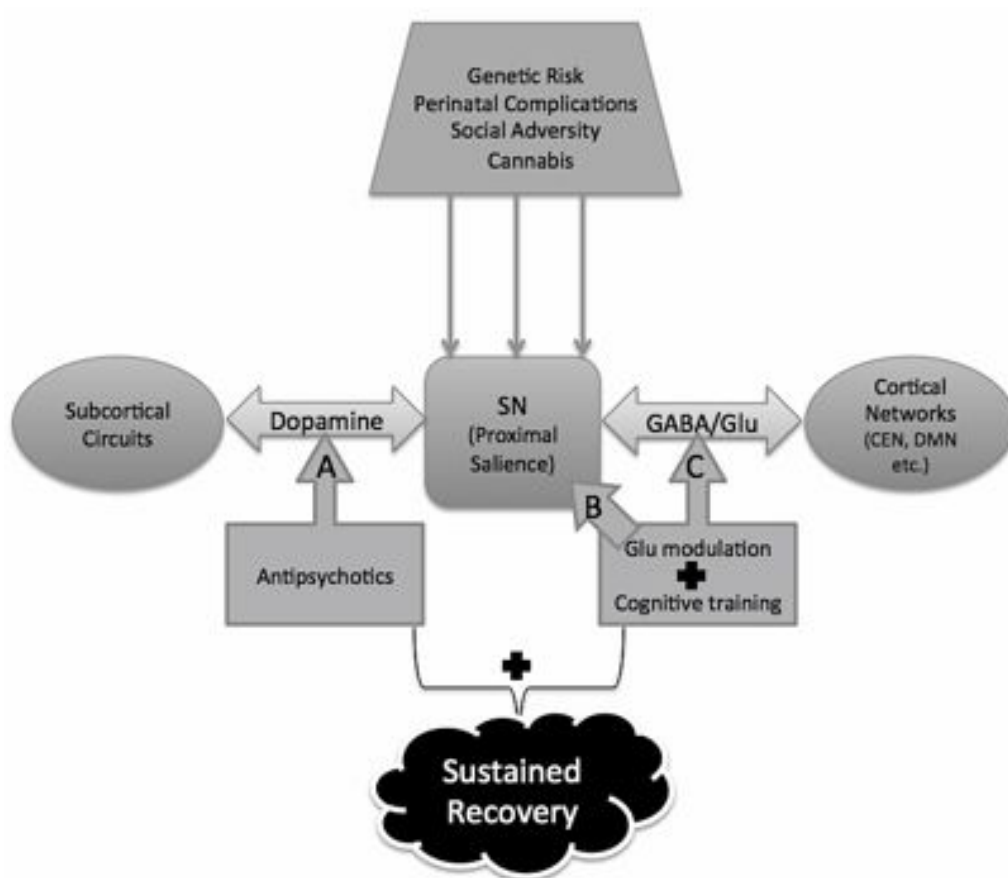


Figure 9.1: A speculative model for targeting dysfunctional SN in schizophrenia. A. Subcortical-SN connectivity likely to be predominantly dopaminergic and affected by antipsychotics. B. Within SN connectivity and C. SN-CEN / SN-DMN connectivity are likely to be predominantly GABA/glutamatergic. Brain Network Modulation (indicated by plus sign) can target the within-network and between-networks dysfunction through a combination of pharmacological and cognitive approaches. SN: Saliency Network, CEN: Central Executive Network, DMN: Default Mode Network

Current therapies produce relatively limited improvement on long-term outcome for schizophrenia. The evidence that the pathophysiology of the

disorder entails subtle but consistent structural abnormalities of cortex, especially in brain regions comprising the SN, suggests that improvement on long-term outcome will require therapies that can alleviate the effects of structural abnormality. The accumulating evidence indicating that various psychological therapies can produce increases in cortical grey matter and/or improved function of SN demonstrate that plasticity exists and suggest that structural lesions are not necessarily irreversible. Furthermore, the preliminary evidence that GABAergic and glutamatergic abnormalities might be involved in developmental deficits in the nodes of the SN suggests appropriate modulation of GABAergic and glutamatergic transmission via pharmacological treatment might act synergistically with neuropsychological strategies to produce enduring changes in structure and function of the SN leading to substantial improvement in long-term outcome of schizophrenia.

REFERENCES

- Afif, A., Bouvier, R., Buenerd, A., Trouillas, J., Mertens, P., 2007. Development of the human fetal insular cortex: study of the gyration from 13 to 28 gestational weeks. *Brain Structure and Function* 212, 335–346.
- Akbarian, S., Bunney, W.E., Potkin, S.G., Wigal, S.B., Hagman, J.O., Sandman, C.A., Jones, E.G., 1993. Altered Distribution of Nicotinamide-Adenine Dinucleotide Phosphate--Diaphorase Cells in Frontal Lobe of Schizophrenics Implies Disturbances of Cortical Development. *Arch Gen Psychiatry* 50, 169–177.
- Albert, N.B., Robertson, E.M., Miall, R.C., 2009. The Resting Human Brain and Motor Learning. *Current Biology* 19, 1023–1027.
- Allen, P., Aleman, A., McGuire, P.K., 2007. Inner speech models of auditory verbal hallucinations: evidence from behavioural and neuroimaging studies. *Int Rev Psychiatry* 19, 407–415.
- Allen, P., Larøi, F., McGuire, P.K., Aleman, A., 2008. The hallucinating brain: A review of structural and functional neuroimaging studies of hallucinations. *Neuroscience & Biobehavioral Reviews* 32, 175–191.
- Ammons, R.B., Ammons, C.H., 1962. The Quick Test (QT): Provisional manual. *Psychological Reports* 11, 111–161.
- Ananth, H., Popescu, I., Critchley, H.D., Good, C.D., Frackowiak, R.S.J., Dolan, R.J., 2002. Cortical and Subcortical Gray Matter Abnormalities in Schizophrenia Determined Through Structural Magnetic Resonance Imaging With Optimized Volumetric Voxel-Based Morphometry. *Am J Psychiatry* 159, 1497–1505.
- Andreasen, N., Nasrallah, H.A., Dunn, V., Olson, S.C., Grove, W.M., Ehrhardt, J.C., Coffman, J.A., Crosssett, J.H.W., 1986. Structural Abnormalities in the Frontal System in Schizophrenia: A Magnetic Resonance Imaging Study. *Archives of General Psychiatry* 43, 136–144.

- Andreasen, N.C., Paradiso, S., O'Leary, D.S., 1998. "Cognitive Dysmetria" as an Integrative Theory of Schizophrenia: A Dysfunction in Cortical-Subcortical-Cerebellar Circuitry? *Schizophrenia Bulletin* 24, 203 –218.
- Anticevic, A., Dierker, D.L., Gillespie, S.K., Repovs, G., Csernansky, J.G., Van Essen, D.C., Barch, D.M., 2008. Comparing surface-based and volume-based analyses of functional neuroimaging data in patients with schizophrenia. *NeuroImage* 41, 835–848.
- Ashburner, J., 2007. A fast diffeomorphic image registration algorithm. *Neuroimage* 38, 95–113.
- Ashburner, J., Friston, K.J., 2000. Voxel-based morphometry--the methods. *Neuroimage* 11, 805–821.
- Ashburner, J., Friston, K.J., 2001. Why voxel-based morphometry should be used. *Neuroimage* 14, 1238–1243.
- Augustine, J.R., 1996. Circuitry and functional aspects of the insular lobe in primates including humans. *Brain Res. Brain Res. Rev* 22, 229–244.
- Aupperle, R.L., Ravindran, L., Tankersley, D., Flagan, T., Stein, N.R., Simmons, A.N., Stein, M.B., Paulus, M.P., 2011. Pregabalin influences insula and amygdala activation during anticipation of emotional images. *Neuropsychopharmacology* 36, 1466–1477.
- Baiano, M., David, A., Versace, A., Churchill, R., Balestrieri, M., Brambilla, P., 2007. Anterior cingulate volumes in schizophrenia: A systematic review and a meta-analysis of MRI studies. *Schizophrenia Research* 93, 1–12.
- Baird, A., Dewar, B.-K., Critchley, H., Gilbert, S.J., Dolan, R.J., Cipolotti, L., 2006. Cognitive functioning after medial frontal lobe damage including the anterior cingulate cortex: a preliminary investigation. *Brain Cogn* 60, 166–175.
- Balthazar, M.L.F., Pereira, F.R.S., Lopes, T.M., Da Silva, E.L., Coan, A.C., Campos, B.M., Duncan, N.W., Stella, F., Northoff, G., Damasceno, B.P., Cendes, F., 2013.

- Neuropsychiatric symptoms in Alzheimer's disease are related to functional connectivity alterations in the salience network. *Hum Brain Mapp.*
- Barbas, H., 2000. Complementary roles of prefrontal cortical regions in cognition, memory, and emotion in primates. *Adv Neurol* 84, 87–110.
- Barta, P.E., Pearlson, G.D., Powers, R.E., Richards, S.S., Tune, L.E., 1990. Auditory hallucinations and smaller superior temporal gyral volume in schizophrenia. *Am J Psychiatry* 147, 1457–1462.
- Bassett, D.S., Bullmore, E., Verchinski, B.A., Mattay, V.S., Weinberger, D.R., Meyer-Lindenberg, A., 2008. Hierarchical Organization of Human Cortical Networks in Health and Schizophrenia. *J. Neurosci.* 28, 9239–9248.
- Binder, J.R., Frost, J.A., Hammeke, T.A., Bellgowan, P.S.F., Rao, S.M., Cox, R.W., 1999. Conceptual Processing during the Conscious Resting State: A Functional MRI Study. *Journal of Cognitive Neuroscience* 11, 80–93.
- Blakemore, S.J., Smith, J., Steel, R., Johnstone, C.E., Frith, C.D., 2000. The perception of self-produced sensory stimuli in patients with auditory hallucinations and passivity experiences: evidence for a breakdown in self-monitoring. *Psychol Med* 30, 1131–1139.
- Bleuler, E., 1950. *Dementia Praecox: Or the Group of Schizophrenias* (Translated by Zinkin, J.). International Universities Press.
- Bodnar, M., Harvey, P.-O., Malla, A.K., Joober, R., Lepage, M., 2011. The parahippocampal gyrus as a neural marker of early remission in first-episode psychosis: a voxel-based morphometry study. *Clin SchizophreniaRelat Psychoses* 4, 217–228.
- Boksman, K., Théberge, J., Williamson, P., Drost, D.J., Malla, A., Densmore, M., Takhar, J., Pavlosky, W., Menon, R.S., Neufeld, R.W.J., 2005. A 4.0-T fMRI study of brain connectivity during word fluency in first-episode schizophrenia. *Schizophrenia Research* 75, 247–263.

- Bonnici, H.M., William, T., Moorhead, J., Stanfield, A.C., Harris, J.M., Owens, D.G., Johnstone, E.C., Lawrie, S.M., 2007. Pre-frontal lobe gyrification index in schizophrenia, mental retardation and comorbid groups: an automated study. *Neuroimage* 35, 648–654.
- Bookstein, F.L., 2001. “Voxel-based morphometry” should not be used with imperfectly registered images. *Neuroimage* 14, 1454–1462.
- Boos, H.B.M., Aleman, A., Cahn, W., Pol, H.H., Kahn, R.S., 2007. Brain Volumes in Relatives of Patients With Schizophrenia: A Meta-analysis. *Arch Gen Psychiatry* 64, 297–304.
- Boos, H.B.M., Cahn, W., Van Haren, N.E.M., Derks, E.M., Brouwer, R.M., Schnack, H.G., Hulshoff Pol, H.E., Kahn, R.S., 2012. Focal And Global Brain Measurements in Siblings of Patients With Schizophrenia. *Schizophrenia Bulletin* 38(4), 814-25.
- Bora, E., Fornito, A., Pantelis, C., Yücel, M., 2012. Gray matter abnormalities in Major Depressive Disorder: a meta-analysis of voxel based morphometry studies. *J Affect Disord* 138, 9–18.
- Bora, E., Fornito, A., Radua, J., Walterfang, M., Seal, M., Wood, S.J., Yücel, M., Velakoulis, D., Pantelis, C., 2011a. Neuroanatomical abnormalities in schizophrenia: a multimodal voxelwise meta-analysis and meta-regression analysis. *Schizophr. Res.* 127, 46–57.
- Bora, E., Fornito, A., Yücel, M., Pantelis, C., 2010. Voxelwise Meta-Analysis of Gray Matter Abnormalities in Bipolar Disorder. *Biological Psychiatry* 67, 1097–1105.
- Bora, E., Fornito, A., Yücel, M., Pantelis, C., 2011b. The Effects of Gender on Grey Matter Abnormalities in Major Psychoses: A Comparative Voxelwise Meta-Analysis of Schizophrenia and Bipolar Disorder. *Psychological Medicine FirstView*, 1–13.
- Borgwardt, S.J., Picchioni, M.M., Ettinger, U., Touloupoulou, T., Murray, R., McGuire, P.K., 2010. Regional Gray Matter Volume in Monozygotic Twins Concordant and Discordant for Schizophrenia. *Biological Psychiatry* 67, 956–964.

- Borgwardt, S.J., Riecher-Rössler, A., Dazzan, P., Chitnis, X., Aston, J., Drewe, M., Gschwandtner, U., Haller, S., Pflüger, M., Rechsteiner, E., D'Souza, M., Stieglitz, R.-D., Radü, E.-W., McGuire, P.K., 2007. Regional Gray Matter Volume Abnormalities in the At Risk Mental State. *Biological Psychiatry* 61, 1148–1156.
- Bossaerts, P., 2010. Risk and risk prediction error signals in anterior insula. *Brain Struct Funct* 214, 645–653.
- Braddick, O., Atkinson, J., Wattam-Bell, J., 2003. Normal and anomalous development of visual motion processing: motion coherence and “dorsal-stream vulnerability”. *Neuropsychologia* 41, 1769–1784.
- Braff, D.L., 1993. Information Processing and Attention Dysfunctions in Schizophrenia. *Schizophrenia Bull* 19, 233–259.
- Brans, R.G.H., Van Haren, N.E.M., Van Baal, G.C.M., Schnack, H.G., Kahn, R.S., Hulshoff Pol, H.E., 2008. Heritability of changes in brain volume over time in twin pairs discordant for schizophrenia. *Arch. Gen. Psychiatry* 65, 1259–1268.
- Braus, D.F., Ende, G., Weber-Fahr, W., Demiralca, T., Henn, F.A., 2001. Favorable effect on neuronal viability in the anterior cingulate gyrus due to long-term treatment with atypical antipsychotics: an MRSI study. *Pharmacopsychiatry* 34, 251–253.
- Braus, D.F., Ende, G., Weber-Fahr, W., Demiralca, T., Tost, H., Henn, F.A., 2002. Functioning and neuronal viability of the anterior cingulate neurons following antipsychotic treatment: MR-spectroscopic imaging in chronic schizophrenia. *Eur Neuropsychopharmacol* 12, 145–152.
- Brett, M., Anton, J., Valabregue, R., Poline, J., 2002. Region of interest analysis using an SPM toolbox. Presented at the Human Brain Mapping. Available in CD-ROM: *Neuroimage* 16(2).
- Brewer, J.A., Worhunsky, P.D., Gray, J.R., Tang, Y.-Y., Weber, J., Kober, H., 2011. Meditation experience is associated with differences in default mode network activity and connectivity. *Proc. Natl. Acad. Sci. U.S.A.* 108, 20254–20259.

- Broca, P., 1878. Anatomie Comparée des circonvolutions cérébrales: le grand lobe limbique dans la série des mammifères. *Revue Antropologique* 384–498.
- Brookes, M.J., Liddle, E.B., Hale, J.R., Woolrich, M.W., Luckhoo, H., Liddle, P.F., Morris, P.G., 2012. Task induced modulation of neural oscillations in electrophysiological brain networks. *Neuroimage* 63, 1918–1930.
- Brüne, M., Lissek, S., Fuchs, N., Witthaus, H., Peters, S., Nicolas, V., Juckel, G., Tegenthoff, M., 2008. An fMRI study of theory of mind in schizophrenic patients with “passivity” symptoms. *Neuropsychologia* 46, 1992–2001.
- Buchanan, K.J., Johnson, J.I., 2011. Diversity of spatial relationships of the claustrum and insula in branches of the mammalian radiation. *Ann. N. Y. Acad. Sci.* 1225 Suppl 1, E30–63.
- Buckner, R.L., Sepulcre, J., Talukdar, T., Krienen, F.M., Liu, H., Hedden, T., Andrews-Hanna, J.R., Sperling, R.A., Johnson, K.A., 2009. Cortical Hubs Revealed by Intrinsic Functional Connectivity: Mapping, Assessment of Stability, and Relation to Alzheimer’s Disease. *J. Neurosci.* 29, 1860–1873.
- Busatto, G.F., 2013. Structural and functional neuroimaging studies in major depressive disorder with psychotic features: a critical review. *Schizophrenia Bull* 39, 776–786.
- Cachia, A., Paillère-Martinot, M.-L., Galinowski, A., Januel, D., De Beaurepaire, R., Bellivier, F., Artiges, E., Andoh, J., Bartrés-Faz, D., Duchesnay, E., Rivière, D., Plaze, M., Mangin, J.-F., Martinot, J.-L., 2008. Cortical folding abnormalities in schizophrenia patients with resistant auditory hallucinations. *Neuroimage* 39, 927–935.
- Calhoun, V.D., Sui, J., Kiehl, K., Turner, J., Allen, E., Pearlson, G., 2012. Exploring the psychosis functional connectome: aberrant intrinsic networks in schizophrenia and bipolar disorder. *Front. Psychiatry* 2, 75.

- Callicott, J.H., Bertolino, A., Mattay, V.S., Langheim, F.J.P., Duyn, J., Coppola, R., Goldberg, T.E., Weinberger, D.R., 2000. Physiological Dysfunction of the Dorsolateral Prefrontal Cortex in Schizophrenia Revisited. *Cerebral Cortex* 10, 1078–1092.
- Cameron, A.M., Oram, J., Geffen, G.M., Kavanagh, D.J., McGrath, J.J., Geffen, L.B., 2002. Working memory correlates of three symptom clusters in schizophrenia. *Psychiatry Research* 110, 49–61.
- Cannon, T.D., Thompson, P.M., Van Erp, T.G.M., Toga, A.W., Poutanen, V.-P., Huttunen, M., Lonnqvist, J., Standerskjold-Nordenstam, C.-G., Narr, K.L., Khaledy, M., Zoumalan, C.I., Dail, R., Kaprio, J., 2002. Cortex mapping reveals regionally specific patterns of genetic and disease-specific gray-matter deficits in twins discordant for schizophrenia. *Proceedings of the National Academy of Sciences* 99, 3228–3233.
- Cannon, T.D., Van Erp, T.G., Huttunen, M., Lönqvist, J., Salonen, O., Valanne, L., Poutanen, V.P., Standerskjöld-Nordenstam, C.G., Gur, R.E., Yan, M., 1998. Regional gray matter, white matter, and cerebrospinal fluid distributions in schizophrenic patients, their siblings, and controls. *Arch. Gen. Psychiatry* 55, 1084–1091.
- Canty, A.J., Dietze, J., Harvey, M., Enomoto, H., Milbrandt, J., Ibáñez, C.F., 2009. Regionalized Loss of Parvalbumin Interneurons in the Cerebral Cortex of Mice with Deficits in GFR α 1 Signaling. *J. Neurosci.* 29, 10695–10705.
- Carlsson, A., Lindqvist, M., 1963. EFFECT OF CHLORPROMAZINE OR HALOPERIDOL ON FORMATION OF 3METHOXYTYRAMINE AND NORMETANEPHRINE IN MOUSE BRAIN. *Acta Pharmacol Toxicol (Copenh)* 20, 140–144.
- Carpenter, W.T., Jr, Buchanan, R.W., Kirkpatrick, B., Tamminga, C., Wood, F., 1993. Strong inference, theory testing, and the neuroanatomy of schizophrenia. *Arch. Gen. Psychiatry* 50, 825–831.
- Casanova, M.F., Tillquist, C.R., 2008. Encephalization, emergent properties, and psychiatry: a minicolumnar perspective. *Neuroscientist* 14, 101–118.

- Castellanos, N.P., Paúl, N., Ordóñez, V.E., Demuynck, O., Bajo, R., Campo, P., Bilbao, A., Ortiz, T., del-Pozo, F., Maestú, F., 2010. Reorganization of functional connectivity as a correlate of cognitive recovery in acquired brain injury. *Brain* 133, 2365–2381.
- Cauda, F., Costa, T., Torta, D.M.E., Sacco, K., D'Agata, F., Duca, S., Geminiani, G., Fox, P.T., Vercelli, A., 2012. Meta-analytic clustering of the insular cortex: Characterizing the meta-analytic connectivity of the insula when involved in active tasks. *NeuroImage* 62, 343–355.
- Cauda, F., D'Agata, F., Sacco, K., Duca, S., Geminiani, G., Vercelli, A., 2011. Functional connectivity of the insula in the resting brain. *Neuroimage* 55, 8–23.
- Cerasa, A., Quattrone, A., Gioia, M.C., Tarantino, P., Annesi, G., Assogna, F., Caltagirone, C., De Luca, V., Spalletta, G., 2011. Dysbindin C-A-T haplotype is associated with thicker medial orbitofrontal cortex in healthy population. *Neuroimage* 55, 508–513.
- Chadwick, P.K., 2007. Peer-Professional First-Person Account: Schizophrenia From the Inside—Phenomenology and the Integration of Causes and Meanings. *Schizophrenia Bulletin* 33, 166–173.
- Chan, R.C.K., Di, X., McAlonan, G.M., Gong, Q., 2009. Brain Anatomical Abnormalities in High-Risk Individuals, First-Episode, and Chronic Schizophrenia: An Activation Likelihood Estimation Meta-analysis of Illness Progression. *Schizophrenia Bull* sbp073.
- Chan, R.C.K., Di, X., McAlonan, G.M., Gong, Q., 2011. Brain anatomical abnormalities in high-risk individuals, first-episode, and chronic schizophrenia: an activation likelihood estimation meta-analysis of illness progression. *Schizophrenia Bull* 37, 177–188.
- Chao-Gan, Y., Yu-Feng, Z., 2010. DPARSF: A MATLAB Toolbox for “Pipeline” Data Analysis of Resting-State fMRI. *Front Syst Neurosci* 4, 13.

- Chee, M.W.L., Zheng, H., Goh, J.O.S., Park, D., Sutton, B.P., 2011. Brain structure in young and old East Asians and Westerners: comparisons of structural volume and cortical thickness. *J Cogn Neurosci* 23, 1065–1079.
- Chen, Y., Bidwell, L.C., Holzman, P.S., 2005. Visual motion integration in schizophrenia patients, their first-degree relatives, and patients with bipolar disorder. *Schizophrenia Research* 74, 271–281.
- Chen, Z., Ma, L., 2010. Grey matter volume changes over the whole brain in amyotrophic lateral sclerosis: A voxel-wise meta-analysis of voxel based morphometry studies. *Amyotroph Lateral Scler* 11, 549–554.
- Chi, J.G., Dooling, E.C., Gilles, F.H., 1977. Gyral development of the human brain. *Annals of Neurology* 1, 86–93.
- Christoff, K., Gordon, A.M., Smallwood, J., Smith, R., Schooler, J.W., 2009. Experience sampling during fMRI reveals default network and executive system contributions to mind wandering. *Proceedings of the National Academy of Sciences* 106, 8719–8724.
- Chua, S., Wright, I., Poline, J., Liddle, P., Murray, R., Frackowiak, R., Friston, K., McGuire, P., 1997. Grey matter correlates of syndromes in schizophrenia. A semi-automated analysis of structural magnetic resonance images. *The British Journal of Psychiatry* 170, 406–410.
- Clark, L., Bechara, A., Damasio, H., Aitken, M.R.F., Sahakian, B.J., Robbins, T.W., 2008. Differential effects of insular and ventromedial prefrontal cortex lesions on risky decision-making. *Brain* 131, 1311–1322.
- Claus, E.D., Blaine, S.K., Filbey, F.M., Mayer, A.R., Hutchison, K.E., 2013. Association Between Nicotine Dependence Severity, BOLD Response to Smoking Cues, and Functional Connectivity. *Neuropsychopharmacology* 38(12), 2363–72.

- Coffeen, U., Lopezavila, A., Ortogalegaspi, J., Delangel, R., Lopezmunoz, F., Pellicer, F., 2008. Dopamine receptors in the anterior insular cortex modulate long-term nociception in the rat. *European Journal of Pain* 12, 535–543.
- Cohen, J.Y., Haesler, S., Vong, L., Lowell, B.B., Uchida, N., 2012. Neuron-type-specific signals for reward and punishment in the ventral tegmental area. *Nature* 482, 85–88.
- Cole, D.M., Oei, N.Y.L., Soeter, R.P., Both, S., Gerven, J.M.A. van, Rombouts, S.A.R.B., Beckmann, C.F., 2012. Dopamine-Dependent Architecture of Cortico-Subcortical Network Connectivity. *Cereb. Cortex* 23, 1509-16.
- Collin, G., Hulshoff Pol, H.E., Haijma, S.V., Cahn, W., Kahn, R.S., Van den Heuvel, M.P., 2011. Impaired Cerebellar Functional Connectivity in Schizophrenia Patients and Their Healthy Siblings. *Front Psychiatry* 2.
- Contreras, M., Ceric, F., Torrealba, F., 2007. Inactivation of the interoceptive insula disrupts drug craving and malaise induced by lithium. *Science* 318, 655–658.
- Corbetta, M., Shulman, G.L., 2002. Control of goal-directed and stimulus-driven attention in the brain. *Nat. Rev. Neurosci* 3, 201–215.
- Corlett, P.R., Taylor, J.R., Wang, X.-J., Fletcher, P.C., Krystal, J.H., 2010. Toward a neurobiology of delusions. *Progress in Neurobiology* 92, 345–369.
- Craig, A.D., 2003. Interoception: the sense of the physiological condition of the body. *Curr. Opin. Neurobiol.* 13, 500–505.
- Craig, A.D., 2009. How do you feel [mdash] now? The anterior insula and human awareness. *Nat Rev Neurosci* 10, 59–70.
- Crespo-Facorro, B., Kim, J.-J., Andreasen, N.C., O’Leary, D.S., Bockholt, H.J., Magnotta, V., 2000. Insular cortex abnormalities in schizophrenia: a structural magnetic resonance imaging study of first-episode patients. *Schizophrenia Research* 46, 35–43.

- Crespo-Facorro, B., Roiz-Santiáñez, R., Quintero, C., Pérez-Iglesias, R., Tordesillas-Gutiérrez, D., Mata, I., Rodríguez-Sánchez, J.M., Gutiérrez, A., Vázquez-Barquero, J.L., 2010. Insular cortex morphometry in first-episode schizophrenia-spectrum patients: Diagnostic specificity and clinical correlations. *J Psychiatr Res* 44, 314–320.
- Crichton-Browne, J., 1879. On the Weight of the Brain and Its Component Parts in the Insane. *Brain* 2, 42–67.
- Critchley, H.D., Wiens, S., Rotshtein, P., Ohman, A., Dolan, R.J., 2004. Neural systems supporting interoceptive awareness. *Nat. Neurosci* 7, 189–195.
- Crow, T.J., 1990. The Continuum of Psychosis and Its Genetic Origins. The Sixty-Fifth Maudsley Lecture. *BJP* 156, 788–797.
- Csernansky, J.G., Gillespie, S.K., Dierker, D.L., Anticevic, A., Wang, L., Barch, D.M., Van Essen, D.C., 2008. Symmetric abnormalities in sulcal patterning in schizophrenia. *Neuroimage* 43, 440–446.
- Curtis, V.A., Dixon, T.A., Morris, R.G., Bullmore, E.T., Brammer, M.J., Williams, S.C., Sharma, T., Murray, R.M., McGuire, P.K., 2001. Differential frontal activation in schizophrenia and bipolar illness during verbal fluency. *J Affect Disord* 66, 111–121.
- Cutting, J., 1987. *The Clinical Roots of the Schizophrenia Concept: Translations of Seminal European Contributions on Schizophrenia*. CUP Archive.
- D'Acemont, M., Lu, Z.-L., Li, X., Van der Linden, M., Bechara, A., 2009. Neural correlates of risk prediction error during reinforcement learning in humans. *Neuroimage* 47, 1929–1939.
- Dale, A.M., Fischl, B., Sereno, M.I., 1999. Cortical Surface-Based Analysis: I. Segmentation and Surface Reconstruction. *NeuroImage* 9, 179–194.
- Daniels, J.K., McFarlane, A.C., Bluhm, R.L., Moores, K.A., Clark, C.R., Shaw, M.E., Williamson, P.C., Densmore, M., Lanius, R.A., 2010. Switching between executive

- and default mode networks in posttraumatic stress disorder: alterations in functional connectivity. *J Psychiatry Neurosci* 35, 258–266.
- Dazzan, P., Morgan, K.D., Orr, K., Hutchinson, G., Chitnis, X., Suckling, J., Fearon, P., McGuire, P.K., Mallett, R.M., Jones, P.B., Leff, J., Murray, R.M., 2005. Different effects of typical and atypical antipsychotics on grey matter in first episode psychosis: the AESOP study. *Neuropsychopharmacology* 30, 765–774.
- Deacon, T.W., 1990. Problems of ontogeny and phylogeny in brain-size evolution. *International Journal of Primatology* 11, 237–282.
- deCharms, R.C., Maeda, F., Glover, G.H., Ludlow, D., Pauly, J.M., Soneji, D., Gabrieli, J.D.E., Mackey, S.C., 2005. Control over brain activation and pain learned by using real-time functional MRI. *PNAS* 102, 18626–18631.
- DeLisi, L.E., Hoff, A.L., Neale, C., Kushner, M., 1994. Asymmetries in the superior temporal lobe in male and female first-episode schizophrenic patients: measures of the planum temporale and superior temporal gyrus by MRI. *Schizophr. Res* 12, 19–28.
- Delvecchio, G., Sugranyes, G., Frangou, S., 2012. Evidence of diagnostic specificity in the neural correlates of facial affect processing in bipolar disorder and schizophrenia: a meta-analysis of functional imaging studies. *Psychological Medicine FirstView*, 1–17.
- Demjaha, A., MacCabe, J.H., Murray, R.M., 2011. How Genes and Environmental Factors Determine the Different Neurodevelopmental Trajectories of Schizophrenia and Bipolar Disorder. *Schizophrenia Bulletin* 38, 209–14.
- Den Ouden, H.E.M., Friston, K.J., Daw, N.D., McIntosh, A.R., Stephan, K.E., 2009. A dual role for prediction error in associative learning. *Cereb. Cortex* 19, 1175–1185.
- Destrieux, C., Fischl, B., Dale, A., Halgren, E., 2010. Automatic parcellation of human cortical gyri and sulci using standard anatomical nomenclature. *Neuroimage* 53, 1–15.

- Dichter, G.S., Bellion, C., Casp, M., Belger, A., 2010. Impaired modulation of attention and emotion in schizophrenia. *Schizophrenia Bull* 36, 595–606.
- Dickinson, D., Goldberg, T.E., Gold, J.M., Elvevag, B., Weinberger, D.R., 2011. Cognitive Factor Structure and Invariance in People With Schizophrenia, Their Unaffected Siblings, and Controls. *Schizophrenia Bull* 37, 1157–1167.
- Dickinson, D., Ramsey, M.E., Gold, J.M., 2007. Overlooking the Obvious: A Meta-analytic Comparison of Digit Symbol Coding Tasks and Other Cognitive Measures in Schizophrenia. *Arch Gen Psychiatry* 64, 532–542.
- Diederer, K.M.J., Daalman, K., De Weijer, A.D., Neggers, S.F.W., Van Gastel, W., Blom, J.D., Kahn, R.S., Sommer, I.E.C., 2011. Auditory Hallucinations Elicit Similar Brain Activation in Psychotic and Nonpsychotic Individuals. *Schizophrenia Bulletin* 38, 1074-82.
- Diwadkar, V.A., Montrose, D.M., Dworakowski, D., Sweeney, J.A., Keshavan, M.S., 2006. Genetically predisposed offspring with schizotypal features: an ultra high-risk group for schizophrenia? *Prog. Neuropsychopharmacol. Biol. Psychiatry* 30, 230–238.
- Dolan, R.J., Fletcher, P., Frith, C.D., Friston, K.J., Frackowiak, R.S.J., Grasby, P.M., 1995. Dopaminergic modulation of impaired cognitive activation in the anterior cingulate cortex in schizophrenia. *Nature* 378, 180–182.
- Doron, G., Rosenblum, K., 2010. c-Fos expression is elevated in GABAergic interneurons of the gustatory cortex following novel taste learning. *Neurobiol Learn Mem* 94, 21–29.
- Dosenbach, N.U.F., Fair, D.A., Miezin, F.M., Cohen, A.L., Wenger, K.K., Dosenbach, R.A.T., Fox, M.D., Snyder, A.Z., Vincent, J.L., Raichle, M.E., Schlaggar, B.L., Petersen, S.E., 2007. Distinct brain networks for adaptive and stable task control in humans. *Proceedings of the National Academy of Sciences* 104, 11073–11078.

- Drzezga, A., Becker, J.A., Dijk, K.R.A.V., Sreenivasan, A., Talukdar, T., Sullivan, C., Schultz, A.P., Sepulcre, J., Putcha, D., Greve, D., Johnson, K.A., Sperling, R.A., 2011. Neuronal dysfunction and disconnection of cortical hubs in non-demented subjects with elevated amyloid burden. *Brain* 134, 1635–1646.
- Du, J., Gray, N.A., Falke, C.A., Chen, W., Yuan, P., Szabo, S.T., Einat, H., Manji, H.K., 2004. Modulation of Synaptic Plasticity by Antimanic Agents: The Role of AMPA Glutamate Receptor Subunit 1 Synaptic Expression. *J. Neurosci.* 24, 6578–6589.
- Duncan, K.J., Pattamadilok, C., Knierim, I., Devlin, J.T., 2009. Consistency and variability in functional localisers. *Neuroimage* 46, 1018–1026.
- Editorial in Nature, 2010. Combating schizophrenia. *Nature* 468, 133–133.
- Ellison-Wright, I., Bullmore, E., 2010. Anatomy of bipolar disorder and schizophrenia: a meta-analysis. *Schizophr. Res* 117, 1–12.
- Ellison-Wright, I., Glahn, D.C., Laird, A.R., Thelen, S.M., Bullmore, E., 2008. The Anatomy of First-Episode and Chronic Schizophrenia: An Anatomical Likelihood Estimation Meta-Analysis. *Am J Psychiatry* 165, 1015–1023.
- Enzi, B., De Greck, M., Prösch, U., Tempelmann, C., Northoff, G., 2009. Is Our Self Nothing but Reward? Neuronal Overlap and Distinction between Reward and Personal Relevance and Its Relation to Human Personality. *PLoS ONE* 4, e8429.
- Essen, D.C.V., 1997. A tension-based theory of morphogenesis and compact wiring in the central nervous system. *Nature* 385, 313–318.
- Eyler, L.T., Prom-Wormley, E., Panizzon, M.S., Kaup, A.R., Fennema-Notestine, C., Neale, M.C., Jernigan, T.L., Fischl, B., Franz, C.E., Lyons, M.J., Grant, M., Stevens, A., Pacheco, J., Perry, M.E., Schmitt, J.E., Seidman, L.J., Thermenos, H.W., Tsuang, M.T., Chen, C.-H., Thompson, W.K., Jak, A., Dale, A.M., Kremen, W.S., 2011. Genetic and Environmental Contributions to Regional Cortical Surface Area in Humans: A Magnetic Resonance Imaging Twin Study. *Cerebral Cortex* 21, 2313–21

- Falkai, P., Honer, W.G., Kamer, T., Dustert, S., Vogeley, K., Schneider-Axmann, T., Dani, I., Wagner, M., Rietschel, M., Müller, D.J., Schulze, T.G., Gaebel, W., Cordes, J., Schönell, H., Schild, H.H., Block, W., Träber, F., Steinmetz, H., Maier, W., Tepest, R., 2007. Disturbed frontal gyrification within families affected with schizophrenia. *Journal of Psychiatric Research* 41, 805–813.
- Falkenberg, L.E., Westerhausen, R., Specht, K., Hugdahl, K., 2012. Resting-state glutamate level in the anterior cingulate predicts blood-oxygen level-dependent response to cognitive control. *PNAS* 109, 5069-73.
- Farb, N.A.S., Anderson, A.K., Segal, Z.V., 2012a. The mindful brain and emotion regulation in mood disorders. *Can J Psychiatry* 57, 70–77.
- Farb, N.A.S., Segal, Z.V., Anderson, A.K., 2012b. Mindfulness meditation training alters cortical representations of interoceptive attention. *Social cognitive and affective neuroscience* 8, 15-26
- Fatemi, S.H., Folsom, T.D., 2009. The Neurodevelopmental Hypothesis of Schizophrenia, Revisited. *Schizophrenia Bulletin* 35, 528 –548.
- Feinberg, I., 1982. Schizophrenia: caused by a fault in programmed synaptic elimination during adolescence? *J Psychiatr Res* 17, 319–334.
- Fellows, L.K., Farah, M.J., 2005. Is anterior cingulate cortex necessary for cognitive control? *Brain* 128, 788–796.
- Ferreira, G., Miranda, M.I., Cruz, V., Rodríguez-Ortiz, C.J., Bermúdez-Rattoni, F., 2005. Basolateral amygdala glutamatergic activation enhances taste aversion through NMDA receptor activation in the insular cortex. *European Journal of Neuroscience* 22, 2596–2604.
- Finlay, B.L., Darlington, R.B., 1995. Linked regularities in the development and evolution of mammalian brains. *Science* 268, 1578–1584.
- Finlay, B.L., Darlington, R.B., Nicastro, N., 2001. Developmental structure in brain evolution. *Behav Brain Sci* 24, 263–278; discussion 278–308.

- Fischl, B., Dale, A.M., 2000. Measuring the thickness of the human cerebral cortex from magnetic resonance images. *Proceedings of the National Academy of Sciences of the United States of America* 97, 11050–11055.
- Fischl, B., Sereno, M.I., Dale, A.M., 1999. Cortical Surface-Based Analysis: II: Inflation, Flattening, and a Surface-Based Coordinate System. *NeuroImage* 9, 195–207.
- Flaum, M., O’Leary, D.S., Swayze, V.W., 2nd, Miller, D.D., Arndt, S., Andreasen, N.C., 1995. Symptom dimensions and brain morphology in schizophrenia and related psychotic disorders. *J Psychiatr Res* 29, 261–276.
- Fletcher, P.C., Frith, C.D., 2009. Perceiving is believing: a Bayesian approach to explaining the positive symptoms of schizophrenia. *Nat. Rev. Neurosci* 10, 48–58.
- Foerster, B.R., Petrou, M., Edden, R.A.E., Sundgren, P.C., Schmidt-Wilcke, T., Lowe, S.E., Harte, S.E., Clauw, D.J., Harris, R.E., 2012. Reduced insular γ -aminobutyric acid in fibromyalgia. *Arthritis & Rheumatism* 64, 579–583.
- Fornito, A., Yücel, M., Dean, B., Wood, S.J., Pantelis, C., 2008. Anatomical Abnormalities of the Anterior Cingulate Cortex in Schizophrenia: Bridging the Gap Between Neuroimaging and Neuropathology. *Schizophrenia Bulletin* 35, 973-93
- Franklin, T.R., Wang, Z., Sciortino, N., Harper, D., Li, Y., Hakun, J., Kildea, S., Kampman, K., Ehrman, R., Detre, J.A., O’Brien, C.P., Childress, A.R., 2011. Modulation of resting brain cerebral blood flow by the GABA B agonist, baclofen: A longitudinal perfusion fMRI study. *Drug and Alcohol Dependence* 117, 176–183.
- Freedman, B.J., 1974. The subjective experience of perceptual and cognitive disturbances in schizophrenia. A review of autobiographical accounts. *Arch. Gen. Psychiatry* 30, 333–340.
- Friston, K.J., 1994. Functional and effective connectivity in neuroimaging: A synthesis. *Human Brain Mapping* 2, 56–78.
- Friston, K.J., 1998. The disconnection hypothesis. *Schizophr. Res* 30, 115–125.

- Friston, K.J., Liddle, P.F., Frith, C.D., Hirsch, S.R., Frackowiak, R.S., 1992. The left medial temporal region and schizophrenia. A PET study. *Brain* 115 (Pt 2), 367–382.
- Frith, C.D., Done, D.J., 1988. Towards a neuropsychology of schizophrenia. *The British Journal of Psychiatry* 153, 437–443.
- Frith, C.D., Friston, K.J., Liddle, P.F., Frackowiak, R.S., 1992. PET imaging and cognition in schizophrenia. *J R Soc Med* 85, 222–224.
- Fusar-Poli, P., Borgwardt, S., Crescini, A., Deste, G., Kempton, M.J., Lawrie, S., Mc Guire, P., Sacchetti, E., 2011a. Neuroanatomy of vulnerability to psychosis: a voxel-based meta-analysis. *Neurosci Biobehav Rev* 35, 1175–1185.
- Fusar-Poli, P., Radua, J., McGuire, P., Stefan, B., 2011b. Neuroanatomical Maps of Psychosis Onset: Voxel-wise Meta-Analysis of Antipsychotic-Naive VBM Studies. *Schizophrenia Bulletin* 38, 1297-307
- Fusar-Poli, P., Smieskova, R., Serafini, G., Politi, P., Borgwardt, S., 2012. Neuroanatomical markers of genetic liability to psychosis and first episode psychosis: A voxelwise meta-analytical comparison. *World Journal of Biological Psychiatry* 1–10.
- García-Martí, G., Aguilar, E.J., Lull, J.J., Martí-Bonmatí, L., Escartí, M.J., Manjón, J.V., Moratal, D., Robles, M., Sanjuán, J., 2008. Schizophrenia with auditory hallucinations: a voxel-based morphometry study. *Prog. Neuropsychopharmacol. Biol. Psychiatry* 32, 72–80.
- Gard, T., Hölzel, B.K., Sack, A.T., Hempel, H., Lazar, S.W., Vaitl, D., Ott, U., 2011. Pain Attenuation through Mindfulness is Associated with Decreased Cognitive Control and Increased Sensory Processing in the Brain. *Cerebral Cortex* 22, 2692-702
- Gardner, D.M., Baldessarini, R.J., Waraich, P., 2005. Modern antipsychotic drugs: a critical overview. *CMAJ* 172, 1703–1711.

- Garrity, A.G., Pearlson, G.D., McKiernan, K., Lloyd, D., Kiehl, K.A., Calhoun, V.D., 2007. Aberrant “Default Mode” Functional Connectivity in Schizophrenia. *Am J Psychiatry* 164, 450–457.
- Gaser, C., Nenadic, I., Volz, H.-P., Büchel, C., Sauer, H., 2004. Neuroanatomy of “hearing voices”: a frontotemporal brain structural abnormality associated with auditory hallucinations in schizophrenia. *Cereb. Cortex* 14, 91–96.
- Gilbert, C.D., Sigman, M., 2007. Brain states: top-down influences in sensory processing. *Neuron* 54, 677–696.
- Glahn, D.C., Laird, A.R., Ellison-Wright, I., Thelen, S.M., Robinson, J.L., Lancaster, J.L., Bullmore, E., Fox, P.T., 2008. Meta-Analysis of Gray Matter Anomalies in Schizophrenia: Application of Anatomic Likelihood Estimation and Network Analysis. *Biological Psychiatry* 64, 774–781.
- Glover, G.H., Li, T.Q., Ress, D., 2000. Image-based method for retrospective correction of physiological motion effects in fMRI: RETROICOR. *Magn Reson Med* 44, 162–167.
- Gogtay, N., Giedd, J.N., Lusk, L., Hayashi, K.M., Greenstein, D., Vaituzis, A.C., Nugent, T.F., Herman, D.H., Clasen, L.S., Toga, A.W., Rapoport, J.L., Thompson, P.M., 2004. Dynamic mapping of human cortical development during childhood through early adulthood. *Proceedings of the National Academy of Sciences of the United States of America* 101, 8174–8179.
- Goldman, A.L., Pezawas, L., Mattay, V.S., Fisl, B., Verchinski, B.A., Zolnick, B., Weinberger, D.R., Meyer-Lindenberg, A., 2008. Heritability of brain morphology related to schizophrenia: a large-scale automated magnetic resonance imaging segmentation study. *Biol. Psychiatry* 63, 475–483.
- Goldman, H.H., Skodol, A.E., Lave, T.R., 1992. Revising axis V for DSM-IV: a review of measures of social functioning. *Am J Psychiatry* 149, 1148–1156.
- Goldman-Rakic, P., Rakic, P., 1984. Experimental modification of gyral patterns., in: *Cerebral Dominance: The Biological Foundations*. Harvard University Press.

- Goldman-Rakic, P.S., Selemon, L.D., 1997. Functional and anatomical aspects of prefrontal pathology in schizophrenia. *Schizophrenia Bull* 23, 437–458.
- Goldstein, J.M., Goodman, J.M., Seidman, L.J., Kennedy, D.N., Makris, N., Lee, H., Tourville, J., Caviness, V.S., Faraone, S.V., Tsuang, M.T., 1999. Cortical abnormalities in schizophrenia identified by structural magnetic resonance imaging. *Arch. Gen. Psychiatry* 56, 537–547.
- Gowland, P.A., Bowtell, R., 2007. Theoretical optimization of multi-echo fMRI data acquisition. *Phys Med Biol* 52, 1801–1813.
- Gradin, V.B., Waiter, G., O'Connor, A., Romaniuk, L., Stickle, C., Matthews, K., Hall, J., Douglas Steele, J., 2013. Salience network-midbrain dysconnectivity and blunted reward signals in schizophrenia. *Psychiatry Res* 211, 104–111.
- Grange, K.M., 1962. Dr. Samuel Johnson's account of a schizophrenic illness in *Rasselas* (1759). *Med Hist* 6, 162–168.
- Greek, M.T., 2010. How a Series of Hallucinations Tells a Symbolic Story. *Schizophrenia Bull* 36, 1063–1065.
- Greve, D.N., Fischl, B., 2009. Accurate and Robust Brain Image Alignment using Boundary-based Registration. *Neuroimage* 48, 63–72.
- Guller, Y., Ferrarelli, F., Shackman, A.J., Sarasso, S., Peterson, M.J., Langheim, F.J., Meyerand, M.E., Tononi, G., Postle, B.R., 2012. Probing Thalamic Integrity in Schizophrenia Using Concurrent Transcranial Magnetic Stimulation and Functional Magnetic Resonance Imaging. *Archives of general psychiatry* 69, 662–71.
- Gussev, A., Rzanny, R., Erdtel, M., Scholle, H.C., Kaiser, W.A., Mentzel, H.J., Reichenbach, J.R., 2010. Time-resolved functional 1H MR spectroscopic detection of glutamate concentration changes in the brain during acute heat pain stimulation. *NeuroImage* 49, 1895–1902.

- Hafeman, D.M., Chang, K.D., Garrett, A.S., Sanders, E.M., Phillips, M.L., 2012. Effects of medication on neuroimaging findings in bipolar disorder: an updated review. *Bipolar Disorders* 14, 375–410.
- Hamilton, J.P., Chen, G., Thomason, M.E., Schwartz, M.E., Gotlib, I.H., 2011a. Investigating neural primacy in Major Depressive Disorder: multivariate Granger causality analysis of resting-state fMRI time-series data. *Molecular Psychiatry* 16, 763–772.
- Hamilton, J.P., Etkin, A., Furman, D.J., Lemus, M.G., Johnson, R.F., Gotlib, I.H., 2012. Functional neuroimaging of major depressive disorder: a meta-analysis and new integration of base line activation and neural response data. *Am J Psychiatry* 169, 693–703.
- Hamilton, J.P., Glover, G.H., Hsu, J.-J., Johnson, R.F., Gotlib, I.H., 2011b. Modulation of Subgenual Anterior Cingulate Cortex Activity With Real-Time Neurofeedback. *Hum Brain Mapp* 32, 22–31.
- Hamm, J.P., Ethridge, L.E., Shapiro, J.R., Stevens, M.C., Boutros, N.N., Summerfelt, A.T., Keshavan, M.S., Sweeney, J.A., Pearlson, G., Tamminga, C.A., Thaker, G., Clementz, B.A., 2012. Spatiotemporal and frequency domain analysis of auditory paired stimuli processing in schizophrenia and bipolar disorder with psychosis. *Psychophysiology* 49, 522–530.
- Harris J.M., Yates S., Miller P., Best J.J, Johnstone E.C, Lawrie S.M., 2004a. Gyrfication in first-episode schizophrenia: A morphometric study. *Biological Psychiatry* 55, 141–147.
- Harris J.M., Whalley, H., Yates S., Miller P., Johnstone E.C, Lawrie S.M., 2004b. Abnormal cortical folding in high-risk individuals: a predictor of the development of schizophrenia? *Biological Psychiatry* 56, 182–89.

- Harris, R.E., Sundgren, P.C., Craig, A.D., Kirshenbaum, E., Sen, A., Napadow, V., Clauw, D.J., 2009. Elevated insular glutamate in fibromyalgia is associated with experimental pain. *Arthritis & Rheumatism* 60, 3146–3152.
- Harris, R.E., Sundgren, P.C., Pang, Y., Hsu, M., Petrou, M., Kim, S.-H., McLean, S.A., Gracely, R.H., Clauw, D.J., 2008. Dynamic levels of glutamate within the insula are associated with improvements in multiple pain domains in fibromyalgia. *Arthritis Rheum* 58, 903–907.
- Hasenkamp, W., James, G.A., Boshoven, W., Duncan, E., 2011. Altered engagement of attention and default networks during target detection in schizophrenia. *Schizophrenia Research* 125, 169–173.
- Haslam, J., 1798. *Observations on Insanity: With Practical Remarks on the Disease, and an Account of the Morbid Appearances on Dissection*. BiblioBazaar.
- Hasson, U., Nusbaum, H.C., Small, S.L., 2009. Task-dependent organization of brain regions active during rest. *Proceedings of the National Academy of Sciences* 106, 10841–10846.
- Haut, K.M., Lim, K.O., MacDonald, A., 2010. Prefrontal Cortical Changes Following Cognitive Training in Patients with Chronic Schizophrenia: Effects of Practice, Generalization, and Specificity. *Neuropsychopharmacology* 35, 1850–1859.
- Havermans, R., Honig, A., Vuurman, E.F., Krabbendam, L., Wilmink, J., Lamers, T., Verheecke, C.J., Jolles, J., Romme, M.A., Van Praag, H.M., 1999. A controlled study of temporal lobe structure volumes and P300 responses in schizophrenic patients with persistent auditory hallucinations. *Schizophr. Res* 38, 151–158.
- Hawkes, E., 2012. Making Meaning. *Schizophrenia Bulletin* 38, 1109-10
- Hebb, D.O., 1949. *The organization of behavior: a neuropsychological theory*. Wiley.
- Henseler, I., Falkai, P., Gruber, O., 2009. A systematic fMRI investigation of the brain systems subserving different working memory components in schizophrenia. *Eur. J. Neurosci* 30, 693–702.

- Herculano-Houzel, S., Mota, B., Wong, P., Kaas, J.H., 2010. Connectivity-driven white matter scaling and folding in primate cerebral cortex. *Proceedings of the National Academy of Sciences* 107, 19008–19013.
- Hermans, E.J., Van Marle, H.J.F., Ossewaarde, L., Henckens, M.J.A.G., Qin, S., Van Kesteren, M.T.R., Schoots, V.C., Cousijn, H., Rijpkema, M., Oostenveld, R., Fernández, G., 2011. Stress-Related Noradrenergic Activity Prompts Large-Scale Neural Network Reconfiguration. *Science* 334, 1151–1153.
- Heuvel, M.P. van den, Mandl, R.C.W., Kahn, R.S., Pol, H.E.H., 2009. Functionally linked resting-state networks reflect the underlying structural connectivity architecture of the human brain. *Human Brain Mapping* 30, 3127–3141.
- Hilgetag, C.C., Barbas, H., 2005. Developmental mechanics of the primate cerebral cortex. *Anat. Embryol* 210, 411–417.
- Hilgetag, C.C., Barbas, H., 2006. Role of Mechanical Factors in the Morphology of the Primate Cerebral Cortex. *PLoS Comput Biol* 2, e22.
- Hill, J., Inder, T., Neil, J., Dierker, D., Harwell, J., Van Essen, D., 2010. Similar patterns of cortical expansion during human development and evolution. *Proceedings of the National Academy of Sciences* 107, 13135–13140.
- Ho, B.-C., Andreasen, N.C., Ziebell, S., Pierson, R., Magnotta, V., 2011. Long-term antipsychotic treatment and brain volumes: a longitudinal study of first-episode schizophrenia. *Arch. Gen. Psychiatry* 68, 128–137.
- Hölzel, B.K., Lazar, S.W., Gard, T., Schuman-Olivier, Z., Vago, D.R., Ott, U., 2011. How Does Mindfulness Meditation Work? Proposing Mechanisms of Action From a Conceptual and Neural Perspective. *Perspectives on Psychological Science* 6, 537–559.
- Honea, R., Crow, T.J., Passingham, D., Mackay, C.E., 2005. Regional Deficits in Brain Volume in Schizophrenia: A Meta-Analysis of Voxel-Based Morphometry Studies. *Am J Psychiatry* 162, 2233–2245.

- Honea, R.A., Meyer-Lindenberg, A., Hobbs, K.B., Pezawas, L., Mattay, V.S., Egan, M.F., Verchinski, B., Passingham, R.E., Weinberger, D.R., Callicott, J.H., 2008. Is gray matter volume an intermediate phenotype for schizophrenia? A voxel-based morphometry study of patients with schizophrenia and their healthy siblings. *Biol. Psychiatry* 63, 465–474.
- Honey, G.D., Pomarol-Clotet, E., Corlett, P.R., Honey, R.A.E., Mckenna, P.J., Bullmore, E.T., Fletcher, P.C., 2005. Functional dysconnectivity in schizophrenia associated with attentional modulation of motor function. *Brain* 128, 2597–2611.
- Hopkins, A.L., 2007. Network pharmacology. *Nature Biotechnology* 25, 1110–1111.
- Horn, D.I., Yu, C., Steiner, J., Buchmann, J., Kaufmann, J., Osoba, A., Eckert, U., Zierhut, K.C., Schiltz, K., He, H., Biswal, B., Bogerts, B., Walter, M., 2010. Glutamatergic and resting-state functional connectivity correlates of severity in major depression - the role of pregenual anterior cingulate cortex and anterior insula. *Front Syst Neurosci* 4.
- Horn, H., Federspiel, A., Wirth, M., Muller, T.J., Wiest, R., Wang, J.-J., Strik, W., 2009. Structural and metabolic changes in language areas linked to formal thought disorder. *The British Journal of Psychiatry* 194, 130–138.
- Howarth, C., Gleeson, P., Attwell, D., 2012. Updated energy budgets for neural computation in the neocortex and cerebellum. *Journal of Cerebral Blood Flow and Metabolism* 32, 1222–32.
- Hulshoff Pol, H.E., Schnack, H.G., Mandl, R.C.W., Brans, R.G.H., Van Haren, N.E.M., Baaré, W.F.C., Van Oel, C.J., Collins, D.L., Evans, A.C., Kahn, R.S., 2006. Gray and white matter density changes in monozygotic and same-sex dizygotic twins discordant for schizophrenia using voxel-based morphometry. *Neuroimage* 31, 482–488.
- Hutton, C., Draganski, B., Ashburner, J., Weiskopf, N., 2009. A comparison between voxel-based cortical thickness and voxel-based morphometry in normal aging. *NeuroImage* 48, 371–380.

- Hyatt, C.J., Haney-Caron, E., Stevens, M.C., 2012. Cortical thickness and folding deficits in conduct-disordered adolescents. *Biol. Psychiatry* 72, 207–214.
- Im, K., Lee, J.-M., Lyttelton, O., Kim, S.H., Evans, A.C., Kim, S.I., 2008. Brain Size and Cortical Structure in the Adult Human Brain. *Cereb. Cortex* 18, 2181–2191.
- Insel, T.R., 2010. Rethinking schizophrenia. *Nature* 468, 187–193.
- Ioannidis, J.P.A., 2011. Excess significance bias in the literature on brain volume abnormalities. *Arch. Gen. Psychiatry* 68, 773–780.
- Ives-Deliperi, V.L., Solms, M., Meintjes, E.M., 2011. The neural substrates of mindfulness: an fMRI investigation. *Soc Neurosci* 6, 231–242.
- Jacobi, W., Winkler, H., 1927. Encephalographische Studien an chronisch Schizophrenen. *European Archives of Psychiatry and Clinical Neuroscience* 81, 299–332.
- Jang, D.-P., Kim, J.-J., Chung, T.-S., An, S.K., Jung, Y.C., Lee, J.-K., Lee, J.-M., Kim, I.-Y., Kim, S.I., 2006. Shape deformation of the insula in schizophrenia. *NeuroImage* 32, 220–227.
- Janssen, J., Reig, S., Alemán, Y., Schnack, H., Udias, J.M., Parellada, M., Graell, M., Moreno, D., Zabala, A., Balaban, E., 2009. Gyral and Sulcal Cortical Thinning in Adolescents with First Episode Early-Onset Psychosis. *Biological Psychiatry* 66, 1047–1054.
- Jardri, R., Pouchet, A., Pins, D., Thomas, P., 2011. Cortical activations during auditory verbal hallucinations in schizophrenia: a coordinate-based meta-analysis. *Am J Psychiatry* 168, 73–81.
- Javitt, D.C., 2009. Sensory Processing in Schizophrenia: Neither Simple nor Intact. *Schizophrenia Bull* 35, 1059–1064.
- Jensen, J., Willeit, M., Zipursky, R.B., Savina, I., Smith, A.J., Menon, M., Crawley, A.P., Kapur, S., 2007. The Formation of Abnormal Associations in Schizophrenia: Neural and Behavioral Evidence. *Neuropsychopharmacology* 33, 473–479.

- Ji, X., Cheng, W., Zhang, J., Ge, T., Sun, L., Wang, Y., Feng, J., 2011. Increased Coupling in the Saliency Network is the main cause/effect of Attention Deficit Hyperactivity Disorder (arXiv e-print No. 1112.3496).
- Job, D.E., Whalley, H.C., Johnstone, E.C., Lawrie, S.M., 2005. Grey matter changes over time in high risk subjects developing schizophrenia. *NeuroImage* 25, 1023–1030.
- Job, D.E., Whalley, H.C., McConnell, S., Glabus, M., Johnstone, E.C., Lawrie, S.M., 2003. Voxel-based morphometry of grey matter densities in subjects at high risk of schizophrenia. *Schizophrenia Research* 64, 1–13.
- Johnston, K., Levin, H.M., Koval, M.J., Everling, S., 2007. Top-down control-signal dynamics in anterior cingulate and prefrontal cortex neurons following task switching. *Neuron* 53, 453–462.
- Johnston, S.J., Boehm, S.G., Healy, D., Goebel, R., Linden, D.E.J., 2010. Neurofeedback: A promising tool for the self-regulation of emotion networks. *Neuroimage* 49, 1066–1072.
- Johnstone, E.C., Crow, T.J., Frith, C.D., Husband, J., Kreel, L., 1976. Cerebral ventricular size and cognitive impairment in chronic schizophrenia. *Lancet* 2, 924–926.
- Jones, S.R., 2010. Do we need multiple models of auditory verbal hallucinations? Examining the phenomenological fit of cognitive and neurological models. *Schizophrenia Bull* 36, 566–575.
- Joyner, A.H., J, C.R., Bloss, C.S., Bakken, T.E., Rimol, L.M., Melle, I., Agartz, I., Djurovic, S., Topol, E.J., Schork, N.J., Andreassen, O.A., Dale, A.M., 2009. A common MECP2 haplotype associates with reduced cortical surface area in humans in two independent populations. *Proc. Natl. Acad. Sci. U.S.A* 106, 15483–15488.
- Kalani, M.Y.S., Kalani, M.A., Gwinn, R., Keogh, B., Tse, V.C.K., 2009. Embryological development of the human insula and its implications for the spread and resection of insular gliomas. *Neurosurgical FOCUS* 27, E2.

- Kanai, R., Rees, G., 2011. The structural basis of inter-individual differences in human behaviour and cognition. *Nature Reviews Neuroscience* 12, 231–242.
- Kane, J.M., Cornblatt, B., Correll, C.U., Goldberg, T., Lencz, T., Malhotra, A.K., Robinson, D., Szeszko, P., 2011. The Field of Schizophrenia: Strengths, Weaknesses, Opportunities, and Threats. *Schizophrenia Bulletin*.
- Kapur, S., 2003. Psychosis as a State of Aberrant Salience: A Framework Linking Biology, Phenomenology, and Pharmacology in Schizophrenia. *Am J Psychiatry* 160, 13–23.
- Kasperek, T., Prikryl, R., Rehulova, J., Marecek, R., Mikl, M., Prikrylova, H., Vanicek, J., Ceskova, E., 2013. Brain functional connectivity of male patients in remission after the first episode of schizophrenia. *Hum Brain Mapp* 34, 726–737.
- Kaufman, J., Plotsky, P.M., Nemeroff, C.B., Charney, D.S., 2000. Effects of early adverse experiences on brain structure and function: clinical implications. *Biological Psychiatry* 48, 778–790.
- Kean, C., 2009. Silencing the Self: Schizophrenia as a Self-Disturbance. *Schizophrenia Bull* 35, 1034–1036.
- Kelly, P.A., Viding, E., Wallace, G.L., Schaer, M., De Brito, S.A., Robustelli, B., McCrory, E.J., 2013. Cortical Thickness, Surface Area, and Gyrfication Abnormalities in Children Exposed to Maltreatment: Neural Markers of Vulnerability? *Biol. Psychiatry*.
- Kennerley, S.W., Walton, M.E., Behrens, T.E.J., Buckley, M.J., Rushworth, M.F.S., 2006. Optimal decision making and the anterior cingulate cortex. *Nat Neurosci* 9, 940–947.
- Kiehl, K.A., Laurens, K.R., Duty, T.L., Forster, B.B., Liddle, P.F., 2001. Neural sources involved in auditory target detection and novelty processing: an event-related fMRI study. *Psychophysiology* 38, 133–142.

- Kilpatrick, L.A., Suyenobu, B.Y., Smith, S.R., Bueller, J.A., Goodman, T., Creswell, J.D., Tillisch, K., Mayer, E.A., Naliboff, B.D., 2011. Impact of Mindfulness-Based Stress Reduction training on intrinsic brain connectivity. *Neuroimage* 56, 290–298.
- Kim, J.J., Youn, T., Lee, J.M., Kim, I.Y., Kim, S.I., Kwon, J.S., 2003. Morphometric abnormality of the insula in schizophrenia: a comparison with obsessive-compulsive disorder and normal control using MRI. *Schizophr. Res* 60, 191–198.
- Klein, T.A., Ullsperger, M., Danielmeier, C., 2013. Error awareness and the insula: links to neurological and psychiatric diseases. *Front. Hum. Neurosci.* 7, 14.
- Ko, J.H., Ptito, A., Monchi, O., Cho, S.S., Van Eimeren, T., Pellecchia, G., Ballanger, B., Rusjan, P., Houle, S., Strafella, A.P., 2009. Increased dopamine release in the right anterior cingulate cortex during the performance of a sorting task: a [¹¹C]FLB 457 PET study. *Neuroimage* 46, 516–521.
- Kochunov, P., Glahn, D.C., Fox, P.T., Lancaster, J.L., Saleem, K., Shelledy, W., Zilles, K., Thompson, P.M., Coulon, O., Mangin, J.F., Blangero, J., Rogers, J., 2010. Genetics of primary cerebral gyration: Heritability of length, depth and area of primary sulci in an extended pedigree of Papio baboons. *Neuroimage* 53, 1126–1134.
- Koechlin, E., Basso, G., Pietrini, P., Panzer, S., Grafman, J., 1999. The role of the anterior prefrontal cortex in human cognition. *Nature* 399, 148–151.
- Komus, K., Westerhausen, R., Hugdahl, K., 2011. The “paradoxical” engagement of the primary auditory cortex in patients with auditory verbal hallucinations: a meta-analysis of functional neuroimaging studies. *Neuropsychologia* 49, 3361–3369.
- Koski, L., Paus, T., 2000. Functional connectivity of the anterior cingulate cortex within the human frontal lobe: a brain-mapping meta-analysis. *Exp Brain Res* 133, 55–65.
- Koutsouleris, N., Gaser, C., Jäger, M., Bottlender, R., Frodl, T., Holzinger, S., Schmitt, G.J.E., Zetsche, T., Burgermeister, B., Scheuerecker, J., Born, C., Reiser, M., Möller, H.-J., Meisenzahl, E.M., 2008. Structural correlates of psychopathological symptom

- dimensions in schizophrenia: a voxel-based morphometric study. *Neuroimage* 39, 1600–1612.
- Kraepelin, E., 1919. *Dementia praecox and paraphrenia*. Livingstone.
- Kühn, S., Gallinat, J., 2010. Quantitative Meta-Analysis on State and Trait Aspects of Auditory Verbal Hallucinations in Schizophrenia. *Schizophrenia Bulletin* 38, 779-86
- Kumar, C.T.S., Christodoulou, T., Vyas, N.S., Kyriakopoulos, M., Corrigall, R., Reichenberg, A., Frangou, S., 2010. Deficits in visual sustained attention differentiate genetic liability and disease expression for Schizophrenia from Bipolar Disorder. *Schizophrenia Research* 124, 152–160.
- Kuperberg, G.R., Broome, M.R., McGuire, P.K., David, A.S., Eddy, M., Ozawa, F., Goff, D., West, W.C., Williams, S.C.R., Van der Kouwe, A.J.W., Salat, D.H., Dale, A.M., Fischl, B., 2003. Regionally Localized Thinning of the Cerebral Cortex in Schizophrenia. *Arch Gen Psychiatry* 60, 878–888.
- Kurth, F., Zilles, K., Fox, P., Laird, A., Eickhoff, S., 2010. A link between the systems: functional differentiation and integration within the human insula revealed by meta-analysis. *Brain Structure and Function* 214, 519-34
- Lahti, A.C., Weiler, M.A., Holcomb, H.H., Tamminga, C.A., Carpenter, W.T., McMahon, R., 2006. Correlations between rCBF and symptoms in two independent cohorts of drug-free patients with schizophrenia. *Neuropsychopharmacology* 31, 221–230.
- Långsjö, J.W., Maksimow, A., Salmi, E., Kaisti, K., Aalto, S., Oikonen, V., Hinkka, S., Aantaa, R., Sipilä, H., Viljanen, T., Parkkola, R., Scheinin, H., 2005. S-ketamine anesthesia increases cerebral blood flow in excess of the metabolic needs in humans. *Anesthesiology* 103, 258–268.
- Laughlin, S.B., Sejnowski, T.J., 2003. Communication in Neuronal Networks. *Science* 301, 1870 –1874.

- Laurens, K.R., Kiehl, K.A., Liddle, P.F., 2005. A supramodal limbic-paralimbic-neocortical network supports goal-directed stimulus processing. *Hum Brain Mapp* 24, 35–49.
- LeBeau, F.E.N., El Manira, A., Griller, S., 2005. Tuning the network: modulation of neuronal microcircuits in the spinal cord and hippocampus. *Trends in Neurosciences* 28, 552–561.
- Leckman, J.F., Sholomskas, D., Thompson, D., Belanger, A., Weissman, M.M., 1982. Best Estimate of Lifetime Psychiatric Diagnosis: A Methodological Study. *Arch Gen Psychiatry* 39, 879–883.
- Legrain, V., Iannetti, G.D., Plaghki, L., Mouraux, A., 2010. The pain matrix reloaded A salience detection system for the body. *Progress in Neurobiology* 93, 111-24
- Lehmann, D., Ozaki, H., Pal, I., 1987. EEG alpha map series: brain micro-states by space-oriented adaptive segmentation. *Electroencephalogr Clin Neurophysiol* 67, 271–288.
- Lehmann, M., Crutch, S.J., Ridgway, G.R., Ridha, B.H., Barnes, J., Warrington, E.K., Rossor, M.N., Fox, N.C., 2009. Cortical thickness and voxel-based morphometry in posterior cortical atrophy and typical Alzheimer’s disease. *Neurobiol. Aging* 32, 1466-76
- Leung, M., Cheung, C., Yu, K., Yip, B., Sham, P., Li, Q., Chua, S., McAlonan, G., 2009. Gray Matter in First-Episode Schizophrenia Before and After Antipsychotic Drug Treatment. *Anatomical Likelihood Estimation Meta-analyses With Sample Size Weighting. Schizophrenia Bulletin* 37, 199-211.
- Levitan, C., Ward, P.B., Catts, S.V., 1999. Superior temporal gyral volumes and laterality correlates of auditory hallucinations in schizophrenia. *Biol. Psychiatry* 46, 955–962.

- Lewis, C.M., Baldassarre, A., Committeri, G., Romani, G.L., Corbetta, M., 2009. Learning sculpts the spontaneous activity of the resting human brain. *Proceedings of the National Academy of Sciences* 106, 17558–17563.
- Lewis, D.A., 2000. Is There a Neuropathology of Schizophrenia? Recent Findings Converge on Altered Thalamic-Prefrontal Cortical Connectivity. *The Neuroscientist* 6, 208–218.
- Lewis, D.A., Hashimoto, T., Volk, D.W., 2005. Cortical inhibitory neurons and schizophrenia. *Nat. Rev. Neurosci.* 6, 312–324.
- Li, X., Xia, S., Bertisch, H.C., Branch, C.A., DeLisi, L.E., 2012. Unique topology of language processing brain network: A systems-level biomarker of schizophrenia. *Schizophrenia Research* 141, 128–136.
- Liang, M., Zhou, Y., Jiang, T., Liu, Z., Tian, L., Liu, H., Hao, Y., 2006. Widespread functional disconnectivity in schizophrenia with resting-state functional magnetic resonance imaging. *Neuroreport* 17, 209–213.
- Liddle, P.F., 1987. The symptoms of chronic schizophrenia. A re-examination of the positive-negative dichotomy. *Br J Psychiatry* 151, 145–151.
- Liddle, P.F., Friston, K.J., Frith, C.D., Hirsch, S.R., Jones, T., Frackowiak, R.S., 1992. Patterns of cerebral blood flow in schizophrenia. *Br J Psychiatry* 160, 179–186.
- Liddle, P.F., Morris, D.L., 1991. Schizophrenic syndromes and frontal lobe performance. *Br J Psychiatry* 158, 340–345.
- Liddle, P.F., Ngan, E.T.C., Duffield, G., Kho, K., Warren, A.J., 2002. Signs and Symptoms of Psychotic Illness (SSPI): a rating scale. *The British Journal of Psychiatry* 180, 45–50.
- Lieberman, J.A., Tollefson, G.D., Charles, C., Zipursky, R., Sharma, T., Kahn, R.S., Keefe, R.S.E., Green, A.I., Gur, R.E., McEvoy, J., Perkins, D., Hamer, R.M., Gu, H., Tohen, M., For the HGDH Study Group, 2005. Antipsychotic Drug Effects on Brain Morphology in First-Episode Psychosis. *Arch Gen Psychiatry* 62, 361–370.

- Linden, D.E.J., Habes, I., Johnston, S.J., Linden, S., Tatineni, R., Subramanian, L., Sorger, B., Healy, D., Goebel, R., 2012. Real-time self-regulation of emotion networks in patients with depression. *PLoS ONE* 7, e38115.
- Lobb, C.J., Wilson, C.J., Paladini, C.A., 2010. A dynamic role for GABA receptors on the firing pattern of midbrain dopaminergic neurons. *J. Neurophysiol.* 104, 403–413.
- Luders, E., Mayer, E.A., Toga, A.W., Narr, K.L., Gaser, C., 2012. The unique brain anatomy of meditation practitioners: alterations in cortical gyrification. *Front. Hum. Neurosci.* 6, 34.
- Luders, E., Thompson, P.M., Narr, K.L., Toga, A.W., Jancke, L., Gaser, C., 2006. A curvature-based approach to estimate local gyrification on the cortical surface. *NeuroImage* 29, 1224–1230.
- Lui, S., Deng, W., Huang, X., Jiang, L., Ouyang, L., Borgwardt, S.J., Ma, X., Li, D., Zou, L., Tang, H., Chen, H., Li, T., McGuire, P., Gong, Q., 2009. Neuroanatomical differences between familial and sporadic schizophrenia and their parents: an optimized voxel-based morphometry study. *Psychiatry Res* 171, 71–81.
- Lui, S., Li, T., Deng, W., Jiang, L., Wu, Q., Tang, H., Yue, Q., Huang, X., Chan, R.C., Collier, D.A., Meda, S.A., Pearlson, G., Mechelli, A., Sweeney, J.A., Gong, Q., 2010. Short-term Effects of Antipsychotic Treatment on Cerebral Function in Drug-Naive First-Episode Schizophrenia Revealed by “Resting State” Functional Magnetic Resonance Imaging. *Arch Gen Psychiatry* 67, 783–792.
- Makris, N., Goldstein, J.M., Kennedy, D., Hodge, S.M., Caviness, V.S., Faraone, S.V., Tsuang, M.T., Seidman, L.J., 2006. Decreased volume of left and total anterior insular lobule in schizophrenia. *Schizophrenia Research* 83, 155–171.
- Mamah, D., Barch, D.M., Repovš, G., 2013. Resting state functional connectivity of five neural networks in bipolar disorder and schizophrenia. *Journal of Affective Disorder* 150, 601-9

- Mangin, J.-F., Jouvent, E., Cachia, A., 2010. In-vivo measurement of cortical morphology: means and meanings. *Current Opinion in Neurology* 1.
- Manoliu, A., Riedl, V., Doll, A., Bauml, J.G., Muhlau, M., Schwerthoffer, D., Scherr, M., Zimmer, C., Forstl, H., Bauml, J., Wohlschlager, A.M., Koch, K., Sorg, C., 2013a. Insular Dysfunction Reflects Altered Between-Network Connectivity and Severity of Negative Symptoms in Schizophrenia during Psychotic Remission. *Front Hum Neurosci* 7.
- Manoliu, A., Riedl, V., Zherdin, A., Mühlau, M., Schwerthöffer, D., Scherr, M., Peters, H., Zimmer, C., Förstl, H., Bäuml, J., Wohlschläger, A.M., Sorg, C., 2013b. Aberrant Dependence of Default Mode/Central Executive Network Interactions on Anterior Insular Salience Network Activity in Schizophrenia. *Schizophrenia Bull.*
- Marcelis, M., Suckling, J., Woodruff, P., Hofman, P., Bullmore, E., Van Os, J., 2003. Searching for a structural endophenotype in psychosis using computational morphometry. *Psychiatry Research: Neuroimaging* 122, 153–167.
- Mars, R.B., Salle, J., Rushworth, M.F.S., Yeung, N., 2012. *Neural Basis of Motivational and Cognitive Control*. MIT Press.
- Marsh, L., Harris, D., Lim, K.O., Beal, M., Hoff, A.L., Minn, K., Csernansky, J.G., DeMent, S., Faustman, W.O., Sullivan, E.V., Pfefferbaum, A., 1997. Structural magnetic resonance imaging abnormalities in men with severe chronic schizophrenia and an early age at clinical onset. *Arch. Gen. Psychiatry* 54, 1104–1112.
- Marsman, A., Van den Heuvel, M.P., Klomp, D.W.J., Kahn, R.S., Luijten, P.R., Hulshoff Pol, H.E., 2011. Glutamate in Schizophrenia: A Focused Review and Meta-Analysis of 1H-MRS Studies. *Schizophrenia Bulletin* 39, 120-9
- Martínez-Cerdeño, V., Noctor, S.C., Kriegstein, A.R., 2006. The role of intermediate progenitor cells in the evolutionary expansion of the cerebral cortex. *Cereb. Cortex* 16 Suppl 1, i152–161.

- Mason, M.F., Norton, M.I., Van Horn, J.D., Wegner, D.M., Grafton, S.T., Macrae, C.N., 2007. Wandering Minds: The Default Network and Stimulus-Independent Thought. *Science* 315, 393–395.
- McCabe, C., Huber, A., Harmer, C.J., Cowen, P.J., 2011. The D2 antagonist sulpiride modulates the neural processing of both rewarding and aversive stimuli in healthy volunteers. *Psychopharmacology (Berl)* 217, 271–278.
- McCarley, R.W., Wible, C.G., Frumin, M., Hirayasu, Y., Levitt, J.J., Fischer, I.A., Shenton, M.E., 1999. MRI anatomy of schizophrenia. *Biol. Psychiatry* 45, 1099–1119.
- McCarthy-Jones, S., 2012. Taking Back the Brain: Could Neurofeedback Training Be Effective for Relieving Distressing Auditory Verbal Hallucinations in Patients With Schizophrenia? *Schizophrenia Bulletin* 38, 678–82
- McDonald, C., Dineen, B., Hallahan, B., 2008. Meta-analysis of brain volumes in unaffected first-degree relatives of patients with schizophrenia overemphasizes hippocampal deficits. *Arch. Gen. Psychiatry* 65, 603–604; author reply 604–605.
- McGrath CL, K.M., 2013. Toward a neuroimaging treatment selection biomarker for major depressive disorder. *JAMA Psychiatry* 1–9.
- McGuire, P.K., David, A.S., Murray, R.M., Frackowiak, R.S.J., Frith, C.D., Wright, I., Silbersweig, D.A., 1995. Abnormal monitoring of inner speech: a physiological basis for auditory hallucinations. *The Lancet* 346, 596–600.
- McIntosh, A.M., Job, D.E., Moorhead, T.W.J., Harrison, L.K., Forrester, K., Lawrie, S.M., Johnstone, E.C., 2004. Voxel-based morphometry of patients with schizophrenia or bipolar disorder and their unaffected relatives. *Biol. Psychiatry* 56, 544–552.
- McIntosh A.M., Moorhead T.W.J, McKirdy J., Hall J., Sussmann J.E.D, Stanfield A.C. ,2009. Prefrontal gyral folding and its cognitive correlates in bipolar disorder and schizophrenia. *Acta Psychiatr Scand* 119, 192–198.

- Mechelli, A., Price, C.J., Friston, K.J., Ashburner, J., 2005. Voxel-Based Morphometry of the Human Brain: Methods and Applications. *CURRENT MEDICAL IMAGING REVIEWS* 1, 105–113.
- Mechelli, A., Riecher-Rössler, A., Meisenzahl, E.M., Tognin, S., Wood, S.J., Borgwardt, S.J., Koutsouleris, N., Yung, A.R., Stone, J.M., Phillips, L.J., McGorry, P.D., Valli, I., Velakoulis, D., Woolley, J., Pantelis, C., McGuire, P., 2011. Neuroanatomical abnormalities that predate the onset of psychosis: a multicenter study. *Arch. Gen. Psychiatry* 68, 489–495.
- Medalla, M., Barbas, H., 2009. Synapses with inhibitory neurons differentiate anterior cingulate from dorsolateral prefrontal pathways associated with cognitive control. *Neuron* 61, 609–620.
- Medford, N., Critchley, H.D., 2010. Conjoint activity of anterior insular and anterior cingulate cortex: awareness and response. *Brain Struct Funct* 214, 535–549.
- Meisenzahl, E.M., Koutsouleris, N., Bottlender, R., Scheuerecker, J., Jäger, M., Teipel, S.J., Holzinger, S., Frodl, T., Preuss, U., Schmitt, G., Burgermeister, B., Reiser, M., Born, C., Möller, H.-J., 2008. Structural brain alterations at different stages of schizophrenia: a voxel-based morphometric study. *Schizophr. Res* 104, 44–60.
- Menon, V., 2011. Large-scale brain networks and psychopathology: a unifying triple network model. *Trends Cogn. Sci. (Regul. Ed.)* 15, 483–506.
- Menon, V., Uddin, L.Q., 2010. Saliency, switching, attention and control: a network model of insula function. *Brain Struct Funct* 214, 655–67.
- Mesulam, M.-M., 2000. *Principles of Behavioral and Cognitive Neurology*, 2nd ed. Oxford University Press, USA.
- Meyer-Lindenberg, A.S., Olsen, R.K., Kohn, P.D., Brown, T., Egan, M.F., Weinberger, D.R., Berman, K.F., 2005. Regionally specific disturbance of dorsolateral prefrontal-hippocampal functional connectivity in schizophrenia. *Arch. Gen. Psychiatry* 62, 379–386.

- Miller, E.K., Cohen, J.D., 2001. An Integrative Theory of Prefrontal Cortex Function. *Annual Review of Neuroscience* 24, 167–202.
- Minzenberg, M.J., Laird, A.R., Thelen, S., Carter, C.S., Glahn, D.C., 2009. Meta-analysis of 41 Functional Neuroimaging Studies of Executive Function in Schizophrenia. *Arch Gen Psychiatry* 66, 811–822.
- Mishara, A.L., 2010. Klaus Conrad (1905-1961): delusional mood, psychosis, and beginning schizophrenia. *Schizophrenia Bulletin* 36, 9–13.
- Mitelman, S.A., Canfield, E.L., Chu, K.-W., Brickman, A.M., Shihabuddin, L., Hazlett, E.A., Buchsbaum, M.S., 2009. Poor outcome in chronic schizophrenia is associated with progressive loss of volume of the putamen. *Schizophr. Res.* 113, 241–245.
- Modinos, G., Costafreda, S.G., Van Tol, M.-J., McGuire, P.K., Aleman, A., Allen, P., 2013. Neuroanatomy of auditory verbal hallucinations in schizophrenia: a quantitative meta-analysis of voxel-based morphometry studies. *Cortex* 49, 1046–1055.
- Modinos, G., Ormel, J., Aleman, A., 2009a. Activation of Anterior Insula during Self-Reflection. *PLoS ONE* 4, e4618.
- Modinos, G., Vercammen, A., Mechelli, A., Knegeting, H., McGuire, P.K., Aleman, A., 2009b. Structural covariance in the hallucinating brain: a voxel-based morphometry study. *J Psychiatry Neurosci* 34, 465–469.
- Molina, V., Solera, S., Sanz, J., Sarramea, F., Luque, R., Rodríguez, R., Jiménez-Arriero, M.A., Palomo, T., 2009. Association between cerebral metabolic and structural abnormalities and cognitive performance in schizophrenia. *Psychiatry Research: Neuroimaging* 173, 88–93.
- Moncrieff, J., Leo, J., 2010. A systematic review of the effects of antipsychotic drugs on brain volume. *Psychol Med* 40, 1409–1422.
- Montagu, A., 1961. Neonatal and Infant Immaturity in Man. *JAMA: The Journal of the American Medical Association* 178, 56–57.

- Moran, L.V., Sampath, H., Stein, E.A., Hong, L.E., 2012. Insular and anterior cingulate circuits in smokers with schizophrenia. *Schizophr. Res.* 142, 223–229.
- Moran, L.V., Tagamets, M.A., Sampath, H., O'Donnell, A., Stein, E.A., Kochunov, P., Hong, L.E., 2013a. Disruption of anterior insula modulation of large-scale brain networks in schizophrenia. *Biol. Psychiatry* 74, 467–474.
- Mountcastle, V., 1997. The columnar organization of the neocortex. *Brain* 120, 701–722.
- Murray, G.K., Corlett, P.R., Clark, L., Pessiglione, M., Blackwell, A.D., Honey, G., Jones, P.B., Bullmore, E.T., Robbins, T.W., Fletcher, P.C., 2008. Substantia nigra/ventral tegmental reward prediction error disruption in psychosis. *Mol. Psychiatry* 13, 239, 267–276.
- Naqvi, N.H., Bechara, A., 2010. The insula and drug addiction: an interoceptive view of pleasure, urges, and decision-making. *Brain Struct Funct* 214, 435–450.
- Narr, K.L., Bilder, R.M., Kim, S., Thompson, P.M., Szeszko, P., Robinson, D., Luders, E., Toga, A.W., 2004. Abnormal gyral complexity in first-episode schizophrenia. *Biol. Psychiatry* 55, 859–867.
- Narr, K.L., Bilder, R.M., Toga, A.W., Woods, R.P., Rex, D.E., Szeszko, P.R., Robinson, D., Sevy, S., Gunduz-Bruce, H., Wang, Y.-P., DeLuca, H., Thompson, P.M., 2005. Mapping Cortical Thickness and Gray Matter Concentration in First Episode Schizophrenia. *Cereb. Cortex* 15, 708–719.
- Narr, K.L., Thompson, P.M., Sharma, T., Moussai, J., Zoumalan, C., Rayman, J., Toga, A.W., 2001. Three-Dimensional Mapping of Gyral Shape and Cortical Surface Asymmetries in Schizophrenia: Gender Effects. *Am J Psychiatry* 158, 244–255.
- Navari, S., Dazzan, P., 2009. Do antipsychotic drugs affect brain structure? A systematic and critical review of MRI findings. *Psychol Med* 39, 1763–1777.
- Neckelmann, G., Specht, K., Lund, A., Ersland, L., Smievoll, A.I., Neckelmann, D., Hugdahl, K., 2006. Mr morphometry analysis of grey matter volume reduction in schizophrenia: association with hallucinations. *Int. J. Neurosci* 116, 9–23.

- Nenadic, I., Smesny, S., Schlösser, R.G.M., Sauer, H., Gaser, C., 2010. Auditory hallucinations and brain structure in schizophrenia: voxel-based morphometric study. *Br J Psychiatry* 196, 412–413.
- Nishida, K., Morishima, Y., Yoshimura, M., Isotani, T., Irisawa, S., Jann, K., Dierks, T., Strik, W., Kinoshita, T., Koenig, T., 2013. EEG microstates associated with salience and frontoparietal networks in frontotemporal dementia, schizophrenia and Alzheimer's disease. *Clin Neurophysiol* 124, 1106–1114.
- Northoff, G., Walter, M., Schulte, R.F., Beck, J., Dydak, U., Henning, A., Boeker, H., Grimm, S., Boesiger, P., 2007. GABA concentrations in the human anterior cingulate cortex predict negative BOLD responses in fMRI. *Nat Neurosci* 10, 1515–1517.
- Nygård, M., Eichele, T., Løberg, E.-M., Jørgensen, H.A., Johnsen, E., Hugdahl, K., 2012. Patients with schizophrenia fail to up-regulate task-positive and down-regulate task-negative brain networks: an fMRI study using an ICA analysis approach. *Front. Hum. Neurosci.* 6, 149.
- O'Daly, O.G., Frangou, S., Chitnis, X., Shergill, S.S., 2007. Brain structural changes in schizophrenia patients with persistent hallucinations. *Psychiatry Res* 156, 15–21.
- Ohara, P.T., Granato, A., Moallem, T.M., Wang, B.-R., Tillet, Y., Jasmin, L., 2003. Dopaminergic input to GABAergic neurons in the rostral agranular insular cortex of the rat. *J. Neurocytol.* 32, 131–141.
- Olabi, B., Ellison-Wright, I., Bullmore, E., Lawrie, S.M., 2012. Structural brain changes in First Episode Schizophrenia compared with Fronto-Temporal Lobar Degeneration: a meta-analysis. *BMC Psychiatry* 12, 104.
- Olson, I.R., Plotzker, A., Ezzyat, Y., 2007. The Enigmatic temporal pole: a review of findings on social and emotional processing. *Brain* 130, 1718–1731.
- Ongür, D., Lundy, M., Greenhouse, I., Shinn, A.K., Menon, V., Cohen, B.M., Renshaw, P.F., 2010. Default mode network abnormalities in bipolar disorder and schizophrenia. *Psychiatry Res* 183, 59–68.

- Onitsuka, T., Shenton, M.E., Salisbury, D.F., Dickey, C.C., Kasai, K., Toner, S.K., Frumin, M., Kikinis, R., Jolesz, F.A., McCarley, R.W., 2004. Middle and inferior temporal gyrus gray matter volume abnormalities in chronic schizophrenia: an MRI study. *Am J Psychiatry* 161, 1603–1611.
- Orliac, F., Naveau, M., Joliot, M., Delcroix, N., Razafimandimby, A., Brazo, P., Dollfus, S., Delamillieure, P., 2013. Links among resting-state default-mode network, salience network, and symptomatology in schizophrenia. *Schizophr. Res.*
- Pagnoni, G., Cekic, M., Guo, Y., 2008. “Thinking about Not-Thinking”: Neural Correlates of Conceptual Processing during Zen Meditation. *PLoS ONE* 3, e3083.
- Palaniyappan, L., Al-Radaideh, A., Mougin, O., Gowland, P., Liddle, P.F., 2013. Combined white matter imaging suggests myelination defects in visual processing regions in schizophrenia. *Neuropsychopharmacology*.
- Palaniyappan, L., Mallikarjun, P., Joseph, V., White, T.P., Liddle, P.F., 2011. Folding of the Prefrontal Cortex in Schizophrenia: Regional Differences in Gyrification. *Biological Psychiatry* 69, 974–979.
- Pan, P.L., Song, W., Shang, H.F., 2011. Voxel-wise meta-analysis of gray matter abnormalities in idiopathic Parkinson’s disease. *Eur J Neurol*.
- Panizzon, M.S., Fennema-Notestine, C., Eyler, L.T., Jernigan, T.L., Prom-Wormley, E., Neale, M., Jacobson, K., Lyons, M.J., Grant, M.D., Franz, C.E., Xian, H., Tsuang, M., Fischl, B., Seidman, L., Dale, A., Kremen, W.S., 2009. Distinct Genetic Influences on Cortical Surface Area and Cortical Thickness. *Cereb. Cortex* 19, 2728–2735.
- Pantelis, C., Velakoulis, D., McGorry, P.D., Wood, S.J., Suckling, J., Phillips, L.J., Yung, A.R., Bullmore, E.T., Brewer, W., Soulsby, B., Desmond, P., McGuire, P.K., 2003. Neuroanatomical abnormalities before and after onset of psychosis: a cross-sectional and longitudinal MRI comparison. *The Lancet* 361, 281–288.
- Parker, J.G., Wanat, M.J., Soden, M.E., Ahmad, K., Zweifel, L.S., Bamford, N.S., Palmiter, R.D., 2011. Attenuating GABA(A) receptor signaling in dopamine neurons selectively

- enhances reward learning and alters risk preference in mice. *J. Neurosci.* 31, 17103–17112.
- Pauli, A., Prata, D.P., Mechelli, A., Picchioni, M., Fu, C.H.Y., Chaddock, C.A., Kane, F., Kalidindi, S., McDonald, C., Kravariti, E., Touloupoulou, T., Bramon, E., Walshe, M., Ehlert, N., Georgiades, A., Murray, R., Collier, D.A., McGuire, P., 2012. Interaction between effects of genes coding for dopamine and glutamate transmission on striatal and parahippocampal function. *Hum Brain Mapp.*
- Paulus, M.P., Feinstein, J.S., Castillo, G., Simmons, A.N., Stein, M.B., 2005. Dose-dependent decrease of activation in bilateral amygdala and insula by lorazepam during emotion processing. *Arch. Gen. Psychiatry* 62, 282–288.
- Payne, R., 2012. Night's End. *Schizophrenia Bull.*
- Peper, J.S., Brouwer, R.M., Boomsma, D.I., Kahn, R.S., Pol, H.E.H., 2007. Genetic influences on human brain structure: A review of brain imaging studies in twins. *Human Brain Mapping* 28, 464–473.
- Pettersson-Yeo, W., Allen, P., Benetti, S., McGuire, P., Mechelli, A., 2011. Dysconnectivity in schizophrenia: where are we now? *Neurosci Biobehav Rev* 35, 1110–1124.
- Picard, F., Sadaghiani, S., Leroy, C., Courvoisier, D.S., Maroy, R., Bottlaender, M., 2013. High density of nicotinic receptors in the cingulo-insular network. *NeuroImage* 79, 42–51.
- Pies, R., 1979. On myths and countermyths: more on Szaszian fallacies. *Arch. Gen. Psychiatry* 36, 139–144.
- Plaze, M., Bartrés-Faz, D., Martinot, J.-L., Januel, D., Bellivier, F., De Beaurepaire, R., Chanraud, S., Andoh, J., Lefaucheur, J.-P., Artiges, E., Pallier, C., Paillère-Martinot, M.-L., 2006. Left superior temporal gyrus activation during sentence perception negatively correlates with auditory hallucination severity in schizophrenia patients. *Schizophrenia Research* 87, 109–115.

- Polli, F.E., Barton, J.J.S., Thakkar, K.N., Greve, D.N., Goff, D.C., Rauch, S.L., Manoach, D.S., 2008. Reduced error-related activation in two anterior cingulate circuits is related to impaired performance in schizophrenia. *Brain* 131, 971–986.
- Posse, S., Wiese, S., Gembris, D., Mathiak, K., Kessler, C., Grosse-Ruyken, M.L., Elghahwagi, B., Richards, T., Dager, S.R., Kiselev, V.G., 1999. Enhancement of BOLD-contrast sensitivity by single-shot multi-echo functional MR imaging. *Magn Reson Med* 42, 87–97.
- Potkin, S.G., Turner, J.A., Brown, G.G., McCarthy, G., Greve, D.N., Glover, G.H., Manoach, D.S., Belger, A., Diaz, M., Wible, C.G., Ford, J.M., Mathalon, D.H., Gollub, R., Lauriello, J., O’Leary, D., Van Erp, T.G.M., Toga, A.W., Preda, A., Lim, K.O., 2009. Working memory and DLPFC inefficiency in schizophrenia: The FBIRN study. *Schizophrenia Bull* 35, 19–31.
- Prasad, K.M.R., Rohm, B.R., Keshavan, M.S., 2004. Parahippocampal gyrus in first episode psychotic disorders: a structural magnetic resonance imaging study. *Prog. Neuropsychopharmacol. Biol. Psychiatry* 28, 651–658.
- Prata, D.P., Mechelli, A., Picchioni, M.M., Fu, C.H.Y., Touloupoulou, T., Bramon, E., Walshe, M., Murray, R.M., Collier, D.A., McGuire, P., 2009. Altered Effect of Dopamine Transporter 3’UTR VNTR Genotype on Prefrontal and Striatal Function in Schizophrenia. *Arch Gen Psychiatry* 66, 1162–1172.
- Preacher, K.J., Hayes, A.F., 2004. SPSS and SAS procedures for estimating indirect effects in simple mediation models. *Behav Res Methods Instrum Comput* 36, 717–731.
- Preacher, K.J., Hayes, A.F., 2008. Asymptotic and resampling strategies for assessing and comparing indirect effects in multiple mediator models. *Behav Res Methods* 40, 879–891.
- Pressler, M., Nopoulos, P., Ho, B.-C., Andreasen, N.C., 2005. Insular cortex abnormalities in schizophrenia: Relationship to symptoms and typical neuroleptic exposure. *Biological Psychiatry* 57, 394–398.

- Preuschoff, K., Quartz, S.R., Bossaerts, P., 2008. Human Insula Activation Reflects Risk Prediction Errors As Well As Risk. *J. Neurosci.* 28, 2745–2752.
- Pu, W., Li, L., Zhang, H., Ouyang, X., Liu, H., Zhao, J., Li, L., Xue, Z., Xu, K., Tang, H., Shan, B., Liu, Z., Wang, F., 2012. Morphological and functional abnormalities of salience network in the early-stage of paranoid schizophrenia. *Schizophrenia Research* 141, 15-21
- Radua, J., Mataix-Cols, D., 2009. Voxel-wise meta-analysis of grey matter changes in obsessive-compulsive disorder. *The British Journal of Psychiatry* 195, 393–402.
- Radua, J., Mataix-Cols, D., Phillips, M.L., El-Hage, W., Kronhaus, D.M., Cardoner, N., Surguladze, S., 2011. A new meta-analytic method for neuroimaging studies that combines reported peak coordinates and statistical parametric maps. *European Psychiatry: The Journal of the Association of European Psychiatrists*.
- Radua, J., Van den Heuvel, O.A., Surguladze, S., Mataix-Cols, D., 2010a. Meta-analytical Comparison of Voxel-Based Morphometry Studies in Obsessive-Compulsive Disorder vs Other Anxiety Disorders. *Arch Gen Psychiatry* 67, 701–711.
- Radua, J., Via, E., Catani, M., Mataix-Cols, D., 2010b. Voxel-based meta-analysis of regional white-matter volume differences in autism spectrum disorder versus healthy controls. *Psychol Med* 1–12.
- Rajagopalan, V., Scott, J., Habas, P.A., Kim, K., Corbett-Detig, J., Rousseau, F., Barkovich, A.J., Glenn, O.A., Studholme, C., 2011. Local Tissue Growth Patterns Underlying Normal Fetal Human Brain Gyrification Quantified In Utero. *The Journal of Neuroscience* 31, 2878 –2887.
- Rajarethinam, R.P., DeQuardo, J.R., Nalepa, R., Tandon, R., 2000. Superior temporal gyrus in schizophrenia: a volumetric magnetic resonance imaging study. *Schizophr. Res* 41, 303–312.
- Rakic, P., 1988. Specification of cerebral cortical areas. *Science* 241, 170–176.

- Repovš, G., Barch, D.M., 2012. Working Memory Related Brain Network Connectivity in Individuals with Schizophrenia and Their Siblings. *Front Hum Neurosci* 6.
- Rescorla, R., Wagner, A., 1972. A theory of Pavlovian conditioning: Variations in the effectiveness of reinforcement and nonreinforcement, in: *Classical Conditioning II: Current Research and Theory*. Appleton-Century-Crofts, pp. 64–99.
- Reynolds, G.P., Zhang, Z.J., Beasley, C.L., 2001. Neurochemical correlates of cortical GABAergic deficits in schizophrenia: selective losses of calcium binding protein immunoreactivity. *Brain Res. Bull.* 55, 579–584.
- Rimol, L.M., Nesvåg, R., Hagler, D.J., Jr, Bergmann, O., Fennema-Notestine, C., Hartberg, C.B., Haukvik, U.K., Lange, E., Pung, C.J., Server, A., Melle, I., Andreassen, O.A., Agartz, I., Dale, A.M., 2012. Cortical volume, surface area, and thickness in schizophrenia and bipolar disorder. *Biol. Psychiatry* 71, 552–560.
- Rimol, L.M., Panizzon, M.S., Fennema-Notestine, C., Eyler, L.T., Fischl, B., Franz, C.E., Hagler, D.J., Lyons, M.J., Neale, M.C., Pacheco, J., Perry, M.E., Schmitt, J.E., Grant, M.D., Seidman, L.J., Thermenos, H.W., Tsuang, M.T., Eisen, S.A., Kremen, W.S., Dale, A.M., 2010. Cortical Thickness Is Influenced by Regionally Specific Genetic Factors. *Biological Psychiatry* 67, 493–499.
- Rodríguez-Sánchez, J.M., Crespo-Facorro, B., González-Blanch, C., Perez-Iglesias, R., Vázquez-Barquero, J.L., PAFIP Group Study, 2007. Cognitive dysfunction in first-episode psychosis: the processing speed hypothesis. *Br J Psychiatry Suppl* 51, s107–110.
- Roiz-Santiáñez, R., Pérez-Iglesias, R., Quintero, C., Tordesillas-Gutiérrez, D., Mata, I., Ayesa, R., Sánchez, J.M.R., Gutiérrez, A., Sanchez, E., Vázquez-Barquero, J.L., Crespo-Facorro, B., 2010. Insular cortex thinning in first episode schizophrenia patients. *Psychiatry Research: Neuroimaging* 182, 216–222.
- Rose, D., Pevalin, D.J., 2003. *A Researcher's Guide to the National Statistics Socio-economic Classification*. Sage Publications, London.

- Ross, C.A., Pearlson, G.D., 1996. Schizophrenia, the heteromodal association neocortex and development: potential for a neurogenetic approach. *Trends Neurosci* 19, 171–176.
- Rowland, L.M., Beason-Held, L., Tamminga, C.A., Holcomb, H.H., 2010. The interactive effects of ketamine and nicotine on human cerebral blood flow. *Psychopharmacology (Berl)* 208, 575–584.
- Rowland, L.M., Bustillo, J.R., Mullins, P.G., Jung, R.E., Lenroot, R., Landgraf, E., Barrow, R., Yeo, R., Lauriello, J., Brooks, W.M., 2005. Effects of Ketamine on Anterior Cingulate Glutamate Metabolism in Healthy Humans: A 4-T Proton MRS Study. *Am J Psychiatry* 162, 394–396.
- Rudnick, A., Rofè, T., Virtzberg-Rofè, D., Scotti, P., 2011. Supported Reporting of First Person Accounts: Assisting People Who Have Mental Health Challenges in Writing and Publishing Reports About Their Lived Experience. *Schizophrenia Bull* 37, 879–881.
- Ruiz, S., Lee, S., Soekadar, S.R., Caria, A., Veit, R., Kircher, T., Birbaumer, N., Sitaram, R., 2011. Acquired self-control of insula cortex modulates emotion recognition and brain network connectivity in schizophrenia. *Human Brain Mapping* 34, 200–12
- Rumelhart, D.E., Group, J.L.M. and the P.R., 1987. *Parallel Distributed Processing - Vol. 1: Foundations*.
- Sadaghiani, S., Scheeringa, R., Lehongre, K., Morillon, B., Giraud, A.-L., Kleinschmidt, A., 2010. Intrinsic Connectivity Networks, Alpha Oscillations, and Tonic Alertness: A Simultaneous Electroencephalography/Functional Magnetic Resonance Imaging Study. *J. Neurosci.* 30, 10243–10250.
- Samanez-Larkin, G.R., Hollon, N.G., Carstensen, L.L., Knutson, B., 2008. Individual differences in insular sensitivity during loss anticipation predict avoidance learning. *Psychol Sci* 19, 320–323.

- Sams-Dodd, F., 2005. Target-based drug discovery: is something wrong? *Drug Discovery Today* 10, 139–147.
- Sanfey, A.G., Rilling, J.K., Aronson, J.A., Nystrom, L.E., Cohen, J.D., 2003. The Neural Basis of Economic Decision-Making in the Ultimatum Game. *Science* 300, 1755–1758.
- Sass, L.A., Parnas, J., 2003. Schizophrenia, Consciousness, and the Self. *Schizophrenia Bull* 29, 427–444.
- Saze, T., Hirao, K., Namiki, C., Fukuyama, H., Hayashi, T., Murai, T., 2007. Insular volume reduction in schizophrenia. *European Archives of Psychiatry and Clinical Neuroscience* 257, 473–479.
- Schaer, M., Cuadra, M.B., Tamarit, L., Lazeyras, F., Eliez, S., Thiran, J.-P., 2008. A surface-based approach to quantify local cortical gyrification. *IEEE Trans Med Imaging* 27, 161–170.
- Schaer, M., Glaser, B., Cuadra, M.B., Debbane, M., Thiran, J.-P., Eliez, S., 2009. Congenital heart disease affects local gyrification in 22q11.2 deletion syndrome. *Dev Med Child Neurol* 51, 746–753.
- Schippers, M.B., Renken, R., Keysers, C., 2011. The effect of intra- and inter-subject variability of hemodynamic responses on group level Granger causality analyses. *Neuroimage* 57, 22–36.
- Schmitt, A., Schulenberg, W., Bernstein, H.-G., Steiner, J., Schneider-Axmann, T., Yeganeh-Doost, P., Malchow, B., Hasan, A., Gruber, O., Bogerts, B., Falkai, P., 2011. Reduction of gyrification index in the cerebellar vermis in schizophrenia: a post-mortem study. *World J. Biol. Psychiatry* 12 Suppl 1, 99–103.
- Schneider, K., 1959. *Clinical psychopathology*. Grune & Stratton.
- Schnell, K., Heekeren, K., Daumann, J., Schnell, T., Schnitker, R., Möller-Hartmann, W., Gouzoulis-Mayfrank, E., 2008. Correlation of passivity symptoms and dysfunctional visuomotor action monitoring in psychosis. *Brain* 131, 2783 – 2797.

- Schultz, W., 2010. Dopamine signals for reward value and risk: basic and recent data. *Behavioral and Brain Functions* 6, 24.
- Seeley, W.W., Menon, V., Schatzberg, A.F., Keller, J., Glover, G.H., Kenna, H., Reiss, A.L., Greicius, M.D., 2007. Dissociable Intrinsic Connectivity Networks for Salience Processing and Executive Control. *J. Neurosci.* 27, 2349–2356.
- Seth, A.K., Suzuki, K., Critchley, H.D., 2011. An interoceptive predictive coding model of conscious presence. *Front Psychol* 2, 395.
- Shapleske, J., Rossell, S.L., Chitnis, X.A., Suckling, J., Simmons, A., Bullmore, E.T., Woodruff, P.W.R., David, A.S., 2002. A Computational Morphometric MRI Study of Schizophrenia: Effects of Hallucinations. *Cereb. Cortex* 12, 1331–1341.
- Shaw, P., Kabani, N.J., Lerch, J.P., Eckstrand, K., Lenroot, R., Gogtay, N., Greenstein, D., Clasen, L., Evans, A., Rapoport, J.L., Giedd, J.N., Wise, S.P., 2008. Neurodevelopmental trajectories of the human cerebral cortex. *J. Neurosci* 28, 3586–3594.
- Shenton, M.E., Dickey, C.C., Frumin, M., McCarley, R.W., 2001. A review of MRI findings in schizophrenia. *Schizophr. Res* 49, 1–52.
- Shenton, M.E., Whitford, T.J., Kubicki, M., 2010. Structural neuroimaging in schizophrenia: from methods to insights to treatments. *Dialogues Clin Neurosci* 12, 317–332.
- Shepherd, A.M., Matheson, S.L., Laurens, K.R., Carr, V.J., Green, M.J., 2012. Systematic Meta-Analysis of Insula Volume in Schizophrenia. *Biological Psychiatry*.
- Sigmundsson, T., Suckling, J., Maier, M., Williams, S.C.R., Bullmore, E.T., Greenwood, K.E., Fukuda, R., Ron, M.A., Toone, B.K., 2001. Structural Abnormalities in Frontal, Temporal, and Limbic Regions and Interconnecting White Matter Tracts in Schizophrenic Patients With Prominent Negative Symptoms. *Am J Psychiatry* 158, 234–243.

- Singer, T., Critchley, H.D., Preuschoff, K., 2009. A common role of insula in feelings, empathy and uncertainty. *Trends in Cognitive Sciences* 13, 334–340.
- Skudlarski, P., Jagannathan, K., Anderson, K., Stevens, M.C., Calhoun, V.D., Skudlarska, B.A., Pearlson, G., 2010. Brain connectivity is not only lower but different in schizophrenia: a combined anatomical and functional approach. *Biol. Psychiatry* 68, 61–69.
- Slotema, C.W., Aleman, A., Daskalakis, Z.J., Sommer, I.E., 2012. Meta-analysis of repetitive transcranial magnetic stimulation in the treatment of auditory verbal hallucinations: Update and effects after one month. *Schizophrenia Research* 142, 40–45.
- Smieskova, R., Fusar-Poli, P., Allen, P., Bendfeldt, K., Stieglitz, R.D., Drewe, J., Radue, E.W., McGuire, P.K., Riecher-Rössler, A., Borgwardt, S.J., 2010. Neuroimaging predictors of transition to psychosis--a systematic review and meta-analysis. *Neurosci Biobehav Rev* 34, 1207–1222.
- Smieskova, R., Fusar-Poli, P., Aston, J., Simon, A., Bendfeldt, K., Lenz, C., Stieglitz, R.-D., McGuire, P., Riecher-Rössler, A., Borgwardt, S.J., 2011. Insular Volume Abnormalities Associated with Different Transition Probabilities to Psychosis. *Psychological Medicine FirstView*, 1–13.
- Smith, B.B., 2003. Medicines Are Not Enough. *Schizophrenia Bull* 29, 139–142.
- Smith, S.M., Miller, K.L., Salimi-Khorshidi, G., Webster, M., Beckmann, C.F., Nichols, T.E., Ramsey, J.D., Woolrich, M.W., 2011. Network modelling methods for FMRI. *Neuroimage* 54, 875–891.
- Sommer, I.E.C., Dierenen, K.M.J., Blom, J.-D., Willems, A., Kushan, L., Slotema, K., Boks, M.P.M., Daalman, K., Hoek, H.W., Neggers, S.F.W., Kahn, R.S., 2008. Auditory verbal hallucinations predominantly activate the right inferior frontal area. *Brain* 131, 3169–3177.

- Southard, E.B., 1915. ON THE TOPOGRAPHICAL DISTRIBUTION OF CORTEX LESIONS AND ANOMALIES IN DEMENTIA PRÆCOX, WITH SOME ACCOUNT OF THEIR FUNCTIONAL SIGNIFICANCE. *Am J Psychiatry* 71, 603–671–20.
- Spence, S.A., Brooks, D.J., Hirsch, S.R., Liddle, P.F., Meehan, J., Grasby, P.M., 1997. A PET study of voluntary movement in schizophrenic patients experiencing passivity phenomena (delusions of alien control). *Brain* 120, 1997 –2011.
- Spencer, M.D., Moorhead, T.W.J., McIntosh, A.M., Stanfield, A.C., Muir, W.J., Hoare, P., Owens, D.G.C., Lawrie, S.M., Johnstone, E.C., 2007. Grey matter correlates of early psychotic symptoms in adolescents at enhanced risk of psychosis: a voxel-based study. *Neuroimage* 35, 1181–1191.
- Sridharan, D., Levitin, D.J., Menon, V., 2008. A critical role for the right fronto-insular cortex in switching between central-executive and default-mode networks. *Proceedings of the National Academy of Sciences* 105, 12569–12574.
- Sripada, R.K., King, A.P., Welsh, R.C., Garfinkel, S.N., Wang, X., Sripada, C.S., Liberzon, I., 2012. Neural dysregulation in posttraumatic stress disorder: evidence for disrupted equilibrium between salience and default mode brain networks. *Psychosom Med* 74, 904–911.
- Stevens, W.D., Buckner, R.L., Schacter, D.L., 2010. Correlated Low-Frequency BOLD Fluctuations in the Resting Human Brain Are Modulated by Recent Experience in Category-Preferential Visual Regions. *Cerebral Cortex* 20, 1997 –2006.
- Stip, E., Lungu, O.V., Anselmo, K., Letourneau, G., Mendrek, A., Stip, B., Lipp, O., Lalonde, P., Bentaleb, L.A., 2012. Neural changes associated with appetite information processing in schizophrenic patients after 16 weeks of olanzapine treatment. *Translational Psychiatry* 2, e128.
- Strauss, J., 2011. Subjectivity and severe psychiatric disorders. *Schizophrenia Bull* 37, 8–13.

- Stroup, D.F., Berlin, J.A., Morton, S.C., Olkin, I., Williamson, G.D., Rennie, D., Moher, D., Becker, B.J., Sipe, T.A., Thacker, S.B., For the Meta-analysis Of Observational Studies in Epidemiology (MOOSE) Group, 2000. Meta-analysis of Observational Studies in Epidemiology. *JAMA: The Journal of the American Medical Association* 283, 2008–2012.
- Su, L., Bowman, H., Barnard, P., 2011. Glancing and Then Looking: On the Role of Body, Affect, and Meaning in Cognitive Control. *Front Psychol* 2.
- Subramanian, L., Hindle, J.V., Johnston, S., Roberts, M.V., Husain, M., Goebel, R., Linden, D., 2011. Real-Time Functional Magnetic Resonance Imaging Neurofeedback for Treatment of Parkinson's Disease. *J. Neurosci.* 31, 16309–16317.
- Suhara, T., 2001. Dopamine D2 Receptors in the Insular Cortex and the Personality Trait of Novelty Seeking. *NeuroImage* 13, 891–895.
- Suhara, T., Okubo, Y., Yasuno, F., Sudo, Y., Inoue, M., Ichimiya, T., Nakashima, Y., Nakayama, K., Tanada, S., Suzuki, K., Halldin, C., Farde, L., 2002. Decreased dopamine D2 receptor binding in the anterior cingulate cortex in schizophrenia. *Arch. Gen. Psychiatry* 59, 25–30.
- Sui, J., Pearlson, G., Caprihan, A., Adali, T., Kiehl, K.A., Liu, J., Yamamoto, J., Calhoun, V.D., 2011. Discriminating schizophrenia and bipolar disorder by fusing fMRI and DTI in a multimodal CCA+ joint ICA model. *Neuroimage* 57, 839–855.
- Sumich, A., Chitnis, X.A., Fannon, D.G., O'Ceallaigh, S., Doku, V.C., Faldrowicz, A., Sharma, T., 2005. Unreality symptoms and volumetric measures of Heschl's gyrus and planum temporal in first-episode psychosis. *Biol. Psychiatry* 57, 947–950.
- Sun, J., Maller, J.J., Guo, L., Fitzgerald, P.B., 2009. Superior temporal gyrus volume change in schizophrenia: a review on region of interest volumetric studies. *Brain Res Rev* 61, 14–32.

- Supekar, K., Menon, V., 2012. Developmental maturation of dynamic causal control signals in higher-order cognition: a neurocognitive network model. *PLoS Comput. Biol.* 8, e1002374.
- Sylvester, C.M., Corbetta, M., Raichle, M.E., Rodebaugh, T.L., Schlaggar, B.L., Sheline, Y.I., Zorumski, C.F., Lenze, E.J., 2012. Functional network dysfunction in anxiety and anxiety disorders. *Trends in neurosciences* 35, 527-35.
- Szasz, T.S., 1976. Schizophrenia: The Sacred Symbol of Psychiatry. *BJP* 129, 308–316.
- Takahashi, H., Higuchi, M., Suhara, T., 2006a. The Role of Extrastriatal Dopamine D2 Receptors in Schizophrenia. *Biological Psychiatry* 59, 919–928.
- Takahashi, T., Suzuki, M., Hagino, H., Zhou, S.-Y., Kawasaki, Y., Nohara, S., Nakamura, K., Yamashita, I., Seto, H., Kurachi, M., 2004. Bilateral volume reduction of the insular cortex in patients with schizophrenia: a volumetric MRI study. *Psychiatry Research: Neuroimaging* 131, 185–194.
- Takahashi, T., Suzuki, M., Zhou, S.-Y., Hagino, H., Tanino, R., Kawasaki, Y., Nohara, S., Yamashita, I., Seto, H., Kurachi, M., 2005. Volumetric MRI study of the short and long insular cortices in schizophrenia spectrum disorders. *Psychiatry Research: Neuroimaging* 138, 209–220.
- Takahashi, T., Suzuki, M., Zhou, S.-Y., Tanino, R., Hagino, H., Kawasaki, Y., Matsui, M., Seto, H., Kurachi, M., 2006b. Morphologic alterations of the parcellated superior temporal gyrus in schizophrenia spectrum. *Schizophr. Res* 83, 131–143.
- Takahashi, T., Wood, S.J., Soulsby, B., McGorry, P.D., Tanino, R., Suzuki, M., Velakoulis, D., Pantelis, C., 2009a. Follow-up MRI study of the insular cortex in first-episode psychosis and chronic schizophrenia. *Schizophrenia Research* 108, 49–56.
- Takahashi, T., Wood, S.J., Soulsby, B., Tanino, R., Wong, M.T.H., McGorry, P.D., Suzuki, M., Velakoulis, D., Pantelis, C., 2009b. Diagnostic specificity of the insular cortex abnormalities in first-episode psychotic disorders. *Progress in Neuro-Psychopharmacology and Biological Psychiatry* 33, 651–657.

- Takahashi, T., Wood, S.J., Yung, A.R., Phillips, L.J., Soulsby, B., McGorry, P.D., Tanino, R., Zhou, S.-Y., Suzuki, M., Velakoulis, D., Pantelis, C., 2009c. Insular cortex gray matter changes in individuals at ultra-high-risk of developing psychosis. *Schizophr. Res* 111, 94–102.
- Takahashi, T., Wood, S.J., Yung, A.R., Soulsby, B., McGorry, P.D., Suzuki, M., Kawasaki, Y., Phillips, L.J., Velakoulis, D., Pantelis, C., 2009d. Progressive gray matter reduction of the superior temporal gyrus during transition to psychosis. *Arch. Gen. Psychiatry* 66, 366–376.
- Tandon, R., Keshavan, M.S., Nasrallah, H.A., 2008. Schizophrenia, “just the facts” what we know in 2008. 2. Epidemiology and etiology. *Schizophr. Res.* 102, 1–18.
- Tang, Y.-Y., Rothbart, M.K., Posner, M.I., 2012. Neural correlates of establishing, maintaining, and switching brain states. *Trends Cogn. Sci. (Regul. Ed.)* 16, 330–337.
- Taylor, K.S., Seminowicz, D.A., Davis, K.D., 2009. Two systems of resting state connectivity between the insula and cingulate cortex. *Hum Brain Mapp* 30, 2731–2745.
- Tian, L., Meng, C., Yan, H., Zhao, Q., Liu, Q., Yan, J., Han, Y., Yuan, H., Wang, L., Yue, W., Zhang, Y., Li, X., Zhu, C., He, Y., Zhang, D., 2011. Convergent Evidence from Multimodal Imaging Reveals Amygdala Abnormalities in Schizophrenic Patients and Their First-Degree Relatives. *PLoS ONE* 6, e28794.
- Tomelleri, L., Jogia, J., Perlini, C., Bellani, M., Ferro, A., Rambaldelli, G., Tansella, M., Frangou, S., Brambilla, P., 2009. Brain structural changes associated with chronicity and antipsychotic treatment in schizophrenia. *Eur Neuropsychopharmacol* 19, 835–840.
- Toro, R., Perron, M., Pike, B., Richer, L., Veillette, S., Pausova, Z., Paus, T., 2008. Brain Size and Folding of the Human Cerebral Cortex. *Cereb. Cortex* 18, 2352–2357.

- Tu, P.-C., Hsieh, J.-C., Li, C.-T., Bai, Y.-M., Su, T.-P., 2012. Cortico-striatal disconnection within the cingulo-opercular network in schizophrenia revealed by intrinsic functional connectivity analysis: a resting fMRI study. *Neuroimage* 59, 238–247.
- Turkeltaub, P.E., Eden, G.F., Jones, K.M., Zeffiro, T.A., 2002. Meta-Analysis of the Functional Neuroanatomy of Single-Word Reading: Method and Validation. *NeuroImage* 16, 765–780.
- Tzourio-Mazoyer, N., Landeau, B., Papathanassiou, D., Crivello, F., Etard, O., Delcroix, N., Mazoyer, B., Joliot, M., 2002. Automated anatomical labeling of activations in SPM using a macroscopic anatomical parcellation of the MNI MRI single-subject brain. *Neuroimage* 15, 273–289.
- Unknown, 1930. The Dementia Praecox Problem. *J Neurol Psychopathol* 11, 60–63.
- Van Haren, N.E.M., Schnack, H.G., Cahn, W., Van den Heuvel, M.P., Lepage, C., Collins, L., Evans, A.C., Pol, H.E.H., Kahn, R.S., 2011. Changes in Cortical Thickness During the Course of Illness in Schizophrenia. *Arch Gen Psychiatry* 68, 871–880.
- Van Snellenberg, J.X., Torres, I.J., Thornton, A.E., 2006. Functional neuroimaging of working memory in schizophrenia: Task performance as a moderating variable. *Neuropsychology* 20, 497–510.
- Van Veen, V., Krug, M.K., Schooler, J.W., Carter, C.S., 2009. Neural activity predicts attitude change in cognitive dissonance. *Nat Neurosci* 12, 1469–1474.
- Venkatasubramanian, G., Puthumana, D.T.K., Jayakumar, P.N., Gangadhar, B.N., 2010. A functional Magnetic Resonance Imaging study of neurohemodynamic abnormalities during emotion processing in subjects at high risk for schizophrenia. *Indian J Psychiatry* 52, 308–315.
- Vercammen, A., Knegeting, H., Liemburg, E.J., Den Boer, J.A., Aleman, A., 2010. Functional connectivity of the temporo-parietal region in schizophrenia: effects of rTMS treatment of auditory hallucinations. *J Psychiatr Res* 44, 725–731.

- Verdoux, H., Van Os, J., Sham, P., Jones, P., Gilvarry, K., Murray, R., 1996. Does familiarity predispose to both emergence and persistence of psychosis? A follow-up study. *The British Journal of Psychiatry* 168, 620–626.
- Villafuerte, S., Heitzeg, M.M., Foley, S., Wendy Yau, W.-Y., Majczenko, K., Zubieta, J.-K., Zucker, R.A., Burmeister, M., 2011. Impulsiveness and insula activation during reward anticipation are associated with genetic variants in GABRA2 in a family sample enriched for alcoholism. *Molecular Psychiatry* 17, 511-9
- Voets, N.L., Hough, M.G., Douaud, G., Matthews, P.M., James, A., Winmill, L., Webster, P., Smith, S., 2008. Evidence for abnormalities of cortical development in adolescent-onset schizophrenia. *Neuroimage* 43, 665–675.
- Vogeley, K., Schneider-Axmann, T., Pfeiffer, U., Tepest, R., Bayer, T.A., Bogerts, B., Honer, W.G., Falkai, P., 2000. Disturbed Gyrfication of the Prefrontal Region in Male Schizophrenic Patients: A Morphometric Postmortem Study. *Am J Psychiatry* 157, 34–39.
- Voss, M.W., Prakash, R.S., Erickson, K.I., Boot, W.R., Basak, C., Neider, M.B., Simons, D.J., Fabiani, M., Gratton, G., Kramer, A.F., 2012. Effects of training strategies implemented in a complex videogame on functional connectivity of attentional networks. *Neuroimage* 59, 138–148.
- Wai, M., Shi, C., Kwong, W., Zhang, L., Lam, W., Yew, D., 2008. Development of the human insular cortex: differentiation, proliferation, cell death, and appearance of 5HT-2A receptors. *Histochemistry and Cell Biology* 130, 1199–1204.
- Wang, G.-J., Volkow, N.D., Fowler, J.S., Ding, Y.-S., Logan, J., Galley, S.J., MacGregor, R.R., Wolf, A.P., 1995. Comparison of two PET radioligands for imaging extrastriatal dopamine transporters in human brain. *Life Sciences* 57, PL187–PL191.
- Waters, F.A., Maybery, M.T., Badcock, J.C., Michie, P.T., 2004. Context memory and binding in schizophrenia. *Schizophrenia Research* 68, 119–125.

- Waters, F.A.V., Badcock, J.C., Michie, P.T., Maybery, M.T., 2006. Auditory hallucinations in schizophrenia: intrusive thoughts and forgotten memories. *Cogn Neuropsychiatry* 11, 65–83.
- Weinberger, D., Berman, K., Suddath, R., Torrey, E., 1992. Evidence of dysfunction of a prefrontal-limbic network in schizophrenia: a magnetic resonance imaging and regional cerebral blood flow study of discordant monozygotic twins. *Am J Psychiatry* 149, 890–897.
- Welker, W., 1990. {Why does cerebral cortex fissure and fold? A review of determinants of gyri and sulci}. *Cerebral cortex* 8, 3–136.
- Wen, X., Yao, L., Liu, Y., Ding, M., 2012. Causal Interactions in Attention Networks Predict Behavioral Performance. *J. Neurosci.* 32, 1284–1292.
- Whalley, H.C., Pappmeyer, M., Sprooten, E., Lawrie, S.M., Sussmann, J.E., McIntosh, A.M., 2012. Review of functional magnetic resonance imaging studies comparing bipolar disorder and schizophrenia. *Bipolar Disord* 14, 411–431.
- Wheeler, D.G., Harper, C.G., 2007. Localised reductions in gyrification in the posterior cingulate: schizophrenia and controls. *Prog. Neuropsychopharmacol. Biol. Psychiatry* 31, 319–327.
- White, T., Hilgetag, C.C., 2011. Gyrification and neural connectivity in schizophrenia. *Dev. Psychopathol* 23, 339–352.
- White, T.P., Joseph, V., Francis, S.T., Liddle, P.F., 2010a. Aberrant salience network (bilateral insula and anterior cingulate cortex) connectivity during information processing in schizophrenia. *Schizophr. Res* 123, 105–115.
- White, T.P., Joseph, V., O'Regan, E., Head, K.E., Francis, S.T., Liddle, P.F., 2010b. Alpha-gamma interactions are disturbed in schizophrenia: A fusion of electroencephalography and functional magnetic resonance imaging. *Clinical Neurophysiology* 121, 1427–1437.

- Whitfield-Gabrieli, S., Ford, J.M., 2012. Default Mode Network Activity and Connectivity in Psychopathology. *Annual Review of Clinical Psychology* 8, 49–76.
- Whitfield-Gabrieli, S., Thermenos, H.W., Milanovic, S., Tsuang, M.T., Faraone, S.V., McCarley, R.W., Shenton, M.E., Green, A.I., Nieto-Castanon, A., LaViolette, P., Wojcik, J., Gabrieli, J.D.E., Seidman, L.J., 2009. Hyperactivity and hyperconnectivity of the default network in schizophrenia and in first-degree relatives of persons with schizophrenia. *Proceedings of the National Academy of Sciences* 106, 1279–1284.
- WHO Collaborating Centre for Drug Statistics and Methodology, 2003. Guidelines for ATC Classification and DDD Assignment.
- Williams, M.R., Chaudhry, R., Perera, S., Pearce, R.K.B., Hirsch, S.R., Ansorge, O., Thom, M., Maier, M., 2012. Changes in cortical thickness in the frontal lobes in schizophrenia are a result of thinning of pyramidal cell layers. *European Archives of Psychiatry and Clinical Neuroscience* 263, 25-39
- Williams, S.M., Goldman-Rakic, P.S., 1998. Widespread origin of the primate mesofrontal dopamine system. *Cerebral Cortex* 8, 321 –345.
- Williamson, P., 2007. Are Anticorrelated Networks in the Brain Relevant to Schizophrenia? *Schizophrenia Bull* 33, 994–1003.
- Williamson, P.C., Allman, J.M., 2012. A framework for interpreting functional networks in schizophrenia. *Front Hum Neurosci* 6.
- Wilmsmeier, A., Ohrmann, P., Suslow, T., Siegmund, A., Koelkebeck, K., Rothermundt, M., Kugel, H., Arolt, V., Bauer, J., Pedersen, A., 2010. Neural correlates of set-shifting: decomposing executive functions in schizophrenia. *J Psychiatry Neurosci* 35, 321–329.
- Winkler, A., Kochunov, P., Fox, P., Duggirala, R., Almasy, L., Blangero, J., Glahn, D., 2009. Heritability of Volume, Surface Area and Thickness for Anatomically Defined

- Cortical Brain Regions Estimated in a Large Extended Pedigree. *NeuroImage* 47, S162.
- Winkler, A.M., Kochunov, P., Blangero, J., Almasy, L., Zilles, K., Fox, P.T., Duggirala, R., Glahn, D.C., 2010. Cortical thickness or grey matter volume? The importance of selecting the phenotype for imaging genetics studies. *NeuroImage* 53, 1135–1146.
- Woodward, N.D., Rogers, B., Heckers, S., 2011. Functional resting-state networks are differentially affected in schizophrenia. *Schizophr. Res.* 130, 86–93.
- Woodward, N.D., Zald, D.H., Ding, Z., Riccardi, P., Ansari, M.S., Baldwin, R.M., Cowan, R.L., Li, R., Kessler, R.M., 2009. Cerebral morphology and dopamine D2/D3 receptor distribution in humans: A combined [¹⁸F]fallypride and voxel-based morphometry study. *NeuroImage* 46, 31–38.
- Wright, I.C., Ellison, Z.R., Sharma, T., Friston, K.J., Murray, R.M., McGuire, P.K., 1999. Mapping of grey matter changes in schizophrenia. *Schizophr. Res* 35, 1–14.
- Wright, I.C., McGuire, P.K., Poline, J.B., Travere, J.M., Murray, R.M., Frith, C.D., Frackowiak, R.S., Friston, K.J., 1995. A voxel-based method for the statistical analysis of gray and white matter density applied to schizophrenia. *Neuroimage* 2, 244–252.
- Wylie, K.P., Tregellas, J.R., 2010. The role of the insula in schizophrenia. *Schizophr. Res.* 123, 93–104.
- Xue, G., Lu, Z., Levin, I.P., Bechara, A., 2010. The impact of prior risk experiences on subsequent risky decision-making: The role of the insula. *NeuroImage* 50, 709–716.
- Xue, T., Yuan, K., Zhao, L., Yu, D., Zhao, L., Dong, T., Cheng, P., Von Deneen, K.M., Qin, W., Tian, J., 2012. Intrinsic brain network abnormalities in migraines without aura revealed in resting-state fMRI. *PLoS ONE* 7, e52927.
- Ye, Z., Hammer, A., Camara, E., Münte, T.F., 2011. Pramipexole modulates the neural network of reward anticipation. *Human Brain Mapping* 32, 800–811.

- Yu, D., 2013. Additional brain functional network in adults with attention-deficit/hyperactivity disorder: a phase synchrony analysis. *PLoS ONE* 8, e54516.
- Yücel, M., Stuart, G.W., Maruff, P., Wood, S.J., Savage, G.R., Smith, D.J., Crowe, S.F., Copolov, D.L., Velakoulis, D., Pantelis, C., 2002. Paracingulate morphologic differences in males with established schizophrenia: a magnetic resonance imaging morphometric study. *Biol. Psychiatry* 52, 15–23.
- Yung, A.R., McGorry, P.D., 1996. The Prodromal Phase of First-episode Psychosis: Past and Current Conceptualizations. *Schizophrenia Bulletin* 22, 353–370.
- Yung, A.R., McGorry, P.D., 2007. Prediction of psychosis: setting the stage. *Br J Psychiatry Suppl* 51, s1–8.
- Zang, Z.-X., Yan, C.-G., Dong, Z.-Y., Huang, J., Zang, Y.-F., 2012. Granger causality analysis implementation on MATLAB: A graphic user interface toolkit for fMRI data processing. *Journal of Neuroscience Methods* 203, 418–426.
- Zeidan, F., Martucci, K.T., Kraft, R.A., Gordon, N.S., McHaffie, J.G., Coghill, R.C., 2011. Brain mechanisms supporting the modulation of pain by mindfulness meditation. *J. Neurosci.* 31, 5540–5548.
- Zhang, Y., Yu, C., Zhou, Y., Li, K., Li, C., Jiang, T., 2009. Decreased gyrification in major depressive disorder. *NeuroReport* 20, 378–380.
- Zhang, Y., Zhou, Y., Yu, C., Lin, L., Li, C., Jiang, T., 2010. Reduced Cortical Folding in Mental Retardation. *American Journal of Neuroradiology* 31, 1063–7.
- Zhou, Y., Liang, M., Tian, L., Wang, K., Hao, Y., Liu, H., Liu, Z., Jiang, T., 2007. Functional disintegration in paranoid schizophrenia using resting-state fMRI. *Schizophrenia Research* 97, 194–205.
- Zilles, K., Armstrong, E., Schleicher, A., Kretschmann, H.-J., 1988. The human pattern of gyrification in the cerebral cortex. *Anatomy and Embryology* 179, 173–179.

- Zipursky, R.B., Marsh, L., Lim, K.O., DeMent, S., Shear, P.K., Sullivan, E.V., Murphy, G.M., Csernansky, J.G., Pfefferbaum, A., 1994. Volumetric MRI assessment of temporal lobe structures in schizophrenia. *Biol. Psychiatry* 35, 501–516.
- Zornberg, G.L., 1999. Elmer E. Southard, M.D. 1876–1920. *Am J Psychiatry* 156, 1263–1263.
- Zou, K.H., Warfield, S.K., Bharatha, A., Tempany, C.M.C., Kaus, M.R., Haker, S.J., Wells, W.M., Jolesz, F.A., Kikinis, R., 2004. Statistical Validation of Image Segmentation Quality Based on a Spatial Overlap Index. *Acad Radiol* 11, 178–189.

APPENDIX 1

Exclusion criteria for motion artefacts in MPRAGE (anatomical image) acquisition

Scans with at least one out of the following three criteria were excluded due to motion artefacts:

1. Images too grainy: GM-WM boundary is clearly invisible in >2 anatomically distinct regions
2. Significant edge ringing artefacts; >2 rings noted with associated blurring of GM_WM boundary in >2 anatomically distinct regions
3. Less severe motion artefacts / grainy image but not satisfying criteria 1 and 2, but either
 - a. Fails Freesurfer cortical reconstruction due to significant topological defects; or
 - b. Presence of >2 handles/holes that require manual intervention (e.g. hole filling, defining control points, removal of obscure/uncertain pia-like tissue) to define GM/WM boundaries despite Freesurfer's automatic topological fixation procedure

APPENDIX 2

PUBLICATIONS (*published/accepted peer reviewed manuscripts arising from the doctoral training; Oct 2009 to July 2013. Chapters of this thesis that are relevant to the published works are highlighted*)

- 1) **Palaniyappan, L.**, Simmonite, M., Liddle, E.B., White, T.P., Liddle, P.F., 2013. Neural primacy of the salience processing system in schizophrenia. *Neuron*. Aug 21;79(4):814-28. CHAPTER 8
- 2) **Palaniyappan, L.**, Reis Marques, T., Taylor, H., Handley, R., Mondelli, V., Bonaccorso, S., Giordano, A., McQueen, A., Simmons, A., Di Forti, M., David, A.S., Pariante, C.M., Murray, R.M., Dazzan, P., in press. Cortical folding defects as markers of poor treatment response in first episode psychosis. *JAMA Psychiatry* (in press, Accepted 01/2013).
- 3) **Palaniyappan, L.**, Crow, T.J., Hough, M., Voets, N.L., Liddle, P.F., James, S., Winmill, L., James, A.C., 2013. Gyrfication of Broca's region is anomalously lateralized at onset of schizophrenia in adolescence and regresses at 2year follow-up. *Schizophrenia Research* 147(1):39-45.
- 4) Fan, Q., **Palaniyappan, L.**, Tan, L., Wang, J., Wang, X., Li, C., Zhang, T., Jiang, K., Xiao, Z., Liddle, P.F., 2013. Surface anatomical profile of the cerebral cortex in obsessive-compulsive disorder: a study of cortical thickness, folding and surface area. *Psychological Medicine*. 43(5):1081-91
- 5) **Palaniyappan, L.**, Liddle, P.F., 2013. Diagnostic Discontinuity in Psychosis: A Combined Study of Cortical Gyrfication and Functional Connectivity. *Schizophrenia Bulletin*. (epub: Apr 24 2013) CHAPTER 7
- 6) **Palaniyappan, L.**, Al-Radaideh, A., Mougín, O., Gowland, P., Liddle, P.F., 2013. Combined white matter imaging suggests myelination defects in visual processing regions in schizophrenia. *Neuropsychopharmacology*. (epub: Apr 4 2013)
- 7) Ecker, C., Ginestet, C., Feng, Y., Johnston, P., Lombardo, M.V., Lai, M.-C., Suckling, J., **Palaniyappan, L.**, Daly, E., Murphy, C.M., Williams, S.C., Bullmore, E.T., Baron-Cohen, S., Brammer, M., Murphy, D.G.M., MRC AIMS Consortium, 2013. Brain surface anatomy in adults with autism: the relationship between surface area, cortical thickness, and autistic symptoms. *JAMA Psychiatry*. 70, 59–70.
- 8) **Palaniyappan, L.**, Liddle, P.F., 2012. Aberrant cortical gyrfication in schizophrenia: a surface-based morphometry study. *Journal of Psychiatry & Neuroscience*. 37, 110-119. CHAPTER 6
- 9) **Palaniyappan, L.**, Liddle, P.F., 2012. Dissociable morphometric differences of the inferior parietal lobule in schizophrenia. *European Archives of Psychiatry & Clinical Neuroscience*. 262(7):579-87

- 10) **Palaniyappan, L., Balain, V., Liddle, P.F., 2012a.** The neuroanatomy of psychotic diathesis: a meta-analytic review. *Journal of Psychiatric Research*. 46, 1249–1256. CHAPTER 3
- 11) Alhusaini, S., Doherty, C.P., **Palaniyappan, L., Scanlon, C., Maguire, S., Brennan, P., Delanty, N., Fitzsimons, M., Cavalleri, G.L., 2012.** Asymmetric cortical surface area and morphology changes in mesial temporal lobe epilepsy with hippocampal sclerosis. *Epilepsia* 53, 995–1003.
- 12) **Palaniyappan, L., Balain, V., Radua, J., Liddle, P.F., 2012.** Structural correlates of auditory hallucinations in schizophrenia: A meta-analysis. *Schizophrenia Research* 137(1-3):169-73 CHAPTER 4
- 13) **Palaniyappan, L., Doege, K., Mallikarjun, P., Liddle, E.B., Liddle, P.F., 2012.** Cortical thickness and oscillatory phase resetting: A proposed mechanism of salience network dysfunction in schizophrenia. *Psychiatry*. 23, 117–129.
- 14) **Palaniyappan, L., Liddle, P.F., 2012.** Differential effects of surface area, gyrification and cortical thickness on voxel based morphometric deficits in schizophrenia. *Neuroimage* 60, 693–699. CHAPTER 5
- 15) **Palaniyappan, L., White, T.P., Liddle, P.F., 2012.** The concept of salience network dysfunction in schizophrenia: from neuroimaging observations to therapeutic opportunities. *Current Topics in Medicinal Chemistry*. 12(21):2324-38. CHAPTERS 1 and 9
- 16) **Palaniyappan, L., Liddle, P.F., 2012.** Does the salience network play a cardinal role in psychosis? An emerging hypothesis of insular dysfunction. *Journal of Psychiatry & Neuroscience* 37, 17–27. CHAPTER 2
- 17) **Palaniyappan, L., Mallikarjun, P., Joseph, V., White, T.P., Liddle, P.F., 2011.** Reality distortion is related to the structure of the salience network in schizophrenia. *Psychological Medicine* 41, 1701–1708
- 18) **Palaniyappan, L., Mallikarjun, P., Joseph, V., White, T.P., Liddle, P.F., 2011.** Regional contraction of brain surface area involves three large-scale networks in schizophrenia. *Schizophrenia Research*. 129, 163–168 CHAPTER 7
- 19) **Palaniyappan, L., Mallikarjun, P., Joseph, V., White, T.P., Liddle, P.F., 2011.** Folding of the Prefrontal Cortex in Schizophrenia: Regional Differences in Gyrification. *Biological Psychiatry* 69, 974–979
- 20) **Palaniyappan, L., Mallikarjun, P., Joseph, V., Liddle, P.F., 2011.** Appreciating symptoms and deficits in schizophrenia: right posterior insula and poor insight. *Progress in Neuropsychopharmacology & Biological Psychiatry* 35, 523–527

CONFERENCE ABSTRACTS (Published in print: Oct 2009 and July 2013)

Palaniyappan, L., Balain, V., Simmonite, M., Carrol, L., McGuffin, P., Aitchison, K., Liddle, P.F., 2012. THE INFLUENCE OF DISC1 SER704CYS POLYMORPHISM ON THE CORTICAL THICKNESS OF SALIENCE NETWORK (INSULA AND ANTERIOR CINGULATE) IN PSYCHOSIS. *Schizophrenia Research*. 136, S319.

Palaniyappan, L., James, A., Crow, T.J., Liddle, P.F., 2012. REPEATED OBSERVATION OF ABNORMAL GYRIFICATION LOCALIZED TO THE FRONTOINSULAR CORTEX FROM FOUR INDEPENDENT SAMPLES WITH SCHIZOPHRENIA. *Schizophrenia Research* 136, S87.

Palaniyappan, L., Park, B., Liddle, P.F., 2012. INCREASED ASSORTATIVITY OF GYRIFICATION BASED BRAIN CONNECTOME IN SCHIZOPHRENIA. *Schizophrenia Research* 136, S206.

Palaniyappan, L., White, T.P., Liddle, P.F., 2012. ABERRANT FUNCTIONAL CONNECTIVITY OF RIGHT ANTERIOR INSULA DURING A WORKING MEMORY TASK IN SCHIZOPHRENIA. *Schizophrenia Research*. 136, S101.

Palaniyappan, L., Balain, V., White, T.P., Jansen, M., Liddle, P.F., 2011. STRUCTURAL ABNORMALITIES IN THE SALIENCE NETWORK ARE COMMON TO BOTH BIPOLAR DISORDER WITH PSYCHOSIS AND SCHIZOPHRENIA. *Bipolar Disorders*, 13, S76.

Palaniyappan, L.K., Doege, K., Mallikarjun, P., Liddle, E.B., Liddle, P.F., 2010. ROLE OF INSULAR CORTEX IN PHASE LOCKING OF FRONTAL THETA OSCILLATIONS IN SCHIZOPHRENIA: PRELIMINARY EVIDENCE FROM CORTICAL SURFACE ANALYSIS. *Schizophrenia Research* 117, 344.